Index

List of Abbreviations

AmB	Amphotericin B
5-BMF	5-Bromomethyl fluorescein
^{13}C NMR	Carbon 13 NMR
CCl_4	Carbon tetrachloride
$CDCl_3$	Deuterated chloroform
CHCA	Cyano-4-hydroxycinnamic acid
d	Doublet
dd	Double doublet
dt	Doublet of triplets
DMAC	Dimethylacetamide
ELISA	Enzyme-linked immunosorbent assay
g	Gram
GC	Gas chromatography
^{1}H NMR	Proton NMR
H_2	Hydrogen
H_2O_2	Hydrogen peroxide
HIV	Human immunodeficiency virus
HMPA	Hexamethylphosphorotriamide
HPLC	High performance liquid chromatography
Hz	Hertz
IMS	Industrial methylated spirits
INH	Isoniazid
IR	Infra red
L	Liter

LDA	Lithium *N*,*N*,-di-isopropylamide
m	multiplet
M	Molar
MA	Mycolic acid
MALDI-TOF MS	Matrix-assisted laser desorption/ionization time-of-flight mass spectrometry
MAs	Mycolic acids
MDR	Multi-drug resistant
MeOH	Methanol
mg	Milligram
ml	Milliliter
mmol	Millimol
MS	Mass spectrometry
M. tb	*Mycobacterium tuberculosis*
M. tuberculosis	*Mycobacterium tuberculosis*
NMR	Nuclear magnetic resonance
OAc	*O*-Acetyl
PCC	Piridinium chlorochromate
Pd on C	Palladium on charcoal
q	Quartet
Rf	Retardation factor
RT	Room temperature
s	Singlet
t	Triplet
TB	Tuberculosis
THF	Tetrahydrofuran

THP	Tetrahydropyran
TLC	Thin layer chromatography
TMDM	Trimethylsilyl diazomethane
WHO	World Health Organisation
XDR	Extreme drug resistant

List of Figures

List of Tables

Acknowledgements

Our God is an awesome God!

My parents, brother and sister for all their love and support.

Prof Verschoor for introducing me to the world of TB research, his guidance and support.

Prof Mark Baird for inviting me to work in his laboratory, his guidance and support.

Sandra van Wyngaardt and the BIA group at the University of Pretoria for their friendship, advise and support.

Dr Juma'a Al-Dulayymi, Mr Roberts, Dr Gianna Sekanka, Gani Koza, Ieuan Roberts and the rest of the students in the organic chemistry lab at the University of Wales Bangor for all their help, advise and friendship.

Glyn, Mike, Gwynfor, Denis and Barry for their help with NMR, MS, MALDI-TOF MS analysis at the University of Wales Bangor.

Dr Gianna Sekanka for helping to understand the chemistry behind the separation of the mycolic acids, and Venessa Roberts for helping with the TLC separation.

MRC and NRF for funding.

Summary

Title: Sturcture-function relationships of mycolic acids in tuberculosis
By: Martha Susanna Madrey Deysel
Promotor: Prof J A Verschoor
Co-promotor: Prof M S Baird (University of Bangor, UK)
Department: Department of Biochemistry
Degree: Philosophiae doctor

Tuberculosis (TB) is the leading cause of death among HIV infected people. *Mycobacterium tuberculosis* (*M. tuberculosis*), the causative agent of TB, features a distinctive lipid-rich cell wall with mycolic acids (MA) the major component in the outer layer. Mycolic acids are α-alkyl β-hydroxy long chain fatty acids, which exist in a number of chemical subclasses depending on the presence of functional oxygenated and non-oxygenated groups in the meromycolate chain. In numerous studies the different MA subclasses have been shown to play different roles in antibody recognition, virulence and the ability to attract cholesterol. It was previously suggested that the oxygenated MA might be important for these properties. Except for the mycolic acid motif, little is known about the stereochemistry of the other chiral centres. The importance of the different functional groups, their position and stereochemistry, for immunological properties, are not yet clarified. This study set out to resolve the structure-activity relationships of mycolic acids from *M. tuberculosis* in terms of their antigenicity and the ability to attract cholesterol. To determine fine specificity of interaction of MA with antibodies, the subclasses of MA from *M. tuberculosis* were separated and the antigenicity of two was determined. TB^+ and TB^- patient sera recognised natural MA, alpha-MA and methoxy-MA. It was confirmed that the carboxylic acid group played a fundamental role in its recognition. Interestingly, cord factor (trehalose-6,6'-dimycolate) was recognised specifically by TB^+ sera. This implies multiple epitopes in the MA structure, some of which are very specific for TB patients. A stereocontrolled diastereomer of *cis*-cyclopropane methoxy-MA was synthesized and along with other synthetic methoxy-, keto- and hydroxy-MAs, were tested for antibody recognition. One diastereomer, *SS*-*SR*-methoxy-MA, was recognised stronger by TB^+ serum than the other, it also is the one that closest approximates the signal strength of antibody binding to natural MA by TB^+ patient sera. While the others are not specifically recognised, this *SS*-*SR*-methoxy-MA may well represent one of the antigenically active

components that occurs in natural MA and that elicits specific antibodies in TB patients. This thesis reports a stereocontrolled chemical synthesis of biologically active mycolic acids and shows that a single component of the mycolic acid mixture can be sufficient to elicit an immunological response.

Chapter 1

General Introduction

1.1 Introduction

1.1.1 Tuberculosis

Tuberculosis (TB) has been called a lot of names. The evangelist John Bunyan named tuberculosis 'the Captain of all these men of Death' and in India it was known as 'the King of Diseases' (69). It appears to be as old as humanity itself, with skeletal remains of prehistoric humans showing evidence consistent with TB of the spine. The early physicians called it *phthisis*, derived from the Greek term for wasting (113).

The World Health Organization reported 9 million new TB cases and about 2 million TB deaths for 2004. The number of TB cases for a few of the WHO regions was stable or decreasing, but in Africa the epidemic is still growing due to the spread of HIV. More than 80% of all TB patients live in sub-Saharan Africa and Asia. South Africa reports more TB cases than any other country in Africa (154).

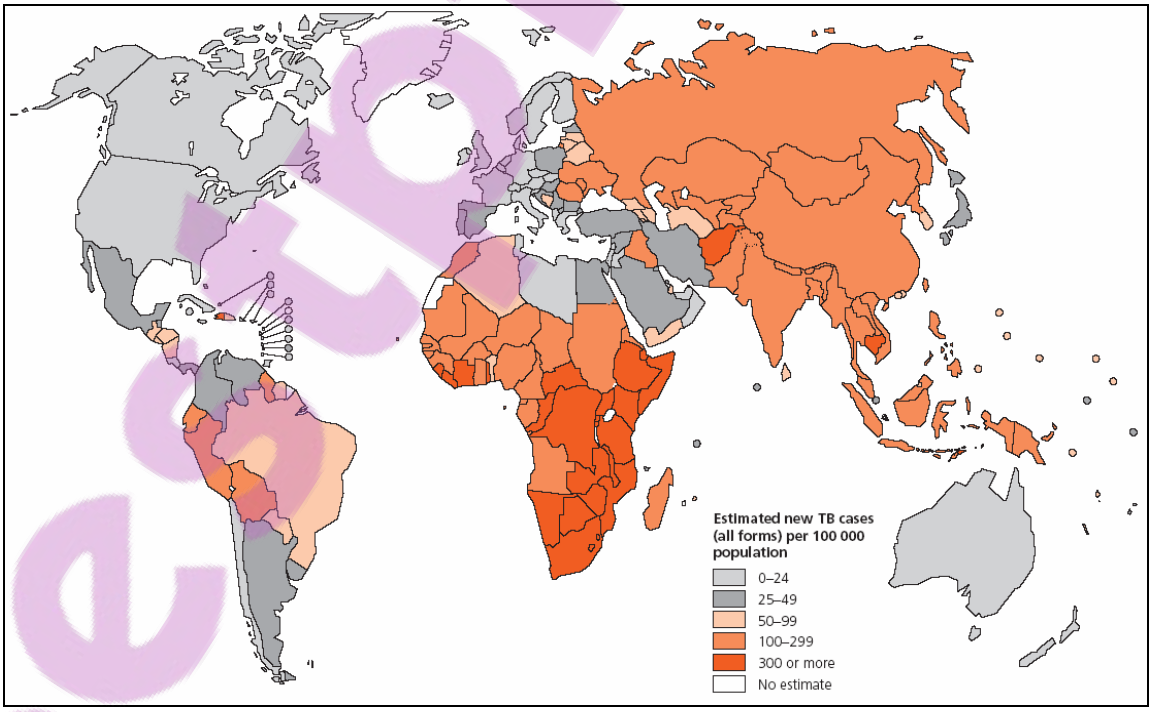

Figure 1.1: *Estimated TB incidence rates, 2004 (154).*

Among the 15 countries with the highest estimated TB incidence rates (Figure 1.1), 11 are in Africa. Incidence rates have been increasing since 1990, especially in African countries. The spread of HIV has driven the TB incidence higher in countries with high rates of HIV infection (154).

TB has been declared a global epidemic in the early 1990s. With the increase of multi-drug resistant (MDR) strains and the newly described extreme drug resistant (XDR) TB strain, the TB epidemic is still growing stronger. The need for quick diagnosis and better treatment of TB is now even bigger than before.

1.1.2 *Mycobacterium tuberculosis*, infection and immunology

In 1868, a French military surgeon, Jean-Antoine Villemin, experimentally demonstrated the transmissibility of tuberculosis in rabbits. It was considered that tuberculosis was likely to be caused by 'germs', and many workers attempted to isolate them. Then in 1882, the famous German Robert Koch, isolated and identified *Mycobacterium tuberculosis* (*M. tuberculosis*) as the causative agent for tuberculosis (69). *M. tuberculosis* is a rod-shaped, Gram positive, aerobic, acid-fast bacillus. The component responsible for acid-fastness is the unique lipid fraction of the cell wall, called mycolic acids. *M. tuberculosis* is an obligate pathogen, totally dependent on a living host for existence (54, 56, 113).

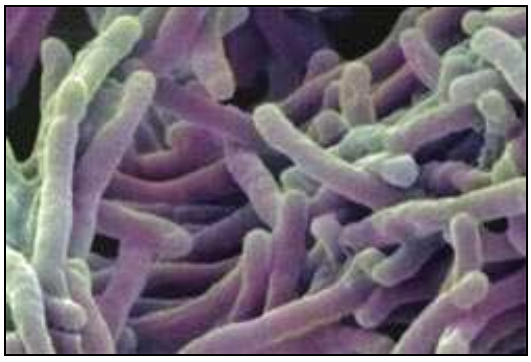

Figure 1.2: *M. tuberculosis.*

Individuals with TB spread *M. tuberculosis* through aerosolized infectious particles generated from coughing and sneezing. These bacilli enter via the respiratory route to infect mainly the lungs. From there, infection can spread through the lymphatic system or blood to other parts of the body (59, 117). After infection one of a few outcomes can occur: first, the bacilli can be destroyed immediately by the host's innate immune responses. Second, a percentage of persons

develop active tuberculosis (141). Third, the majority of people develop a clinical latent infection. These have a positive reaction to the skin test, but show no clinical symptoms and are not contagious (72, 138). About 5-10% of latent infections will reactivate and cause active tuberculosis (131).

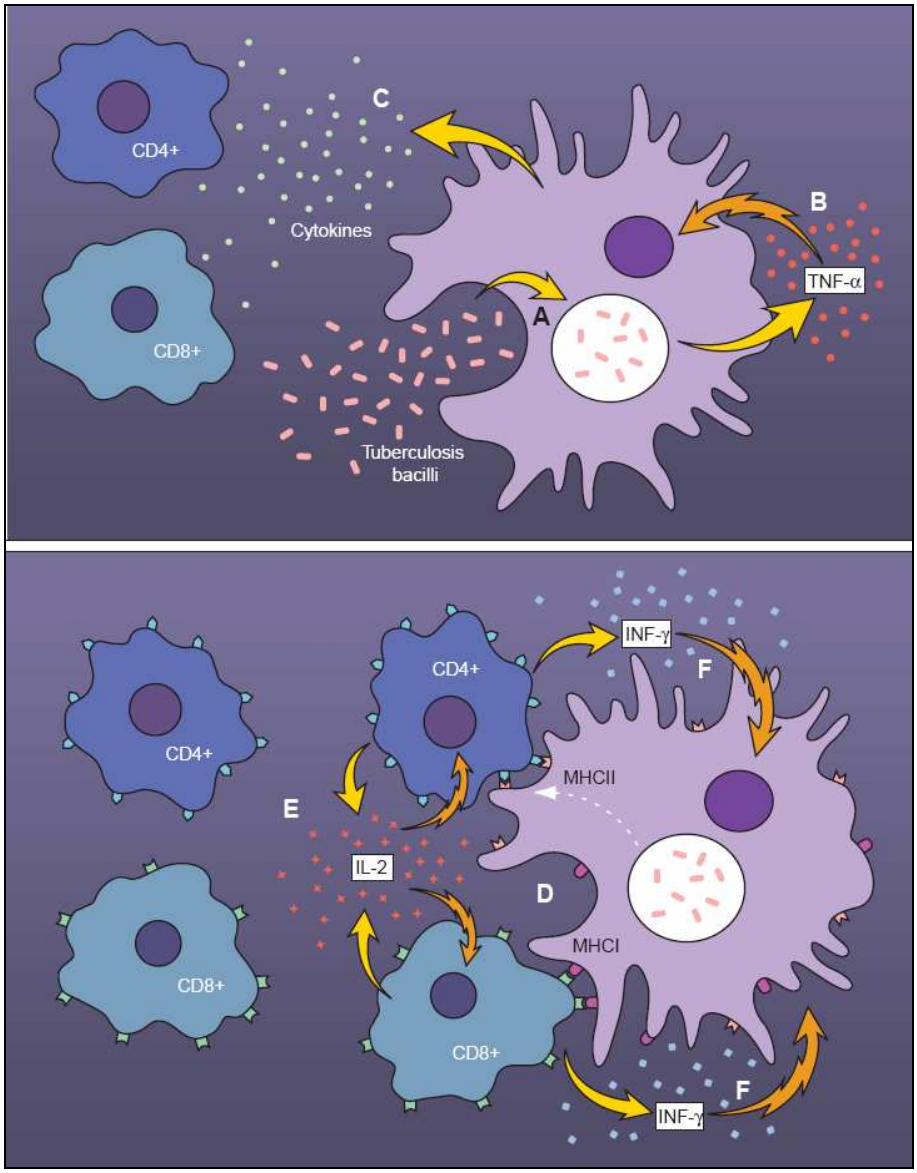

Figure 1.3: *The role of cytokines in TB. The macrophage (A) phagocytoses the invading mycobacteria, this results in the release of TNF-α (B) and other cytokines (C), the effect of which is further activation of cell-mediated immunity. The early release of TNF-α enhances the ability of macrophages to phagocytose and kill mycobacteria. Antigen presentation through MHC leads to the release (D) of interleukin-2 (IL-2) with further recruitment of T cells (E). T-cell release of interferon-γ (F) further activates the macrophage to enhance bacterial killing (94).*

Alveolar macrophages infected with *M. tuberculosis* interact with T lymphocytes via important cytokines. The T-cell response is antigen specific and is influenced by the major histocompatibility complexes (MHC) (60, 128). Infected macrophages release interleukins 12 and 18 which stimulate $CD4^+$ and $CD8^+$ T cells to secrete interferon-gamma (IFN-γ), which stimulates the phagocytosis of *M. tuberculosis* by the macrophage (55, 135). The macrophages also release tumour necrosis factor-alpha (TNF-α), which enables the macrophage to phagocytose and kill the mycobacteria (94) (Figure 1.3).

TNF-α plays a crucial role in the formation of granulomas and to control infection (20, 61, 107, 143). The granulomas isolate the infection and prevent their continued growth and spread to the rest of the lung and other organs and so concentrate the immune response to the site of infection (59).

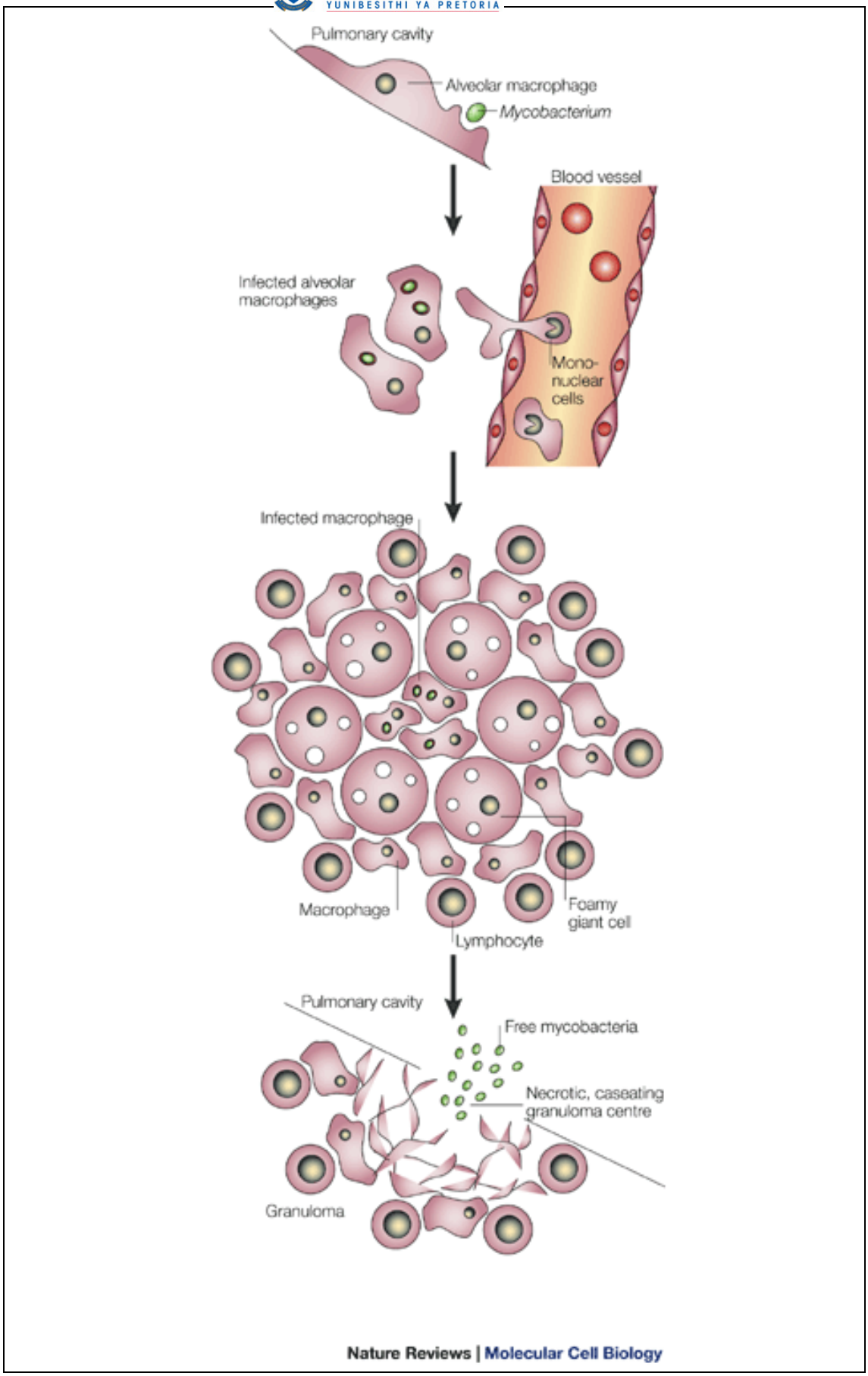

Figure 1.4: *Cellular events and granuloma formation following infection with* M. tuberculosis *(122).*

The success of granulomas depends on the number of macrophages present at the site of infection as well as on the number of organisms (56). The granuloma consists of a centre of infected macrophages surrounded by foamy giant cells, macrophages and lymphocytes (122). Figure 1.4 shows the cellular events and granuloma formation following infection.

The bacilli are unable to multiply within the granulomas due to a low pH and low availability of oxygen. With good host cell-mediated immunity, the infection may be stopped permanently at this point. The granulomas start to heal and leave small calcified lesions (137).

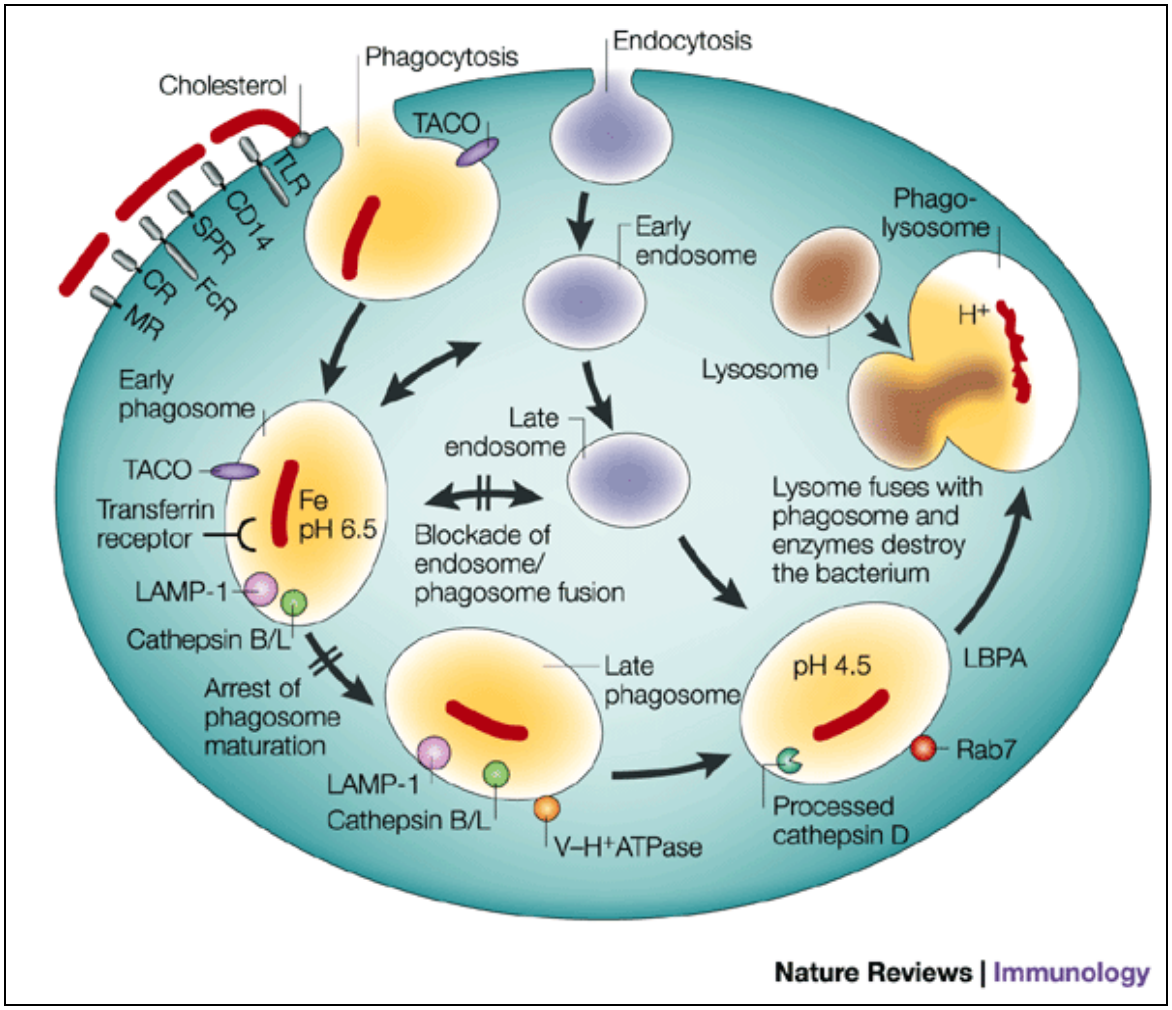

Figure 1.5: *The intracellular lifecycle of* M. tuberculosis. *CR, complement receptor; FcR, receptor for the constant fragment of immunoglobulin; LAMP-1 lysosomal-associated membrane protein 1; LBPA, lysobiphosphatic acid; MR, mannose receptor; Rab7, member of the small GTPase family; SPR, surfactant protein receptor; TACO, tryptophane aspartate-containing coat protein; TLR, Toll-like receptor; V–H$^+$ATPase, vacuolar ATP-dependent proton pump (83).*

Only a few organisms can survive inside the macrophage, due to hydrolytic enzymes and acidic phagocytic vacuoles. *M. tuberculosis* has immune evasive strategies to survive and multiply within the macrophage, probably because of the unusual mycobacterial cell surface (28). An important mechanism to the persistence and pathogenicity of mycobacteria in phagosomes is their ability to avoid fusion with lysosomes (73) that would destroy the bacteria. This process is dependent on living bacteria, as killed bacteria land up in the phago-lysosomes (13, 74).

Tryptophan-aspartate-containing coat protein (TACO) is absent from phagosomes containing killed bacilli, and from any of the endosomal/lysosomal organelles purified from uninfected cells. It was shown that TACO is retained by live mycobacteria at the mycobacterial phagosome membrane and that it prevents maturation and fusion with lysosomes, thus allowing the mycobacteria to survive inside the macrophage (2, 57), as shown in Figure 1.5.

1.1.3 Diagnosis of TB

Common clinical symptoms of TB infection include fever, night sweats, weight loss and shortness of breath, haemoptysis and chest pain. Laboratory tests for diagnosis of TB vary in specificity, sensitivity, speed and cost. Even though other tests are available, bacterial cell culture is still required for accurate diagnosis and drug-susceptibility testing (62). The other tests include the tuberculin skin test - of which the specificity is low and false positive and false negative reactions are frequent, direct microscopy - that is not adequately sensitive and requires a high level of bacteremia of more than 10 000 bacilli/ml sputum, ELISA to detect antibodies to *M. tuberculosis* - which is relatively simple and inexpensive, but most studies yielded poor sensitivity and specificity, chest X-rays - that can miss tuberculosis in HIV positive patients and cannot distinguish between lesions from current or past infections, and polymerase chain reaction (PCR) - that has created new possibilities for rapid and sensitive diagnosis, but still require a few days of culture (142).

1.1.4 Association with HIV/AIDS

TB is the leading cause of death amongst HIV infected people. According to WHO it accounts for about 13% of AIDS deaths worldwide and in Africa, HIV is the single most important factor playing a role in the increased incidence of TB in the past 10 years. TB and HIV together form a lethal combination (152). HIV prevalence in new TB cases in South Africa is 60% (Figure 1.6) (154).

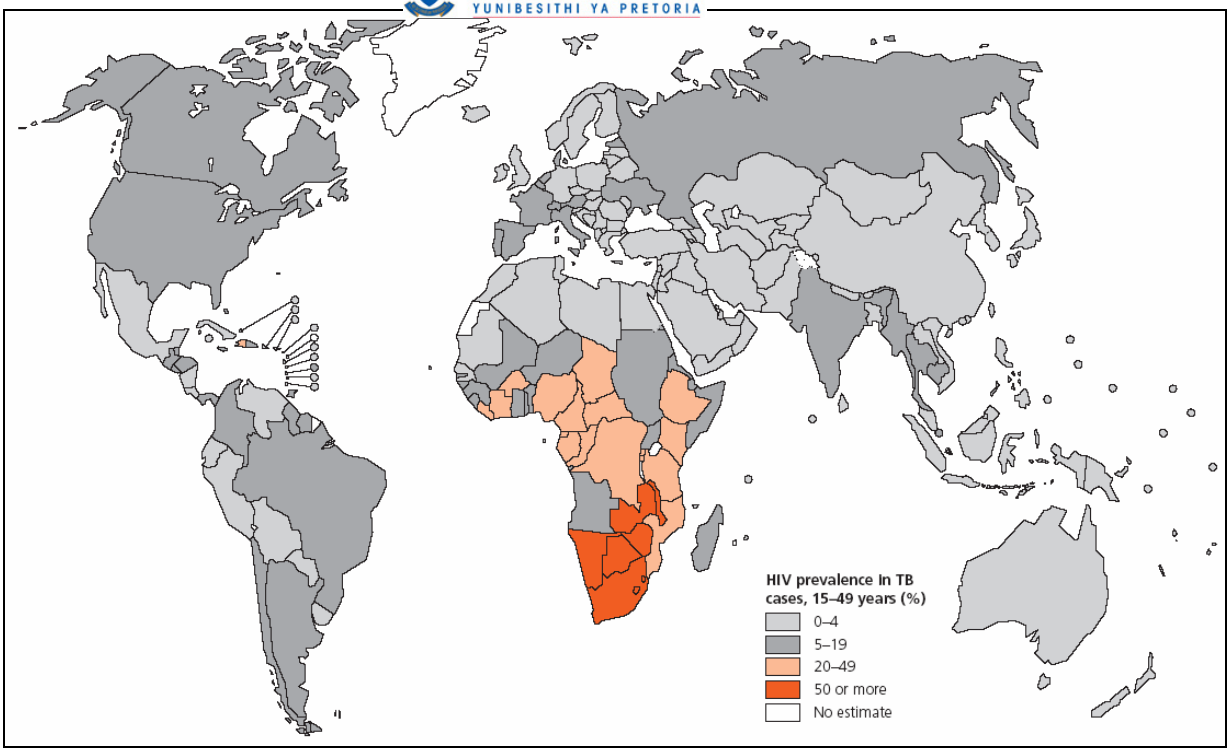

Figure 1.6: *Estimated HIV prevalence in new adult TB cases, 2004 (154).*

Human immunodeficiency virus (HIV) is a major risk factor for developing TB. In patients infected with HIV, the $CD4^+$ T cell count steadily decline as the infection progresses and the ability to restrict the bacilli to only a few infected macrophages decreases (111). Healthy people have about 1 000 $CD4^+$ T cells per microlitre of blood, which decline at a rate of about 100 cells per microlitre per year after HIV infection. A person usually develops TB at a count of approximately 187 $CD4^+$ T cells per microlitre of blood (156). The loss of T cell function reduces cytokine production, which compromises activation of macrophages. The activation of macrophages is required to control *M. tuberculosis* infection.

The risk of developing TB in patients co-infected with HIV and *M. tuberculosis* by reactivating latent tuberculosis infection increases to 5-15% annually, concurrent with the development of immune deficiency (12). In the 1993 classification of AIDS by the Centres for Disease Control, pulmonary TB was considered a true AIDS-defining illness in HIV-infected patients. It should be noted that there is a mutual interaction between *M. tuberculosis* and HIV: the immunosuppression induced by HIV infection, modifies the clinical presentation of TB resulting in atypical symptoms. Moreover, the immune restoration induced by highly active anti-retroviral therapy (HAART) may be associated with paradoxical worsening of TB manifestation related to immune reconstitution. TB, on the other hand, enhances the

progression of HIV infection, while anti-tuberculosis drugs interfere with anti-retroviral drugs (1).

In HIV negative patients infected with *M. tuberculosis*, clinical manifestations are pulmonary cavitation in the upper lobes and detectable bacilli in the sputum. With HIV infection this changes to extrapulmonary disease or infiltrating non-cavitating pulmonary disease in the lower lobes with no visible bacilli in sputum (111), which makes diagnosis of TB in HIV positive patients very difficult if not impossible. This strongly emphasises the need of a serodiagnostic test to accurately diagnose TB in a high HIV burdened population.

1.1.5 Diagnosis of TB in patients co-infected with HIV

Currently diagnosis of TB by growth of the Mycobacterium from sputum samples takes several weeks and is not always reliable (95), especially among HIV-infected communities. Different new methods for diagnosis are under investigation, of which the detection of antibodies in the sera of TB patients would be the most convenient and affordable (142). Protein and lipopolysaccharide antigens of TB are not good ligands for the antibodies, as antibody production to these antigens are paralysed by HIV co-infection, giving rise to false-negative results. This is not so with the mycolic acid antigens that make up the dominant part of the mycobacterial cell wall of *M. tuberculosis*. Tuberculosis patients produce antibodies directed against *M. tuberculosis* mycolic acids (112, 115). These antibodies were detected by an enzyme-linked immunosorbent assay (ELISA). This principle was reported by Schleicher *et al.* (127) to work especially well in HIV-co-infected patients, showing that HIV-infected patients were not disabled in any way to produce these antibodies in comparison to HIV-non-infected control, although the predictiveness of the test was still too low for practical application in diagnosis. The reason for this is that antibodies to the mycolic acids come about in a very different way in the body that is not affected by the human immunodeficiency virus (114, 133).

1.1.6 Other mycobacteria causing diseases

Besides *M. tuberculosis*, there are some other pathogenic mycobacteria as well, for example *Mycobacterium bovis, Mycobacterium africanum* and *Mycobacterium microti*, which are all related and members of the *M. tuberculosis* complex, (all members of *M. tuberculosis* complex cause tuberculosis). *M. bovis* is a causative agent of TB in many animals, the most significant being cattle, and some wildlife, like lions, buffalo and baboons which is an increasing problem

in the Kruger National Park (88, 99, 120). *M. microti* is a pathogen of voles and other small mammals, and *M. africanum* was isolated from man in equatorial Africa (69).

Then there are other mycobacteria including *Mycobacterium avium* complex (the avian tubercle bacillus), *Mycobacterium kansasii*, *Mycobacterium marinum* responsible for granulomatous skin disease of man, *Mycobacterium fortuitum* and *Mycobacterium chelonae* (69). Most of these mycobacteria cause TB-like diseases and opportunistic disease in immune deficient people, particular in AIDS patients (30).

There are also several non-tuberculous mycobacteria (NTM) that cause human diseases but not TB. *Mycobacterium avium paratuberculosis* has been identified as a possible cause of Crohn's disease in humans (129) and Johne's disease in animals. *Mycobacterium leprae* causes leprosy, which has declined to such an extent that it was eliminated from the list of global public health problems in 2000 (155). Buruli ulcer is a disease caused by *Mycobacterium ulcerans*, first described in Australia, which emerged in 1980 as an important cause of human suffering, making it the third most common mycobacterial infection after TB and leprosy (153).

1.1.7 Mycolic acids

1.1.7.1 History and properties of mycolic acid

An 'unsaponifiable' wax was first isolated from the human tubercle bacillus by Anderson and co-workers in 1938. He proposed to call this ether-soluble, unsaponifiable, high-molecular weight hydroxy acid 'mycolic acid'. Mycolic acid (MA) was described as an acid-fast, saturated acid with a low dextrorotation that contained hydroxyl and methoxy-groups. It was difficult to purify and impossible to crystallize. Pyrolytic cleavage yielded hexacosanoic acid and a non-volatile residue which showed no acidic properties. Together it showed an empirical formula of $C_{88}H_{172}O_4$ or $C_{88}H_{176}O_4$ (11, 140). In 1950, Asselineau proved that MAs contained a long alkyl branch in the α-position and a hydroxyl group in the β-position, thereby explaining the pyrolysis as a reversed Claisen reaction (14, 16). As the ability to elucidate the structure of such molecules advanced, the complexity of MA became more apparent. What was once described as a single component that was isolated from *M. tuberculosis* is now recognized as a family of over 500 related chemical structures. This amazing number of MA types that make up the major part of the cell wall of a single bacterium is an indication of the biological importance of these molecules (19).

Mycolic acids are very long, α-alkyl-β-hydroxy fatty acids present as mixtures of different types and homologues. All of the known MAs have the basic structure $R_2CH(OH)CH(R_1)COOH$ wherein R_1 is a C_{22} or C_{24} linear alkane and R_2, also known as the mero chain, is a more complex structure of 30-60 carbon atoms and contains a variety of functional groups (100, 101). Mycobacterial MAs are distinguished from those of the other genera by the following features: (i) they are the largest MAs; (ii) they have the largest side chain; (iii) they contain one or two unsaturated carbon moieties, which may be double bonds or cyclopropane rings; (iv) they contain oxygen functions additional to the α-hydroxy group; and (v) they have methyl branches in the main carbon backbone (101).

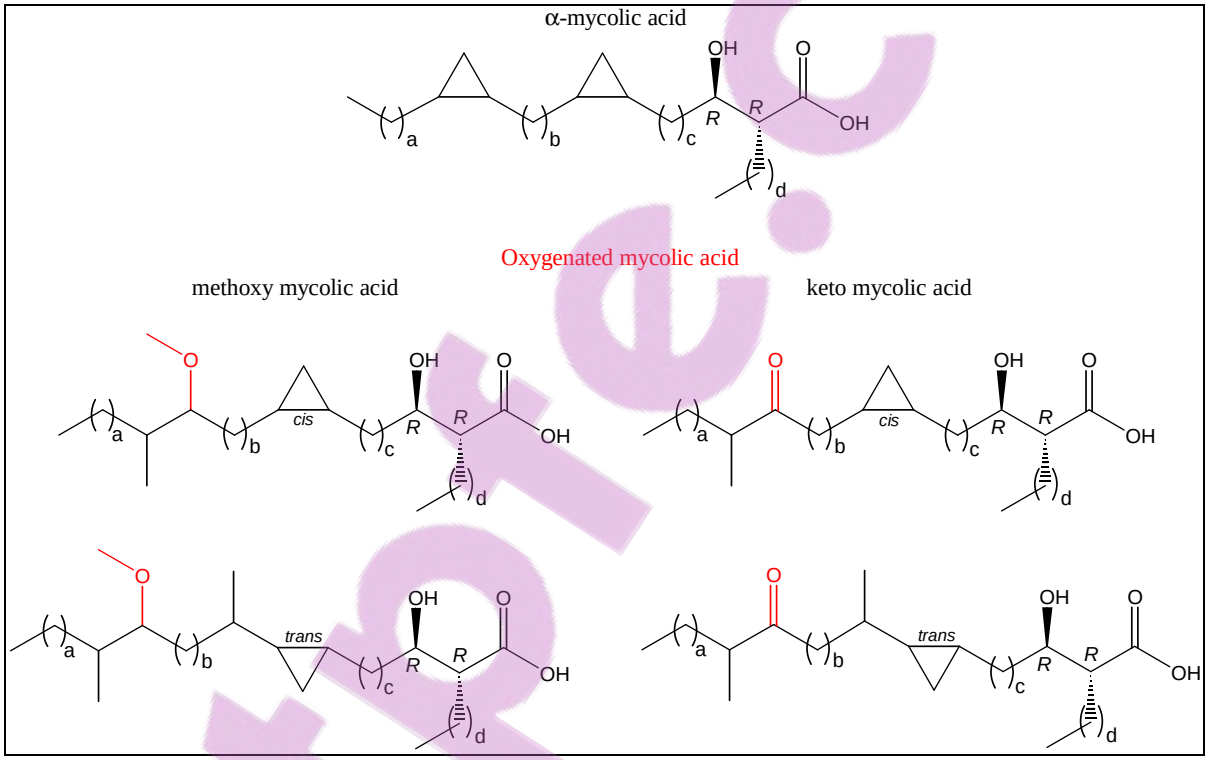

Figure 1.7: *Mycolic acid subclasses from* M. tuberculosis.

Mycolic acids from *M. tuberculosis* can be divided into three subclasses: α-MA, methoxy-MA and keto-MA (Figure 1.7). The prefix 'alpha' has been assigned to the acid lacking oxygen functions in addition to the 3-OH acid unit. The other mycolates are named according to the oxygen functions in the mero chain (15, 100, 101). α-Mycolic acid contains two *cis*-cyclopropanes, one in the proximal position (closer to the hydroxyacid) and one in the distal position (further away from the hydroxyacid) in the mero chain. Methoxy-mycolate has a *cis*- or *trans*-cyclopropane in the proximal position with a α-methyl-β-methoxy in the distal

position, whereas keto-MA also has a *cis*- or *trans*-cyclopropane in the proximal position, but with a α-methyl-β-keto in the distal position. When a cyclopropane ring is in the *trans*-orientation, it also contains an adjacent methyl branch (105, 106).

Mycolic acids show a variety of structural features in the meromycolate chain, including *cis*-cyclopropanes and α-methyl-*trans*-cyclopropanes with various combinations of α-methyl-β-keto, α-methyl-β-methoxy, *cis*-alkene, α-methyl-*trans*-alkene, and α-methyl-*trans*-epoxy fragments (100, 101). These acids are usually present as mixtures of various chain lengths. Although the hydroxyacid grouping is of the *R*,*R*-configuration, little is known about the absolute stereochemistry of the other groups. There is some evidence that the α-methyl-β-methoxy unit at the distal position from the hydroxyacid in MAs is of *S*,*S*-configuration (Figure 1.8) (44, 51).

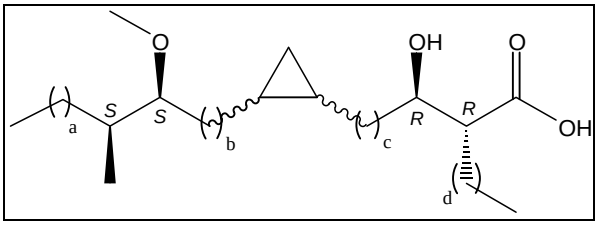

Figure 1.8: *The stereochemistry of the hydroxyacid group and the α-methyl-β-methoxy-group.*

Two-dimensional TLC (48, 104), GC (81) and HPLC (32, 116, 139) together with MS, IR and NMR techniques, made the identification of the different MAs present in each Mycobacterium possible. HPLC patterns are characteristic for each Mycobacterium and have been used as a rapid diagnostic tool (32).

Watanabe *et al.* (149, 150) isolated MA methyl esters from 24 strains of the *M. tuberculosis* complex and related mycobacteria. These were separated into the different subclasses and each subclass was further separated by argentation chromatography into mycolates with no double bonds, those with one *trans*-double bond and those with one *cis*-double bond. Mass spectrometry (MS) gave information about the chain lengths, while nuclear magnetic resonance (NMR) revealed the content of double bonds and cyclopropane rings. They further prepared mero MAs by pyrolysis of the methyl esters and submitted them to high-energy collision-induced dissociation/fast atom bombardment MS (CID/FAB MS) to reveal the exact location of the different functional groups within the merochain. These included double bonds,

cyclopropane rings, keto- and methoxy-groups. This revealed considerable variation in the mycolate composition. In the strains of the *M. tuberculosis* complex there are keto-, methoxy-, and α-MA that have a double bond in the proximal position in either the *cis*- or *trans*-configuration, instead of a cyclopropane ring. Watanabe *et al.* (149, 150) presented a possible classification of all these lipids. Type 1 defines the MAs with a cyclopropane (*cis*- or *trans*-), type 2 those with a *trans*-double bond and type 3 with a *cis*-double bond (149, 150) as shown in Figure 1.9. It was also shown that in several mero aldehyde homologues the values for a, b and c differed, with a and b more conserved than c.

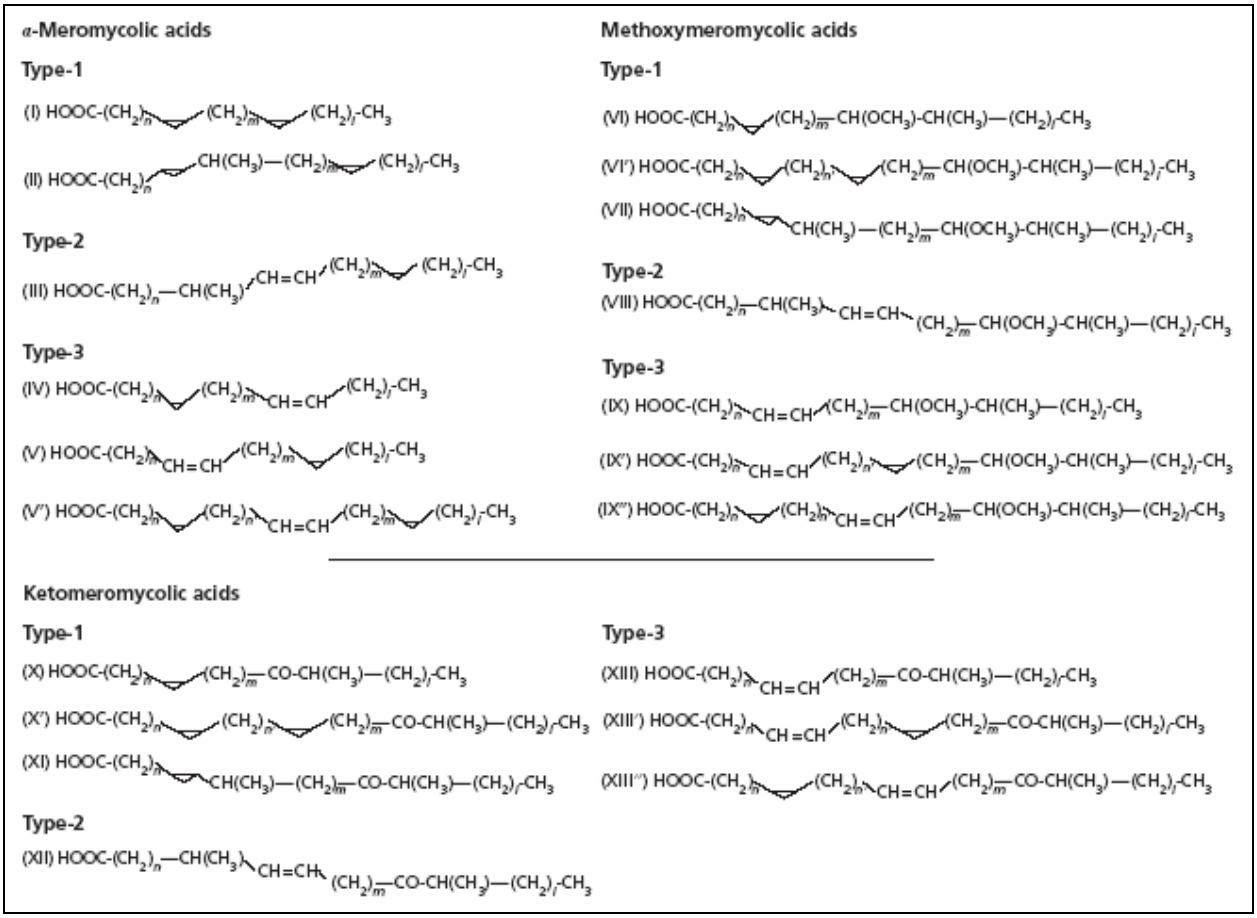

Figure 1.9: *Chemical structures for a-mero acids, methoxy-mero acids and keto-mero acids derived from MAs (149), n = c, m = b and l = a.*

Other mycobacteria contain different sets of MAs (Table 1.1 and Figure 1.10). For example, these can range from α'- and α- MA with either one or two double bonds, either in the *cis*- or the *trans*-configuration, and epoxy-MA in *M. smegmatis* and *M. fortuitum* (45, 71, 91, 103) to wax esters, ω-carboxy-MA and ω-1-methoxy-MA (92, 96) isolated from other mycobacteria.

A recent review confirmed that the most widespread of the different MAs is the α-mycolates, with either two cyclopropane rings or two double bonds (48, 148, 150). Keto-MAs are the second most widely distributed and are found in pathogenic and saprophytic mycobacteria. Wax esters and the α'-MA are next on the list.

Methoxy-MA are not frequently found in non-pathogenic mycobacteria (only about 12%), but are present in less than half of the mycobacteria that cause diseases in HIV co-infected individuals (Table 1.1)

Table 1.1: *Distribution of MA subclasses in several mycobacterial species (19)*

Species	α	α'	methoxy	Keto	epoxy	wax ester	ω-1 methoxy
M. abscessus	+	+					
M. africanum	+		+	+			
M. avium complex	+			+		+	
M. bovis	+		+	+			
M. chelonae	+	+					
M. fortuitum	+	+			+		+
M. gordonae	+		+	+			
M. intracellulare	+			+		+	
M. kansasii	+		+	+			
M. marinum	+		+	+			
M. scrofulaceum	+			+		+	
M. simiae	+	+		+			
M. tuberculosis	+		+	+			

Besides these major types of MAs, there are also other types present in mycobacteria; some in minor quantities. In 19 strains of the *M. tuberculosis* complex there are keto-, methoxy-, and α-MA which have a double bond in the proximal position either in the *cis*- or *trans*-configuration, instead of a cyclopropane ring (149, 150).

Although MAs are characteristic of all the mycobacteria, they are also present in genera other than *Mycobacterium*: in *Corynobacterium*, *Dietzia*, *Nocardia*, *Rhodococcus* and *Tsukamurella*, but all these bacteria have different kinds of MAs present in the cell envelope.

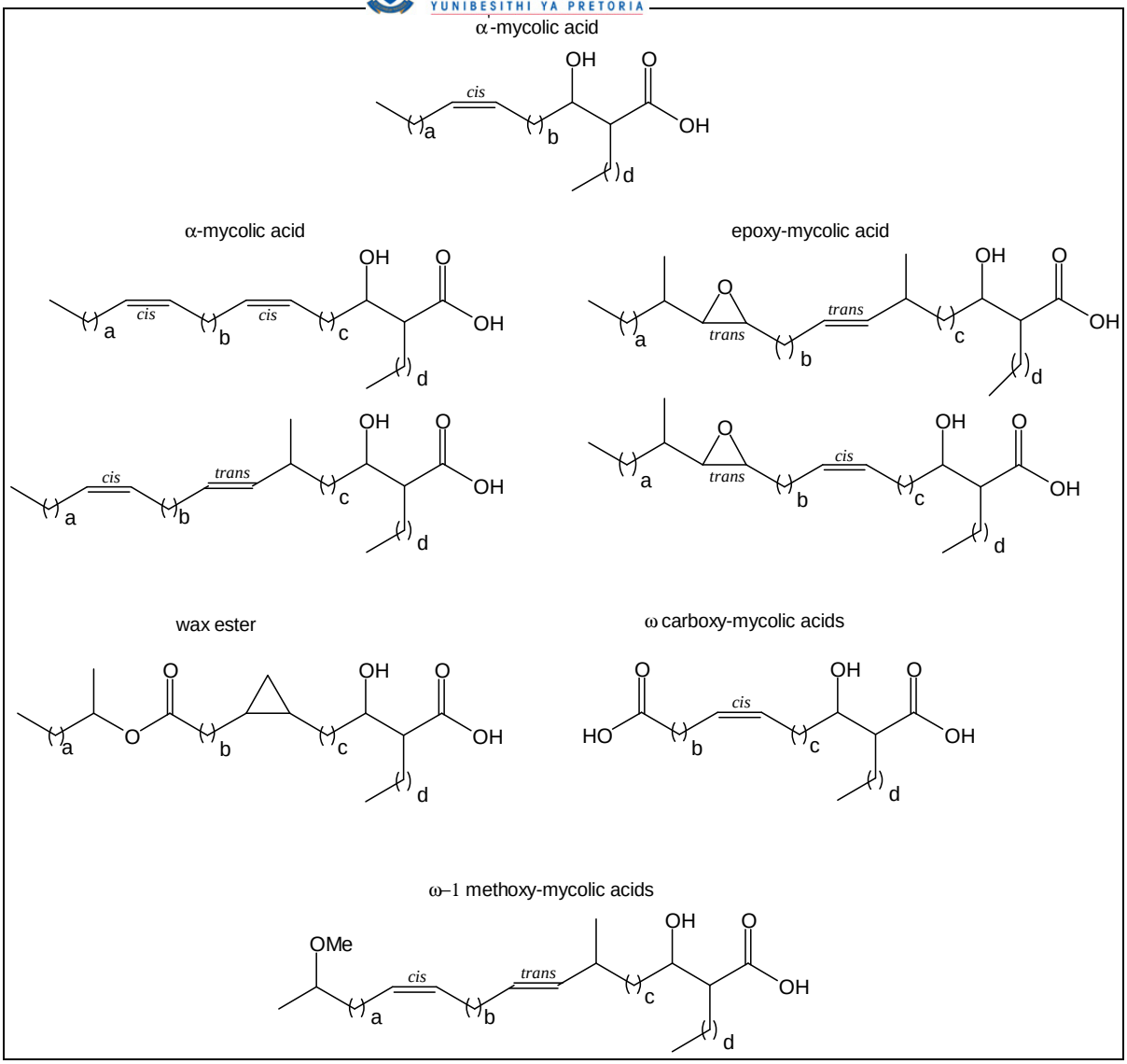

Figure 1.10: *Other MA subclasses found in* Mycobacterium spp.*, beside those in Figure 1.7.*

1.1.7.2 Mycolic acid and the cell wall

Mycolic acids are the major constituent of the cell envelope of *M. tuberculosis* and similar species, making up about 60% of the dry weight of the cell wall of the organism (30). Mycolic acids are present as organic solvent extractable lipids, mainly in the form of trehalose 6,6'-dimycolate also known as cord factor, but for the most part as bound esters of arabinogalactan, a peptidoglycan-linked polysaccharide (30, 100, 101).

The mycobacterial cell wall has a more complex structure compared to other Gram positive bacteria. The cell envelope consists of three structural components: the plasma membrane, the cell wall and the capsular layer (30, 42, 49), as shown in Figure 1.11. The mycobacterial cell wall is made up of three covalently linked macromolecules, namely peptidoglycan,

arabinogalactan and MA (29, 30, 98). Peptidoglycan is covalently attached to the mycolylarabinogalactan (mAG) through a phosphodiester bond. mAG, also called the cell wall core, constitutes the underlying framework of the cell wall and consists of MA covalently linked to arabinogalactan. The MAs are orientated perpendicular with respect to the plasma membrane. The C-2 branching position in the MA allows the meromycolate chain to pack closely in parallel with the saturated alkyl side chain. This packing is made possible by the flexibility of the arabinogalactan molecule and its linkage unit and is possibly stabilized by intramolecular hydrogen bonds between the MAs (100). Embedded into this framework is a uniquely large number of different lipids, several different multi-methyl branched fatty acids (25, 43, 100, 102), cell wall proteins, the phosphatidylinositol mannosides (PIMs), the phthiocerol-containing lipids, lipomannan (LM), lipoarabinomannans (LAM) (34, 35) and trehalose 6,6'-dimycolate (33).

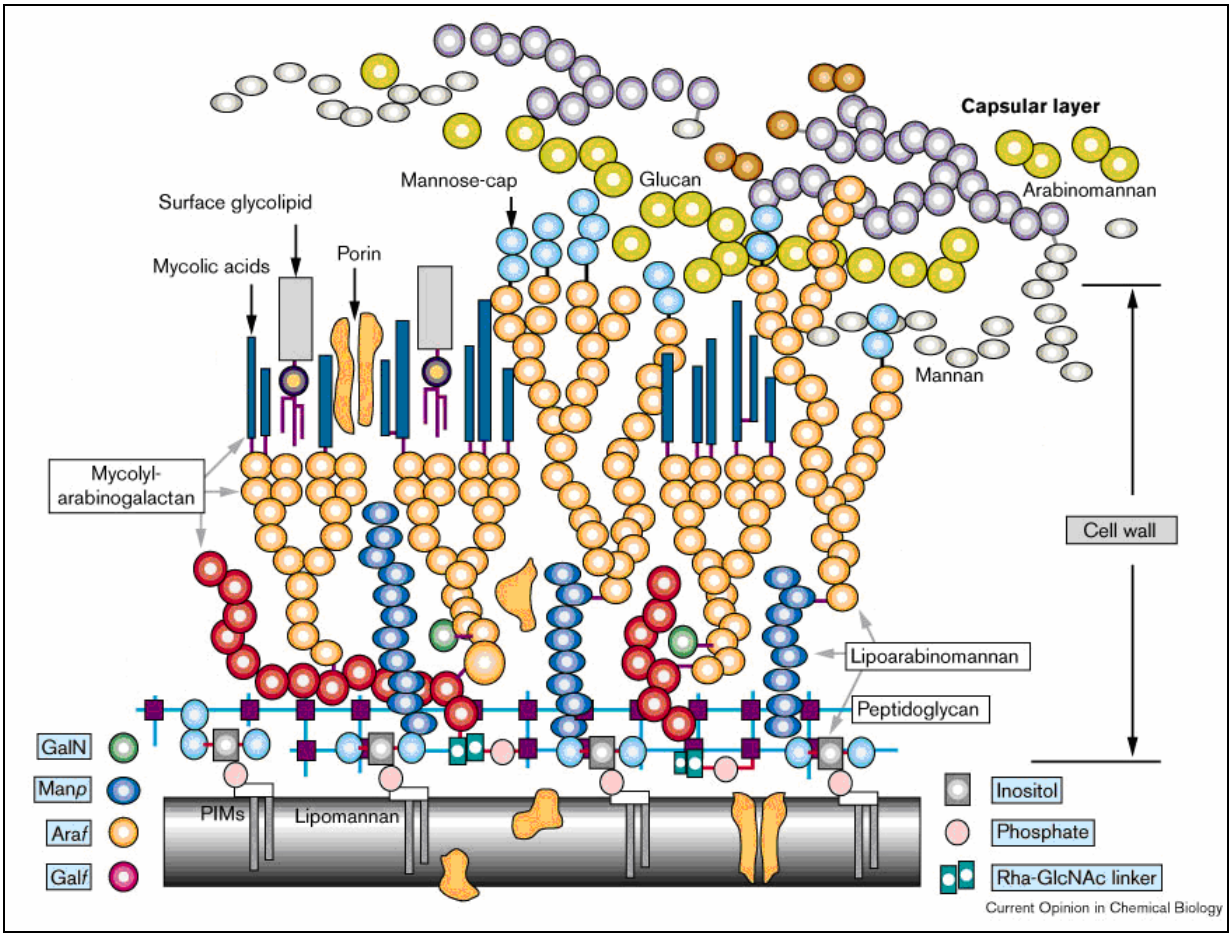

Figure 1.11: *A model of the mycobacterial cell wall (33).*

The cell wall, in particular MAs, is critical for growth and survival of *M. tuberculosis* in the infected host and they form an effective barrier against the penetration of antibiotics and chemotherapeutic agents (30). Some of the effective drugs are known to inhibit biosynthesis of the cell wall components. Mycobacterial pathogens are resistant to most common antibiotics and chemotherapeutics, and this might be due to the unusual structure and low permeability of the cell wall. Relatively hydrophobic antibiotics may be able to cross the cell wall by diffusing through the hydrophobic bilayer of MA and glycolipids, but hydrophilic antibiotics and nutrients cannot diffuse across this layer and make use of porin channels to cross (40, 136). There are various other lipids present in the mycobacterial cell envelope and these lipids may also take part in the permeability function of the cell envelope (100, 102). However, this study will focus on MA containing glycolipids.

1.1.7.3 Immunological properties of cord factor and mycolic acids

Trehalose 6,6'-dimycolate (cord factor) was discovered in 1950 by Bloch (27) and is an interesting glycolipid isolated from tubercle bacilli, a trehalose esterified at both primary alcohol groups with MAs (110), as shown in Figure 1.12.

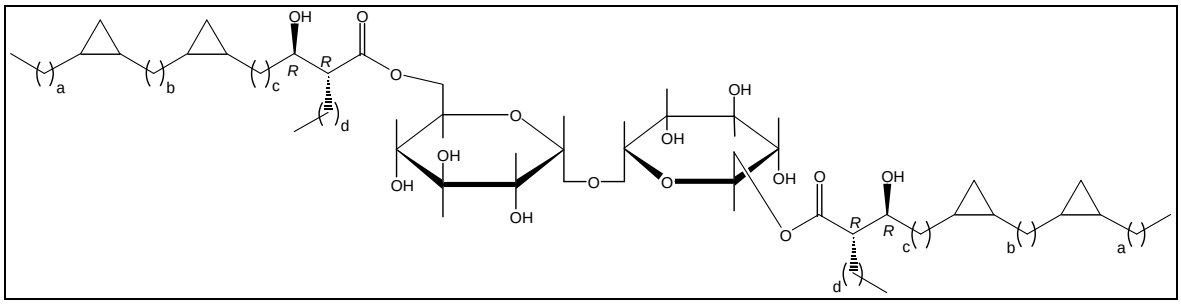

Figure 1.12: *Cord factor - trehahose esterified at both primary alcohol groups with MAs.*

Cord factor is considered a "free lipid" since it can be extracted from the cell wall, while the other MAs that are covalently linked to arabinogalactan cannot without hydrolysis. Cord factor has been shown to possess an array of immunological properties such as granuloma formation (18, 22), angiogenesis (125, 126) and anti-tumoral activity (23). It also protects against infection with other pathogenic micro-organisms and it is a potent adjuvant enhancing the immune system's response to diverse antigens (119, 123). Cord factor is important for the survival of *M. tuberculosis* in the macrophage as it appears to prevent fusion of phospholipid vesicles. Cord factor is stimulates innate, rather than adaptive immunity.

In 1971 Bekierkunst (23) indicated antibody production against cord factor, and in 1972, Kato speculated that it was the sugar part of cord factor that was recognised and not the lipid part (82). Recently a number of publications contradicted this as it was shown that the MA part may indeed be recognised (63, 64). It was reported that the detection of anti-cord factor IgG antibody by ELISA in active and inactive TB patients is a useful serodiagnostic tool and is applicable in various tuberculous diseases (78, 87, 97). In preliminary studies, Pan *et al.* (112) found that serum from tuberculosis patients were highly reactive against cord factor isolated from *M. tuberculosis*, whereas they were less reactive against cord factor from *Mycobacterium avium*. They also reported that *M. avium* patients' sera were highly reactive against *M. avium* cord factor, but less reactive against *M. tuberculosis* cord factor, thus suggesting that specific MA subclasses may be the antigenic epitope for the anti-cord factor antibody. They further demonstrated the antigenicity of MA by coating ELISA plate wells with the pure, separated MA methyl esters from hexane solutions and showed that among the three subclasses of MA present in *M. tuberculosis*, sera from TB patients reacted most prominently against the methoxy-MA and less against the α-MA and keto-MA. There was no reaction against either straight-chain fatty acid such as palmitic acid or shorter-chain MAs such as the C44-C46 nocardo-MAs.

Mycolic acids are extremely hydrophobic and dissimilar to other, more common antigens. The first evidence for immunoregulatory properties of MAs was obtained by the observation that presentation of MA to T-cells occurred by professional antigen-presenting cells (APC) in a major histocompatibility complex (MHC)-independent manner through CD1b molecules (21). It was also shown that MA were able to stimulate CD4, CD8-double negative (DN) T-cell proliferation (21, 67).

Other studies showed that immunoassays prepared with MA derivatives from *M. fortuitum* were highly effective for the serodiagnosis of TB. This organism also contains oxygenated MAs, but they are of a different subclass from the one present in *M. tuberculosis*. Therefore, some MA types are more helpful than others in the preparation of immunodiagnostic devices for TB detection (95).

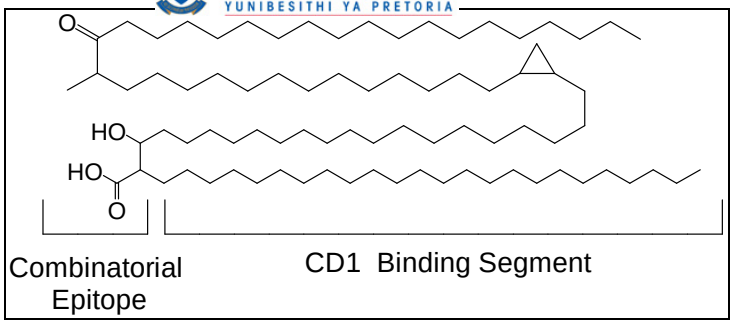

Figure 1.13: *A proposed folded conformation for keto-MA (70), (note that figure from refence is incorrect: the keto group and methyl branch are the wrong way around, the number of carbons between the hydroxyl group and the cyclopropane must be an odd number and those between the cyclopropane and the methyl-branched keto group must be an even number).*

More recently, Grant *et al.* (70) suggested that the keto-MA fold in a way that allows the three polar functions of the lipid chain to be in close proximity to form a combinatorial epitope presented on the CD1 surface protein (Figure 1.13), giving a possible reason for the stronger recognition of the oxygenated MAs. Hasegawa *et al.* (75, 76) also proposed that MAs could exist in folded conformations, although this was in the context of arrangement in monolayer films. These conformations are thought to be very stable in keto-MAs due to strong molecular interactive forces.

Recently, free MAs have been demonstrated to be able to adopt a “W” conformation with all four alkyl chains folded parallel to each other (130, 145, 146). The existence of this conformation has been suggested by Langmuir analyses of monolayers consisting of free MAs over a wide range of temperatures (145, 146).

1.1.7.4 Cholesterol in Tuberculosis

It appears that both the entry and the survival of the pathogen in the macrophage host cell depend on its attraction to cholesterol. Gatfield and Pieters (66) demonstrated that cholesterol concentrated at the specific site where mycobacteria enter the macrophage and that cholesterol depletion of the macrophage membrane prevented entry of the mycobacteria into the macrophage. This implies a mechanism of infection whereby the Mycobacterium, after docking to the macrophage, accrues cholesterol from the host membrane to the parasite cell wall and then penetrates the macrophage. The cholesterol enriched endosomic membrane then attracts and holds Tryptophan-Aspartate Coat (TACO) protein to prevent fusion of the infected organelle with the destructive lysosome (2, 58) (Figure 1.5). *M. tuberculosis* may facilitate its uptake into the host macrophage via the cholesterol binding Scavenger Type A receptor (159).

This molecular association between membrane cholesterol and mycobacterial MAs may also explain why the membrane of the phagosome appears to be tightly associated with the engulfed pathogen (46, 47). Av-gay and Sobouti (17) observed that pathogenic mycobacteria uniquely accumulates, but does not consume cholesterol from the growth medium, in contrast to the non-pathogenic mycobacteria that could rely on cholesterol as a major carbon source. Kaul *et al.* (85) discovered an infection-facilitating role for a "Human Receptor C_k-like" protein expressed in *M. tuberculosis*, of which the human equivalent is known for its function as a cholesterol sensor to regulate various genes for cholesterol homeostasis (84, 86). In addition, Korf *et al.* (89) showed that intraperitoneal MA administration into mice affectes mainly the macrophages and convert them into cholesterol-rich foam cells.

Mycolic acid can be considered as a likely candidate to attract cholesterol. It is the most abundant lipid of the outer layer of the mycobacterial cell wall. The “W” conformation of MAs could be imagined to resemble the shape of cholesterol; otherwise the structure of these two lipids upon first inspection appears to be very different. The waxy nature makes it highly hydrophobic, thereby making it possible to accumulate the hydrophobic cholesterol (30, 148). There is, however, much more involved than just hydrophobic interaction. In 2000, Dubnau *et al.* (50) demonstrated that recombinant *M. tuberculosis*, without the ability to oxygenate the MA side chains, could survive normally outside the macrophage in *in vitro* cell culture, but was unable to enter the macrophage. It could well be that an oxygenated group in the meromycolate chain is required for selective affinity towards binding cholesterol. This becomes an even likelier hypothesis by the discovery that the protein product of *M. tuberculosis’* inhA gene, an enzyme involved in the catalysis of the mero chain of the MA molecule, belongs to the family of the steroid dehydrogenases (121) and may therefore accommodate the meromycolate intermediates in its active site in a steroidal conformation.

1.2 Hypothesis

The recognition of MAs by TB patient serum antibodies, and the binding of MAs to cholesterol reside in only one of the subclasses of MAs that can be chemically synthesized and stereochemically characterized.

1.3 Aims

The aims of this study are to:

- Successfully separate natural mycolic acids into the different subclasses
- Determine antigenicity of the different subclasses
- Synthesize a stereochemically controlled methoxy-MA
- Determine the antigenicity of different types and diastereomers of synthetic mycolic acids
- Explore the binding of cholesterol to synthetic mycolic acids
- Determine structure-function relationships of mycolic acids

Chapter 2

Purification and characterization of mycolic acids and their methyl esters

2.1 Introduction

In order to investigate the properties and specific biological activities of the different subtypes of MAs in *M. tuberculosis*, they had to be separated. Different methods of separation have been described. Minnikin *et al.*, (48, 104) have used two-dimensional TLC to separate MAs into the different subclasses in order to determine specific patterns of MAs from different mycobacterial species for classification and identification.

Dubnau *et al.* (50) reported that the oxygenated MAs are necessary for virulence by infecting mice with a *M. tuberculosis* H37Rv strain and a mutant strain which is unable to synthesize oxygenated MAs. Yuan *et al.* (158) showed that not only the methoxy, but also the keto-function played an important role in cell wall function, as the *in vitro* growth of a *M. tuberculosis* strain lacking keto-mycolates was impaired at reduced temperatures and that glucose uptake was significantly reduced. The effect of INH did not change, but the sensitivity to ampicillin and rifampin increased. It could well be that each of the different subclasses of MA plays an important role in the sustenance and virulence of the organism.

2.2 Aim

It has been indicated that the immunological properties of the various subclasses of MA differ from one another (Chapter 1). In order to investigate this in more detail, pure fractions of each had to be prepared. This chapter describe the successful separation and then confirmation by structural analysis of the different subclasses of MAs harvested from *M. tuberculosis* H37Rv. The antigenicity of the different subtypes of natural MAs were then determined by using ELISA.

2.3 Esterification and separation of mycolic acids

2.3.1 Results and Discussion

2.3.1.1 Preliminary experiments

In order to exclude any factors that could influence the outcome of this experiment, the natural MAs that were isolated from *M. tuberculosis* H37Rv were analysed for purity. Analysis on HPLC gave a profile that corresponded with data reported in the literature. NMR spectra also corresponded with the data reported in literature, except that the sample contained some other minor components (150). To estimate the amount of these components in the natural MA sample, a small amount of the natural MA was loaded on a TLC plate which was developed, only once, using petroleum ether/ethyl acetate (4/1, v/v). The spots were visualized by dipping the plate into a molybdophosphoric acid (10%) solution in ethanol, followed by heating.

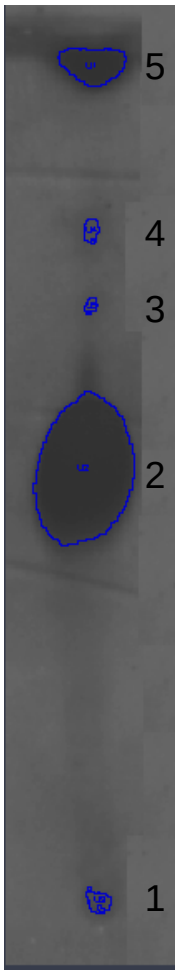

Figure 2.1: *TLC of natural MAs and impurities from M. tuberculosis H37RV prepared in the laboratory.*

Then the dry TLC plate (Figure 2.1) was scanned and the results listed in Table 2.1. This confirmed that the sample contained less than 10% of other components.

Table 2.1: *Analysis of the impurities in the sample of natural MAs from M. tuberculosis H37Rv prepared in the laboratory. Quantification of individual spots was carried out on a Versadoc (Model 3000) imaging system which measured the area and optical density of each spot. From this the density (optical density/area) and volume (Optical density*area) for each spot could be calculated. The values for the volume for each spot were given as % of the total.*

Name	Area mm^2	Density ODu/mm^2	Volume $ODu*mm^2$	% Vol.
1	33.30	4.61	52.67	1.04
2 (Mycolic acids)	976.76	5.28	1769.82	91.36
3	12.70	4.47	19.49	0.18
4	25.75	4.50	39.76	0.42
5	161.02	5.30	292.85	6.99

The ^{1}H NMR spectrum of the natural MAs showed a singlet at δ 3.34 for the methoxy-group (methoxy-MA), the proton next to the methoxy-group appeared as a multiplet at δ 2.96, the α-proton appeared as a double of triplets at δ 2.44 (*J* 5.4, 8.9 Hz). The *cis*-cyclopropane ring protons appeared as a multiplet at δ 0.65, a triplet of doublets at δ 0.57 (*J* 4.1, 8.2 Hz) and a broad double doublet at δ -0.33 (*J* 5.0, 8.9 Hz), the spectrum also showed two multiplets at δ 0.4 and δ 0.1 for the *trans*-cyclopropane ring protons. The ^{13}C NMR spectrum included a carbonyl signal at δ 176.21, a signal at δ 85.48 for the carbon next to the methoxy-group and at δ 57.72 for the carbon of the methoxy-group. The β-carbon appeared at δ 72.33, the α-carbon at δ 50.98 and the carbon next to the methyl group in the meromycolate chain appeared at δ 35.41. The spectrum showed signals for the carbons of the cyclopropane ring at δ 15.78 and δ 10.91.

Using a similar method to that described by Watanabe *et al.* (150, 151), it was possible to estimate the mycolate composition of the samples from NMR analyses (Table 2.2).

Table 2.2: *Estimation of the ratios among the different subclasses from analyses of ^{1}H NMR spectrum of MAs.*

Signal		**Area**	**%**	**Ratios**
cyclopropane *cis*		1.36	93.04	1
cyclopropane *trans*		0.10	6.51	0.08
3 different equations can be described:				
total cyclopropanes	= 2 (alpha) + 1 (methoxy) + 1 (keto)	1.47		
H in β-position	= 1 (alpha) + 1 (methoxy) + 1 (keto)	1		
H next to methoxy	= 1 (methoxy)	0.51		
From these 3 equations it was possible to estimate				
Subclass		**Area**	**%**	**Ratios**
Alpha		0.465	46.54	1
Methoxy		0.509	50.93	1.09
Keto		0.025	2.53	0.05

Explanation for the equations: Total cyclopropane = 2(alpha) + 1(methoxy) + 1 (keto): α-MA has 2 cyclopropanes, both cis, methoxy-MA and keto-MA have only 1 cyclopropane each, mostly cis, but trans as well. H in β position = 1(alpha) + 1(methoxy) + 1(keto): all 3 different subclasses have 1 proton on the β carbon. H next to methoxy = 1(methoxy): only methoxy-MA has a methoxy group in the meromycolate chain.

The sample contained a negligible amount of double bond MAs, while *cis*- and *trans*-cyclopropanes were in a ratio equal to 1:0.08, and the ratios among α, methoxy and keto were equal to 1:1.09:0.05.

2.3.1.2 Esterification of natural mycolic acids

According to Laval *et al.* (48, 93, 100, 101), MA may be separated into its different subgroups with TLC after it has been esterified with trimethylsilyl diazomethane (TMDM). The unmethylated MAs have a polar carboxylic acid group which strongly associates with the silica on the TLC plate causing the sample to smear, thus making separation incomplete. By methyl-esterification of the carboxylic acid, the MA subclasses separate simply due to the differences in functional groups in the meromycolate chain. The different subclasses were separated using a mobile phase containing 9:1 (v/v) petroleum ether:diethyl ether (147).

Twenty microlitres of the MA samples (10 mg/ml chloroform, *M. tuberculosis* MA batch A0698, MB - synthetic α-MA, kindly provided by Prof M.S. Baird (University of Wales, Bangor, UK); MA from Sigma; *M. tuberculosis* MA batch A1198) were incubated with 5µl of *n*-hexane-dissolved TMDM (2 M) at room temperature for one hour. The total volume of the TMDM incubated samples was loaded onto a silica plate that had been dried for two hours at

110 °C. After loading, the plate was dried briefly at 80 °C and then developed five times consecutively in a mobile phase containing 9:1 (v/v) petroleum ether:diethyl ether. Between developments, the plate was dried at 80 °C for ten minutes. Visualisation was done by sulfuric acid charring. Results are shown in Figure 2.2.

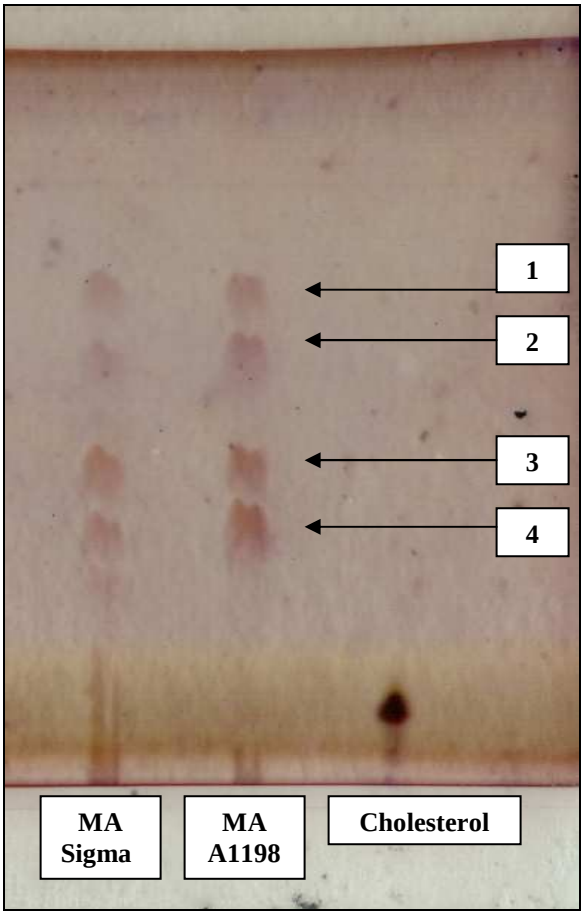

Figure 2.2: *TLC of esterified MA from various sources (see text), compared to cholesterol. The four distinct spots in the MA lanes might be: 1 α-MA, 2 methoxy-MA, 3 keto-MA and 4 unesterified MA. (MA A1198 refers to a batch purified from M. tuberculosis by Sandra van Wyngaardt).*

Four distinct spots were observed after development with mobile phase. The R_f values of the spots were (from bottom to top) 0.37, 0.48, 0.62 and 0.73. Three of these spots were expected to be the subclasses α-, keto- and methoxy-MA. The first spot was thought to be alpha-MA, as it is less polar than the oxygenated MAs, the second spot should then be methoxy and the third the keto-MA. Although the identity of the fourth (lowest) spot was unclear, it was thought to represent unesterified MA (Figure 2.2).

For the preparative TLC of the esterified MA, a total of 10 mg (ten times 10 µl of a 100 mg/ml chloroform solution) *M. tuberculosis* MA that had been esterified, was striped on a preparative TLC plate. The plate was developed as described, the sides removed and visualised by sulfuric acid charring before being compared with the remainder of the plate to identify the spots to be eluted (139, 150, 151). The different spots/fractions were eluted from the silica gel with chloroform, dried under nitrogen and submitted for NMR analysis. NMR analysis showed totally different results from what was expected.

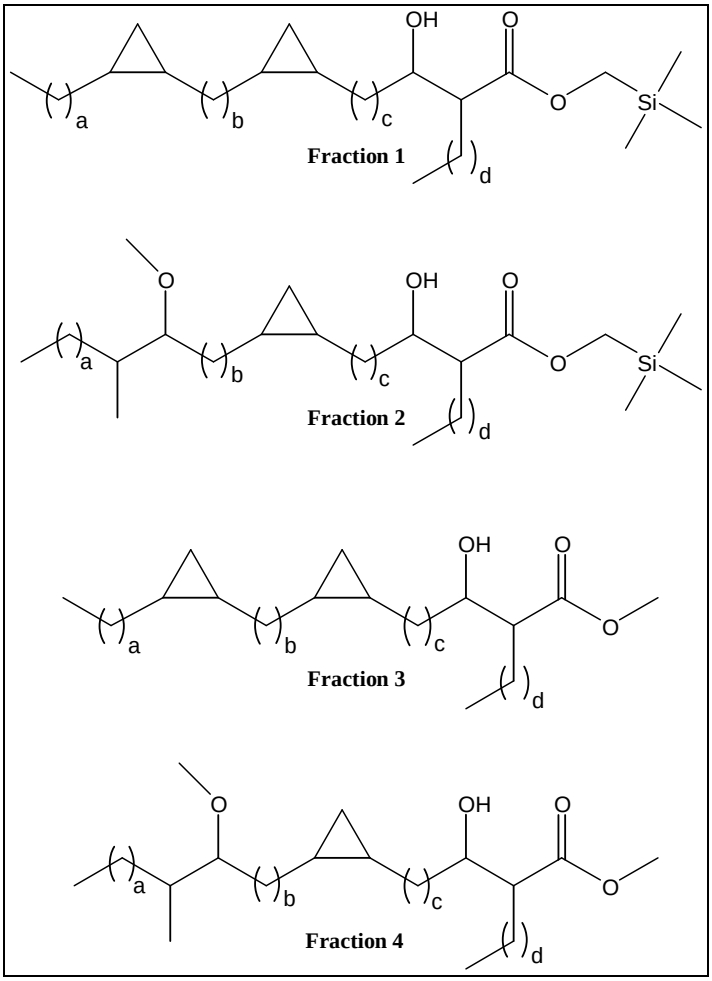

Figure 2.3: *Structures of the different fractions of TLC separated natural MA determined by NMR analysis.*

Fraction 1 was indeed alpha-MA, but with a silyl group attached to the acid instead of a methyl, fraction 2 was methoxy-MA, also with a silyl group. Surprisingly, the third and fourth fractions were not keto- and unesterified MA, NMR showed it to be esterified α- and esterified methoxy MA. There was no detectable keto-MA present in any of the fractions (Figure 2.3).

Next, the esterification method of the MAs was reviewed. Trimethylsilyl diazomethane (TMDM) is a convenient methylating agent since it can be purchased commercially and is much safer to use than diazomethane. It is, however, important to include methanol in the solvent. Without methanol in the reaction, two products form, i.e. the methyl ester and trimethylsilyl methyl ester, which explains the products obtained previously (Figure 2.2). The methanol suppresses the following mechanism (Figure 2.4).

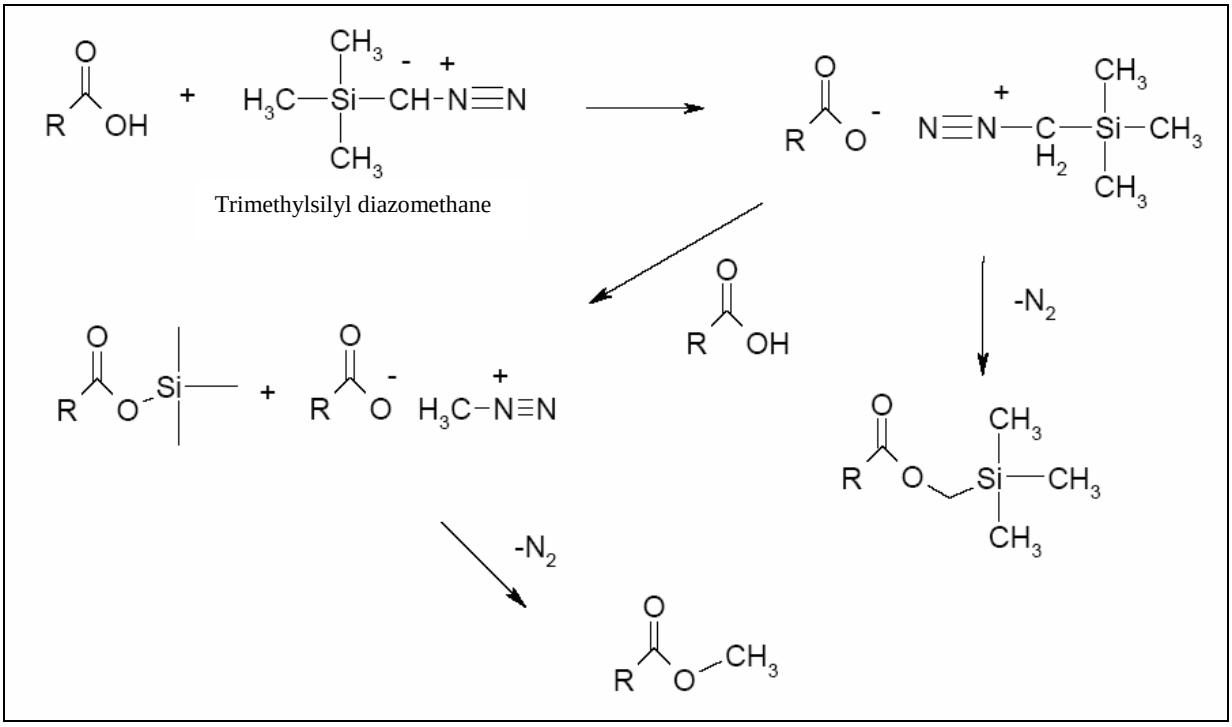

Figure 2.4: *Reaction mechanism of trimethylsilyl diazomethane without methanol (132).*

The reaction of TMDM with carboxylic acids including methanol makes the reaction proceed according to the mechanism shown in Figure 2.5.

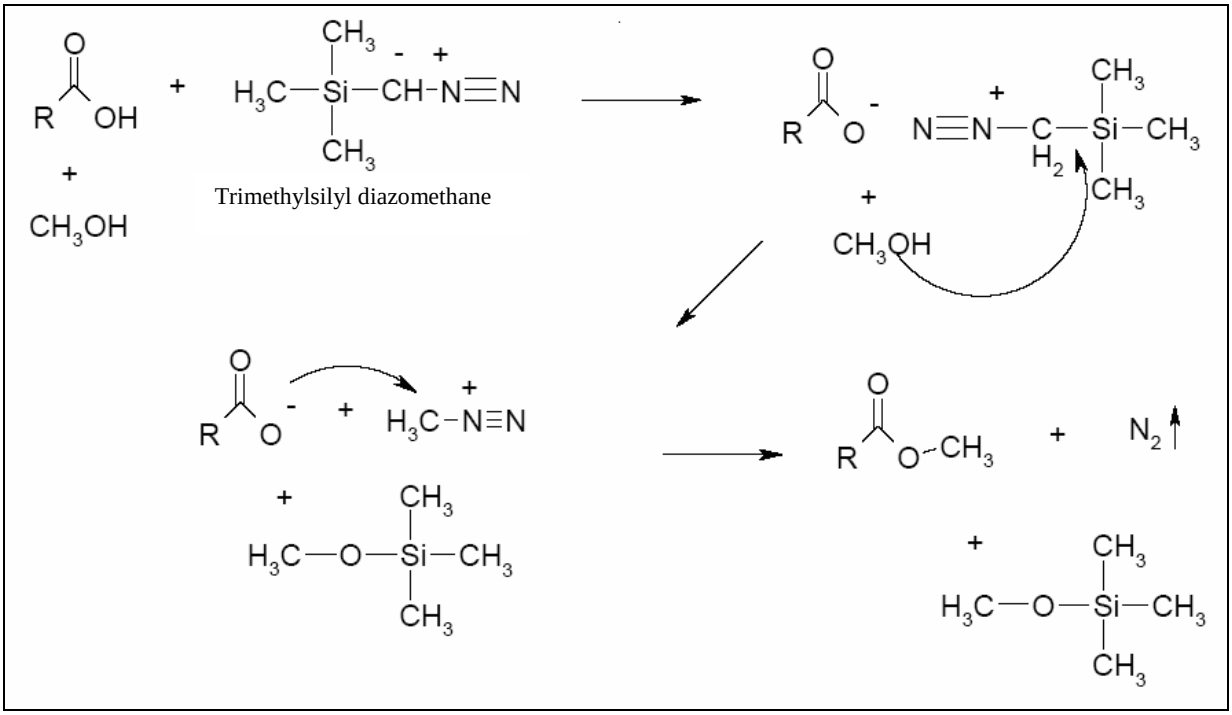

Figure 2.5: *Reaction mechanism of trimethylsilyl diazomethane mediated methylesterification of carboxylic acids (132).*

In order to form the methyl esters, MAs were dissolved in a mixture of toluene and methanol (5:1) whereafter TMDM was added in a few small portions. After 72 hours of stirring, the reaction mixture was quenched and extracted with dichloromethane to give a high yield of 97% of mycolic acids methyl esters.

The ^{1}H NMR spectrum of the esterified, unseparated natural MA corresponded to that reported in the literature for mycolic acid methyl esters (77, 132). It showed the same peaks present in the natural MAs before methylation and an additional singlet at δ 3.72 for the methyl group in the MA motif (Figure 2.6).

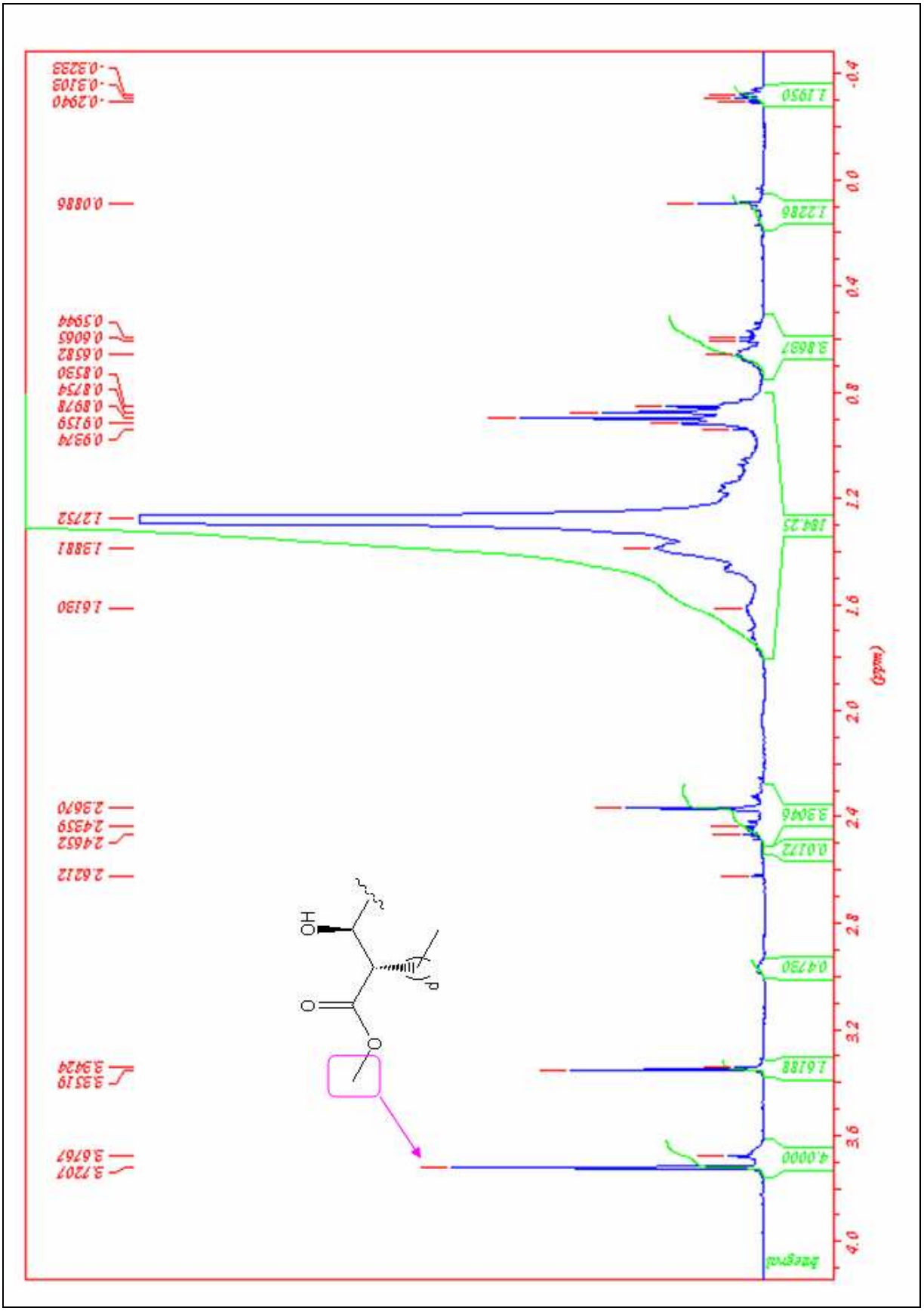

Figure 2.6: *^{1}H NMR spectrum of natural mycolic acid methyl esters.*

TLC analysis of the product showed the presence of three spots. The spots were thought to be the three mycolic acid methyl ester subclasses (Figure 2.7).

After optimization, we were finally able to successfully separate the MAs into the three different subclasses after methylation of the natural MA. Separation of the different fractions of MAs was done by preparative TLC. Each fraction was purified by column chromatography, which eliminated all the impurities, except for the methyl keto-MA fraction which needed to be harvested and combined from more preparative TLC plates in order to come to a realistic yield for further work.

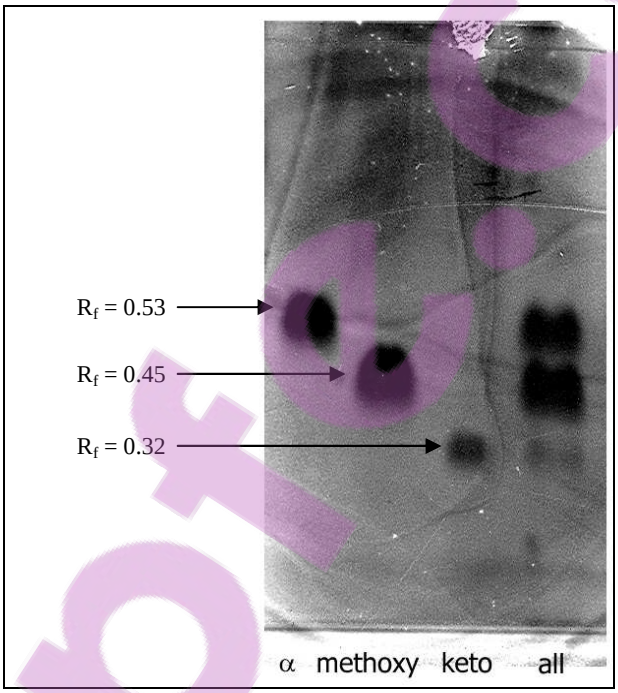

Figure 2.7: *TLC of the different subclasses of mycolic acid methyl esters obtained after separation of the natural MA into the subclasses and extracted from preparative TLC plates. Lane 1 α-MA, lane 2 methoxy-MA, lane 3 keto-MA and lane 4 natural MA before separation.*

TLC confirmed the presence of alpha mycolic methyl ester (R_f = 0.53), methoxy mycolic acid methyl ester (R_f = 0.45) and keto mycolic acid methyl ester (R_f = 0.32) as shown in Figure 2.7 [lit. respectively R_f = 0.50, 0.46 and 0.36 (93)]. The quantification of individual spots showed that alpha:methoxy:keto mycolic acid methyl esters were in ratios of 1:1.29:0.06 (Table 2.3), which was in agreement with the results previously found by NMR analysis (Table 2.2).

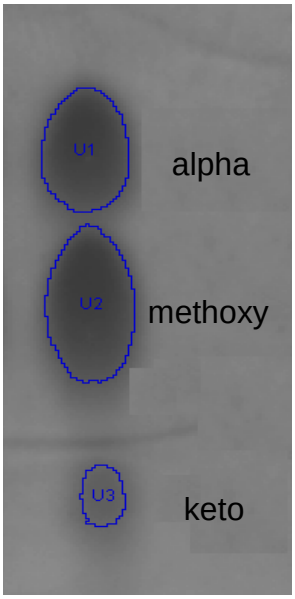

Figure 2.8: *TLC, showing the different subclasses, used to determine the ratios of the different subclasses by spot quantification. TLC was performed on Silica Gel 60 using petroleum ether/ethyl acetate (4/1, v/v); lipid spots were revealed by dipping the plates into a molybdophosphoric acid (10%) solution in ethanol, followed by heating.*

Table 2.3: *Estimation of the ratios amongst the different subclasses. Quantification of individual spots was done on a Versadoc (Model 3000) imaging system which measured the area and optical density of each spot. From this the density (optical density/area) and volume (optical density*area) for each spot could be calculated. The values for the volume for each spot were given as % of the total. From this the ratios were calculated.*

Name	Area mm2	Density ODu/mm2	Volume ODu*mm2	% Adj. Vol.	Ratios
alpha	357.74	4.67	573.34	42.26	1
methoxy	448.38	4.69	721.33	54.32	1.29
keto	90.98	3.91	121.98	3.42	0.06

After purification the amounts of the different fractions recovered (Table 2.4) were comparable to the results calculated from the NMR spectrum (Table 2.2) and to the results of the spot quantification (Table 2.3 and Figure 2.8)

Table 2.4: *The quantities of different fractions recovered.*

Type of MA	mg extracted	Ratio among different fractions after extraction
α	44.4	1
Methoxy	49.5	1.1
Keto	1.8	0.04

It is clear from the NMR and TLC analysis that the MAs isolated from *M. tuberculosis* H37Rv gave a higher percentage of methoxy-MA and a much lower percentage of keto-MA than reported in literature (93, 149, 150), where all three subclasses were found in approximately equal amounts.

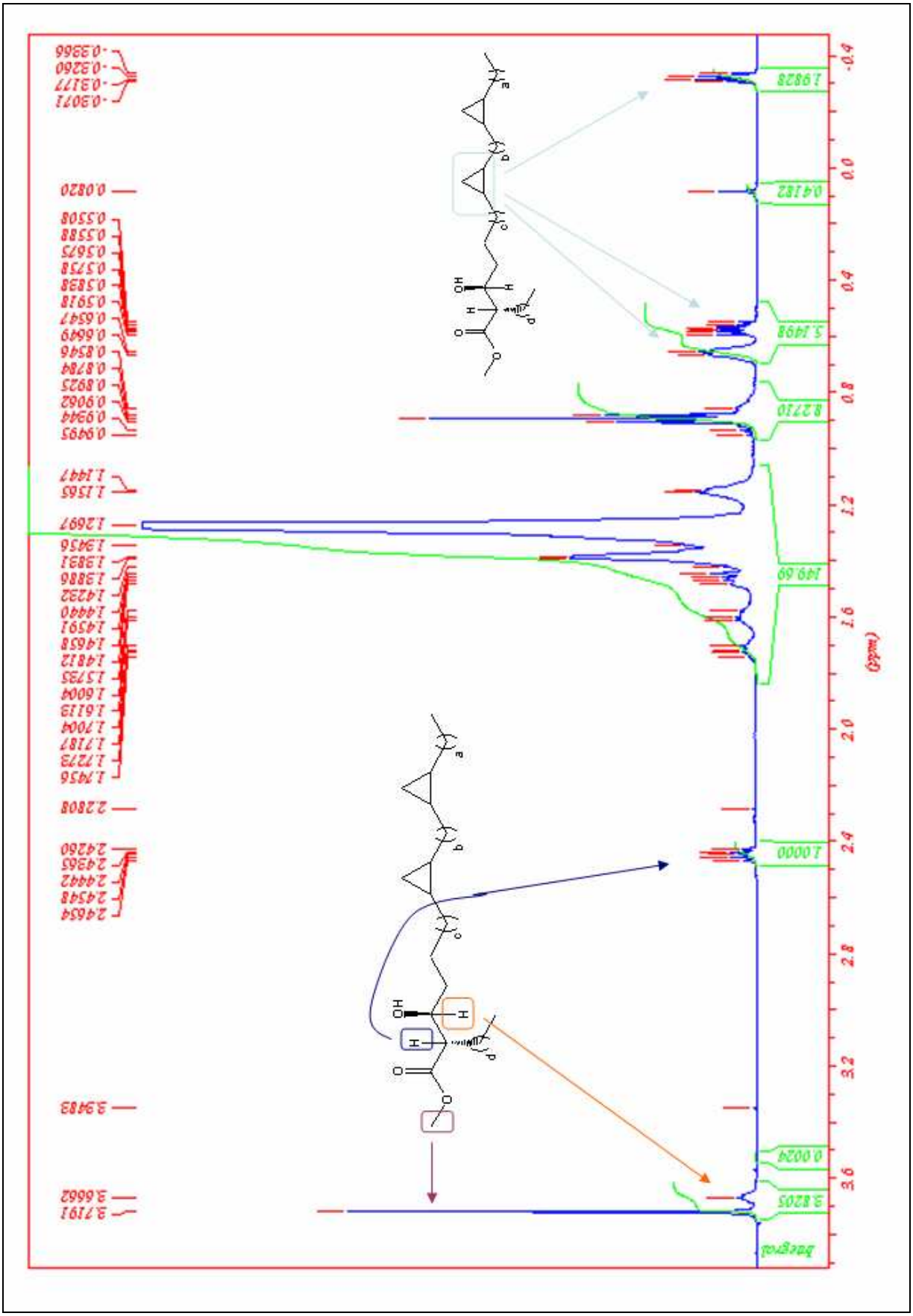

Figure 2.9: *^{1}H NMR spectrum of α mycolic acid methyl ester.*

The ^{1}H NMR spectrum of the α mycolic acid methyl ester showed a singlet at δ 3.72 for the methyl group in the mycolic acid motif. The β-proton appeared as a multiplet at δ 3.66 and the α-proton as a double of triplets at δ 2.44. The *cis*-cyclopropane ring protons appeared as a multiplet at δ 0.65, a triplet of doublets at δ 0.57 (*J* 4.1, 8.2 Hz) and another multiplet at δ -0.33 (Figure 2.9). The ^{13}C NMR spectrum included a carbonyl signal at δ 176.20 and a signal at δ 51.47 for the carbon of the methyl group in the mycolic acid motif. The β-carbon appeared at δ 72.32 and the α-carbon at δ 51.00. The spectrum showed signals for the carbons of the cyclopropane ring at δ 15.80 and 10.94 (Figure 2.10).

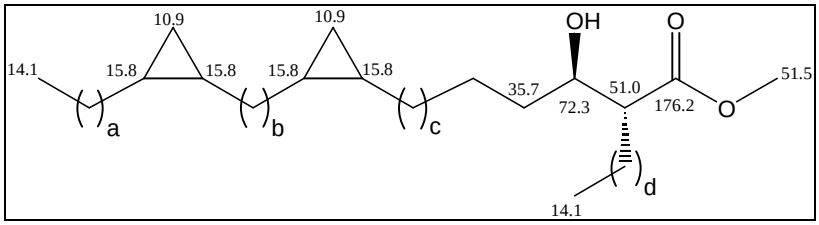

Figure 2.10: *α mycolic acid methyl ester with ^{13}C signals. Chemical shifts are quoted in δ relative to the trace resonance of $CDCl_3$ (δ 77.0 ppm).*

The NMR spectrum also showed minute amounts of impurities (1:191), as shown in Figure 2.11, which showed a peak at δ 3.35. These belong to methoxy-MA.

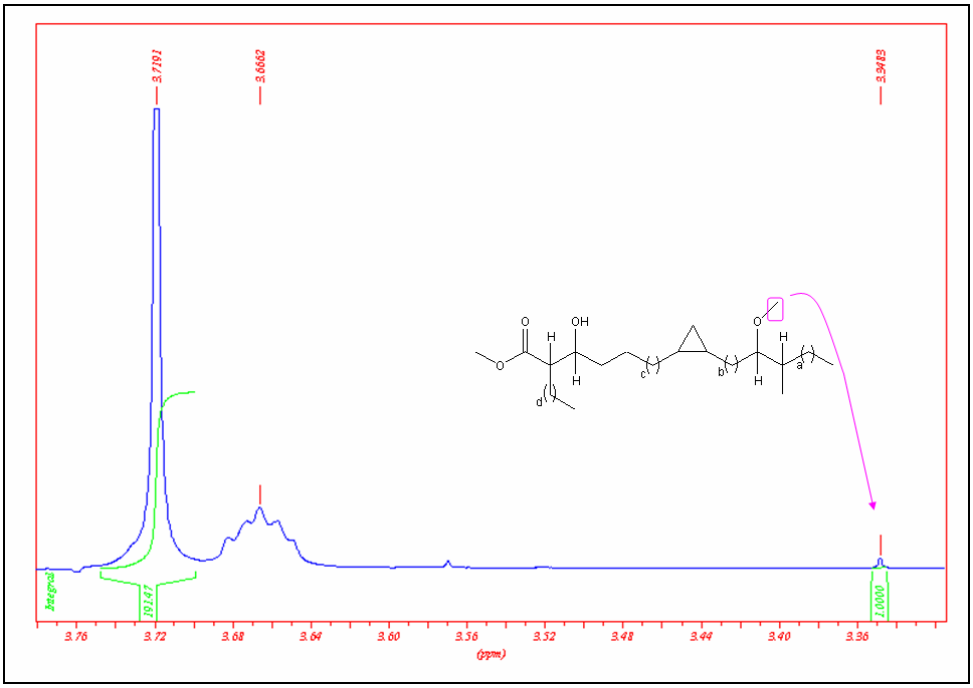

Figure 2.11: *^{1}H NMR of alpha mycolic acid methyl ester showing impurities from methoxy mycolic acid methyl ester.*

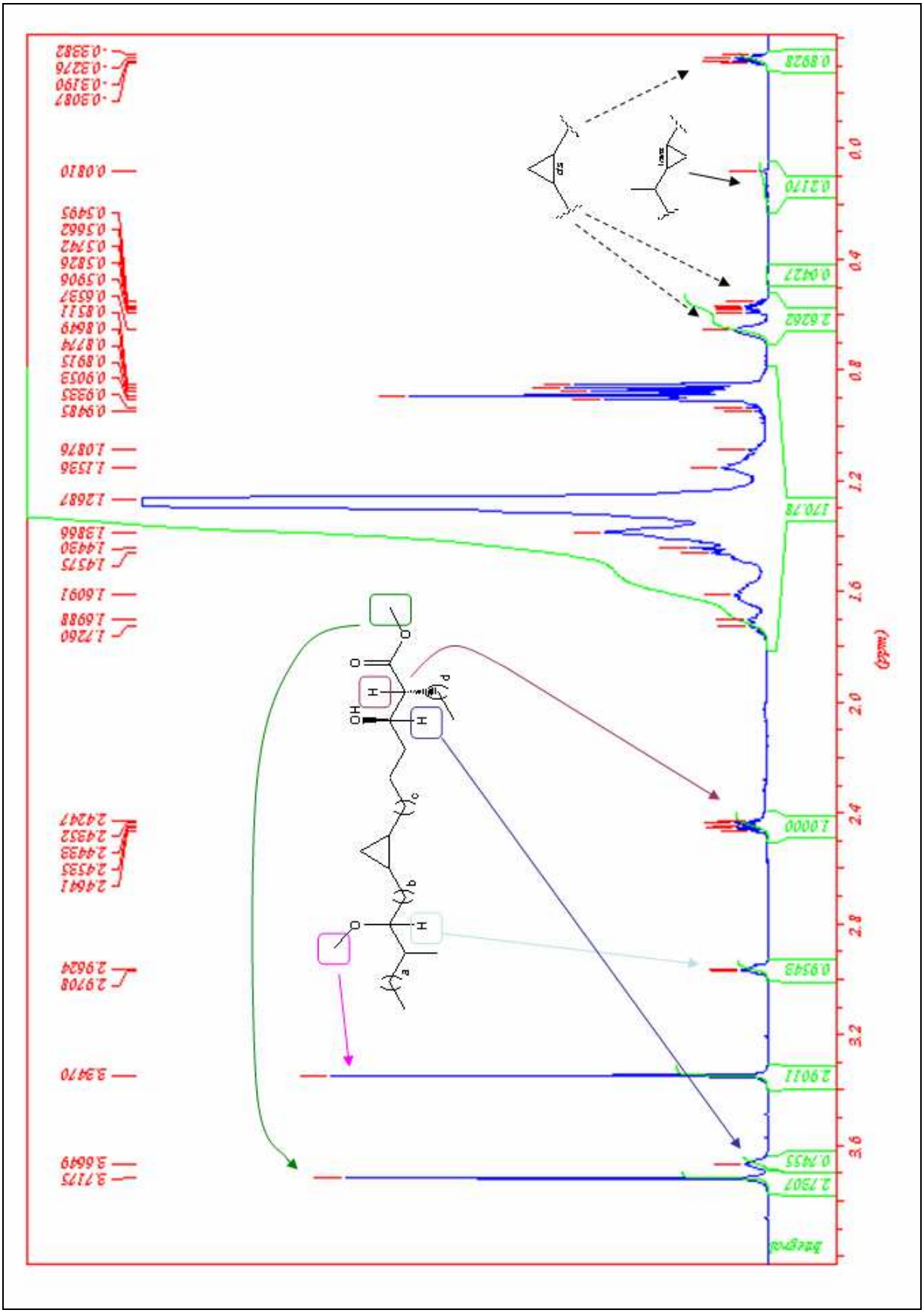

Figure 2.12: *^{1}H NMR spectrum of methoxy mycolic acid methyl ester.*

The ^{1}H NMR spectrum of the methoxy mycolic acid methyl ester showed a singlet at δ 3.72 for the methyl group in the mycolic acid motif, a multiplet at δ 3.66 for the proton on the β-carbon and a double of triplets at δ 2.44 (*J* 5.3, 9.2 Hz) for the proton of the α-carbon. The protons of the methoxy-group in the meromycolate chain appeared as a singlet at δ 3.32 and the proton next to the methoxy-group as a multiplet at δ 2.96. The spectrum showed a multiplet at δ 0.65, a triplet of doublets at δ 0.57 (*J* 4, 8.2 Hz) and a multiplet at δ -0.33 for the *cis*-cyclopropane ring protons. The *trans*-cyclopropane ring protons appeared as multiplets at δ 0.45 and 0.02-0.0. The *trans*-cyclopropane was less than 6% (Figure 2.12). The ^{13}C NMR spectrum included a carbonyl signal at δ 176.20, a signal at δ 85.47 for the carbon next to the methoxy-group and at δ 57.71 for the carbon of the methoxy-group. The β-carbon appeared at δ 72.32 and the α-carbon at δ 51.00. The carbons of the *cis*-cyclopropane ring appeared at δ 15.80 and 10.94, and the carbons of the *trans*-cyclopropane ring at δ 26.16, δ 18.62, δ 14.88 and δ 10.54 (Figure 2.13).

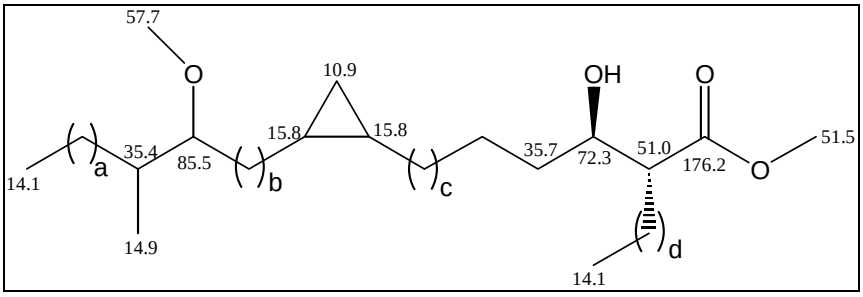

Figure 2.13: *Methoxy mycolic acid methyl ester with ^{13}C signals. Chemical shifts are quoted in δ relative to the trace resonance of $CDCl_3$ (δ 77.0 ppm).*

Figure 2.14 shows the ratios of one the *cis*-cyclopropane ring protons to the four ring protons of the *trans*-cyclopropane. The *trans*-cyclopropane was calculated to be less than 6%, Watanabe *et al*. the *cis*-cyclopropane to *trans*-cyclopropane ration to be 1:0.14 (150).

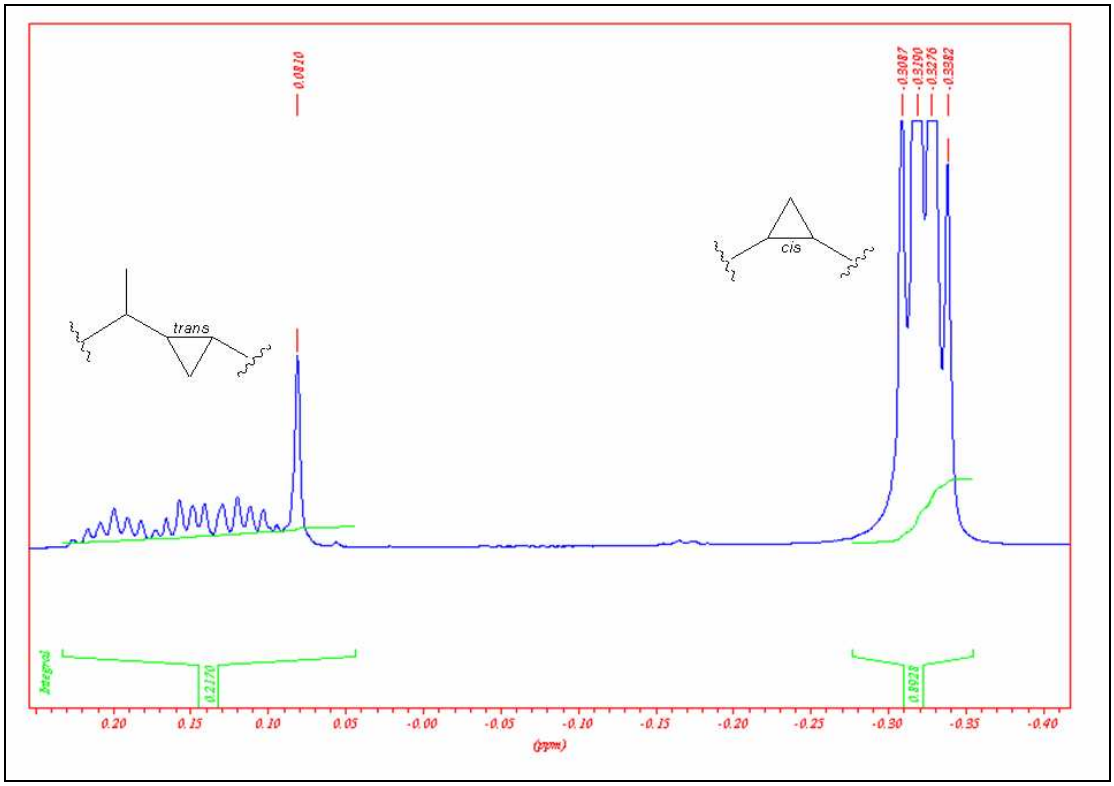

Figure 2.14: *^{1}H NMR spectrum of methoxy mycolic acid methyl ester showing the trans-cyclopropane.*

The ^{1}H NMR spectrum of the keto mycolic acid methyl ester showed a singlet at δ 3.72 for the methyl group in the mycolic acid motif. The β-proton appeared as a multiplet at δ 3.66 and the α-proton as a double of triplets at δ 2.44 (*J* 5.3, 9.2 Hz). The proton next to the keto-group appeared at δ 2.49. The *cis*-cyclopropane ring protons appeared as a multiplet at δ 0.65, a triplet of doublets at δ 0.57 (*J* 4.1, 8.2 Hz) and a double doublet at δ -0.33 (*J* 4.1, 5.3 Hz). The protons of the *trans*-cyclopropane ring appeared as multiplets at δ 0.45 and 0.02-0.0, the *trans*-cyclopropane was more than 10%. As shown in Table 2.4, a very small amount of the keto mycolic acid methyl ester was recovered; therefore the signals were not as strong as would have been ideal for interpretation (Figure 2.15). The ^{13}C NMR spectrum included carbonyl signals at δ 215.3 and δ 176.20. The β-carbon appeared at δ 72.33, the α-carbon at δ 51.00 and the carbon of the methyl ester at δ 51.47. The spectrum showed signals for the *cis*-cyclopropane ring at δ 15.80 and 10.94 (Figure 2.16).

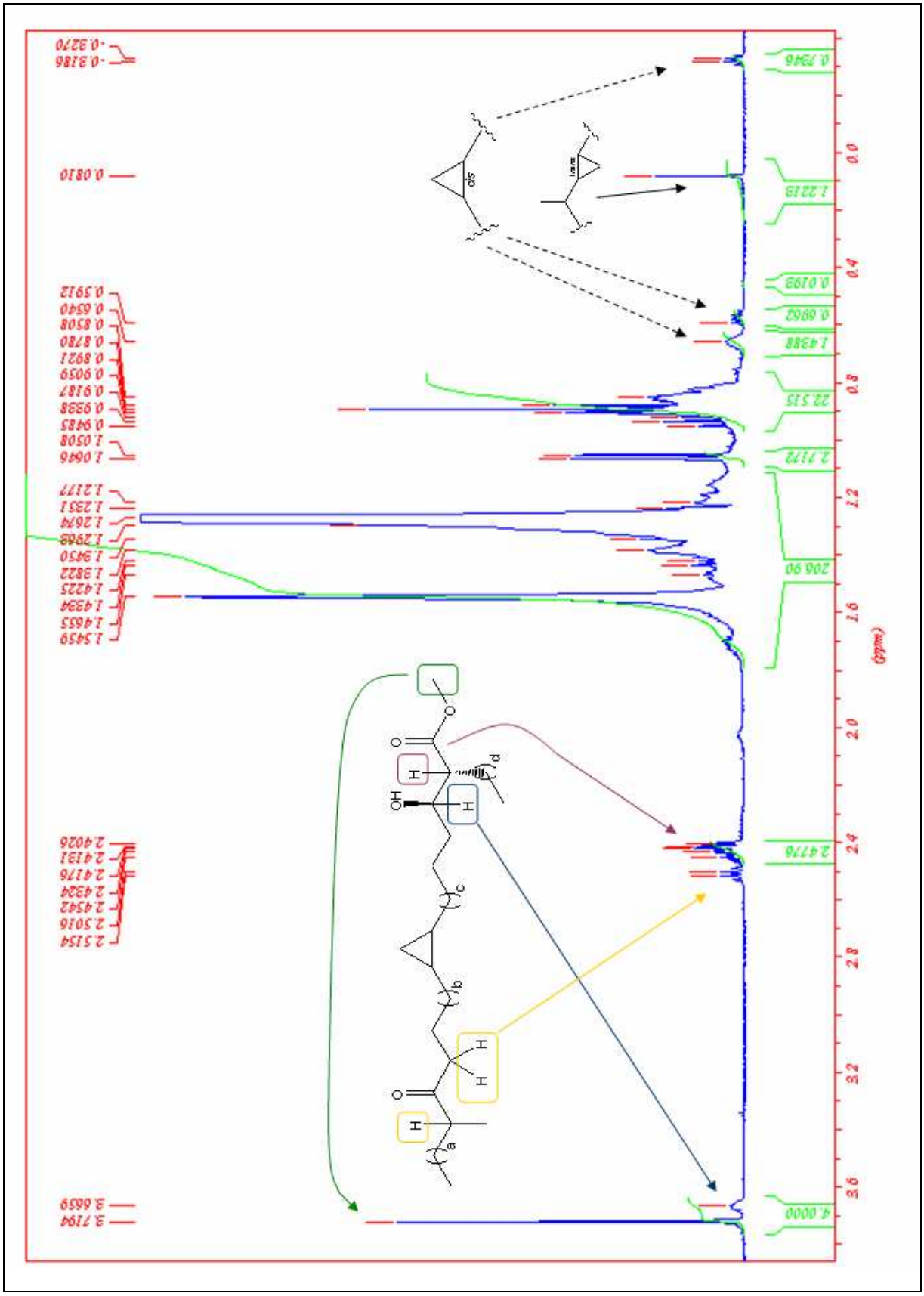

Figure 2.15: *^{1}H NMR spectrum of keto mycolic acid methyl ester.*

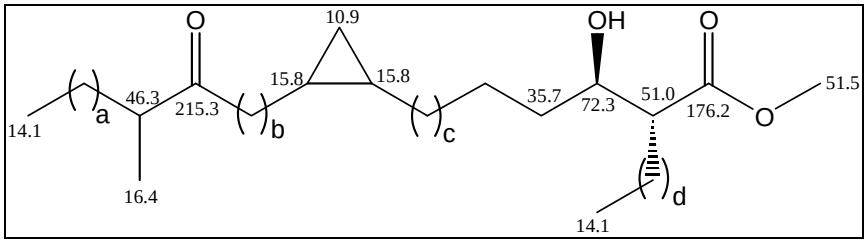

Figure 2.16: *Keto mycolic acid methyl ester with ^{13}C signals. Chemical shifts are quoted in δ relative to the trace resonance of $CDCl_3$ (δ 77.0 ppm).*

Figure 2.17 shows the ratios of the four *trans*-cyclopropane ring protons to the four protons of the *cis*-cyclopropane ring in the keto mycolic acid methyl ester.

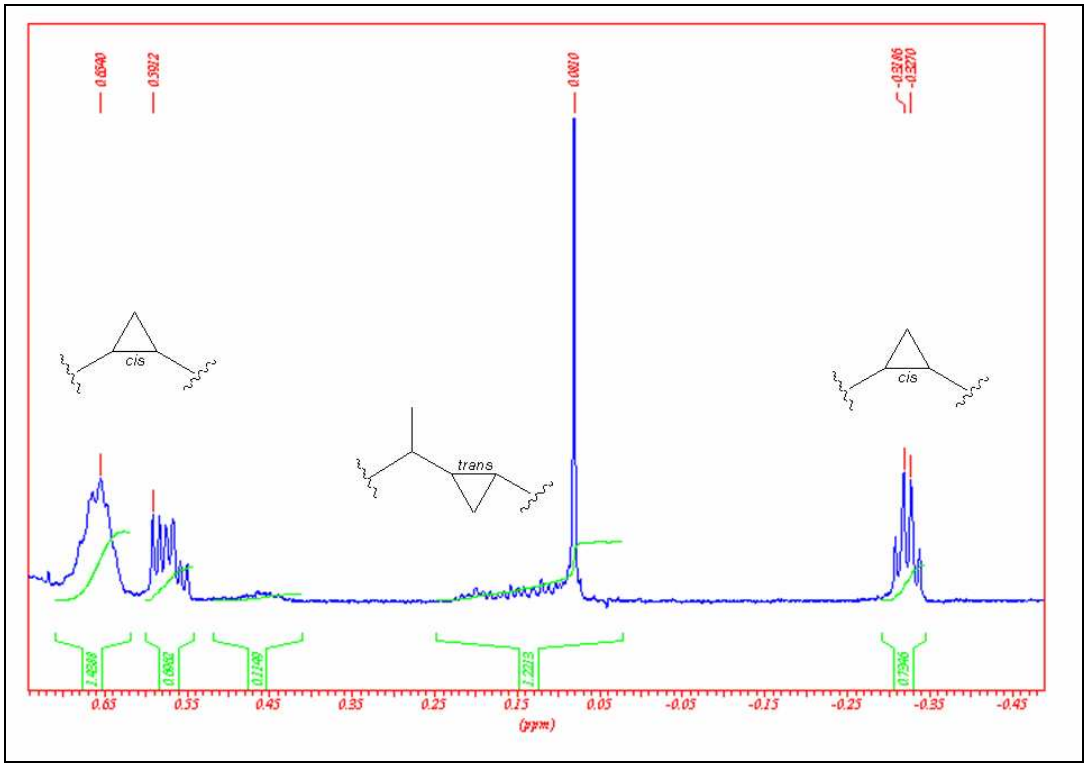

Figure 2.17: *^1H NMR spectrum of keto mycolic acid methyl ester showing trans-cyclopropane.*

Molecular weights of α-MA methyl esters, methoxy-MA methyl ester and keto-MA methyl esters were evaluated by MALDI-TOF/MS. The spectra obtained were in agreement with those reported in the literature (93). The pseudo-molecular mass of the major component of each subclass [M + Na^+] corresponded to 1174, 1290 and 1246 respectively, as shown in Figures 2.18, 2.19 and 2.20.

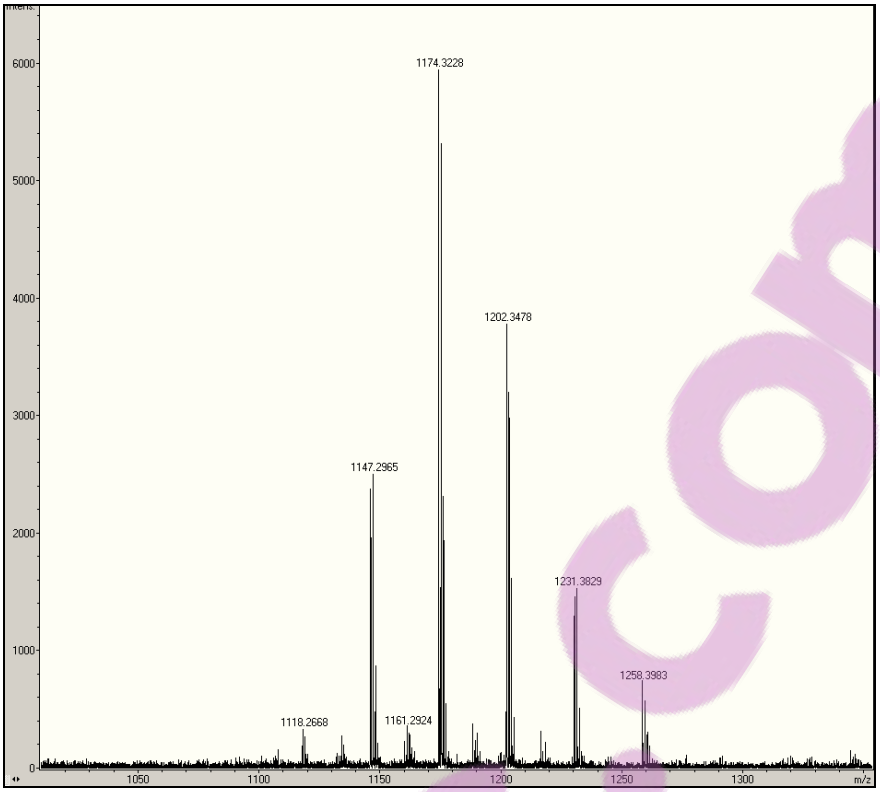

Figure 2.18: *MALDI-TOF MS spectrum of α-MA methyl ester. The total carbon number of the free acid is 78.*

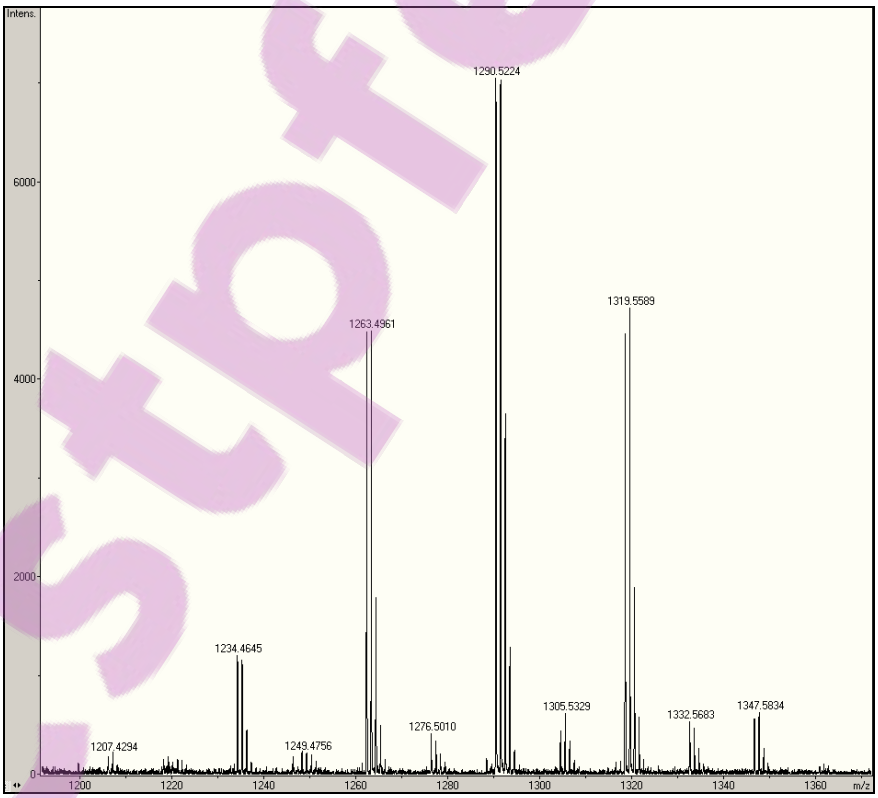

Figure 2.19: *MALDI-TOF MS spectrum of methoxy-MA methyl ester. The total carbon number of the free acid is 85.*

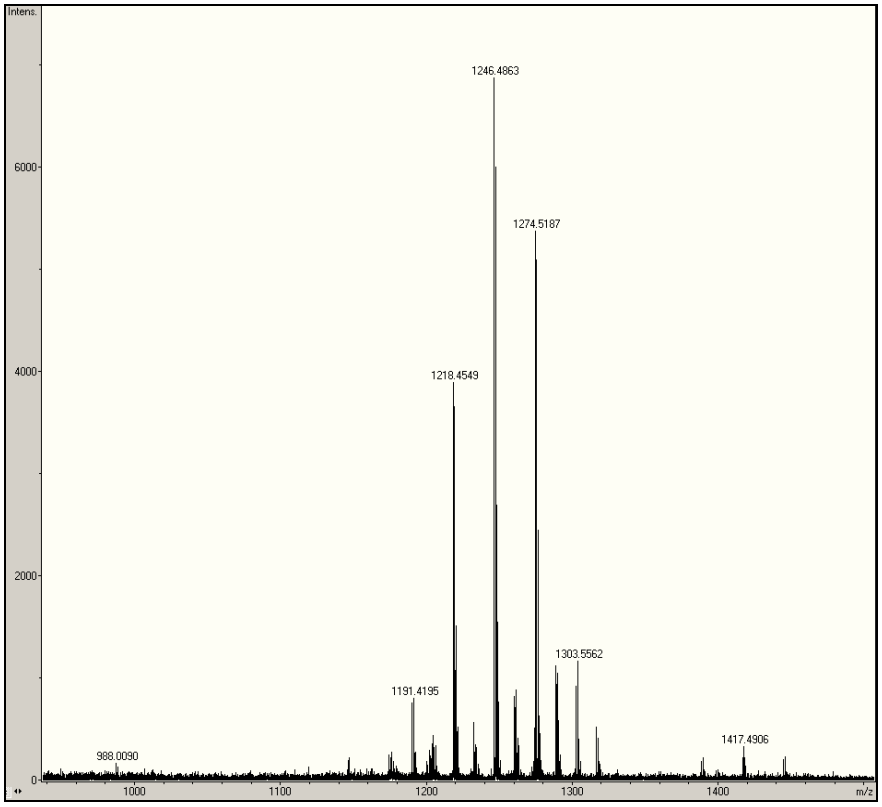

Figure 2.20: *MALDI-TOF MS spectrum of keto-MA methyl ester. The total carbon number of the free acid is 82.*

2.3.2 Materials and methods

2.3.2.1 General considerations

The MA sample was isolated from *M. tuberculosis* H37Rv and purified as described (67). HPLC was performed on a Phenomenex Luna 5 µ C18 column in a Merck Hitachi Chromatograph fitted with a Merck Hitachi L-4500 Diode Array Detector. NMR spectra were recorded either on a Bruker Advance 500 spectrometer with 5 mm BBO probe. Compounds analysed were solutions in deuterated chloroform ($CDCl_3$). All chemical shifts are quoted in δ relative to the trace resonance of protonated chloroform (δ 7.27 ppm) and $CDCl_3$ (δ 77.0 ppm). HPLC and NMR spectra were in agreement with the data reported in literature except that the sample contained some minor impurities (139, 150, 151).

2.3.2.2 Estimation of other components in natural mycolic acids

A TLC was performed on Silica Gel 60 using petroleum ether/ethyl acetate (4/1, v/v); lipid spots were revealed by dipping the plates into a molybdophosphoric acid (10%) solution in ethanol, followed by heating. Quantification of individual spots was carried out on a Versadoc (Model 3000) imaging system. This confirmed that the sample contained less than 10% of impurities.

2.3.2.3 NMR analysis of the natural mycolic acids

δ_H: 3.34 (3H, s, CHOC<u>H</u>$_3$), 2.96 (1H, m, C<u>H</u>OCH$_3$), 2.44 (1H, dt, *J 5.4*, 8.9 Hz, C<u>H</u>(CH$_2$)$_{23}$CH$_3$), 1.8-0.7 (other H, multiplets including a d at δ 1.05, *J* 6.9 Hz, 3H, C<u>H</u>$_3$CHCO), 0.65 (2H, m, *cis*-cyclopropane), 0.57 (1H, ddd, *J* 4.1, 8.2 Hz, CH *cis*-cyclopropane), 0.4 (3H, m, *trans*-cyclopropane), 0.1 (1H, m, *trans*-cyclopropane), -0.33 (1H, broad dd, *J* 5.0, 8.9 Hz, *cis*-cyclopropane).

δ_C: 176.21 (<u>C</u>O$_2$CH$_3$), 85.48 (<u>C</u>OCH$_3$), 72.33 (<u>C</u>HOH), 57.72 (CO<u>C</u>H$_3$), 51.48 (CO$_2$<u>C</u>H$_3$), 50.98 (<u>C</u>H(CH$_2$)$_{23}$CH$_3$), 35.59 (CH$_2$), 35.41 (<u>C</u>HCH$_3$), 32.43 (CH$_2$), 31.94 (CH$_2$), 31.59 (CH$_2$), 30.53 (CH$_2$), 30.22 (CH$_2$), 29.99 (CH$_2$), 29.94 (CH$_2$), 29.71 (CH$_2$), 29.58 (CH$_2$), 29.51 (CH$_2$), 29.43 (CH$_2$), 29.37 (CH$_2$), 28.74 (CH$_2$), 28.09 (CH$_2$), 27.57 (CH$_2$), 27.33 (CH$_2$), 26.17 (CH$_2$), 25.74 (CH$_2$), 22.69 (CH$_2$), 15.78 (CHcyclopropane), 14.88 (CH<u>C</u>H$_3$), 14.11 (CH$_3$), 10.91 (CH$_2$cyclopropane).

2.3.2.4 Esterification of mycolic acids

To form the methyl esters, MAs (100 mg, ~ 0.1 mmol) were dissolved in a mixture of toluene:methanol (5:1, 18 ml). Thereafter trimethylsilyl diazomethane (TMDM, 2 M solution, Fluka, 0.2 ml, 0.4 mmol) was added, followed by further 4 additions of TMDM (0.1 ml, 0.2 mmol) every 45 minutes. The mixture was stirred for 72 hours, and then quenched by evaporation. The residue was dissolved in dichloromethane (15 ml) and water (10 ml) was added. The two layers were separated and the water layer extracted with dichloromethane (2 x 10 ml). The combined organic layers were dried and the solvent evaporated to give the desired compound (98 mg, ~ 97%). The NMR spectra of the compounds obtained, corresponded to those reported in the literature for methyl MAs (149, 150).

2.3.2.5 NMR analysis of the mycolic acids methyl esters

δ_H: 3.72 (3H, s, CO$_2$C<u>H</u>$_3$), 3.66 (1H, m, C<u>H</u>OH), 3.34 (3H, s, CHOC<u>H</u>$_3$), 2.95 (1H, m, C<u>H</u>OCH$_3$), 2.44 (1H, dt, J 5.4, 8.9 Hz, C<u>H</u>(CH$_2$)$_{23}$CH$_3$), 1.8-0.7 (other H, multiplets including a d at δ 1.05, *J* 6.9 Hz, 3H, C<u>H</u>$_3$CHCO), 0.65 (2H, m, *cis*-cyclopropane), 0.57 (2H, ddd, *J* 4.1, 8.2 Hz, CH *cis*-cyclopropane), 0.4 (m, *trans*-cyclopropane), 0.1 (m, *trans*-cyclopropane), -0.33 (1H, broad dd, *J* 5.0, 8.9 Hz, *cis*-cyclopropane).

δ_C: 176.21 (<u>C</u>O$_2$CH$_3$), 85.48 (<u>C</u>OCH$_3$), 72.33 (<u>C</u>HOH), 57.72 (CO<u>C</u>H$_3$), 51.48 (CO$_2$<u>C</u>H$_3$), 50.98 (<u>C</u>H(CH$_2$)$_{23}$CH$_3$), 35.73 (CH$_2$), 35.40 (<u>C</u>HCH$_3$), 32.43 (CH$_2$), 31.93 (CH$_2$), 30.54 (CH$_2$), 30.22 (CH$_2$), 29.99 (CH$_2$), 29.95 (CH$_2$), 29.71 (CH$_2$), 29.51 (CH$_2$), 29.43 (CH$_2$), 29.37 (CH$_2$),

29.15 (CH_2), 28.74 (CH_2), 28.09 (CH_2), 27.58 (CH_2), 27.43 (CH_2), 26.18 (CH_2), 25.74 (CH_2), 22.69 (CH_2), 15.78 (CHcyclopropane), 14.88 ($CH\underline{C}H_3$), 14.11 (CH_3), 10.91 (CH_2cyclopropane).

2.3.2.6 Separation of the different subclasses of mycolic acids

Separation of the different fractions of MAs was achieved by preparative TLC (Silica Gel 60, Merck) using the same procedures for elution and the revealing of the spots at the two extremities of the plates as described in section *2.3.2.2*. The mycolic acid methyl esters were eluted from the silica gel with dichloromethane. Then each fraction was purified by Flash column chromatography using Fluorosil (60-100 mesh, Aldrich) and eluting with a solution of petroleum ether:diethyl ether (9:1). This method proved efficient for the α-MA methyl ester and methoxy-MA methyl ester fractions, while the keto-MA methyl ester subclass was further purified by preparative TLC. The purity of the various types of mycolates was checked by analytical TLC, as described in section *2.3.2.2*.

2.3.2.7 Estimation of different subclasses of mycolic acids

A TLC was performed on Silica Gel 60 developed in petroleum ether/ethyl acetate (4/1, v/v). Lipid spots were revealed by dipping the plates into a molybdophosphoric acid (10%) solution in ethanol, followed by heating. Quantification of individual spots was done on a Versadoc (Model 3000) imaging system.

2.3.2.8 NMR analysis of α-mycolic acid methyl esters

δ_H (500 MHz): 3.72 (3H, s, $OC\underline{H}_3$), 3.66 (1H, m, $C\underline{H}OH$), 2.44 (1H, dt, *J* 5.3, 9.2 Hz, $C\underline{H}(CH_2)_{23}CH_3$), 1.8-1.0 (other H, m), 0.95-0.7 (other H, m), 0.65 (4H, m, $C\underline{H}$ *cis*-cyclopropane), 0.57 (2H, td, *J* 4, 8.2 Hz, CH *cis*-cyclopropane), -0.33 (2H, m, $C\underline{H}_2$ *cis*-cyclopropane).

δ_C (125.8 MHz): 176.20 ($\underline{C}O_2CH_3$), 72.32 ($\underline{C}HOH$), 51.47 ($CO_2\underline{C}H_3$), 51.00 ($\underline{C}H(CH_2)_{23}CH_3$), 35.73, 31.93, 29.71, 29.62, 29.59, 29.57, 29.51, 29.42, 29.36, 28.74, 27.43, 25.74, 22.69, 15.80 (CH *cis*-cyclopropane), 14.10 (CH_3), 10.94 (CH_2 *cis*-cyclopropane).

2.3.2.9 NMR analysis of methoxy mycolic acid methyl esters

δ_H (500 MHz): 3.72 (3H, s, $OC\underline{H}_3$), 3.66 (1H, m, $C\underline{H}OH$), 3.32 (3H, s, $CHOC\underline{H}_3$), 2.96 (1H, m, $C\underline{H}OCH_3$), 2.44 (1H, dt, *J* 5.3, 9.2 Hz, $C\underline{H}(CH_2)_{23}CH_3$), 3.72 (3H, s, $OC\underline{H}_3$), 3.66 (1H, m,

CHOH), 2.44 (1H, dt, *J* 5.3, 9.2 Hz, CH$(CH_2)_{23}CH_3$), 1.8-1.0 (other H, m), 0.95-0.7 (other H, m), 0.65 (2H, m, CH *cis*-cyclopropane), 0.57 (1H, td, *J* 4, 8.2 Hz, CH *cis*-cyclopropane), 0.45 (1H, m, CH-*trans*-cyclopropane, less than 6%), 0.2-0.0 (3H, m, *trans*-cyclopropane), -0.33 (1H, m, CH_2 *cis*-cyclopropane).

δ_C (125.8 MHz): 176.20 (CO_2CH_3), 85.47 ($COCH_3$), 72.32 (CHOH), 57.71 ($COCH_3$), 51.47 (CO_2CH_3), 51.00 (CH$(CH_2)_{23}CH_3$), 38.2 ($CHCH_3$ *trans*-cyclopropane) 35.73, 35.41, 32.43, 31.93, 30.54, 29.92, 29.71, 29.61, 29.57, 29.50, 29.43, 29.36, 28.73, 27.59, 27.44, 26.16 (CH *trans*-cyclopropane), 22.69 (CH_2), 2.16, 19.72 (CH_3CH), 18.62 (CH *trans*-cyclopropane), 15.80 (CH *cis*-cyclopropane), 14.88 ($CHCH_3$ *trans*-cyclopropane), 14.10 (CH_3), 10.94 (CH_2 *cis*-cyclopropane), 10.54 (CH_2 *trans*-cyclopropane).

2.3.2.10 NMR analysis of keto mycolic acid methyl ester

δ_H (500 MHz): 3.72 (3H, s, OCH_3), 3.66 (1H, m, CHOH), 2.49 (1H, q, *J* 6.9 Hz, $COCHCH_3$), 2.44 (1H, dt, *J* 5.3, 9.2 Hz, CH$(CH_2)_{23}CH_3$), 2.41 (2H, td, *J* 1.8, 7.0 Hz, CH_2CO), 1.8-1.0 (other H, multiplet including a d at δ 1.05, *J* 6.9 Hz, 3H, CH_3CH), 0.65 (2H, m, CH *cis*-cyclopropane), 0.57 (1H, ddd, *J* 4.1, 8.2 Hz, CH *cis*-cyclopropane), 0.45 (1H, m, CH *trans*-cyclopropane, more than 10%), 0.2-0.0 (3H, m, *trans*-cyclopropane), -0.33 (1H, dd, *J* 4.1, 5.3 Hz, CH_2 *cis*-cyclopropane).

δ_C (125.8 MHz): 215.3 (C=O), 176.20 (CO_2CH_3), 72.33 (CHOH), 51.47 (CO_2CH_3), 51.00 (CH$(CH_2)_{23}CH_3$), 46.35, 41.14, 35.73, 31.93, 30.23, 29.70, 29.50, 29.43, 29.36, 28.73, 27.44, 27.34, 23.75, 22.69, 16.36 ($CHCH_3$ keto-group), 15.80 (CH *cis*-cyclopropane), 14.10 (CH_3), 10.94 (CH_2 *cis*-cyclopropane).

2.3.2.11 MALDI-TOF Mass Spectrometry

Dried samples (5 mg) were redissolved in 1.0 ml of chloroform. An aliquot was mixed with an equal volume of 2,5 dihydroxybenzoic acid (2,5-DHB) matrix solution [10 mg/ml 2,5-DHB in chloroform : methanol (1:1)] and 0.7 µl spotted onto a MALDI target that had been seeded with a layer of 2,5-DHB (in ethanol). Mass spectra were acquired in reflectron mode with delayed ion extraction using 40 laser shots per acquisition. Between 120 and 160 laser shots were accumulated into the final summed spectrum. Spectra were externally calibrated using a peptide mixture in CHCA matrix (93).

2.4 Biological activity/antigenicity of subclasses of mycolic acids

2.4.1 Results and discussion

After a few attempts, the natural MA was successfully separated into the different subclasses and purified. The next step was to determine the biological activity/antigenicity of these different subtypes by using ELISA. Pan *et al.* (112) showed that by using ELISA, the methoxy-MA was recognised better than the α- and keto-MA by sera from TB positive patients. They applied the MAs as methyl esters in *n*-hexane solution to the ELISA plate wells.

With ELISA being the easiest and quickest way to obtain results for antibody recognition against certain antigens, ELISA plate wells were coated with MAs as methyl esters and as free acids in chloroform, as shown in Figure 2.21. MA had to be esterified in order to be separated into the different subclasses. However, the methyl esters were not recognised by antibodies in TB^+ patient serum, therefore the hydrolysis (de-esterification) of the different subclasses was required. Pan *et al.* (112) and Fujita *et al.* (64) showed that cord factor was recognised by antibodies in TB^+ patient serum. Cord factor was therefore included as control.

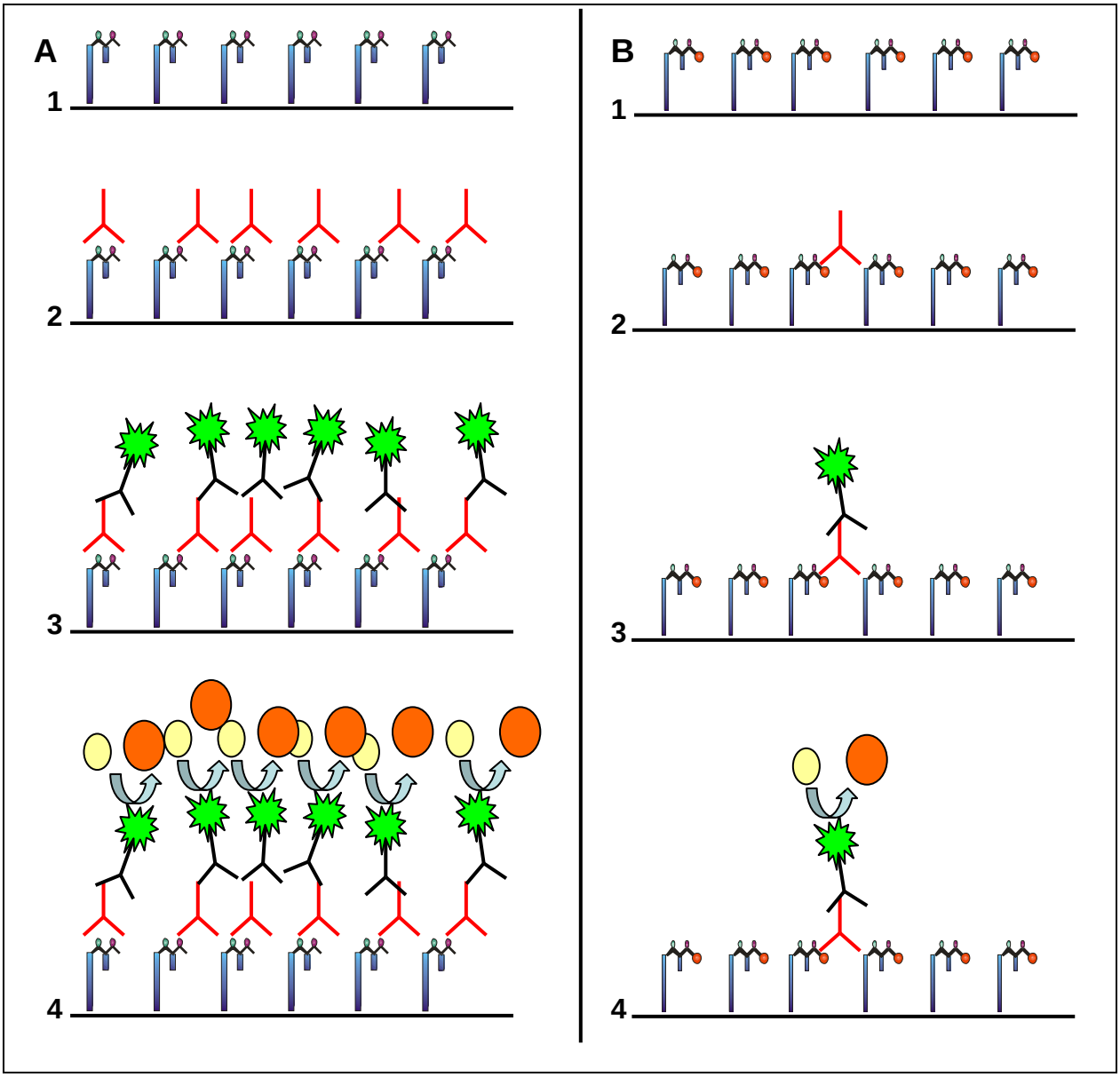

Figure 2.21: *Schematic presentation of ELISA.* ***A*** *shows results of antibody binding to the antigen (in this case natural MA).* ***B*** *shows the results of no antibody binding to the antigen (in this case MA methyl ester). 1. Coating with antigen. 2. Incubation with serum. 3. Addition of conjugate and 4. Addition of substrate and monitoring of colour change.*

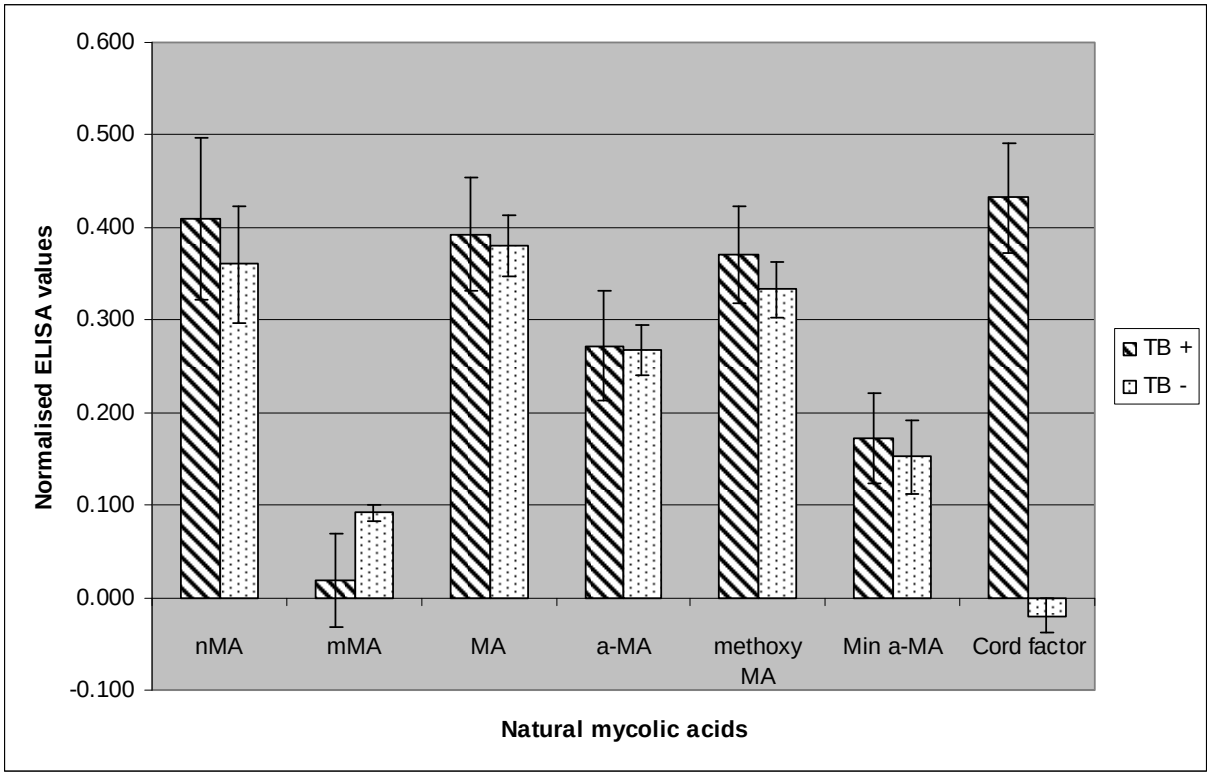

Figure 2.22: *ELISA results of antibody binding to natural MA (nMA, n=92), natural mycolic aicd methyl esters (mMA, n=20), MA (MA, n=18), alpha-MA (α-MA, n=20), methoxy-MA (methoxy-MA, n=20), α-MA (Min α-MA, n=20) and cord factor (n=20). The source of the antibodies was sera collected from either TB positive, kindly provided by Dr AC Stoltz from the Pretoria Academic Hospital, or TB negative South African hospitalised patients of various adult age groups* (127). *(Values are given as a mean ± standard deviation).*

Figure 2.22 summarises the results obtained with ELISA. TB^+ patient serum gave a relatively strong signal against natural MA (nMA) and cord factor, as well as against the MA (MA) and methoxy-MA (methoxy-MA), but weaker signals against the α-MA (α-MA) and the α-MA (Min α-MA). TB^+ patient serum did not recognise the methylated MA (mMA).

TB^- patient serum, just like TB^+ sera, also recognised MA (nMA), MA, alpha-MA, methoxy-MA and the alpha-MA (Min α-MA), and it also did not give a signal against the esterified MA (mMA). Interestingly, however, TB^- patient serum did not recognise cord factor, which gave among the strongest of signals with TB^+ sera.

Statistically (Student's t test), compared to MA, there was no significant difference in the binding of TB^+ patient serum antibodies to MA, methoxy-MA or to cord factor. Antibody binding to the methylated MA was very low compared to natural MA. The ELISA signal against the alpha-MA was much higher compared to the esterified MA, but significantly lower

compared to natural MA ($P < 0.0001$). Antibodies recognised the natural MA (Min α-MA) a little less than the MA, but significantly less than methoxy-MA ($P < 0.0001$).

Closer analyses of ^{1}H NMR spectra of both separated natural alpha-MA (Figure 2.11) and natural alpha-MA from Prof D.E. Minnikin (University of Birmingham, UK) showed a small amount of methoxy-MA present. This might explain the signals obtained against these antigens, as the more hydrophilic oxygenated MA may preferentially orientate itself in the antigen coat to be more accessible for antibody binding than the majority of α-MA.

The results found contradicted that reported by Pan and his co-workers (112). We found that the methyl esters of the MAs were not recognised by TB positive patient serum in the ELISA assay. Pan *et al.* (112) showed recognition of the methoxy-MA methyl esters. This might be due to small differences in the method followed by Pan *et al.*, and the method used for this study. Pan *et al.* coated the ELISA plate wells with MA methyl esters in *n*-hexane and used 0.05% Tween-20 in PBS as blocking solution, whereas in this study the MA methyl esters and free MA were coated from hot PBS solutions, while 0.5% casein in PBS was used as blocking solution. Deposition of MA from an aqueous, rather than a hydrophobic environment, may influence the conformation assumed by the immobilised MA.

Esterified MA was used as negative control in order to prove that a specific conformation, which can be destroyed by the elimination of the hydrogen bonding capacity of the carboxylic acid in the α- and the hydroxyl group in β-position, is important for defining the "cholesteroid" nature of MAs. The formation of a hydrogen bond between the α-carboxylic and the β-hydroxyl of MA is particularly stable for the natural *erythro* configuration of *2R,3R* 2-alkyl,3-hydroxy acids and has been shown to have a stabilising effect on the alignment of the alkyl chains affecting the physical properties of these acids (52, 53). Sugar esters, such as trehalose mono- or dimycolates, may also suffice to stabilise the folding of the mero chain by hydrogen bonding, as it retains hydroxyl groups in the vicinity of the α-carboxylic group of MA, but the methyl ester of MA substitutes the hydrogen atom on the carboxylic acid with a hydrophobic moiety that has no possibility for hydrogen bonding with the oxygenated group of the mero chain. This may explain why the recognition of cord factor by TB^{+} patient serum was still allowed, despite the esterification of the mycolates. In corroboration of the results obtained here, Grant *et al.* (70) reported that the ability of the T-cell antigen receptor to recognise MA

presented to the T-cell on the CD1b protein of an antigen presenting cell was abolished when the methyl ester of MA was presented instead.

The loss of antigenicity of the mycolic acid methyl ester indicated that the mycolic motif plays an important role in recognition by antibodies. The importance of the mero chain was shown by the difference in antibody recognition of the alpha-MA and the methoxy-MA.

From these results it is clear that both the mycolic motif and the mero chain play and important role in antigenicity of MAs.

Much can be learned from the different results obtained with TB^+ and TB^- patient sera against cord factor, as opposed to the similar signals that were obtained with TB^+ and TB^- patient sera against all the free hydroxy acid MAs. With cord factor, only TB^+ patient sera showed recognition, whereas TB^- patient serum did not recognise cord factor at all. The results can be interpreted in a way similar to that applied to the antigenicity of virus particles of the development of subcomponent vaccines for viral diseases in humans and animals (144).

In the case of viruses, different types of virus particles are secreted from infected cells that will be recognised by antibodies of the host. Virus particles also self-assemble with different virus particles into whole or partial virus coats and these may also be brought into contact with the immune system during the course of infection. In this way, three categories of antigenic epitopes may be recognised per virus particle that are necessary to explain the immune phenomena that are observed. These categories are metatopes, cryptotopes and neotopes. Metatopes are antigenic epitopes that are recognised on both individual virus particles and on the same particle that has been wholly or partially self-assembled into virus coats. Cryptotopes are types of epitopes occurring on the facet of the virus particle that is obscured by self-assembly with other virus particles. These epitopes are therefore hidden from interaction with antibodies, hence the name *crypto*-tope. When two viral particles combine, they may create a single epitope that spans over both particles, thereby creating a new epitope (neotope) that cannot be recognised on either of the two particles alone before their assembly into a single antigenic entity. This concept is illustrated in Figure 2.23.

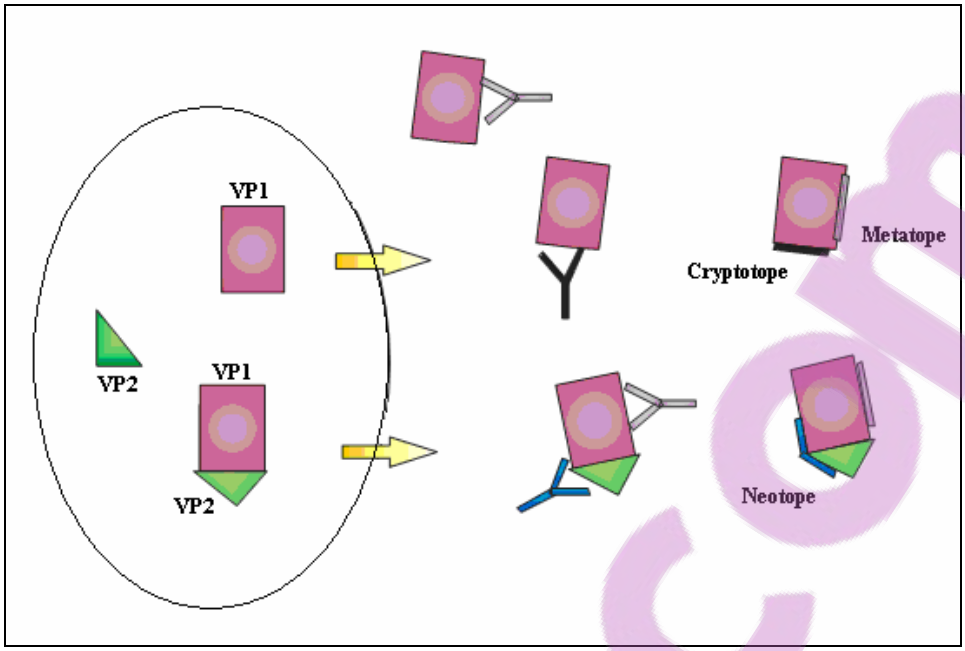

Figure 2.23: *Cartoon drawing of the different viral epitopes that are formed in the host cell and are recognised by different antibodies when secreted from the infected cell: cryptotope in black, metatope in lilac and neotope in blue.*

By analogy to the above figure, insight can be gained in the antibodies from TB^+ and TB^- patients recognising MAs and cord factor. The MA might have a cryptotope that can be recognised by anti-MA antibodies, as well as by anti-cholesterol antibodies that occur in all humans at different levels of expression and affinity. When MAs are linked to trehalose to form cord factor, this epitope might be hidden (cryptotope) and a new epitope (neotope) might form, one that can then only be recognised by anti-cord factor antibodies that occur in TB^+, but not in TB^- patient sera (Figure 2.24). The results imply that free MA may not be very useful in the serodiagnosis of TB, at least not when ELISA is used as the immunoassay. In contrast, cord factor appears as a very strong candidate to base TB serodiagnosis on. This finding corroborates the results reported by Fujita *et al.* in 2005 (64).

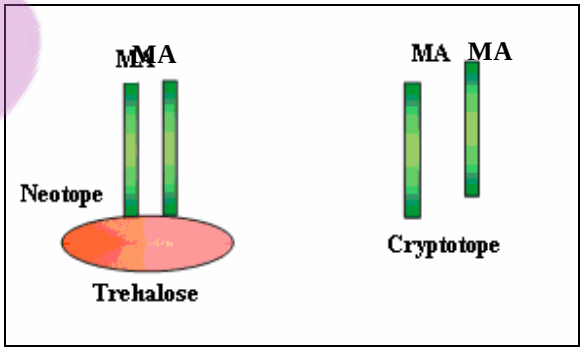

Figure 2.24: *Possible epitopes in MAs and cord factor that are recognised by different antibodies.*

2.4.2 Materials and methods

2.4.2.1 Mycolic acids used as antigens

2.4.2.1.1 Natural MA (nMA)

Natural MA was isolated from *M. tuberculosis* H37Rv, as described by Goodrum *et al.* (67), as a mixture of α-, keto- and methoxy-MAs as shown in Figure 1.7.

2.4.2.1.2 Natural mycolic aicd methyl esters (mMA)

Natural MA had to be esterified in order to be separated into the different subclasses. The COOH was methylated (67) to give COOMe as shown in Figure 2.25.

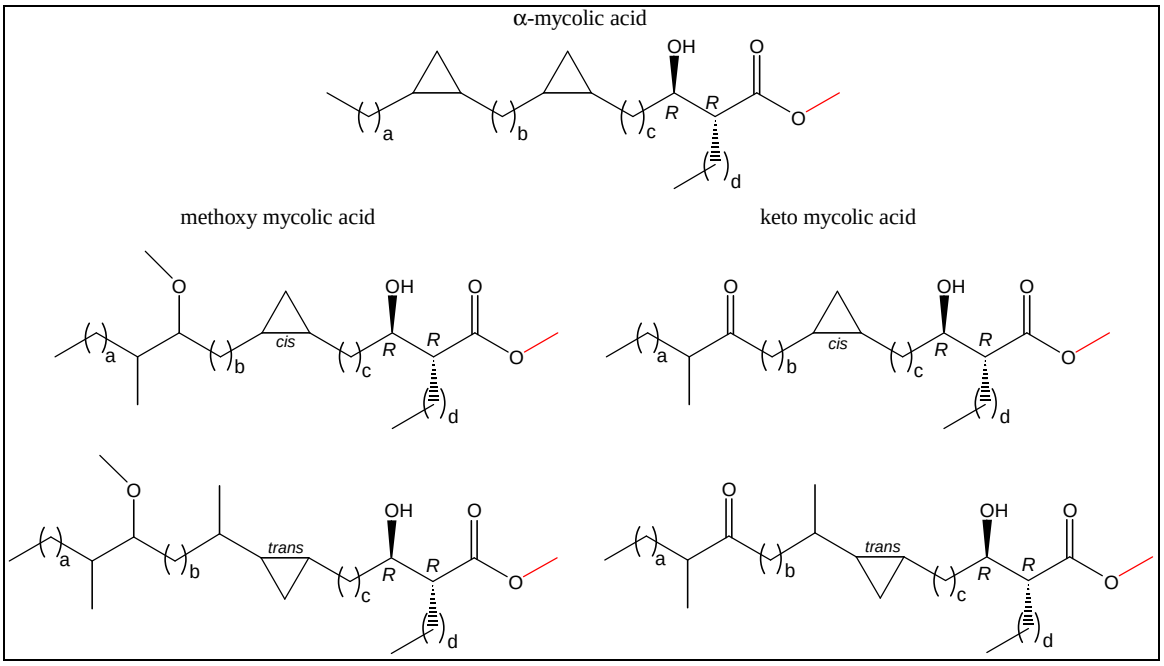

Figure 2.25: *Natural mycolic acid methyl esters.*

2.4.2.1.3 Mycolic acids (MA)

The methyl group from the natural mycolic acid methyl ester was removed by dissolving MA (10 mg) in a solution of potassium hydroxide and propan-2-ol (100 mg/ml, 1 ml). The mixture was stirred at 85 ºC for 3½ hours. The reaction was quenched by adding water (1 ml) and the MA was extracted 15 times with hexane. The organic layers were collected and dried over anhydrous calcium chloride, filtered and the hexane evaporated.

2.4.2.1.4 Alpha-MA (α-MA) and methoxy-MA (methoxy-MA)

The methylated natural MA was separated into the different subclasses and each subclass was demethylated as described in section *2.4.2.1.3*.

2.4.2.1.5 Natural alpha-MA from Prof Minnikin (Min α-MA)

Natural deprotected α-MA, from *M. tuberculosis*, was kindly provided by Prof D.E. Minnikin (University of Birmingham, UK). ^{1}H NMR showed minute amounts (about 1%) of methoxy-MA.

2.4.2.1.6 Cord factor (Trehalose-6,6'-dimycolate)

Commercial cord factor (Fig 2.26) was bought from Sigma, (Steinheim, Germany).

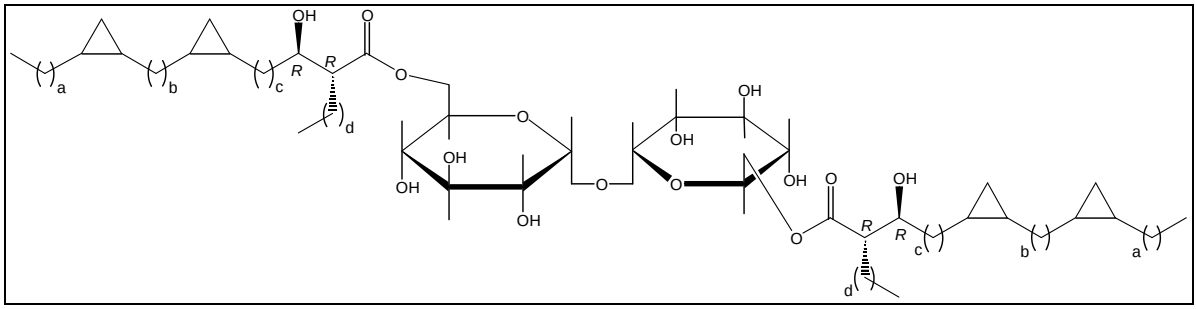

Figure 2.26: *Cord factor.*

2.4.2.2 Reagents and apparatus used in ELISA

ELISA plates: flat bottom, 96 wells (Bibby Sterilin Ltd., Sterilab, UK).

Phosphate buffered saline (PBS): 20 x PBS stock was prepared by dissolving sodium chloride (160 g; 99%, Merck, SA), potassium chloride (4 g; 99%, Merck, SA), di-hydrogen potassium phosphate (4 g, 99%, Merck, SA) and di-sodium hydrogen phosphate (23 g; 99%, Merck, SA) in double distilled de-ionized water to a final volume of 1000 ml.

PBS (1 x): 50 ml of the 20 x PBS solution was diluted in 950 ml dddH_2O. The pH of the solution was adjusted to 7.4 with 1 M NaOH.

Casein-PBS (0.5%): 5 g of casein (0.1% fat, 0.1% fatty acids; Merck, SA) were dissolved in a final volume of 1000 ml PBS by stirring at 37 °C for 2 hours. The pH was adjusted to 7.4 with 1 M sodium hydroxide and then stored at 4 °C overnight for use within the next day.

Goat anti-human IgG peroxidase conjugate: A 1/1000 dilution of the conjugate was prepared by adding peroxidase conjugate (10 µl; whole molecule, Sigma, Steinheim, Germany) to 0.5% casein PBS (10 ml) five minutes prior to use.

O-Phenylenediamine (OPD): (Sigma, St. Louis, MD, USA).
Hydrogen peroxide (H_2O_2): Tablets of urea, 33-35% per gram (Sigma, St. Louis, MD, USA).

0.1 M Citrate buffer: citric acid (0.1 M, 450 ml; Sigma, USA) was added to citrate tri-sodium (0.1 M, 450 ml; Sigma USA) until a pH of 4.5. The solution was brought to a final volume of 1000 ml with double distilled de-ionized water.

2.4.2.3 Human sera

TB positive, HIV positive, patient serum was kindly provided by Dr. A.C. Stoltz, Pretoria Academic Hospital, Pretoria, South Africa. TB negative, HIV negative, hospitalized patient serum were kindly provided by Dr. G. Schleicher, Helen Joseph Hospital, Auckland Park, Johannesburg, South Africa (127).

2.4.2.4 Preparation of coating solutions

The antigens were heated in PBS buffer (4 ml) for 20 minutes at 85 ºC on a heatblock. The hot solutions were vortexed for 10 seconds and sonified (Virsonic 600 – Ultrasonic cell disrupter, United Scientific, New York, USA), output level 2, 1 minute, 30 sec on and 30 sec off). The plates were coated by adding the hot solutions at 50 µl per well and storing at 4 ºC overnight. The final antigen load was approximately 3 µg/well for MAs. PBS was included as control. Coating of the wells was confirmed under the microscope as visible fatty deposits adsorbed on the polystyrene.

2.4.2.5 Blocking step

After 16 hours of incubation with antigen solution, the plates were aspirated and blocked with casein-PBS (400 µl per well) for 2 hours at room temperature.

2.4.2.6 Antibody binding

The blocking solution was aspirated before the serum was added (TB positive and TB negative, 1:20 dilution in casein-PBS, 50 µl per well). The plates were incubated for 1 hour at

room temperature, then washed with casein-PBS (3 times) using the ELISA plate washer (Anthos Autowash automatic ELISA plate washer, Labsystems) and aspirated.

2.4.2.7 Addition of conjugate and substrate

The goat anti-human IgG peroxidase conjugate (50 µl per well) was added and incubated for 30 minutes at room temperature. The plates were then washed with casein-PBS (3 times) and aspirated. The substrate solution (10 mg OPD, 8 mg H_2O_2 in 10 ml citrate buffer) was prepared immediately before use and added to the plates (50 µl per well). The plates were incubated at room temperature and the colour development was monitored at 10, 30, 40 and 50 minutes after addition of the substrate using a photometer (SLT 340 ATC photometer, Thermo-Labsystems, Finland) at wavelength of 450 nm.

Chapter 3

Synthesis of a methoxy mycolic acid

3.1 Introduction

3.1.1 Why synthesize mycolic acids?

Except for the mycolic acid motif, very little is known about the stereochemistry of the other chiral centres in the mero chain. It is also not known whether the stereochemistry is important at all. There are a few unanswered questions that need investigation: does the stereochemistry influence the folding of the molecule? Is it necessary for infection, evasion of the immune system, for survival in the host or any for biological activity? Is the methoxy-MA really more important than the α- and keto-MA? Is there one specific MA responsible for all this, or is it a combination of some of them, or all of them? These are complex molecules that are found in a variety of combinations of different functional groups as well as different chain lengths. How important the chain length and the position of the functional groups are and what exactly the structural requirements for functionality and antibody recognition are, remain to be discovered.

Apart from separation of MAs by TLC and HPLC, chemical synthesis provides another way for investigating the structure of MAs. Stereochemically controlled single enantiomers and diastereomers, which can not be separated and purified from natural MAs extracts, can be synthesized and the biological activity of each can be investigated separately.

3.1.2 Previous synthesis of mycolic acids

In 1982 Huang *et al.* (80) reported the total synthesis of naturally occurring monoalkene MAs from *M. smegmatis*. They synthesized *(E)*- and *(Z)-threo*-2-docosyl-3-hydroxytetracont-21-enoate. The key feature of this synthesis was the incorporation of the 2-docosyl side chain and functionalized main chain (R) in a regiospecific manner. The mycolic acid motif was synthesized by alkylation of methyl aceto acetate at C-2 with 1-iododocosane (Figure 3.1).

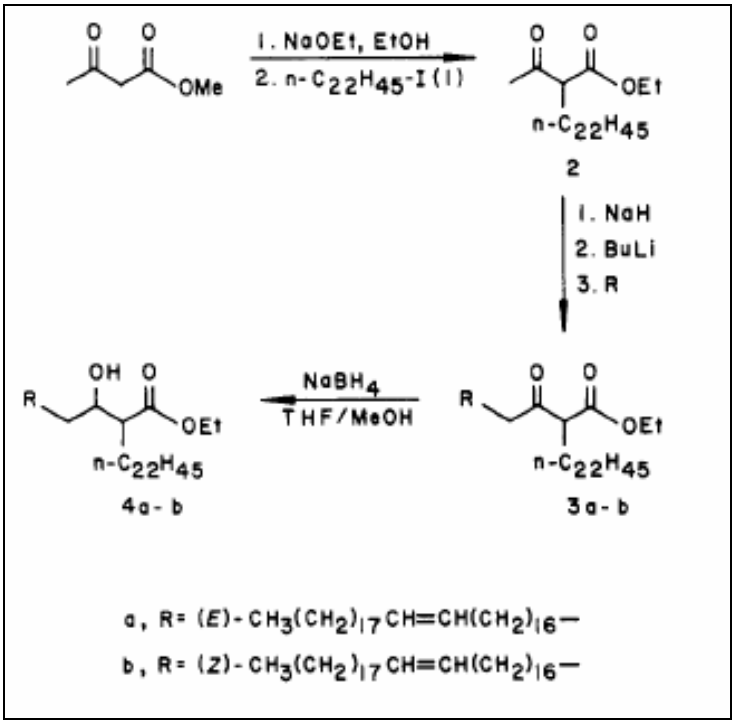

Figure 3.1: *Synthesis of a monoalkene MA from M. smegmatis (80).*

Al Dulayymi *et al.* (6, 7) described the synthesis of a single enantiomer of a major α-MA of *M. tuberculosis* (labelled MB for this study). They had a different approach to synthesizing the mycolic acid motif than reported by Huang *et al.* (80). Figure 3.2 shows how they started from a ring opening of the epoxide **(a)** with a Grignard reagent prepared from 9-bromo-nonan-1-ol tetrahydropyranyl ether which led to a single enantiomer of **(b)**. This was converted, in a few steps, to the diol **(c)**. The next step was the protection of the primary alcohol and the alkylation of the α-carbon to give the ester **(d)**. Acetylation of the β-hydroxy, deprotection and oxidation of the primary alcohol yielded the aldehyde **(e)**, which was coupled to the dicyclopropane sulfone **(f)** in a modified Julia reaction to give the protected α-MA **(g)**.

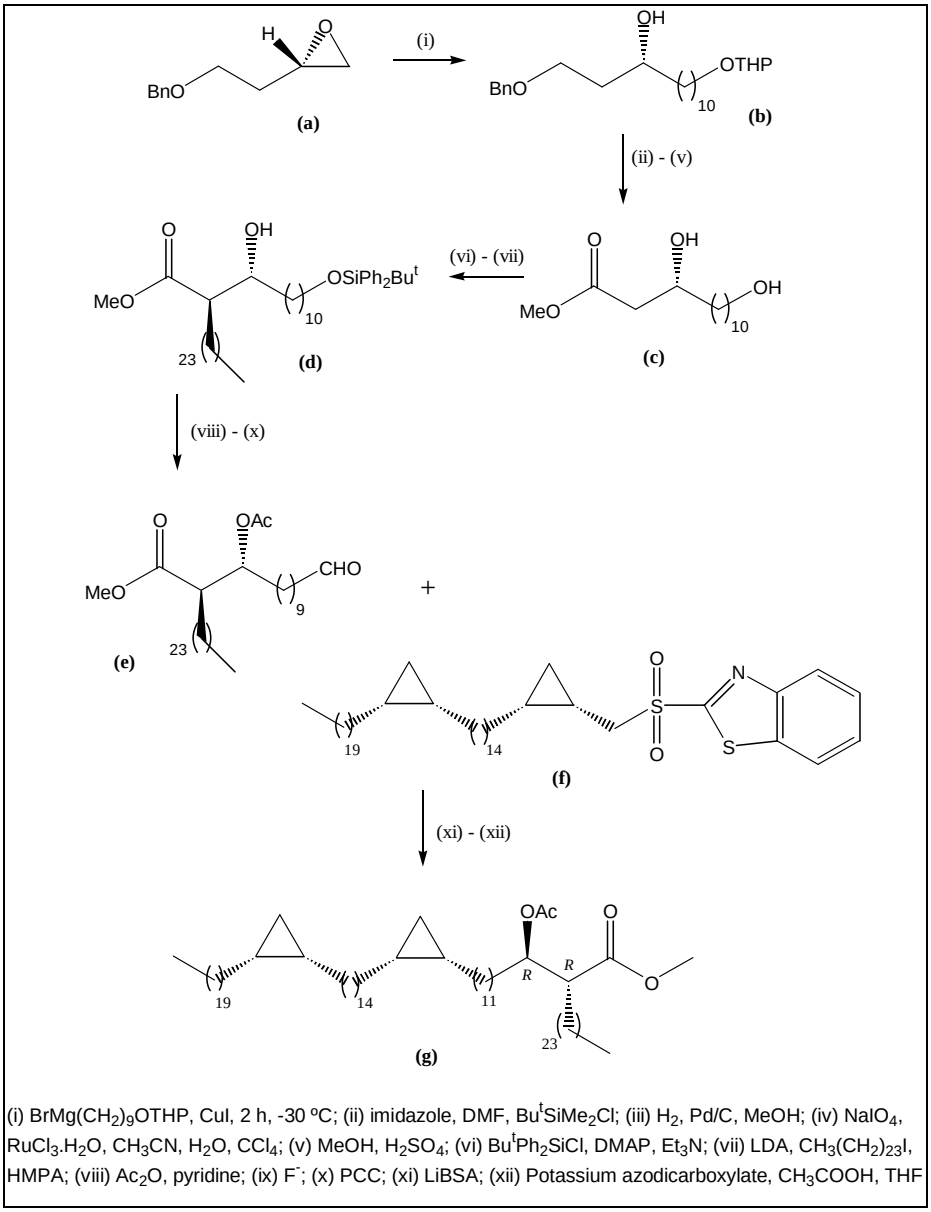

Figure 3.2: *Synthesis of protected α-MA, modified from (7).*

They also reported the synthesis of single enantiomers of a mero MA (8) and one isomer of the α-methyl-*trans*-cyclopropane unit (5) (Figure 3.3).

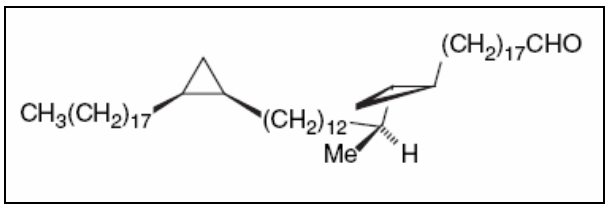

Figure 3.3: *α-Methyl-trans-cyclopropane mero aldehyde (5).*

Coxon *et al.* described the synthesis of enantiomers of lactobacillic acid and MA analogues (37, 39) containing *cis*-cyclopropanes, as well as the synthesis of methyl 5-(1'*R*,2'*S*)-(2-octadecylcyclopropane-1-yl)pentanoate and other ω-19 chiral cyclopropane fatty acids and esters related to mycobacterial MAs (38). These (shown in Figure 3.4) were assayed for inhibition of MA biosynthesis using a cell-wall preparation from *M. smegmatis*. The assay measured elongation of endogenous fatty acid precursors associated with the cell wall extracts. From all the analogues tested, **(V)** and **(XII)** showed marginal inhibition of MA biosynthesis, whereas the other all stimulated biosynthesis. Stimulation might be a result of direct incorporation of the long-chain cyclopropane compounds, but extensive investigation is necessary.

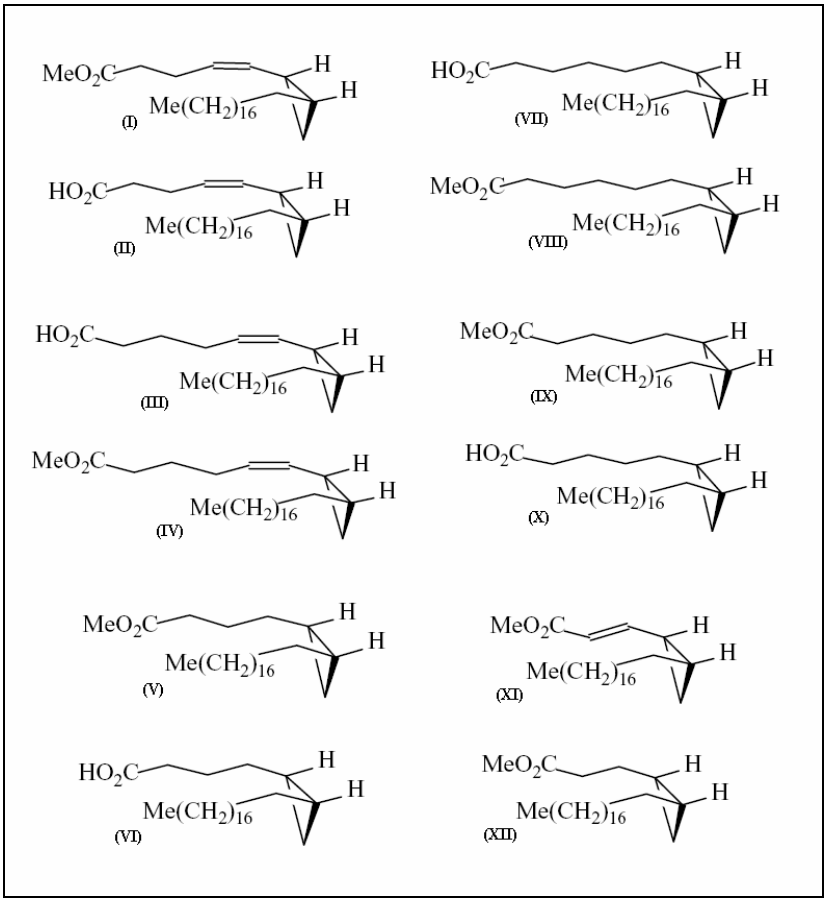

Figure 3.4: *(1*R,*2*S*) Long-chain ω-19 cyclopropane fatty acids and esters related to mycobacterial MAs (38).*

3.1.3 Cholesterol and mycolic acids

Siko (134) investigated cholesterol binding to MAs and found that if a biosensor cuvette surface was coated with natural MAs in liposomes, cholesterol accumulated onto the surface. This was not seen when empty PC liposomes were added to the MA surface (Figure 3.5).

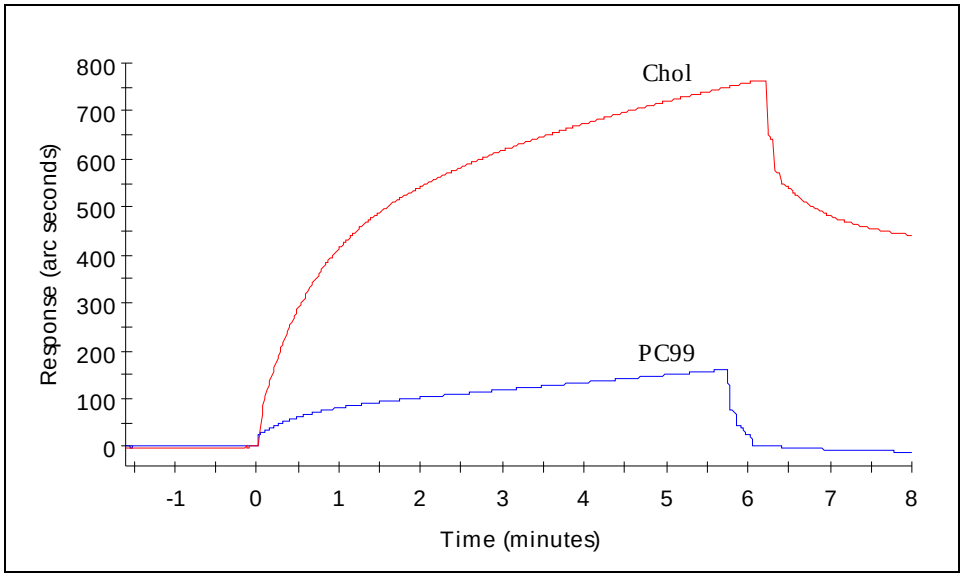

Figure 3.5: *Biosensor binding profile of cholesterol on a MA-coated surface. Chol = binding profile after addition of cholesterol/PC99 liposomes; PC99 = binding profile after adding PC99 liposomes (134).*

Based on this observation and results from ELISA, where antibody binding to MAs were also found to bind cholesterol, a possible existence of molecular relatedness between MAs and cholesterol and different MAs folding structures was investigated. Benadie (24) found that if a biosensor surface was coated with either MA or cholesterol, Amphotericin B (a known bactericide) accumulated onto the MA or cholesterol surface. This further supports a structural and functional relation between MA and cholesterol. A folded structure of the oxygenated MA species (methoxy-MAs and keto-MAs, Figure 3.6) was drawn that could explain such a possible structural relation. The methoxy-MAs could assume a folded structure in which relation to cholesterol could be seen. The methoxy-group of MAs corresponds to the hydroxyl position of cholesterol. In the folded structure with all the oxygenated groups on one side of the molecule and a hairpin bend induced by the cyclopropane moiety in the long hydrocarbon chain of MAs, a ‘mimicry’ of the structure of cholesterol appeared feasible. Keto-MAs would probably not ‘mimic’ cholesterol, as the plane introduced by the double bond between the oxygen and carbon might prevent formation of such a structure.

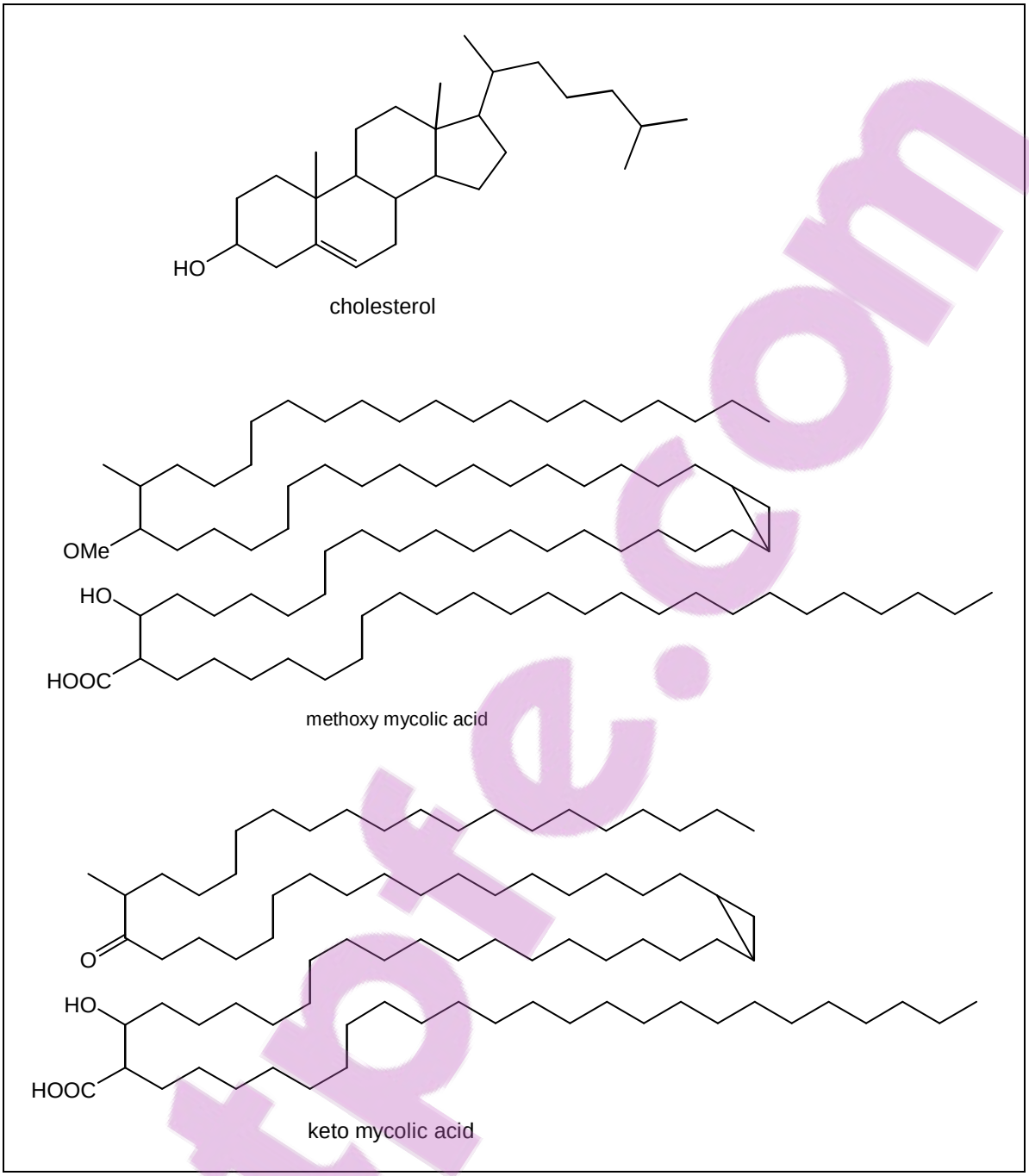

Figure 3.6: *The structures representing the possible molecular mimicry between the methoxy-MAs, keto-MAs and cholesterol (134).*

3.2 Aim

The aim was to synthesize the diastereomer (Figure 3.7 - **A**) of the previously synthesized *cis*-cyclopropane methyl methoxy-MA, synthesised by Dr J. Al Dulayymi (University of Wales, Bangor, UK) (Figure 3.7 - **B**), in order to prove the stereochemistry of the *cis*-cyclopropane and to determine the biological activity/antigenicity of different synthesized MAs.

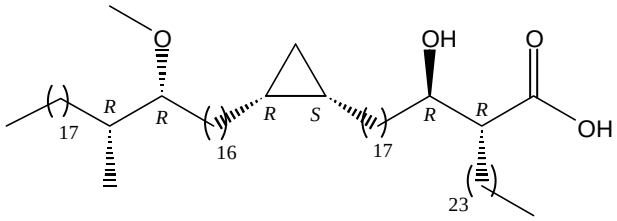

(A)

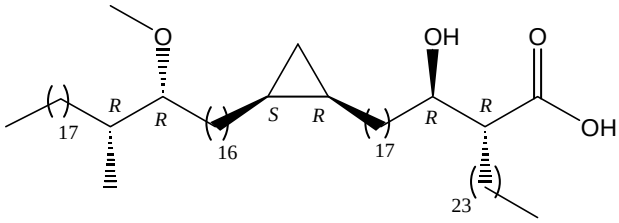

(B)

Figure 3.7: *The two diastereomers of cis-cyclopropane methyl methoxy-MA*

3.3 Synthesis of a methoxy mycolic acid

3.3.1 Results and discussion

The MA can be decoupled to give the mycolic acid motif and the meromycolate chain. In turn, the meromycolate chain can be decoupled to give the methoxy part and the cyclopropane part as shown in Figure 3.8. The synthesis of these different parts and the coupling to get the full MA is described and shown in Figures 3.9-3.19.

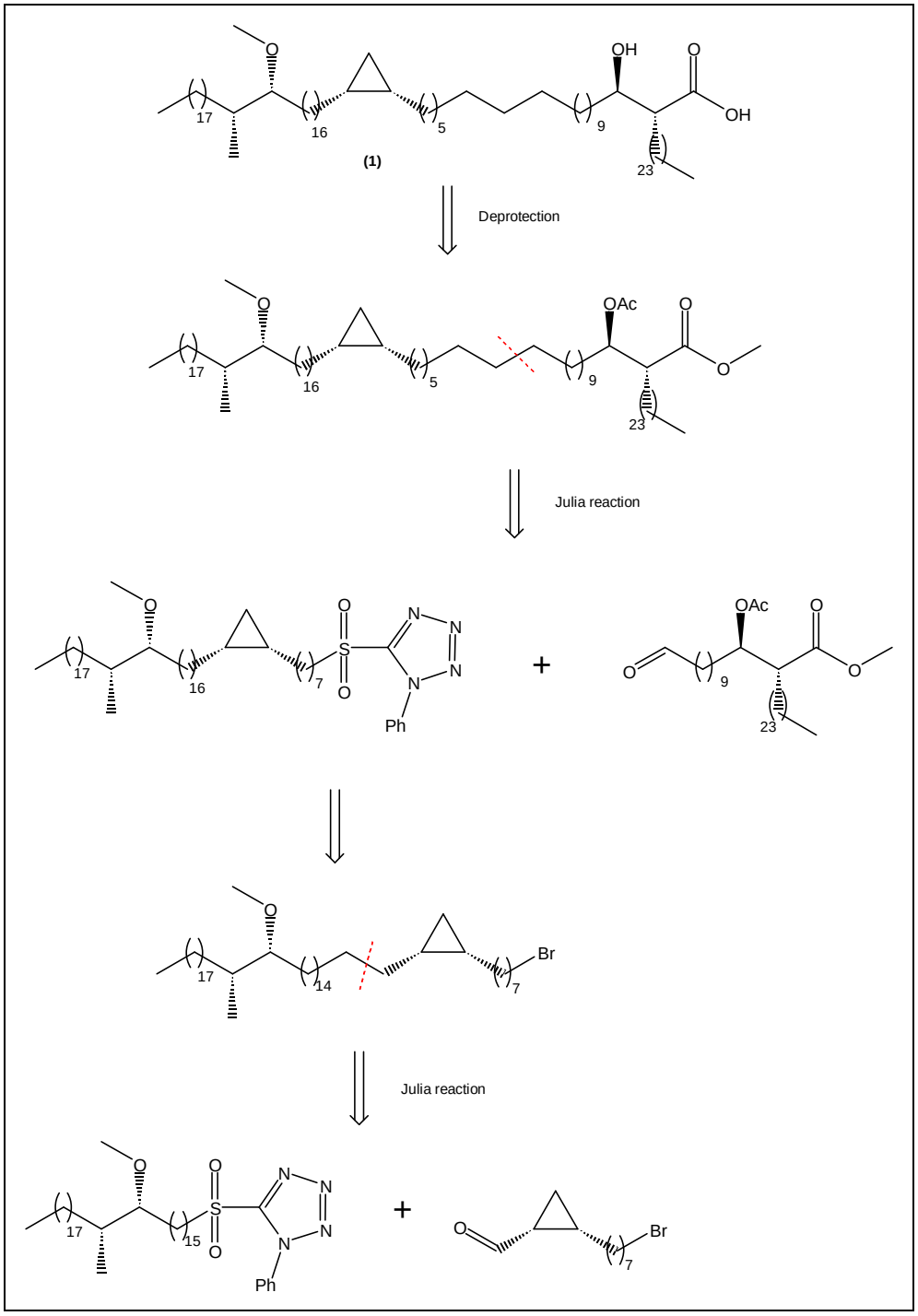

Figure 3.8: *Retrosynthesis of (R)-2-{(R)-1-acetoxy-18-(1S,2R)-2-((17R,18R)-17-methoxy-18-methylhexatri-acontyl)-cyclopropyl}-octadecyl}-hexacosanoic acid.*

To synthesize *cis*-methyl methoxy-MA **(1)**, *D*-mannitol was used as starting material. The two terminal hydroxyl groups on each end were protected by being stirred in acetone and $ZnCl_2$, then the 1,2 diol was oxidised to the aldehyde and attached to triethyl phosphonoacetate in a Wittig reaction to give the alkene **(3)**. A methyl group was added to the β-carbon in a Michael addition in dry ether at -78 °C. The reduction of the ester **(4)** using lithium aluminium hydride

in dry THF gave the alcohol **(5)**, which was oxidised using PCC in dichloromethane to give the aldehyde **(6)** as shown in Figure 3.9.

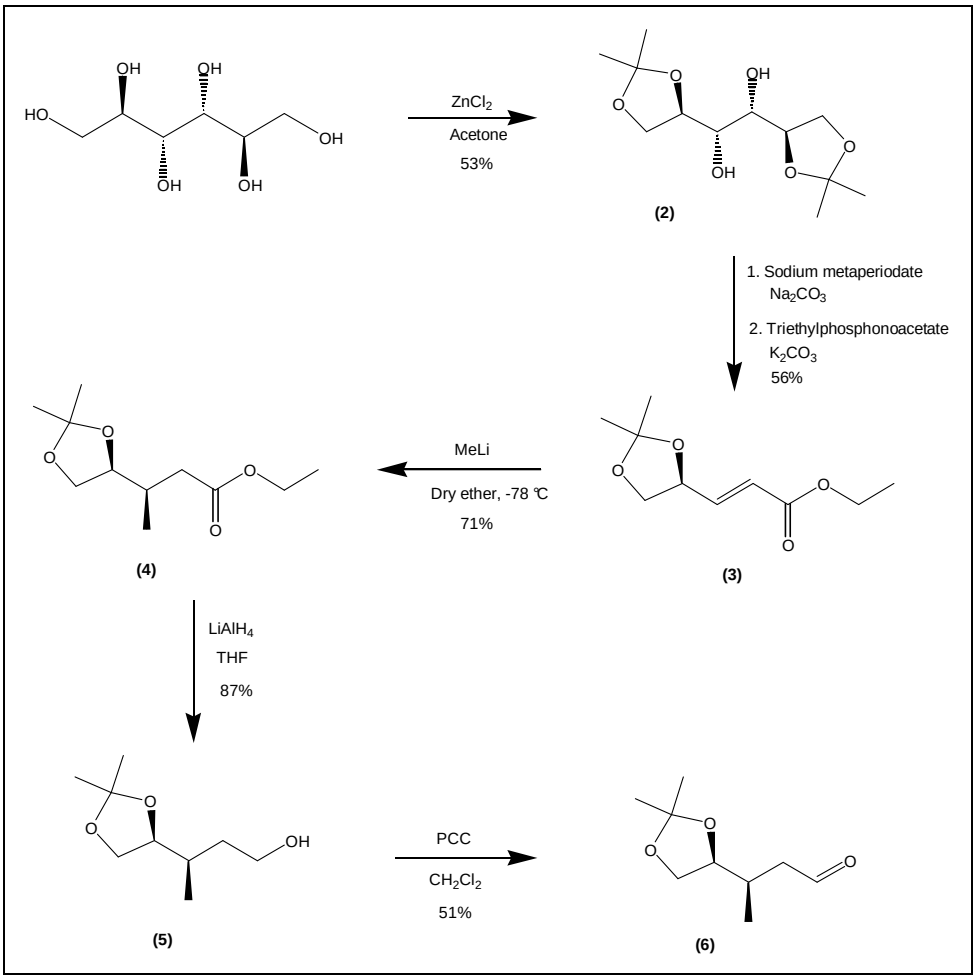

Figure 3.9: *Synthesis of (R)-3-((S)-2,2-dimethyl-[1,3]-dioxolan-4-yl)-butyraldehyde.*

The ^{1}H NMR spectrum of **(3)** showed two double doublets for the protons at the double bond at δ 6.85 (*J* 5.65, 15.75 Hz) and 6.07 (J 1.6, 15.75 Hz) respectively. In the ^{1}H NMR of **(4),** these signals disappeared and it showed a doublet at δ 0.98 (*J* 6.6 Hz) for the methyl group. The IR spectrum of the alcohol **(5)** showed a broad peak at 3426 cm^{-1} for O-H stretching. The ^{1}H NMR spectrum of the aldehyde **(6)** showed a triplet for the proton of the aldehyde at δ 9.79 (*J* 1.9 Hz) and the ^{13}C NMR spectrum included the carbonyl signal at δ 201.7.

5-(Hexadecane-1-sulfonyl)-1-phenyl-1*H*-tetrazole **(9)** was synthesized, as shown in Figure 3.10, to extend the chain length of the aldehyde **(6)** from C_2 to C_{17}. 1-Bromohexadecane **(7)** was reacted with 1-phenyl-1*H*-tetrazole-5-thiol and anhydrous potassium carbonate in acetone

to give the sulfide **(8)** which was oxidised with ammonium molybdate (VI) tetrahydrate and H_2O_2 in THF and IMS to give **(9)**.

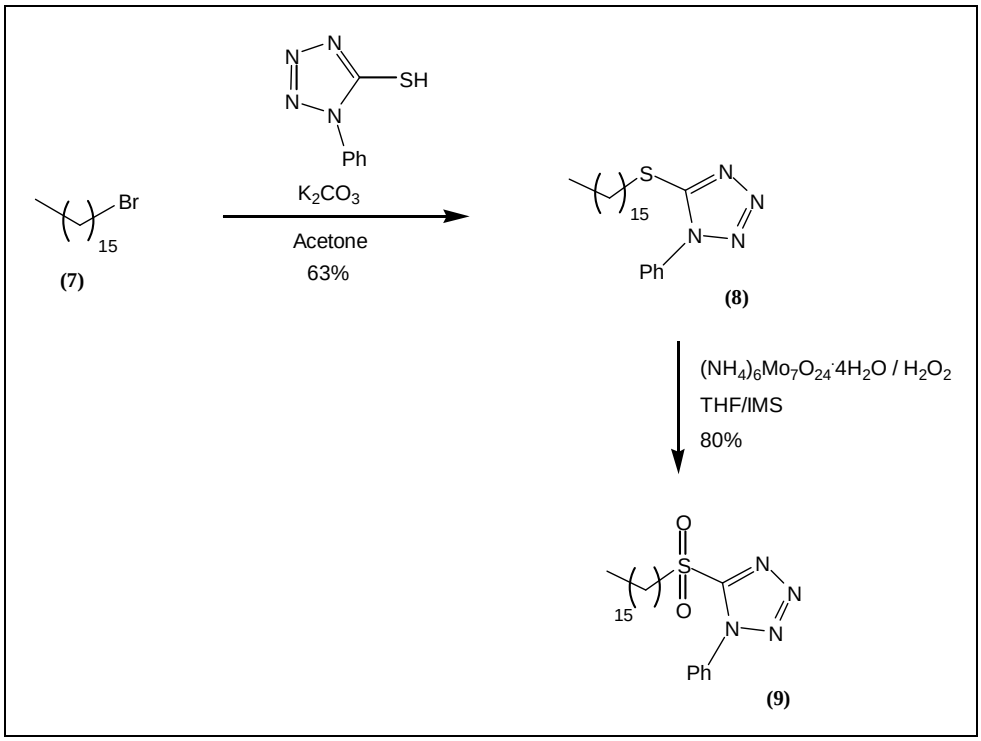

Figure 3.10: *Synthesis of 5-(Hexadecane-1-sulfonyl)-1-phenyl-1H-tetrazole.*

The ^{1}H NMR spectrum of **(9)** showed the phenyl group protons as two multiplets at δ 7.70 and 7.61, and a distorted triplet at δ 3.73 (*J* 7.85 Hz) for the two chain protons next to the sulfone.

The aldehyde **(6)** was reacted with 5-(hexadecane-1-sulfonyl)-1-phenyl-1H-tetrazole **(9)** in a Julia reaction using lithium bis(trimethylsilyl)amide in dry THF to give two isomers of the olefin. These both gave (*S*)-2,2-dimethyl-4-((*R*)-1-methyl-nonadecyl-[1,3]-dioxolane **(10)** after being hydrogenated by using Pd on C as a catalyst, as shown in Figure 3.11. The dioxolane group was deprotected using *p*-toluenesulfonic acid in methanol, THF and water to give the diol **(11)**. The epoxide **(12)** was formed by reacting the diol **(11)** with *p*-toluenesulfonic chloride, sodium hydroxide and cetrimide in dichloromethane and this was protected and the chain length extended in a Grignard reaction with 6-tetrahydropyranyloxyheptyl magnesium bromide and copper iodide in THF to give 2-((8*R*,9*R*)-8-hydroxy-9-methyl-heptacosyloxy)-tetrahydropyran **(13)**. The hydroxyl group was changed to a methoxy-group in a reaction with methyl iodide and sodium hydride in THF to give the methyl methoxy-compound **(14)**. The

THP group was deprotected by using *p*-toluenesulfonic acid monohydrate and the alcohol **(15)** was oxidized to the aldehyde (**16**) using PCC in dichloromethane as shown in Figure 3.11.

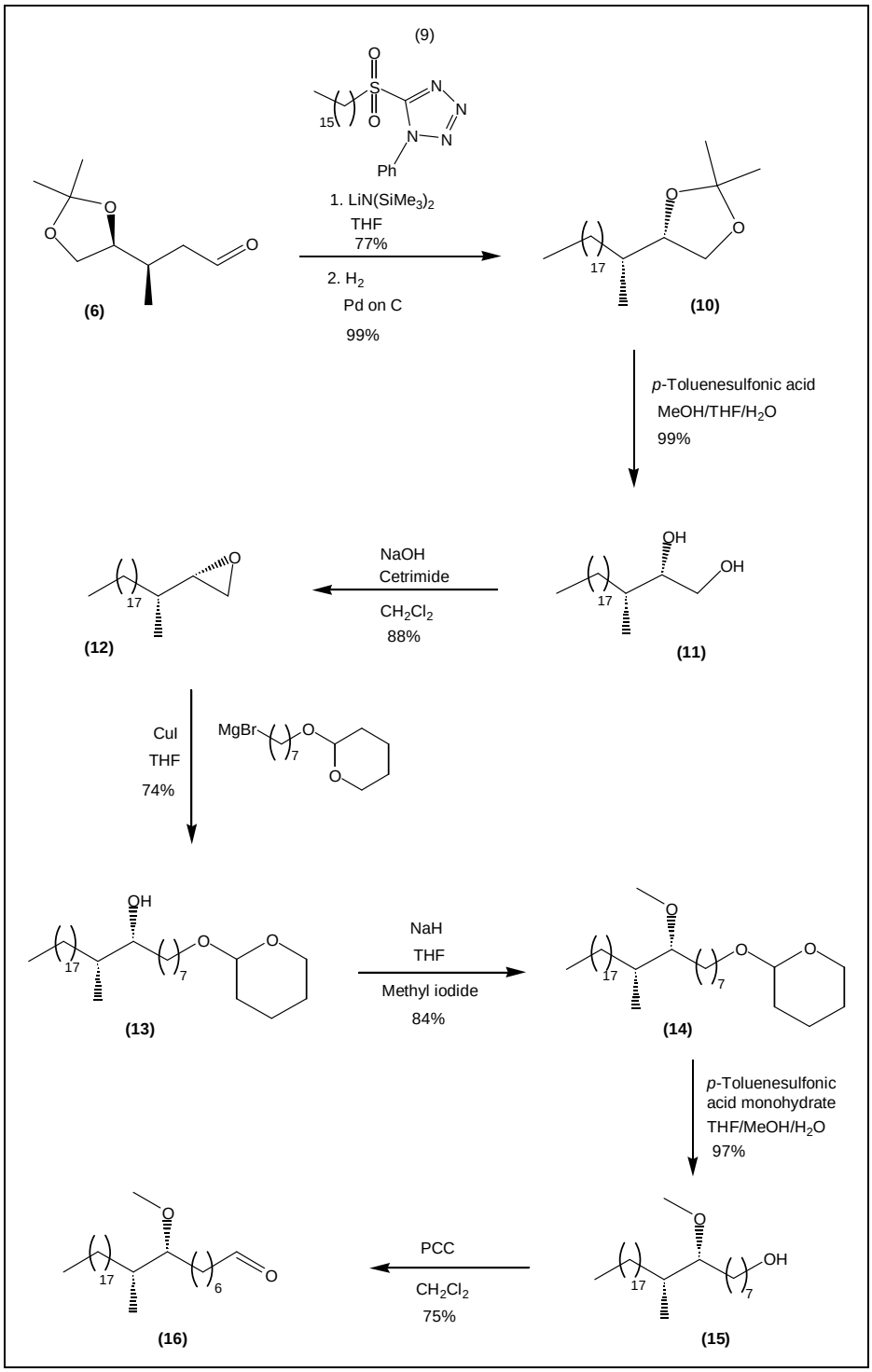

Figure 3.11: *Synthesis of (8R,9R)-8-methoxy-9-methyl-heptacosanal.*

The ^{1}H NMR spectrum of **(10)** showed two singlets at δ 1.41 and 1.36 for the two methyl groups of the protecting group which disappeared after deprotection. The IR spectrum of the

diol **(11)** showed a broad peak at 3283 cm^{-1} and that of **(13)** showed a broad peak at 3360 cm^{-1}, both for O-H stretching. The ^{1}H NMR spectrum of the methyl methoxy-compound **(14)** showed a singlet at δ 3.34 for the methyl group on the oxygen. The IR spectrum of the alcohol **(15)** showed a broad peak at 3373 cm^{-1} for the O-H stretching. The ^{1}H NMR spectrum of the aldehyde **(16)** included a triplet for the proton of the aldehyde at δ 9.79 (*J* 1.9 Hz) and the ^{13}C NMR spectrum included the carbonyl signal at δ 201.7.

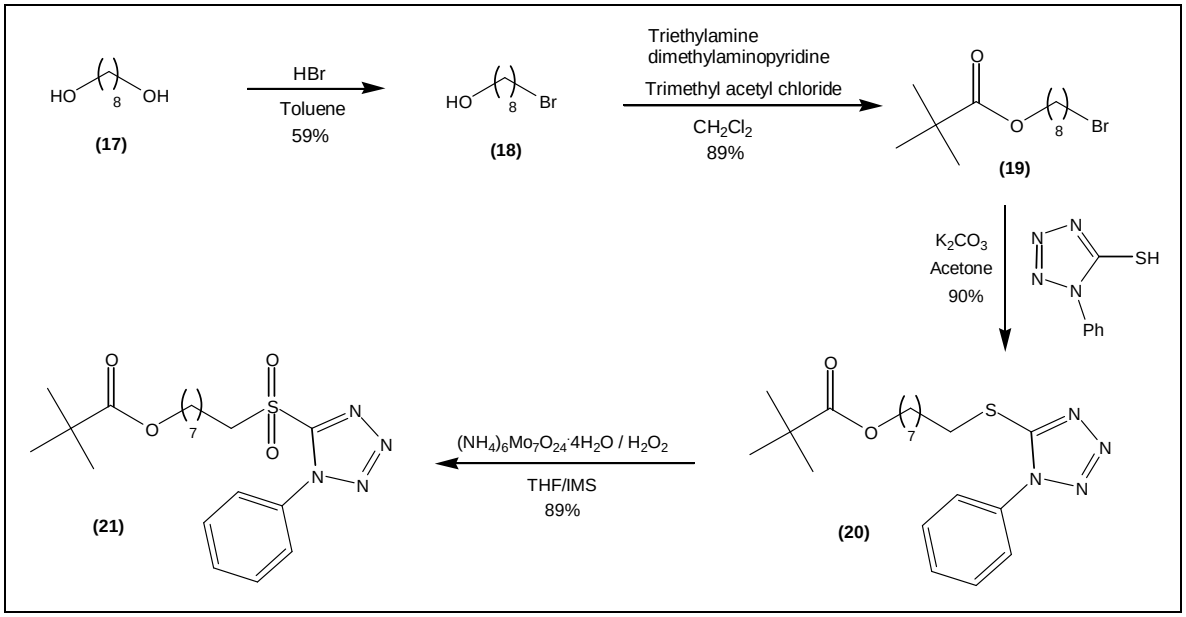

Figure 3.12: *Synthesis of 5-(1-octanolpivalate-8-sulfonyl)-1-phenyl-1H-tetrazole.*

5-(1-Octanolpivalate-8-sulfonyl)-1-phenyl-1*H*-tetrazole **(20)** was prepared to extend the chain of the aldehyde **(16)** from C_7 to C_{15}, as shown in Figure 3.12. Bromination of the diol **(17)** was done by refluxing the diol with HBr in toluene, and then the alcohol group on 8-bromo-octan-1-ol **(18)** was protected with trimethyl acetyl chloride, triethylamine and dimethylaminopyridine in dichloromethane to give 2,2-dimethyl-propionic acid 8-bromo-octyl ester **(19)**. The Julia reagent **(21)** was then prepared as described before for **(9)**.

The ^{1}H NMR spectrum of **(21)** showed the phenyl group protons as two multiplets at δ 7.69 and 7.61, a triplet for the two protons next to the oxygen at δ 4.04 (*J* 6.6 Hz), a distorted triplet at δ 3.73 (*J* 7.85 Hz) for the two protons next to the sulfone and a singlet at δ 1.19 for the three methyl groups of the protecting group. The ^{13}C NMR spectrum included the carbonyl signal at δ 178.5.

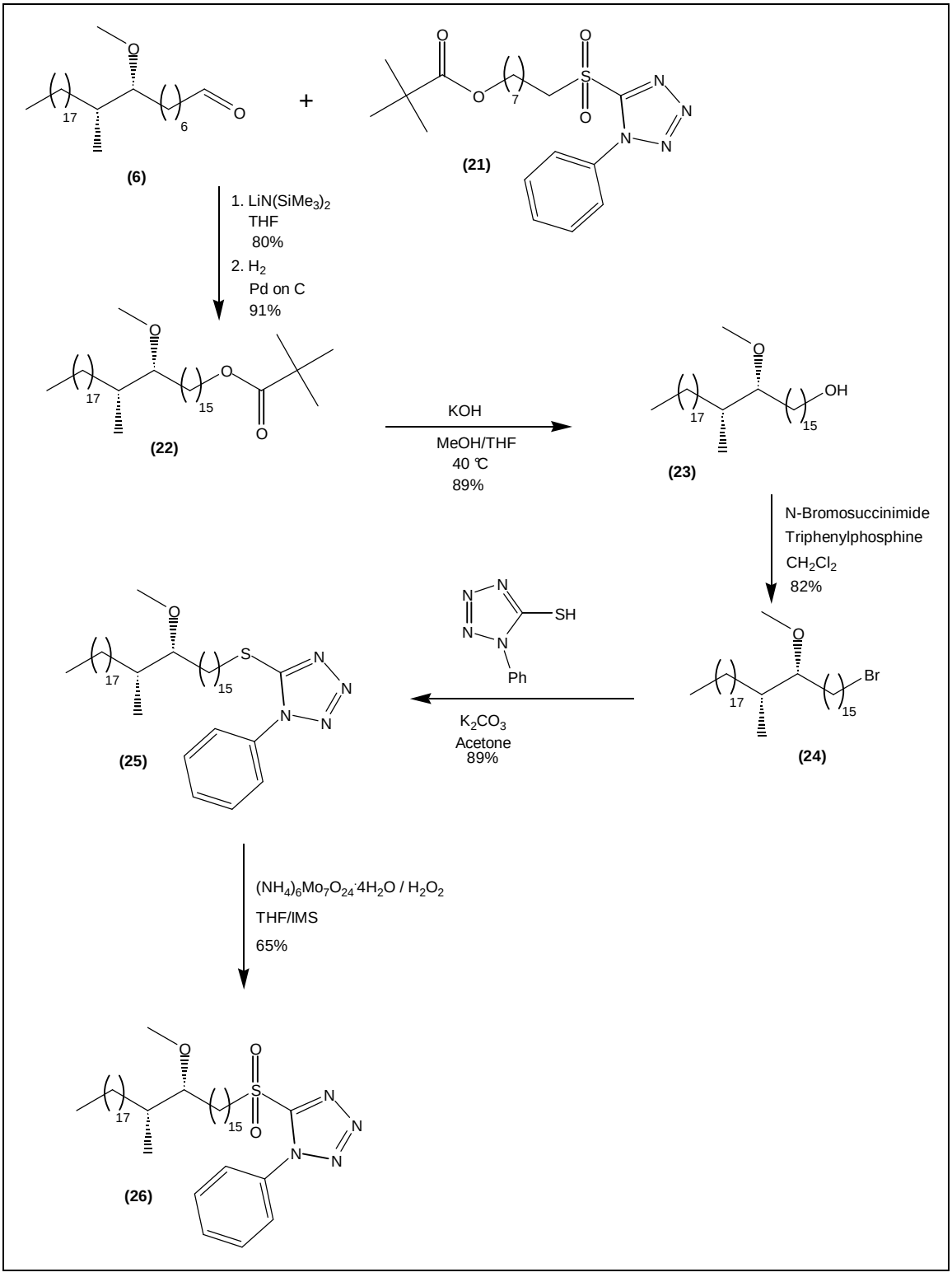

Figure 3.13: *Synthesis of 5-((16R,17R)-16-methoxy-17-methyl-pentatriacontane-1-sulfanyl)-1-phenyl-1H-tetrazole.*

The tetrazole **(21)** was then reacted with the aldehyde **(6)** using lithium bis(trimethylsilyl)amide in dry THF to give two isomers of the olefin which were saturated with hydrogen using Pd on C as catalyst to give compound **(22)**, as shown in Figure 3.13. The

ester **(22)** was hydrolised to the alcohol **(23)** using KOH in MeOH and THF, which was then brominated using *N*-bromosuccinimide and triphenylphosphine in dichloromethane to give **(24)**. The Julia reagent **(26)** was prepared as described before for **(9)**.

The ^{1}H NMR spectrum of **(22)** showed a singlet at δ 1.19 for the three methyl groups of the protecting group which disappeared after deprotection of the THP group. The IR spectrum of the alcohol **(23)** showed a broad peak at 3426 cm^{-1} for O-H stretching which disappeared after bromination **(24)**.

The addition of sodium methoxide to a mixture of methyl chloroacetate and methyl acrylate gave the *cis*- and *trans*- isomers of the cyclopropane ester **(27a, 27b)**. The *cis*-isomer was successfully separated by column chromatography and was reduced to the diol **(28)** with lithium aluminium hydride in THF. The diol was then protected with butyric anhydride to give the diester **(29)**, which was enzymatically hydrolysed to give a single enantiomer of the hydroxyl cyclopropane ester **(30)**. The Julia reagent **(33)** was prepared from the bromo cyclopropane ester **(31)** as shown in Figure 3.14.

The ^{1}H NMR spectrum of the *cis*-cyclopropane **(27b)** showed a double doublet at δ 2.08 (*J* 6.9, 8.5 Hz) and two triplet of doublets at δ 1.70 (*J* 5, 6.6, 13.2 Hz) and δ 1.26 (*J* 5.05, 8.55, 16.7 Hz) for the four protons of the cyclopropane, and a singlet at δ 3.70 for the two methyl groups of the diester, which disappeared after reduction to the alcohol. The ^{13}C NMR spectrum of showed the carbonyl signal at δ 170.21. The ^{1}H NMR spectrum of the alcohol **(30)** showed a double doublet at δ 4.46 (*J* 5.7, 12 Hz), a multiplet at δ 3.83 and a double doublet at δ 3.39 (*J* 9.15, 11.65 Hz) for the protons next to the oxygen atoms. The cyclopropane ring protons appeared as a multiplet at δ 1.30, a triplet of doublets at δ 0.84 (*J* 5.05, 8.5, 16.7 Hz) and a quartet at δ 0.22 (*J* 5.65 Hz). The IR spectrum showed a broad peak at 3426 cm^{-1} for O-H stretching and the optical rotation was +16.95. The ^{1}H NMR spectrum of the Julia reagent **(33)** showed the phenyl group protons as two multiplets at δ 7.70 and 7.63, four double doublets at δ 4.37 (*J* 5.7, 12.3 Hz), δ 4.03 (*J* 5.4, 14.85 Hz), δ 3.92 (*J* 8.2, 12 Hz) and δ 3.67 (*J* 8.85, 15.15 Hz) for the protons next to the sulfone and oxygen atoms, respectively. The protons of the cyclopropane ring appeared as a multiplet at δ 1.49, a triplet of doublets at δ 1.03 (*J* 5.7, 8.5 Hz) and a quartet at δ 0.60 (*J* 5.7 Hz).

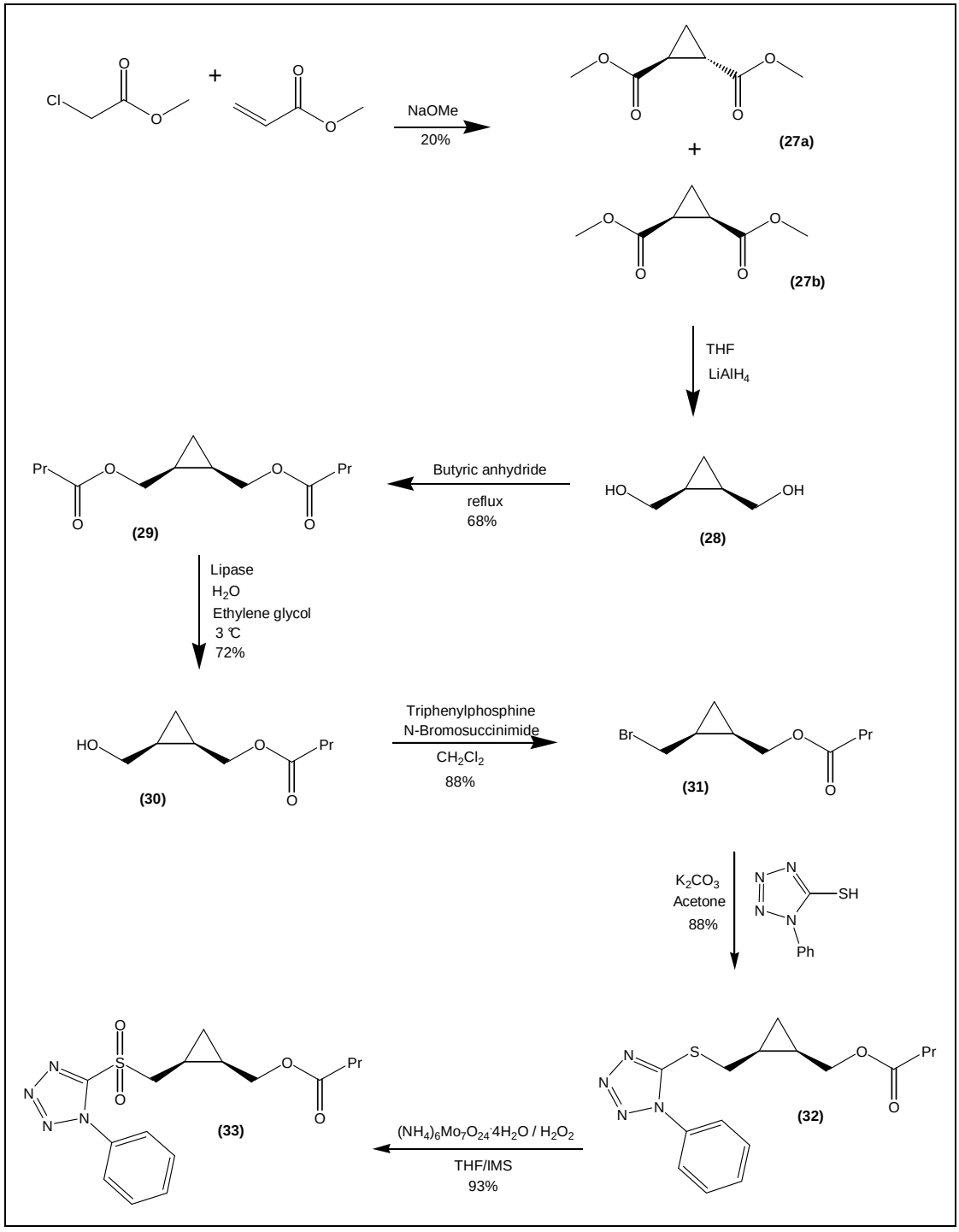

Figure 3.14: *Synthesis of butyric acid cis-2-(1-phenyl-1H-tetrazole-5-sulfonylmethyl)-cyclopropyl methyl ester.*

The Julia reagent **(33)** was coupled with 6-bromo-hexanal **(34)** to elongate the carbon chain next to the cyclopropane from C_1 to C_6 using lithium bis(trimethylsilyl)amide in dry THF to give two isomers of the olefin which were saturated with hydrogen using 2,4,6-triisopropylbenzene sulfonohydrazide to give butyric acid 2-(7-bromo-heptyl)-cyclopropyl methyl ester **(35)**, as shown in Figure 3.15. The ester **(35)** was then hydrolysed to the alcohol

(36) and then oxidised to the aldehyde **(37)** by using PCC in dichloromethane to be coupled to the Julia reagent **(26)**.

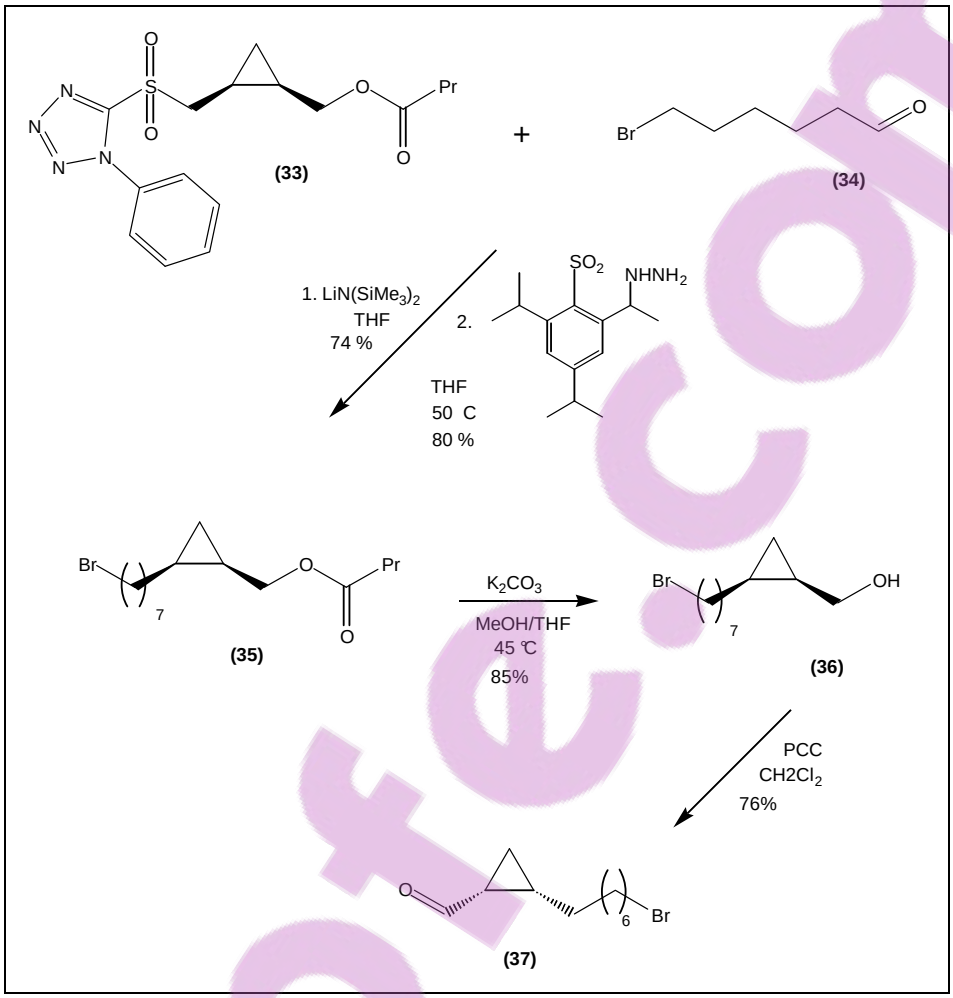

Figure 3.15: *Synthesis of 2-(7-bromo-heptyl)-cyclopropane carbaldehyde.*

The ^{1}H NMR spectrum of the bromocyclopropane ester **(35)** showed two double doublets at δ 4.19 (*J* 6.9, 11.65 Hz) and δ 3.93 (*J* 8.8, 11.65 Hz) for the two protons next to the oxygen which shifted to δ 3.65 (*J* 7.25, 11.35 Hz) and δ 3.57 (*J* 8.2, 11.35 Hz) for the two protons next to the hydroxyl group of the bromo cyclopropane alcohol **(36)**. The optical rotation for the alcohol was +12.87. The ^{1}H NMR spectrum of the aldehyde **(37)** showed the proton of the aldehyde as a doublet at δ 9.37 (*J* 5.4 Hz), a triplet at δ 170.21 (*J* 6.6 Hz) for the two protons next to the bromine and the protons of the cyclopropane appeared as a multiplet at δ 1.49, and two triplet of doublets at δ 1.24 (*J* 4.75, 7.9 Hz) and δ 1.19 (*J* 5.05, 6.6 Hz). The ^{13}C NMR spectrum included the carbonyl signal at δ 201.64 and the optical rotation was measured as +8.19 (-10.1 reported by Dr. J. Al Dulayymi for the enantiomer).

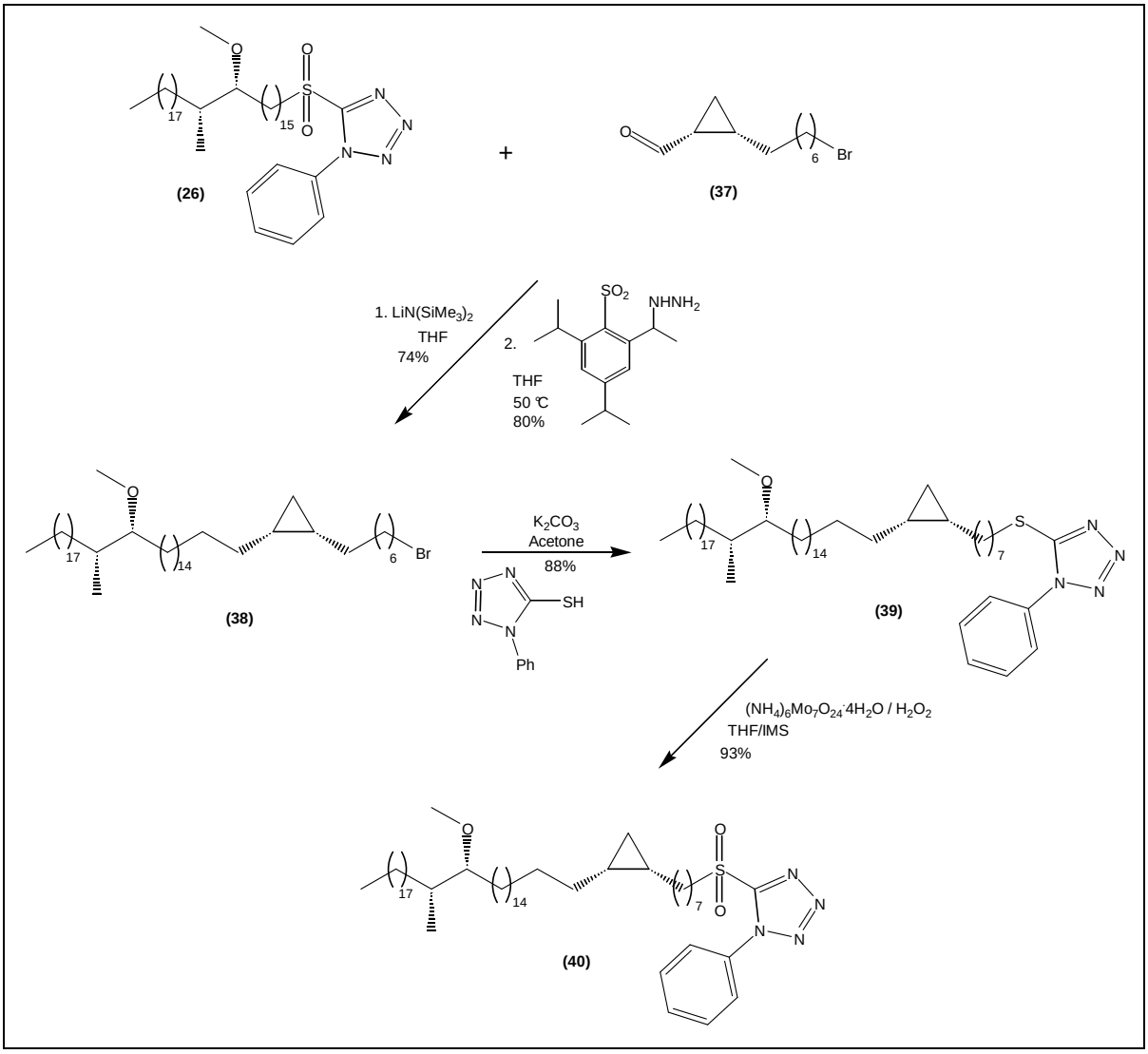

Figure 3.16: *Synthesis of 5-(7-[1R,2S]-2-((17R,18R)-17-methoxy-18-methyl-hexatriacontyl)-cyclopropyl)-heptyl sulfanyl)-1-phenyl-1H-tetrazole.*

The Julia reagent **(26)** and the aldehyde **(37)** was coupled using lithium bis(trimethylsilyl)amide in dry THF to give two isomers of the olefin which were saturated with hydrogen using 2,4,6-triisopropylbenzene sulfonohydrazide to give 1-(7-bromo-heptyl)-2-((17*R*,18*R*)-17-methoxy-18-methyl-hexatriacontyl)-cyclopropane **(38)** from which the Julia reagent **(40)** was prepared, as shown in Figure 3.16. This was prepared to be coupled to the mycolic acid motif.

The ^{1}H NMR spectrum of the Julia reagent **(40)** showed two multiplets at δ 7.71 and δ 1.70 for the protons of the phenyl group and a distorted triplet at δ 3.74 (*J* 7.9 Hz) for the two protons next to the sulfone. The methyl group on the oxygen appeared as a singlet at δ 3.35, the other

two methyl groups as a triplet at δ 0.89 (*J* 6.65 Hz) and a doublet at δ 0.86 (*J* 6.65 Hz). The cyclopropane ring protons appeared as a multiplet at δ 0.66, a triplet of doublets at δ 0.58 (*J* 3.75, 7.85 Hz) and a quartet at δ -0.32 (*J* 5.05 Hz) and the optical rotation was measured as +4.4 (+4.13 reported by Dr J. Al Dulayymi for a diastereomer).

To synthesize the mycolic acid motif, 8-bromo-octan-1-ol was used as starting material, the alcohol was protected with THP in dry dichloromethane and the bromide was replaced with iodide while being stirred in acetone and $NaHCO_3$ to give **(41)**. This was coupled with propagyl alcohol in liquid ammonia to extend the carbon chain from C_8 to C_{11} to give two isomers of the olefin which were saturated with hydrogen using nickel acetate tetrahydrate to give the alcohol **(42),** which was protected with trimethyl acetyl chloride in dichloromethane to give the ester **(43)** as shown in Figure 3.17. The ester **(43)** was then hydrolysed to the alcohol **(44)** by using *p*-toluenesulfonic acid monohydrate in THF, methanol and water. The alcohol was then oxidised to the aldehyde **(45)** by using PCC in dichloromethane to be coupled to (methoxycarbonylmethylene)-triphenylphosphorane as shown in Figure 3.17.

The ^{1}H NMR spectrum of the alcohol **(44)** showed a singlet at δ 1.19 for the three methyl groups of the protecting group and the IR spectrum showed a broad peak at 3384 cm^{-1} for O-H stretching. The ^{1}H NMR spectrum of the aldehyde **(45)** showed the proton of the aldehyde as a triplet at δ 9.76 (*J* 1.55 Hz) and a singlet at δ 1.19 for the three methyl groups of the protecting group. The ^{13}C NMR spectrum included the carbonyl signals at δ 202.83 for the aldehyde and at δ 178.62 for the protecting group.

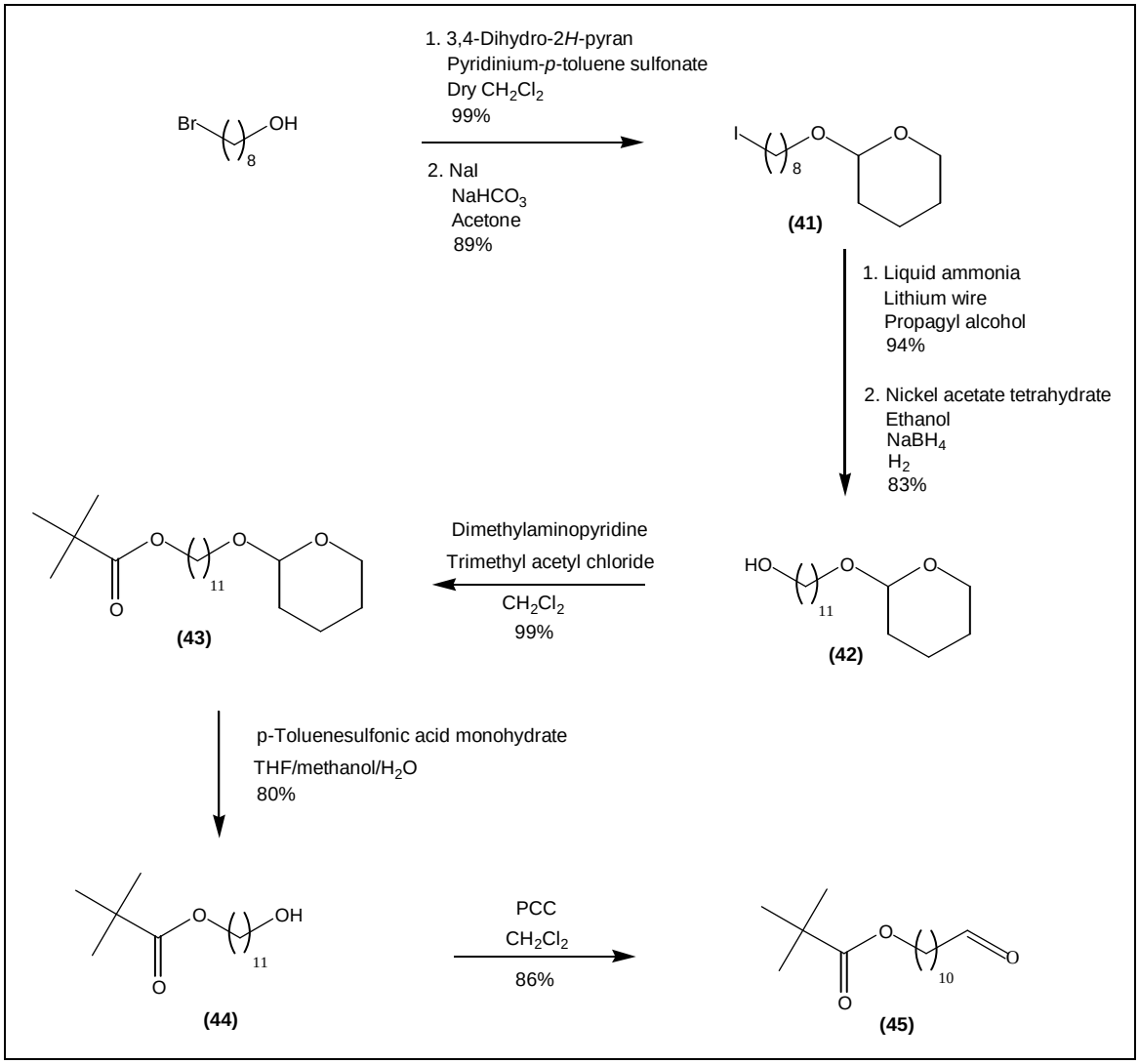

Figure 3.17: *Synthesis of 2,2-dimethyl-propionic acid-11-oxo-undecyl ester.*

The aldehyde **(45)** was coupled to (methoxycarbonylmethylene) triphenylphosphorane to give 13-(2,2-dimethyl-propionyloxy)-tridec-2-enoic acid methyl ester **(46)** which was oxidized using $(DHQD)_2PHAL$, K_3Fe_6, potassium carbonate, osmium tetroxide and methane sulfone amide to give the diol **(47)**. This was reacted with thionyl chloride in CCl_4 and then oxidized with $NaIO_4$ and ruthenium trichloride hydrate to give the cyclic sulfone ester **(48),** which was stirred in DMAC and sodium borohydrate to give the alcohol ester **(49)**. The acidic proton between the hydroxyl and the carbonyl groups was removed with freshly prepared LDA and coupled to allylic iodide to give the allyl ester **(50)**, as shown in Figure 3.18.

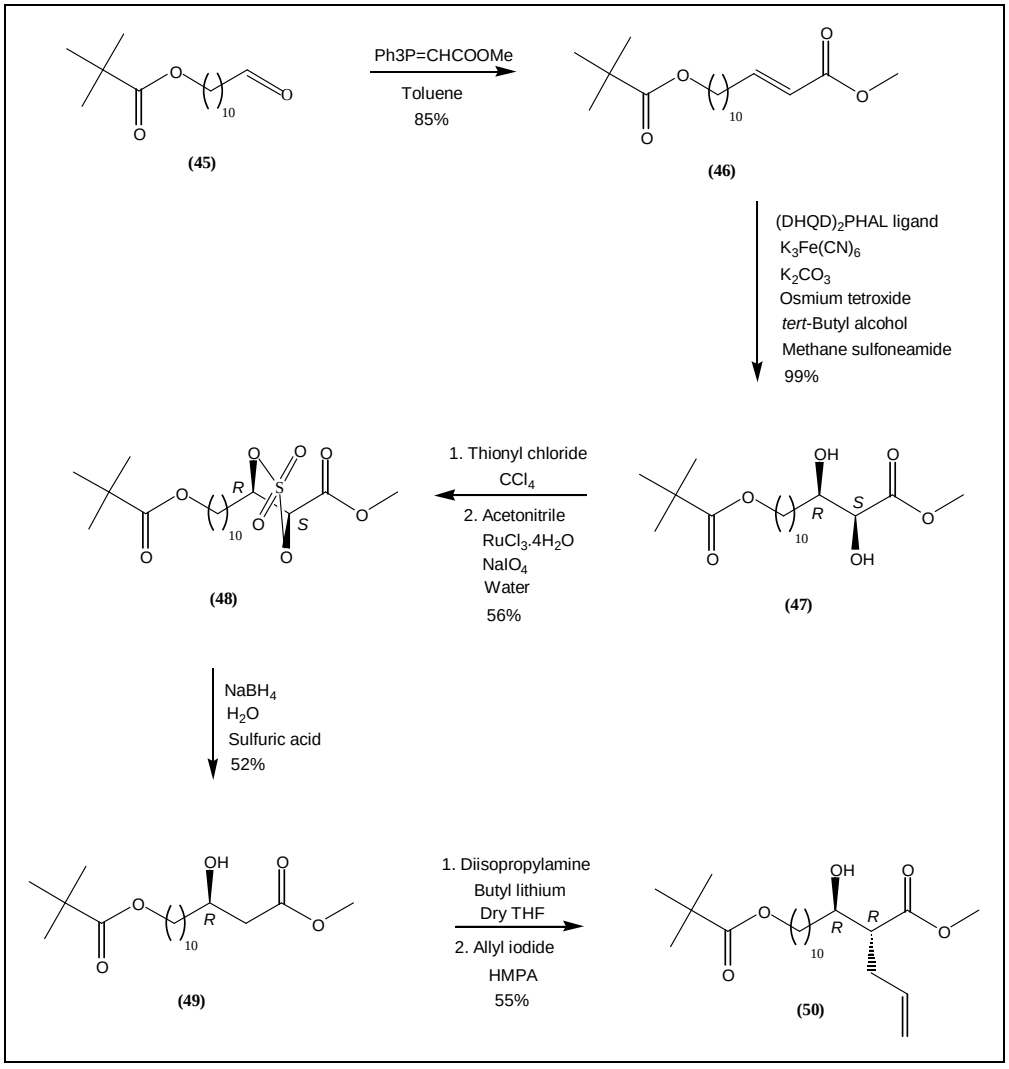

Figure 3.18: *Synthesis of (2R,3R)-2-allyl-[11-(2,2-dimethyl-propionyloxy)-1-hydroxy-undecyl]-pent-4-enoic acid methyl ester.*

The ^{1}H NMR spectrum of **(46)** showed the two protons of the double bond as two double triplets at δ 6.79 (*J* 6.95, 15.45 Hz) and at δ 5.81 (*J* 1.6, 15.45 Hz) which disappeared after the oxidation to the diol **(47)**. IR spectrum of **(47)** showed a broad peak at 3449 cm^{-1} for the OH-stretching. The ^{1}H NMR spectrum of the cyclic sulfone **(48)** showed the two protons next to the oxygens bound to the sulfone as a double of triplets at δ 4.95 (*J* 5.05, 7.25 Hz) and a doublet at δ 4.89 (*J* 7.25 Hz). The ^{1}H NMR spectrum of the alcohol **(54)** showed two double doublets for the two protons between the hydroxyl group and the carbonyl group at δ 2.51 (*J* 3.15, 16.4 Hz) and δ 2.41 (*J* 9.15, 16.5 Hz) and the IR spectrum showed a broad peak at 3517 cm^{-1} for OH-stretching. The ^{1}H NMR spectrum of the allylic ester **(50)** showed a multiplet at δ 5.75, a double doublet at δ 5.11 (*J* 0.95, 17 Hz) and a broad doublet at δ 5.05 (*J* 10.05 Hz) for

the three protons of the double bond. The IR spectrum showed a peak at 3524 cm^{-1} for OH-stretching and a peak at 1642 cm^{-1} for the double bond.

Methyl (2*R*,3*R*)-3-acetoxy-2-tetracosanyl-13-hydroxytridecanoate **(51)** (kindly provided by Dr J. Al Dulayymi, University of Wales, Bangor, UK) was oxidised to the aldehyde **(52)** by using PCC in dichloromethane. This was coupled to the Julia reagent **(40)** using lithium bis(trimethylsilyl)amide in dry THF to give two isomers of the olefin, which were saturated with hydrogen using dipotassium azodicarboxylate to give the full protected methoxy-MA **(53)** The final step was the elimination of the OAc and the methyl group to give the final product **(1)** as shown in Figure 3.19.

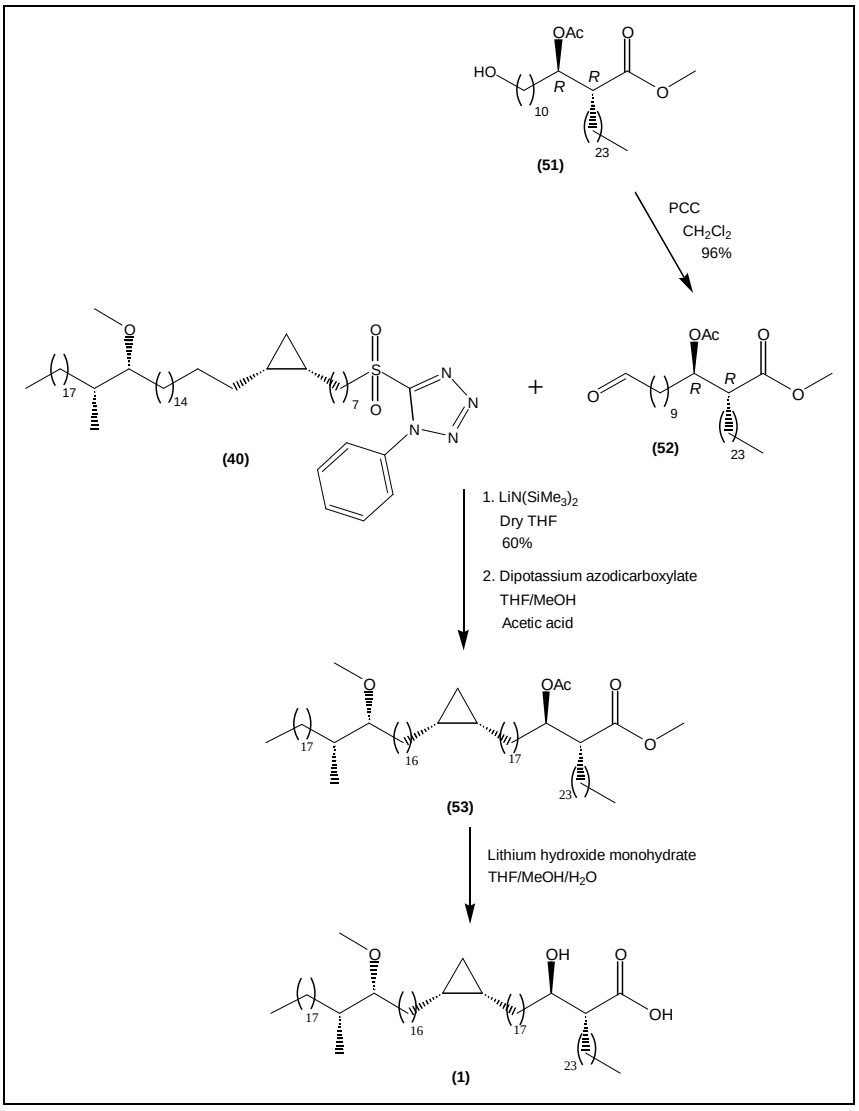

Figure 3.19: *Synthesis of (R)-2-{(R)-1-hydroxy-18-(1S,2R)-2-((17R,18R)-17-methoxy-18-methyl hexatri acontyl)-cyclopropyl}-octadecyl-hexacosanoic acid.*

The ^{1}H NMR spectrum of the protected MA **(53)** showed double triplets at δ 5.09 (J 3.8, 7.9 Hz) for the proton next to the OAc group and two singlets at δ 3.69 and δ 3.35 for the protons of the two methoxy groups. The proton next to the methoxy-group appeared as a multiplet at δ 2.96, the α proton appeared as a double double doublet at δ 2.62 (J 4.4, 6.95, 14.8 Hz) and the protons of the methyl group of the OAc group appeared as a singlet at δ 2.04. The spectrum also showed a triplet at δ 0.89 (*J* 6.6 Hz) for the six protons of the two terminal methyl groups and a doublet at δ 0.85 (*J* 6.9 Hz) for the methyl group next to the methoxy in the meromycolate chain. The cyclopropane ring protons appeared as a multiplet at δ 0.65, a triplet of doublets at δ 0.58 (*J* 4.1, 7.9 Hz) and a quartet at δ -0.32 (*J* 5.05 Hz). The ^{13}C NMR spectrum included two carbonyl signals at δ 173.65 and δ 170.33. The optical rotation was measured as +7.69 (+7.17 reported by Dr. J. Al Dulayymi for a diastereomer). In the ^{1}H NMR spectrum for the final MA **(1)**, the double of triplets at δ 5.09 (J 3.8, 7.9 Hz) for the proton next to the OAc group, and the singlet at δ 3.69 for the protons of the methyl ester group disappeared. Instead, the proton next to the β-OH group appeared as a multiplet at δ 2.99-2.95. The optical rotation was measured as +6.95.

3.3.2 Experimental

General considerations

All chemicals were purchased form Lancaster Synthesis Ltd. (UK), Aldrich Chemical Co. Ltd. (UK), or Avocado Chemical Co. Ltd (UK). Diethyl ether and THF were distilled over sodium and benzophenone under a nitrogen atmosphere, while dichloromethane was distilled over calcium hydride. Distilled solvents were used within one day. Organic solutions were dried over anhydrous magnesium sulfate. Bulk solvents were removed under vacuum at 14 mm Hg and residual traces of solvent were finally removed at 0.1 mm Hg. All glassware used in anhydrous reactions were dried for not less than 5 hours at 250 °C. Column chromatography was done under medium pressure using silica gel (particle size 33-70 μm) from DBH Chemicals (UK); thin layer chromatography (TLC) was carried out on pre-coated Kieselgel 60 F254 (Art. 5554, Merck, UK) plates. Routine gas liquid chromatography (GLC) was performed using a temperature programmable Hewlett-Packard (Agilent) 5890 Gas Chromatograph with manual injection. The carrier gas was 5.0 grade helium with a column head pressure of 100 KPa supplied by Air Products plc (UK). The column was Rtx-5 supplied by Restek Corporation (USA). The phase thickness was 25 μm, the column internal diameter 0.31 mm and the column length 15 m. Optical rotations of compounds were measured in solutions of

chloroform at known concentration using a Polar 2001 Automatic Polarimeter, with the assistance of Dr J. Al Dulayymi (University of Wales, Bangor, UK). Infra-red spectra were recorded as KBr disc (solid) or thin films (liquid) on NaCl windows using a Perkin Elmer 1600 series FT-IR spectrometer. NMR spectra were recorded either on a Bruker AC 250 spectrometer with 5 mm dual probe or on Bruker Advance 500 spectrometer with 5 mm BBO probe. Compounds analysed were solutions in denatured chloroform ($CDCl_3$), unless indicated differently. All chemical shifts are quoted in δ relative to the trace resonance of protonated chloroform (δ 7.27 ppm) and $CDCl_3$ (δ 77.0 ppm). Low resolution mass spectra using electron impact (EI) were measured at 70 eV on a Hewlett-Packard (Agilent) 5970 quadrupole mass selective detector where the Gas Chromatograph was a Hewlett-Packard (Agilent) 5890 Gas Chromatograph with a 5975 auto sampler. It contained a Rtx-5 column supplied by Restek Corporation (USA). The phase thickness was 25 μm, the column diameter 0.25 mm and the column length 25 m.

3.3.2.1 Preparation of 1,2,5,6-di-O-isopropylidene-D-mannitol (2)

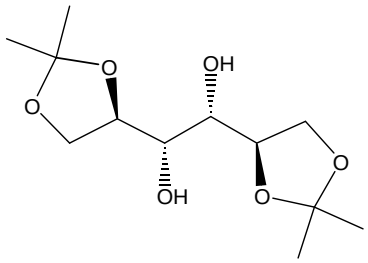

D-Mannitol **(1)** (30.31 g, 166.38 mmol) was added to a stirring solution of zinc chloride (60.75 g, 445.74 mmol, 2.7 mol eq.) in acetone (300 ml) at RT and the mixture was stirred for 18 hours at RT. Potassium carbonate (50.23 g, 363.43 mmol) in water (50 ml) was added to the reaction mixture resulting in the precipitation of a white crystalline solid (zinc chloride and potassium carbonate). The mixture was vacuum filtered, the precipitate washed with dichloromethane (4 x 100 ml) and the solvent evaporated to yield a viscous oil. This oil was dissolved in dichloromethane (200 ml) and washed with water (2 x 75 ml). The organic layer was separated and washed with brine (150 ml), dried and evaporated to give a white solid. The crude product was recrystallised from ethyl acetate (60 ml) and petroleum ether (300 ml) to give *1,2,5,6-di-O-isopropylidene-D-mannitol* **(2)** as a white solid (18.76 g, 43%).

Physical properties:

ν_{max}/cm^{-1}: 3288, 2987, 1371, 1208, 1157, 1065

δ_H (500 MHz, $CDCl_3$): 4.21 (2H, q, *J* 6.3 Hz), 4.13 (2H, dd, *J* 6.6, 8.5 Hz), 3.98 (2H, dd, *J* 5.65, 8.5 Hz), 3.76 (2H, t, *J* 6 Hz), 2.55 (2H, d, *J* 6.3 Hz), 1.43 (6H, s), 1.37 (6H, s)

δ_C (500 MHz, $CDCl_3$): 109.39, 76.37(-), 71.29(-), 66.73(+), 26.70(-), 25.18(-), [+ = CH_2, - = CH, CH_3]

3.3.2.2 Preparation of ethyl-4,5-O-isopropylidene-(S)-4,5-dihydroxy-2-pentanoate (3)

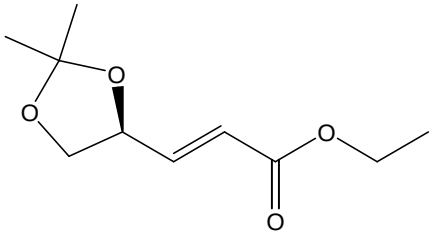

A solution of sodium metaperiodate (18.38 g, 85.92 mmol, 1.20 mol eq.) in water (100 ml) was added to a stirring solution of sodium carbonate (9.59 g, 90.48 mmol, 1.25 mol eq.) and 1,2,5,6-di-O-isopropylidene-D-mannitol **(2)** (18.76 g, 71.60 mmol) in water (150 ml) at 5 °C (the temperature was kept below 5 °C). The reaction mixture was allowed to reach RT and stirred for 1 hour. The mixture was then cooled to 0 °C and triethylphosphonoacetate (34.3 ml, 30.45 g, 136.04 mmol) and potassium carbonate (37.60 g, 272.08 mmol) in water (50 ml) was added and the mixture stirred for 20 hours at RT. The product was extracted with dichloromethane (3 x 200 ml) and the combined organic layers were washed with brine (200 ml), dried and evaporated to give a oily residue which was purified by column chromatography on silica gel eluted with petroleum ether/diethyl ether (5:1) to give *ethyl-4,5-O-isopropylidene-(S)-4,5-dihydroxy-2-pentanoate* **(3)** (15.10 g, 56%) (109).

Physical properties:

ν_{max}/cm^{-1}: 2985, 2937, 2875, 1725, 1662

δ_H (500 MHz, $CDCl_3$): 6.85 (1H, dd, *J* 5.65, 15.75 Hz), 6.07 (1H, dd, *J* 1.6, 15.75 Hz), 4.64 (1H, dd, *J* 1.25, 6.9 Hz), 4.17 (3H, m including q, *J* 7.25 Hz), 3.65 (1H, dd, *J* 7.55, 8.2 Hz), 1.42 (3H, s), 1.38 (3H, s), 1.27 (3H, t, *J* 7.25 Hz)

δ_C (500 MHz, $CDCl_3$): 165.9, 144.5(-), 122.4(-), 110.1, 74.9(-), 68.7(+), 60.5(+), 26.4(-), 25.6(-), 14.1(-), [+ = CH_2, - = CH, CH_3]

$[\alpha]_D^{24}$: +40.4 ° (c = 1.09, $CHCl_3$)

3.3.2.3 Preparation of (R)-3-((S)-2,2-dimethyl-[1,3]-dioxolan-4-yl)-butyric acid ethyl ester (4)

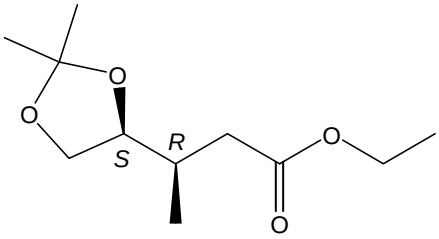

Methyl lithium (81 ml, 120 mmol, 1.50 M, 2 mol eq.) was added to a stirring solution of 3-(2,2-dimethyl-(1,3)-dioxolan-4-yl)-acrylic acid **(3)** (12 g, 60 mmol) in dry diethyl ether (300 ml) at -78 °C under nitrogen atmosphere. The reaction mixture was stirred at -78 °C for 2½ hours and allowed to reach -60 °C. Water was then added (10 ml) and after 5 minutes a saturated solution of ammonium chloride (80 ml), where upon the temperature rose to -40 °C. The cooling bath was removed, the mixture was allowed to reach 0 °C and the reaction was quenched with water (100 ml). The organic layer was separated and the aqueous layer extracted with diethyl ether (2 x 100 ml). The combined organic layers were washed with brine (2 x 150 ml), dried and evaporated to give a yellow oily residue, which was purified by column chromatography on silica gel eluted with petroleum ether/diethyl ether (4:1) to give *(R)-3-((S)-2,2-dimethyl-[1,3]-dioxolan-4-yl)-butyric acid ethyl ester* **(4)** (9.17 g, 71%) (109).

Physical properties:

ν_{max}/cm^{-1}: 2984, 2980, 1732, 1012

δ_H (500 MHz, $CDCl_3$): 4.12 (2H, q, *J* 7.25 Hz), 3.99 (2H, m), 3.61 (1H, t, *J* 6.6), 2.38 (1H, dd, *J* 4.75, 14.85 Hz), 2.19 (1H, m), 2.11 (1H, dd, *J* 8.8, 14.8 Hz), 1.38 (3H, s), 1.32 (3H, s), 1.24 (3H, t, *J* 7.25 Hz), 0.98 (3H, d, *J* 6.6 Hz)

δ_C (500 MHz, $CDCl_3$): 172.57, 108.85, 78.74(+), 66.71(-), 60.31(-), 37.51(-), 32.94(+), 26.31(+), 25.19(+), 15.33(+), 14.16(+), [- = CH_2, + = CH, CH_3]

$[\alpha]_D^{22}$: +10.29 ° (c = 2.02, $CHCl_3$)

3.3.2.4 Preparation of (R)-3-((S)-2,2-dimethyl-[1,3]-dioxolan-4-yl)-butan-1-ol (5)

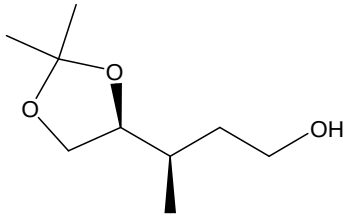

(*R*)-3-((*S*)-2,2-Dimethyl-[1,3]dioxolan-4-yl)-butyric acid ethyl ester **(4)** (6.90 g, 31.94 mmol) in dry THF (30 ml) was added drop-wise over a period of 15 minutes to a suspension of lithium aluminium hydride (1.46 g, 38.33 mmol) in dry THF (160 ml) under nitrogen atmosphere at RT. The reaction mixture was refluxed for 1 hour. When TLC showed that no more starting material was left, the mixture was cooled to RT and carefully quenched with freshly prepared saturated aqueous sodium sulfate decahydrate (10 ml) until a white precipitate was formed. This was followed by addition of magnesium sulfate (10 g). The mixture was stirred vigorously for 10 minutes, filtered through a pad of celite and washed thoroughly with THF (2 x 50 ml). The combined organic layers were evaporated to give a residue which was dissolved in a mixture of petroleum ether/diethyl ether (1:1, 150 ml) and triethylamine (2 drops). The solution was dried by stirring for one hour over anhydrous potassium carbonate. Filtration yielded a solution which was concentrated by evaporation to yield a colourless liquid of *(R)-3-((S)-2,2-dimethyl-[1,3]-dioxolan-4-yl)-butan-1-ol* **(5)** (4.8 g, 87%) (124).

Physical properties:

ν_{max}/cm^{-1}:	3423, 2933
δH (500 MHz, CDCl3):	3.99 (2H, m), 3.72 (1H, m), 3.64 (2H, m), 2.08 (1H, broad s), 1.82 (1H, m), 1.64 (1H, m), 1.45-1.37 (4H, m including s), 1.34 (3H, m), 0.97 (3H, dd, *J* 2.55, 6.95 Hz)
δC (500 MHz, CDCl3):	108.75, 79.69(+), 67.20(-), 60.35(-), 35.68(-), 32.81(+), 26.42(+), 25.32(+), 15.17(+), [- = CH_2, + = CH, CH_3]
$[\alpha]_D^{22}$:	+16.1 ° (c = 1.35, $CHCl_3$); *reported as* $[\alpha]_D^{22}$*: +16.8 ° (*$CHCl_3$*) by Ryosuke et al. (124)*

3.3.2.5 Preparation of (R)-3-((S)-2,2-dimethyl-[1,3]-dioxolan-4-yl)-butyraldehyde (6)

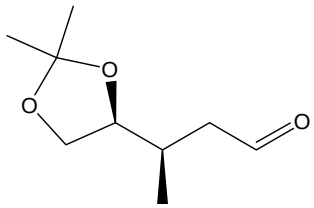

(*R*)-3-((*S*)-2,2-Dimethyl-[1,3]-dioxolan-4-yl)-butan-1-ol **(5)** (6.10 g, 35.06 mmol) in dichloromethane (30 ml) was added to a stirring suspension of pyridinium chlorochromate (16.07 g, 92.00 mmol) in dichloromethane (500 ml) at RT. The mixture was refluxed for 30 minutes. When TLC indicated that no starting material was left, the mixture was cooled down and poured into diethyl ether (200 ml), filtered through a pad of silica gel and washed thoroughly with diethyl ether. The filtrate was evaporated to give a residue which was purified by column chromatography on silica gel eluted with petroleum ether (BP 40-60 °C)/diethyl ether (1:1) to give *(R)-3-((S)-2,2-dimethyl-[1,3]-dioxolan-4-yl)-butyraldehyde* **(6)** as a colourless oil (3.05 g, 51%) (36).

Physical properties:

ν_{max}/cm^{-1}:	2985, 1725, 1215, 1066
δ_H (500 MHz, $CDCl_3$):	9.79 (1H, t, *J* 1.9 Hz), 4.09 (1H, m), 4.00 (1H, dd, *J* 6.6, 8.2 Hz), 3.65 (1H, dd, *J* 7.3, 8.2 Hz), 2.57 (1H, m), 2.40 (1H, m), 2.29 (1H, m), 1.43 (3H, s), 1.36 (3H, s), 1.01 (3H, d, *J* 6.9 Hz)
δ_C (500 MHz, $CDCl_3$):	201.7(-), 109.1, 78.6(-), 66.3(+), 46.6(+), 30.4(-), 26.2(-), 25.1(-), 15.5(-), [+ = CH_2, - = CH, CH_3]
$[\alpha]_D^{22}$:	+8.27 ° (c = 1.44, $CHCl_3$)

*3.3.2.6 Preparation of 5-hexadecylsulfanyl-1-phenyl-1*H*-tetrazole (8)*

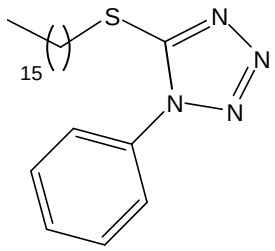

1-Bromohexadecane **(7)** (16.20 g, 53.05 mmol) was added to a stirring solution of 1-phenyl-1*H*-tetrazole-5-thiol (9.69 g, 54.37 mmol) and anhydrous potassium carbonate (15.24 g, 110.27 mmol) in acetone (165 ml). The mixture was vigorously stirred and refluxed for 2½ hours. When TLC showed that no starting material was left, the inorganic salts were filtered off and washed with acetone. The acetone solution was evaporated to a small bulk and dissolved in dichloromethane (150 ml). The solution was washed with water (300 ml), the organic layer separated and the aqueous layer re-extracted with dichloromethane (2 x 50 ml). The combined organic phases were washed with water (300 ml), dried and the solvent evaporated to give a solid. This was dissolved in acetone (50 ml) and diluted with methanol (100 ml). The mixture was left at ambient temperature for 1 hour and then at 0 °C for 1 hour. A white solid crystallised out; this was filtered off and washed with cold acetone/methanol (1:2) to give a white solid of *5-hexadecylsulfanyl-1-phenyl-1H-tetrazole* **(8)** (13.92 g, 63%).

Physical properties:

ν_{max}/cm^{-1}:	2917, 1501, 1091, 759
m.p.	48-50 ºC
δ_H (500 MHz, $CDCl_3$):	7.56 (5H, m), 3.40 (2H, t, *J* 7.55 Hz), 1.82 (2H, pent, *J* 7.25 Hz), 1.44 (2H, pent, *J* 6.95 Hz), 1.35-1.24 (24H, m including s), 0.88 (3H, t, *J* 6.95 Hz)
δ_C (500 MHz, $CDCl_3$):	154.46, 133.82, 129.98(-), 129.70(-), 123.83(-), 33.39(+), 31.88(+), 29.64(+), 29.62(+), 29.60(+), 29.57(+), 29.49(+), 29.39(+), 29.30(+), 29.08(+), 28.99(+), 28.60(+), 22.64(+), 14.04(-), [+ = CH_2, - = CH, CH_3]

*3.3.2.7 Preparation of 5-(hexadecane-1-sulfonyl)-1-phenyl-1*H*-tetrazole (9)*

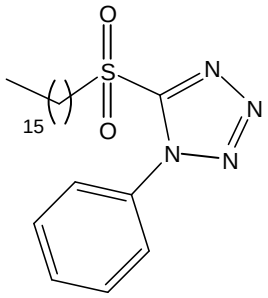

A solution of ammonium molybdate (VI) tetrahydrate (18.90 g, 15.31 mmol) in ice cold H_2O_2 35% (w/w, 50 ml) was added to a stirring solution of 5-hexadecylsulfanyl-1-phenyl-1*H*-tetrazole **(8)** (13.50 g, 33.58 mmol) in THF (150 ml) and IMS (300 ml) at 12 °C and stirred at RT for 2 hours. A further solution of ammonium molybdate (VI) tetrahydrate (7.20 g, 5.83 mmol) in ice cold H_2O_2 35% (w/w, 20 ml) was added and the mixture was stirred at RT for 18 hours. The mixture was poured into 3 L of water and extracted with dichloromethane (3 x 400 ml). The combined organic phases were washed with water (2 x 500 ml), dried and the solvent was evaporated. The residue was dissolved in methanol (200 ml) and the mixture left at RT for 1 hour and then at 0 °C for 1 hour. A white solid crystallised out; this was filtered off and washed with cold methanol to give a white solid of *5-(hexadecane-1-sulfonyl)-1-phenyl-1H-tetrazole* **(9)** (12.42 g, 80%).

Physical properties:

ν_{max}/cm^{-1}:	2918, 1470, 1343, 1154, 770
m.p.	65-67 ºC
δ_H (500 MHz, $CDCl_3$):	7.70 (2H, m), 7.61 (3H, m), 3.73 (2H, distorted t, *J* 7.85 Hz), 1.96 (2H, m), 1.50 (2H, pent, *J* 6.95 Hz), 1.34-1.25 (24H, m including s), 0.89 (3H, t, *J* 6.9 Hz)
δ_C (500 MHz, $CDCl_3$):	153.56, 133.11, 131.39(+), 129.66(+), 125.09(+), 56.06(-), 31.89(-), 29.65(-), 29.64(-), 29.62(-), 29.59(-), 29.52(-), 29.42(-), 29.31(-), 29.16(-), 28.87(-), 28.12(-), 22.64(-), 21.92(-), 14.05(+), [- = CH_2, + = CH, CH_3]

3.3.2.8 Preparation of (S)-2,2-dimethyl-4-((R)-1-methyl-nonadecyl)-[1,3]-dioxolane (10)

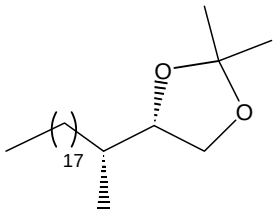

Lithium bis(trimethylsilyl)amide (27 ml, 28.60 mmol, 1.06 M) was added drop-wise to a stirring solution of (*R*)-3-((*S*)-2,2dimethyl-[1,3]-dioxolan-4-yl)-butyraldehyde **(6)** (3.05 g, 17.73 mmol) and 5-(hexadecane-1-sulfonyl)-1-phenyl-1*H*-tetrazole **(9)** (9.30 g, 20.17 mmol) in dry THF (130 ml) under nitrogen at - 2 °C. The reaction mixture was allowed to reach RT and stirred for 16 hours, then quenched with water (100 ml) and petroleum ether/diethyl ether (1:1, 100 ml). The organic layer was separated and the aqueous layer re-extracted with petroleum ether/diethyl ether (1:1, 2 x 50 ml). The combined organic layers were washed with brine (2 x 100 ml), dried and evaporated to give a thick oil which was purified by column chromatography on silica gel eluting with petroleum ether/diethyl ether (10:0.5) to give *(S)-2,2-dimethyl-4-((E,Z)-(R)-1-methyl-nonadec-3-enyl)-[1,3]-dioxolane* (5.18 g, 77%).

Palladium on charcoal (10%, 1.20 g) was added to a stirring solution of (*S*)-2,2-dimethyl-4-((*E,Z*)-(*R*)-1-methyl-nonadec-3-enyl)-[1,3]-dioxolane (5.18 g, 13.63 mmol) in IMS (125 ml) and methanol (30 ml). The mixture was stirred while being hydrogenated under hydrogen atmosphere. When no more hydrogen was absorbed the mixture was filtered through a pad of celite and washed with warmed ethyl acetate (100 ml). The clear colourless filtrate was evaporated at 14 mm Hg to give a white solid of *(S)-2,2-dimethyl-4-((R)-1-methyl-nonadecyl-[1,3]-dioxolane* **(10)** (5.18 g, 99%).

Physical properties:

ν_{max}/cm^{-1}: 2919, 2851, 1467, 1076, 856

δ_H (500 MHz, $CDCl_3$): 4.01 (1H, dd, *J* 5.95, 7.55 Hz), 3.87 (1H, q, *J* 7.2 Hz), 3.61 (1H, t, *J* 7.55 Hz), 1.55 (1H, m), 1.41 (3H, s), 1.36 (3H, s), 1.34-1.20 (33H, m including s), 1.09 (1H, m), 0.97 (3H, d, *J* 6.6 Hz), 0.89 (3H, t, *J* 6.6 Hz)

δ_C (500 MHz, $CDCl_3$): 108.50, 80.42(-), 67.82(+), 36.51(-), 32.76(+), 31.93(+), 29.87(+), 29.69(+), 29.66(+), 29.64(+), 29.61(+), 29.36(+),

26.99(+), 26.64(-), 25.54(-), 22.68(+), 15.61(-), 14.09(-), [+ = CH_2, - = CH, CH_3]

$[\alpha]_D^{22}$: *reported as +23.01 ° (c = 0.62, $CHCl_3$)*

3.3.2.9 Preparation of (2S,3R)-3-methyl-henicosane-1,2-diol (11)

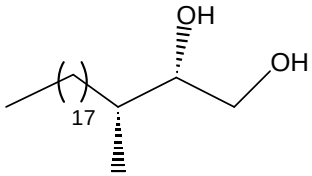

p-Toluenesulfonic acid (0.48 g, 2.51 mmol, 1.90 mol eq.) was added to a stirring solution of (*S*)-2,2-dimethyl-4-((*R*)-1-methyl-nonadecyl)-[1,3]-dioxolane **(10)** (5.04 g, 13.19 mmol) in THF (35 ml), methanol (50 ml) and water (5 ml) at RT. The reaction mixture was refluxed for 3½ hours. When TLC showed that no starting material was left, the solvent was evaporated and the residue diluted with petroleum ether/diethyl ether (1:1, 150 ml). Then a solution of saturated sodium bicarbonate (50 ml) was added, the organic layer separated and the aqueous layer re-extracted with diethyl ether (2 x 300 ml). The combined organic layers were washed with brine (250 ml), dried and evaporated to give a white solid of *(2S,3R)-3-methyl-henicosane-1,2-diol* **(11)** (4.58 g, >99%).

Physical properties:

ν_{max}/cm^{-1}: 3420

m.p. 67-68 ºC

δ_H (500 MHz, $CDCl_3$): 3.69 (1H, m), 3.59 (2H, m), 2.04 (1H, d, *J* 4.1 Hz), 1.95 (1H, dd, *J* 4.8, 7.0 Hz), 1.57 (1H, m), 1.28 (34 H, m), 0.95 (3H, d, *J* 7.0 Hz), 0.90 (3H, t, *J* 7.0 Hz)

δ_C (500 MHz, $CDCl_3$): 75.75(-), 65.15(+), 35.71(-), 32.98(+), 31.91(+), 29.85(+), 29.69(+), 29.68(+), 29.35(+), 27.10(+), 22.68(+), 14.55(-), 14.10(-), [+ = CH_2, - = CH, CH_3]

$[\alpha]_D^{22}$: *reported as +12.7 ° (c = 1.11, $CHCl_3$*

3.3.2.10 Preparation of (S)-2-((R)-1-methyl-nonadecyl)-oxirane (12)

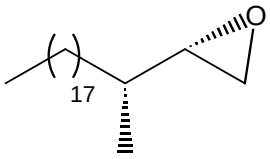

Sodium hydroxide solution (50%, 17.5 ml) was added to a vigorously stirring solution of (2*S*,3*R*)-3-methyl-henicosane-1,2-diol **(11)** (4.58 g, 13.39 mmol) and cetrimide (0.50 g) in dichloromethane (200 ml) at RT. To this, a solution of *p*-toluenesulfonyl chloride (3.15 g, 16.35 mmol) in dichloromethane (20 ml) was added over 10 minutes. The mixture was stirred for 30 minutes at RT and when TLC showed that no starting material was left, the mixture was quenched with water (150 ml). The organic layer was separated and the aqueous layer extracted with dichloromethane (2 x 50 ml). The combined organic layers were washed with water (100 ml), dried and evaporated to give a residue which was purified by column chromatography on silica gel eluting with petroleum ether/diethyl ether (10:0.5) to give *(S)-2-((R)-1-methyl-nonadecyl)-oxirane* **(12)** as a white solid (3.82 g, 88%).

Physical properties:

ν_{max}/cm^{-1}:	2919, 1473, 1261, 892, 729
m.p.	45-47 ºC
δ_H (500 MHz, $CDCl_3$):	2.78 (1H, dd, *J* 3.8, 4.75 Hz), 2.68 (1H, m), 2.54 (1H, dd, *J* 2.8, 5.0 Hz), 1.32-1.24 (35H, m including s), 1.03 (3H, d, *J* 6 Hz), 0.89 (3H, t, *J* 6.6 Hz)
δ_C (500 MHz, $CDCl_3$):	57.17(-), 47.03(+), 36.23(-), 33.57(+), 31.92(+), 29.87(+), 29.69(+), 29.65(+), 29.63(+), 29.58(+), 29.36(+), 27.12(+), 22.68(+), 17.13(-), 14.11(-), [+ = CH_2, - = CH, CH_3]
$[\alpha]_D^{22}$:	*reported as +0.3 ° (c = 1.01, $CHCl_3$)*

3.3.2.11 Preparation of 6-bromo-hexan-1-ol

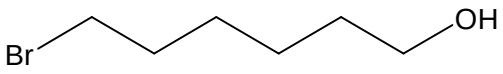

HBr (48%, 44.51 g, 30 ml, 0.55 mol) was added to a stirring solution of 1,6-hexanediol (25 g, 0.21 mol) in toluene (300 ml). The mixture was refluxed overnight, cooled down and the toluene was evaporated. A saturated solution of $NaHCO_3$ (200 ml) was added and the mixture was extracted with dichloromethane (3 x 150 ml). The combined organic layers were dried and evaporated, the product was purified by column chromatography on silica gel eluting with petroleum ether/diethyl ether (5:1, then 1:1) to give *6-bromohexan-1-ol* (26.83 g, 71%) (108).

Physical properties:

ν_{max}/cm^{-1}: 3357, 2937, 1638, 1054

δ_H (500 MHz, $CDCl_3$): 3.56 (2H, t, *J* 6.6 Hz), 3.36 (2H, t, *J* 6.95 Hz), 2.63 (1H, s), 1.82 (2H, pent, *J* 6.95 Hz), 1.51 (2H, pent, *J* 6.95 Hz), 1.41 (2H, pent, *J* 6.95 Hz), 1.33 (2H, m)

δ_C (500 MHz, $CDCl_3$): 62.27(+), 33.74(+), 32.53(+), 32.23(+), 27.75(+), 24.76(+), [+ = CH_2, - = CH, CH_3]

3.3.2.12 Preparation of 1-bromo-6-tetrahydropyranyloxynonane

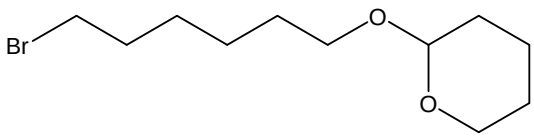

3,4-Dihydro-2*H*-pyran (26.50 g, 0.32 mol, 2.1 mol eq.) and pyridinium-*p*-toluene sulfonate (3 g) were added to a stirring solution of 6-bromo-hexan-1-ol (26.80 g, 0.15 mol) in dry dichloromethane (250 ml) under nitrogen at RT. The reaction was stirred at RT for 3 hours. When TLC showed that no starting material was left, the reaction mixture was filtered through a pad of silica gel and washed with dichloromethane (200 ml). The dichloromethane was evaporated and the residue purified by column chromatography on silica gel eluted with petroleum ether/diethyl ether (9:1) to give *1-bromo-6-tetrahydropyranyloxynonane* (38.08 g, 93%) (108).

Physical properties:

ν_{max}/cm^{-1}: 2939, 2865, 1440, 1120

δ_H (500 MHz, $CDCl_3$): 4.54 (1H, m), 3.83 (1H, m), 3.71 (1H, ddd, *J* 6.6, 9.45, 16.4 Hz), 3.47 (1H, m), 3.38 (2H, t, *J* 6.6 Hz), 3.34 (1H, m), 1.89-1.76 (3H, m), 1.71-1.64 (1H, m), 1.60-1.33 (10H, m)

δ_C (500 MHz, $CDCl_3$): 98.73(-), 67.25(+), 62.21(+), 33.70(+), 32.63(+), 30.65(+), 29.43(+), 27.88(+), 25.34(+), 25.35(+), 19.57(+), [+ = CH_2, - = CH, CH_3]

*3.3.2.13 Preparation of (8**R**,9**R**)-9-methyl-1-(tetrahydropyran-2-yloxy)-heptacosan-8-ol (13)*

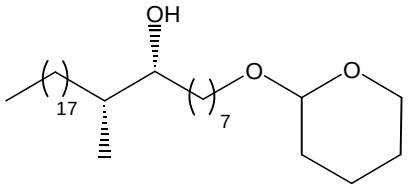

A solution of 1-bromo-6-tetrahydropyranyloxynonane (9.38 g, 35.39 mmol) in dry THF (25 ml) was added drop wise to a suspension of magnesium turnings (1.70 g, 70.83 mmol) in dry THF (30 ml) under nitrogen. The mixture was refluxed for 1 hour, then cooled down to RT and added drop wise to a stirring solution of purified copper iodide (0.59 g, 3.11 mmol) in dry THF (40 ml) at -30 °C. After 30 min a solution of (*S*)-2-((*R*)-1-methyl-nonadecyl)-oxirane **(12)** (3.82 g, 11.79 mmol) in dry THF (30 ml) was added drop-wise. The reaction mixture was stirred for another 2 ½ hours, then allowed to reach RT and stirred overnight. The mixture was quenched with saturated aqueous ammonium chloride (100 ml) and extracted with diethyl ether (3 x 200 ml). The combined organic layers were washed with brine (250 ml), dried and evaporated to give a colourless oil which was purified by column chromatography on silica gel eluted with petroleum ether/diethyl ether (9:1 changing to 3:1, 2:1 and 1:1) to give *(8*R,9R*)-9-methyl-1-(tetrahydropyran-2-yloxy)-heptacosan-8-ol* as a colouless oil **(13)** (4.45 g, 74%).

Physical properties:

ν_{max}/cm^{-1}: 3450, 2921, 2851, 1465, 1033

δ_H (500 MHz, $CDCl_3$): 4.57 (1H, m), 3.87 (1H, m), 3.73 (1H, ddd, *J* 6.9, 9.75, 16.7 Hz), 3.39 (2H, m), 3.38 (1H, ddd, *J* 6.6, 9.45, 16.05 Hz), 1.83 (1H, m), 1.72 (1H, m), 1.63-1.49 (6H, m), 1.42 (4H, m), 1.33 (7H, m),

1.29-1.20 (33H, m including s), 0.88 (3H, t, *J* 6.6 Hz), 0.85 (3H, d, *J* 6.65 Hz)

δ_C (500 MHz, $CDCl_3$): 98.80(-), 75.13(-), 67.61(+), 62.27(+), 38.17(-), 34.43(+), 33.33(+), 31.90(+), 30.75(+), 29.24(+), 29.71(+), 29.67(+), 29.63(+), 29.44(+), 29.33(+), 27.40(+), 26.21(+), 26.18(+), 25.48(+), 22.66(+), 22.58(+), 19.66(+), 14.08(-), 13.54(-), [+ = CH_2, - = CH, CH_3]

$[\alpha]_D^{22}$: *reported as +9.15 (c = 1.28, $CHCl_3$)*

*3.3.2.14 Preparation of 2-((8**R**,9**R**)-8-methoxy-9-methyl-heptacosyloxy)-tetrahydropyran (14)*

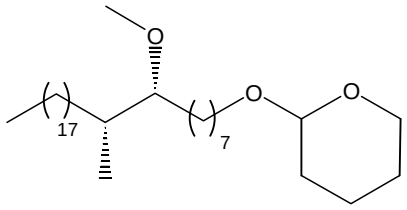

Sodium hydride (1.42 g, 58.1 mmol, 60% dispersion) was washed with petroleum ether (3 x 20 ml) and then suspended in dry THF (35 ml). The suspension was cooled to 5 °C and (8*R*,9*R*)-9-methyl-1-(tetrahydropyran-2-yloxy)-heptacosan-8-ol **(13)** (4.45 g, 8.73 mmol) in THF (35 ml) was added over 5 minutes. After 15 minutes methyl iodide (7.31 g, 51.5 mmol) was added. The mixture was stirred for 16 hours at RT. When TLC showed that no starting material was left, saturated ammonium chloride solution (50 ml) was added carefully followed by the addition of diethyl ether (100 ml). The organic layer was separated and the aqueous layer re-extracted with petroleum ether/diethyl ether (1:1, 2 x 50 ml). The combined organic layers were washed with brine (2 x 80 ml), dried and evaporated to give a residue which was purified by column chromatography on silica gel eluted with petroleum ether/diethyl ether (10:2) to give *2-((8R,9R)-8-methoxy-9-methyl-heptacosyloxy)-tetrahydropyran* **(14)** as a pale yellow oil (3.83 g, 84%).

Physical properties:

ν_{max}/cm^{-1}: 2928, 2846, 1077

δ_H (500 MHz, $CDCl_3$): 4.60 (1H, t, *J* 2.3 Hz), 3.80 (1H, m), 3.74 (1H, dt, *J* 7, 9.45 Hz), 3.52 (1H, m), 3.40 (1H, dt, *J* 6.6, 9.45 Hz), 3.35 (3H, s), 2.97

(1H, m), 1.90-1.82 (1H, m), 1.76-1.70 (1H, m), 1.68-1.50 (6H, m), 1.45-1.25 (44H, m), 1.10 (1H, m), 0.91 (3H, t, *J* 7 Hz), 0.86 (3H, d, *J* 6.65 Hz)

δ_C (500 MHz, $CDCl_3$): 98.84, 85.43, 67.67, 62.30, 57.70, 35.30, 32.35, 31.91, 30.82, 30.47, 30.01, 29.89, 29.76, 29.70, 29.67, 29.50, 29.42, 27.59, 26.20, 26.14, 25.48, 22.17, 19.70, 14.89, 14.13, [+ = CH_2, - = CH, CH_3]

$[\alpha]_D^{22}$: *reported as +8.76 ° (c = 1.45, $CHCl_3$)*

3.3.2.15 Preparation of (8R,9R)-8-methoxy-9-methyl-heptacosan-1-ol (15)

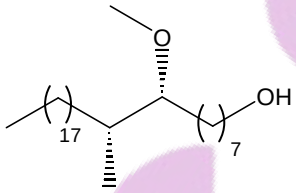

p-Toluenesulfonic acid monohydrate (0.36 g, 1.89 mmol) was added to a stirring solution of 2-((8*R*,9*R*)-8-methoxy-9-methyl-heptacosyloxy)-tetrahydro-pyran **(14)** (3.80 g, 7.25 mmol) in THF (20 ml), methanol (70 ml) and water (1 ml) at RT. The reaction mixture was refluxed for 30 min. When TLC showed that no starting material was left, the solution was evaporated to approximately half of the volume and diluted with a saturated solution of sodium bicarbonate (50 ml). A mixture of petroleum ether/diethyl ether (1:1, 150 ml) was added and extracted. The organic layer was separated and the aqueous layer re-extracted with petroleum ether/diethyl ether (1:1, 2 x 50 ml). The combined organic layers were washed with brine (100 ml), dried and evaporated to give a residue which was purified by column chromatography on silica gel eluted with petroleum ether/diethyl ether (5:2) to give *(8R,9R)-8-methoxy-9-methyl-heptacosan-1-ol* **(15)** as a colourless liquid, which solidified later (3.23 g, 97%).

Physical properties:

ν_{max}/cm^{-1}: 3463, 2912, 2846, 1078

m.p. 33-35 ºC

δ_H (500 MHz, $CDCl_3$): 3.63 (2H, t *J* 6.6 Hz), 3.33 (3H, s), 2.95 (1H, m), 1.54 (4H, m), 1.45-1.20 (44H, m including s), 0.88 (3H, t, *J* 6.3 Hz), 0.84 (3H, d, *J* 6.9 Hz)

δ_C (500 MHz, $CDCl_3$): 85.46(-), 62.94(+), 57.66(-), 35.37(-), 32.78(+), 32.35(+), 31.91(+), 30.49(+), 29.97(+), 29.86(+), 29.68(+), 29.63(+), 29.42(+), 29.33(+), 27.56(+), 26.09(+), 25.71(+), 22.66(+), 14.87(-), 14.05(-), [+ = CH_2, - = CH, CH_3]

$[\alpha]_D^{26}$: +9.88 °, (c = 1.29, $CHCl_3$); *reported as* $[\alpha]_D^{22}$*: +11.05 ° (c = 1.19)*

3.3.2.16 Preparation of (8R,9R)-8-methoxy-9-methyl-heptacosanal (16)

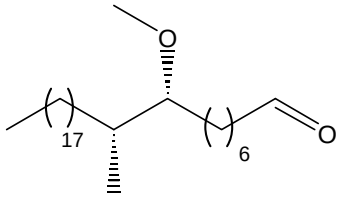

(8*R*,9*R*)-8-Methoxy-9-methyl-heptacosan-1-ol **(15)** (3.1 g, 7.05 mmol) in dichloromethane (30 ml) was added to a stirring suspension of pyridinium chlorochromate (3.8 g, 17.6 mmol) in dichloromethane (200 ml) at RT. The mixture was stirred vigorously and refluxed for 3 hours. When TLC showed that no starting material was left, the mixture was cooled down and poured into diethyl ether (200 ml) and filtered through a pad of silica gel, washed with diethyl ether and the filtrate evaporated to give a residue that was purified by column chromatography on silica gel eluted with petroleum ether/diethyl ether (10:1) to give *(8R,9R)-8-methoxy-9-methyl-heptacosanal* **(16)** as a colourless liquid (2.31 g, 75%).

Physical properties:

ν_{max}/cm^{-1}: 2924, 2850, 1729, 1465, 1097

δ_H (500 MHz, $CDCl_3$): 9.78 (1H, s), 3.40 (3H, s), 2.96 (1H, m), 2.44 (2H, t, *J* 7.25 Hz), 1.65 (4H, m), 1.45-1.25 (40H, m), 1.10 (1H, m), 0.88 (3H, t, *J* 6.3 Hz), 0.85 (3H, d, *J* 6.6 Hz)

δ_C (500 MHz, $CDCl_3$): 202.88, 85, 50, 57.70, 43.91, 35.29, 32.25, 30.00, 29.72, 29.66, 29.63, 29.17, 27.58, 25.97, 22.69, 22.10, 14.94, 14.11, [+ = CH_2, - = CH, CH_3]

$[\alpha]_D^{22}$: *reported as +11.6 ° (c = 1.16, $CHCl_3$)*

3.3.2.17 Preparation of 8-bromo-octan-1-ol (18)

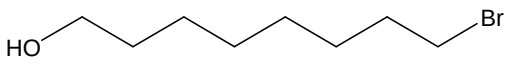

HBr (48%, 34.79 g, 25 ml, 0.43 mol) was added to a stirring solution of 1,8-octanediol **(17)** (25 g, 0.17 mol) in toluene (350 ml). The mixture was refluxed overnight, cooled down and the toluene was evaporated. A saturated solution of $NaHCO_3$ (200 ml) was added and the mixture was then extracted with dichloromethane (3 x 150 ml). The combined organic layers were dried and evaporated and the product was purified by column chromatography on silica gel eluted with petroleum ether/diethyl ether (1:2) to give *8-bromo-octan-1-ol* **(18)** (21.2 g, 59%) (108).

Physical properties:

ν_{max}/cm^{-1}: 3353, 2928, 2855,

δ_H (500 MHz, $CDCl_3$): 3.59 (2H, m), 3.38 (2H, m), 1.84 (2H, m), 1.54 (2H, m), 1.42 (2H, m), 1.32 (6H, broad s)

δ_C (500 MHz, $CDCl_3$): 62.72(+), 33.82(+), 32.69(+), 32.58(+), 29.11(+), 28.60(+), 27.99(+), 25.54(+), [+ = CH_2, - = CH, CH_3]

3.3.2.18 Preparation of 2,2-dimethyl-propionic acid 8-bromo-octyl ester (19)

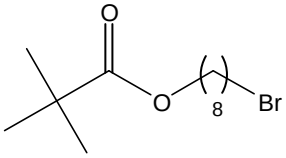

A solution of trimethyl acetyl chloride (14.47 g, 120 mmol, 1.20 mol eq.) in dichloromethane (45 ml) was added over 15 minutes to a stirring solution of bromo alcohol **(18)** (21 g, 100 mmol), triethylamine (42 ml, 300 mmol, 3 mol eq.) and 4-dimethylaminopyridine (0.25 g, 2 mmol) in dichloromethane (160 ml). The reaction mixture was stirred overnight at RT. Diluted hydrochloric acid (150 ml, 5%) was added and the organic layer separated and washed with diluted hydrochloric acid (1 x 100 ml) and then with brine (2 x 200 ml), dried and evaporated. The residue was dissolved in petroleum ether (200 ml), filtered through a pad of silica gel and washed with petroleum ether (50 ml). The silica gel pad was washed with petroleum

ether/diethyl ether (1:1, 150 ml) and the solvent evaporated to give *2,2-dimethyl-propionic acid 8-bromo-octyl ester* **(19)** as a colourless oil (26.09 g, 89%).

Physical properties:

ν_{max}/cm^{-1}: 2930, 2857, 1810, 1728

δ_H (500 MHz, $CDCl_3$): 4.03, (2H, t, *J* 6.6 Hz), 3.38 (2H, t, *J* 6.65 Hz), 1.84 (2H, pent, *J* 6.95 Hz), 1.61 (2H, m), 1.42 (2H, m), 1.32 (6H, m), 1.18 (9H, s)

δ_C (500 MHz, $CDCl_3$): 178.45, 64.25(-), 38.64, 33.71(-), 32.69(-), 28.94(-), 28.55(-), 28.51(-), 27.98(-), 27.13(+), 26.44(+), 25.73(-), 22.53(+), [- = CH_2, + = CH, CH_3]

*3.3.2.19 Preparation of 5-(1-octanolpivalate-8-sulfanyl)-1-phenyl-1*H*-tetrazole (20)*

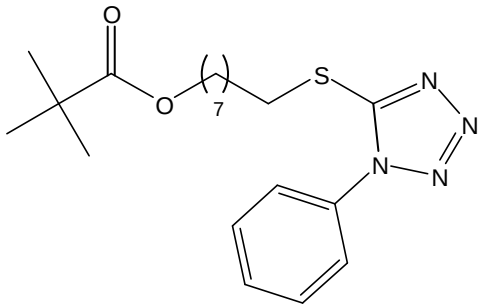

2,2-Dimethyl-propionic acid 8-bromo-octyl ester **(19)** (26 g, 88.73 mmol) was added to a stirring solution of 1-phenyl-1*H*-tetrazole-5-thiol (17.40 g, 97.63 mmol, 1.10 mol eq.) and anhydrous potassium carbonate (25.80 g, 186.67 mmol, 2.1 mol eq.) in acetone (300 ml) and stirred overnight at RT. When TLC showed no starting material was left, the mixture was added to water (1L) and extracted with dichloromethane (1 x 150 ml, 2 x 25 ml). The combined organic layers were washed with brine (2 x 200 ml), dried and evaporated to give a dark yellow oil which was purified by column chromatography on silica gel eluted with petroleum ether/diethyl ether (7:2.5) to give *5-(1-octanolpivalate-8-sulfanyl)-1-phenyl-1H-tetrazole* **(20)** (31 g, 90%).

Physical properties:

ν_{max}/cm^{-1}: 2931, 2856, 1725

δ_H (500 MHz, $CDCl_3$): 7.55 (5H, m), 4.02 (2H, t, *J* 6.65 Hz), 3.37 (2H, t, *J* 7.55 Hz), 1.81 (2H, pent, *J* 7.25 Hz), 1.59 (2H, m), 1.43 (2H, m), 1.31 (6H, m), 1.17 (9H, s)

δ_C (500 MHz, $CDCl_3$): 178.51, 154.38, 133.65, 129.97(+), 129.67(+), 123.74(+), 64.23(-), 38.62, 33.20(-), 28.96(-), 28.92(-), 28.79(-), 28.45(-), 28.44(-), 27.11(+), 25.70(-), 22.52(+), 14.23(+), 11.33(+), [- = CH_2, + = CH, CH_3]

*3.3.2.20 Preparation of 5-(1-octanolpivalate-8-sulfonyl)-1-phenyl-1*H*-tetrazole (21)*

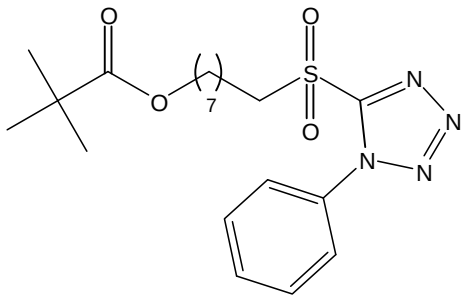

A solution of ammonium molybdate(VI)tetrahydrate (24.50 g, 19.88 mmol) in ice cold H_2O_2 35% (w/w, 48 ml) was added to a stirring solution of 5-(1-octanolpivalate-8-sulfanyl)-1-phenyl-1*H*-tetrazole **(20)** (15.54 g, 39.75 mmol) in THF (225 ml) and IMS (420 ml) at 10 °C and stirred at RT for 2 hours. A further solution of ammonium molybdate(VI)tetrahydrate (12.90 g) in ice cold H_2O_2 35% (w/w, 30 ml) was added and the mixture was stirred overnight at RT. The mixture was poured into water (1.8 ℓ) and extracted with dichloromethane (1 x 200 ml, 3 x 30 ml). The combined organic layers were washed with water (1 x 500 ml), dried and evaporated to give a colourless oil which was purified by column chromatography on silica gel eluted with petroleum ether/diethyl ether (3:1, changing to 2:1 and then to 1:1) to give *5-(1-octanolpivalate-8-sulfonyl)-1-phenyl-1H-tetrazole* **(21)** (14.93 g, 89%).

Physical properties:

ν_{max}/cm^{-1}: 2934, 2860, 1723

δ_H (500 MHz, $CDCl_3$): 7.69 (2H, m), 7.61 (3H, m), 4.04 (2H, t, *J* 6.6 Hz), 3.73 (2H, distorted t, *J* 7.85 Hz), 1.95 (2H, m), 1.61 (2H, m), 1.50 (2H, m), 1.34 (6H, m), 1.19 (9H, s)

δ_C (500 MHz, $CDCl_3$): 178.53, 153.42, 132.97, 131.39(+), 129.64(+), 125.00(+), 64.19(-), 55.87(-), 38.65, 28.72(-), 28.45(-), 27.97(-), 27.13(+), 25.68(-), 21.87(-), 15.20(+), [- = CH_2, + = CH, CH_3]

*3.3.2.21 Preparation of 2,2-dimethyl-propionic acid-(16**R**,17**R**)-16-methoxy-17-methyl-pentatriacontyl ester (22)*

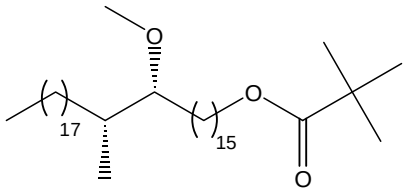

Lithium bis(trimethylsilyl)amide (9.88 ml, 10.50 mmol, 1.06 M) was added drop-wise to a stirring solution of (8R,9R)-8-methoxy-9-methyl-heptacosanal **(6)** (2.30 g, 5.24 mmol) and 5-(1-octanolpivalate-8-sulfonyl)-1-phenyl-1*H*-tetrazole **(21)** (3.32 g, 7.86 mmol) in dry THF (100 ml) under nitrogen at -2 °C. The reaction mixture was allowed to reach RT and stirred for 16 hours, then quenched with saturated solution of ammonium chloride (50 ml) and petroleum ether/diethyl ether (1:1, 100 ml). The organic layer was separated and the aqueous layer re-extracted with petroleum ether/diethyl ether (1:1, 2 x 50 ml). The combined organic layers were washed with brine (2 x 100 ml), dried over magnesium sulfate and evaporated to give a thick oil, which was purified by column chromatography on silica gel eluted with petroleum ether/diethyl ether (10:0.3) to give *(E/Z)-2,2-dimethyl-propionic acid-(16R, 17R)-16-methoxy-17-methyl-pentatriacont-8-enyl ester* as a colourless liquid (2.65 g, 80%).

Physical properties:

δ_H (500 MHz, $CDCl_3$): 5.39 (1H, m), 5.35 (1H, m), 4.05 (2H, t, *J* 6.6 Hz), 3.34 (3H, s), 2.96 (1H, m), 1.99 (4H, m), 1.63 (4H, m), 1.37-1.24 (48 H, m including s), 1.20 (9H, s), 0.88 (3H, t, *J* 6.95 Hz), 0.85 (3H, d, *J* 6.9 Hz)

δ_C (500 MHz, $CDCl_3$): 178.56, 130.41(-), 130.21(-), 85.45(-), 64.41(+), 57.68(-), 38.70, 35.38(-), 32.57(+), 32.53(+), 32.39(+), 31.92(+), 30.52(+), 29.69(+), 29.35(+), 29.17(+), 29.07(+), 29.00(+), 28.62(+), 27.58(+), 27.20(-), 26.14(-), 25.87(+), 22.67(+), 14.88(-), 14.07(-), [+ = CH_2, - = CH, CH_3]

Palladium on charcoal (10%, 0.70 g) was added to a stirring solution of *(E/Z)-2,2-dimethyl-propionic acid-(16R, 17R)-16-methoxy-17-methyl-pentatriacont-8-enyl ester* (2.60 g, 4.11 mmol) in IMS (100 ml) and ethyl acetate (25 ml). The mixture was stirred while being hydrogenated under hydrogen atmosphere. When no more hydrogen was absorbed the mixture

was filtered through a pad of celite and washed with warmed ethanol (100 ml). The clear colourless filtrate was evaporated to give a white solid of *2,2-dimethyl-propionic acid-(16R, 17R)-16-methoxy-17-methyl-pentatriacontyl ester* **(22)** as a colourless oil (2.36 g, 91%).

Physical properties:

ν_{max}/cm^{-1}: 2922, 2852, 1731, 1155

δ_H (500 MHz, $CDCl_3$): 4.04 (2H, t, *J* 6.65 Hz), 3.34 (3H, s), 2.95 (1H, m), 1.33-1.23 (56 H, m including s), 1.19 (9H, s), 0.88 (3H, t, *J* 6.95 Hz), 0.85 (3H, d, *J* 6.9 Hz)

δ_C (500 MHz, $CDCl_3$): 178.56, 85.44(-), 64.43(+), 57.67(-), 38.70, 35.37(-), 32.40(+), 31.91(+), 30.51(+), 29.96(+), 29.92(+), 29.68(+), 29.55(+), 29.51(+), 29.34(+), 29.22(+), 28.62(+), 27.56(+), 27.18(-), 26.16(+), 25.90(+), 22.66(+), 20.97(-), 14.86(-), 14.17(-), 14.07(-), [+ = CH_2, - = CH, CH_3]

$[\alpha]_D^{24}$: +6.08 °, (c = 1.19, $CHCl_3$); *reported as* $[\alpha]_D^{22}$*: +6.8 ° (c = 1.49, $CHCl_3$)*

3.3.2.22 Preparation of (16R,17R)-16-methoxy-17-methyl-pentatriacontan-1-ol (23)

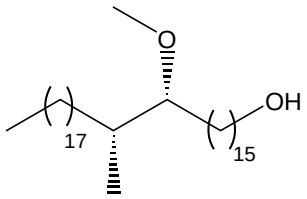

Potassium hydroxide (0.84 g, 14.97 mmol) in methanol (20 ml) was added to a stirring solution of (16*R*,17*R*)-1-*tert*-butoxy-16-methoxy-17-methyl-pentatriacontane **(22)** (2.35 g, 3.71 mmol) in THF (50 ml) at RT. The reaction mixture was stirred overnight at 40 °C. When TLC showed that no starting material was left, the reaction was quenched with water (100 ml) and a mixture of petroleum ether/diethyl ether (1:1, 100 ml). The organic layer was separated and the aqueous layer re-extracted with petroleum ether/diethyl ether (2 x 50 ml). The combined organic layers were washed with brine (60 ml), dried and evaporated to give a white solid which was purified by column chromatography on silica gel eluted with petroleum ether/diethyl ether (2:1) to give a white solid of *(16R,17R)-16-methoxy-17-methyl-pentatriacontan-1-ol* **(23)** (1.81 g, 89%).

Physical properties:

ν_{max}/cm^{-1}:	3373, 2921, 1098, 1076
m.p.	46-48 ºC
δ_H (500 MHz, $CDCl_3$):	3.65 (2H, q, *J* 6.6 Hz), 3.35 (3H, s), 2.96 (1H, m), 1.64 (1H, m), 1.58, (6H, pent, J 6.9 Hz), 1.4-1.24 (54H, m including s), 1.10 (1H, m), 0.89 (3H, t *J* 6.95 Hz), 0.85 (3H, d, *J* 6.95 Hz)
δ_C (500 MHz, $CDCl_3$):	85.45(-), 63.10(+), 57.71(-), 35.30(-), 32.81(+), 32.34(+), 31.92(+), 30.46(+), 29.98(+), 29.93(+), 29.69(+), 29.60(+), 29.42(+), 29.36(+), 27.56(+), 26.16(+), 25.73(+), 22.68(+), 14.88(-), 14.11(-), [+ = CH_2, - = CH, CH_3]
$[\alpha]_D^{24}$:	+7.76 °, (c = 1.03, $CHCl_3$); *reported as* $[\alpha]_D^{22}$*: +7.9 ° (c = 1.40, $CHCl_3$)*

*3.3.2.23 Preparation of (16**R**,17**R**)-1-bromo-16-methoxy-17-methyl-pentatriacontane (24)*

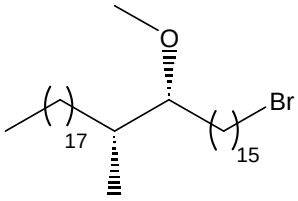

N-Bromosuccinimide (0.75 g, 4.21 mmol, 1.3 mol eq.) was added in portions over 15 minutes to a stirring solution of (16*R*,17*R*)-16-methoxy-17-methyl-pentatriacontan-1-ol **(23)** (1.80 g, 3.26 mmol) and triphenylphosphine (0.94 g, 3.58 mmol, 1.1 mol eq.) in dichloromethane (50 ml) at 0 °C. The reaction mixture was stirred at RT for 1 hour. When TLC showed that no starting material was left, the reaction was quenched with saturated solution of sodium meta-bisulfite (50 ml). The organic layer was separated and the aqueous layer re-extracted with dichloromethane (2 x 30 ml). The combined organic layers were washed with water, dried and evaporated to give a residue which was treated with a mixture of petroleum ether/diethyl ether (1:1, 100 ml). The mixture was refluxed for 30 minutes. The triphenylphosphine oxide was filtered off and washed with petroleum ether/diethyl ether (50 ml). The filtrate was evaporated and the residue was purified by column chromatography on silica gel eluted with petroleum ether/diethyl ether (10:0.2) to give *(16R,17R)-1-bromo-16-methoxy-17-methyl-pentatriacontane* **(24)** as a white solid (1.65 g, 82%).

Physical properties:

ν_{max}/cm^{-1}:	2929, 2849, 1099,717
m.p.	38-40 ºC
δ_H (500 MHz, $CDCl_3$):	3.42 (2H, t, *J* 6.9 Hz), 3.35 (3H, s), 2.96 (1H, m), 1.86 (2H, pent, *J* 6.95 Hz), 1.64 (1H, m), 1.45-1.2 (60 H, m including s), 0.89 (3H, t, *J* 6.6 Hz), 0.85 (3H, d, *J* 6.95 Hz)
δ_C (500 MHz, $CDCl_3$):	85.44(-), 57.71(-), 35.29(-), 34.06(+), 32.84(+), 32.34(+), 31.92(+), 30.46(+), 29.98(+), 29.93(+), 29.70(+), 29.62(+), 29.54(+), 29.44(+), 29.36(+), 28.77(+), 28.18(+), 27.57(+), 26.16(+), 22.69(+), 14.89(-), 14.12(-), [+ = CH_2, - = CH, CH_3]
$[\alpha]_D^{20}$:	+5.98 °, (c = 1.06, $CHCl_3$); *reported as* $[\alpha]_D^{22}$*: +6.5 ° (c = 1.16, $CHCl_3$)*

*3.3.2.24 Preparation of 5-((16**R**,17**R**)-16-methoxy-17-methyl-pentatriacontyl-1- sulfanyl)-1-phenyl-1**H**-tetrazole (25)*

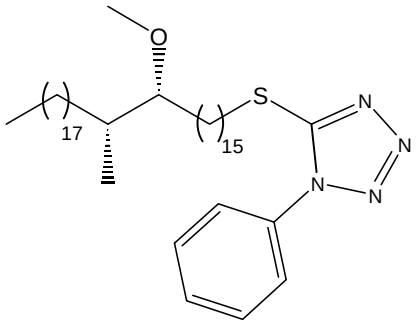

(16*R*,17*R*)-1-Bromo-16-methoxy-17-methyl-pentatriacontane **(24)** (1.60 g, 2.60 mmol) was added to a stirring solution of 1-phenyl-1*H*-tetrazol-5-thiol (0.51 g, 2.86 mmol) and potassium carbonate (1.44 g, 10.42 mmol) in acetone (60 ml) at RT. After 23 hours of stirring, TLC still showed that starting material was left. A further amount of 1-phenyl-1*H*-tetrazol-5-thiol (0.2 g) was added and the mixture was stirred overnight at RT. Then the solvent was evaporated and the residue diluted with a mixture of petroleum ether/diethyl ether (1:1, 150 ml) and water (100 ml). The organic layer was separated and the aqueous layer re-extracted with petroleum ether/diethyl ether (2 x 50 ml). The combined organic layers were dried and evaporated to give a pale yellow viscous oil which was purified by column chromatography on silica gel eluting

with petroleum ether/diethyl ether (10:1) to give *5-((16R,17R)-16-methoxy-17-methyl-pentatriacontyl-1-sulfanyl)-1-phenyl-1H-tetrazole* **(25)** as colourless viscous oil (1.65 g, 89%).

Physical properties:

ν_{max}/cm^{-1}: 2928, 2861, 1097

δ_H (500 MHz, $CDCl_3$): 7.58 (5H, m), 3.41 (2H, t, *J* 7.25 Hz), 3.35 (3H, s), 2.96 (1H, m), 1.83 (2H, pent, *J* 7.25 Hz), 1.63 (1H, m), 1.47-1.20 (62H, m including s), 1.10 (1H, m), 0.89 (3H, t, *J* 6.65 Hz), 0.85 (3H, d, *J* 6.95 Hz)

δ_C (500 MHz, $CDCl_3$): 130.03(-), 129.75(-), 123.88(-), 85.48(-), 57.72 (-), 35.40(-), 33.42(+), 32.42(+), 31.93(+), 30.54(+), 29.98(+), 29.95(+), 29.70(+), 29.63(+), 29.55(+), 29.44(+), 29.36(+), 29.11(+), 29.04(+), 28.66(+), 27.58(+), 26.19(+), 22.68(+), 14.89(-), 14.10(-), [+ = CH_2, - = CH, CH_3]

$[\alpha]_D^{18}$: +6.79 °, (c = 1.03, $CHCl_3$); *reported as* $[\alpha]_D^{22}$*: +6.18 (c = 1.12, $CHCl_3$)*

*3.3.2.25 Preparation of 5-((16*R*,17*R*)-16-methoxy-17-methyl-pentatriacontane-1-sulfonyl)-1-phenyl-1*H*-tetrazole (26)*

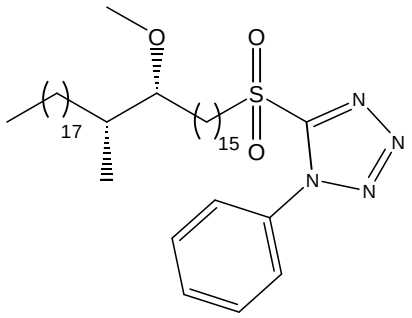

A solution of ammonium heptamolybdate(VI)tetrahydrate (2.48 g, 2.30 mmol, 1.1 mol eq.) in ice cold H_2O_2 35% (w/w, 11 ml) was added to a stirring solution of 5-((16*R*,17*R*)-16-methoxy-17-methyl-pentatriacontyl-1-sulfanyl)-1-phenyl-1*H*-tetrazole **(25)** (1.62 g, 2.28 mmol) in THF (30 ml) and IMS (70 ml) at 5 °C and stirred at RT for 1 hour. A further solution of ammonium heptamolybdate(VI)tetrahydrate (1.42 g, 1.15 mmol) in ice cold H_2O_2 35% (w/w, 5 ml) was added and the mixture was stirred overnight at RT. Dichloromethane (60 ml) and water (300 ml) was added, the organic layer separated and the aqueous layer re-extracted with

dichloromethane (2 x 30 ml). The combined organic layers were washed with water, dried and evaporated to give a residue which was purified by column chromatography on silica gel eluting with petroleum ether/diethyl ether (10:1) to give *5-((16R,17R)-16-methoxy-17-methyl-pentatriacontane-1-sulfonyl)-1-phenyl-1H-tetrazole* **(26)** as a white solid (1.1 g, 65%).

Physical properties:

ν_{max}/cm^{-1}:	2924, 2849, 1343, 1157, 1096
m.p.	42-44 ºC
δ_H (500 MHz, $CDCl_3$):	7.71 (2H, m), 7.61 (3H, m), 3.74 (2H, distorted t, *J* 7.85 Hz), 3.34 (3H, s), 2.96 (1H, m), 1.96 (2H, m), 1.63 (1H, m), 1.50-1.20 (63H, m including s), 0.89 (3H, t, *J* 6.65 Hz), 0.86 (3H, d, *J* 6.6 Hz)
δ_C (500 MHz, $CDCl_3$):	153.56, 133.11, 131.44(-), 129.70(-), 125.10(-), 85.48(-), 57.72(-), 56.07(+), 35.40(-), 33.42(+), 32.42(+), 31.93(+), 30.54(+), 29.98(+), 29.95(+), 29.70(+), 29.66(+), 29.57(+), 29.47(+), 29.36(+), 29.19(+), 29.11(+), 28.90(+), 28.66(+), 28.16(+), 27.58(+), 26.19(+), 22.68(+), 21.20(+), 14.89(-), 14.10(-), [+ = CH_2, - = CH, CH_3]
$[\alpha]_D^{26}$:	+5.46 °, (c = 1.08, $CHCl_3$); *reported as* $[\alpha]_D^{22}$*: +5.65 ° (c = 1.90, $CHCl_3$)*

3.3.2.26 Preparation of* cis-*cyclopropane-1,2-dicarboxylic acid dimethyl ester (27b)

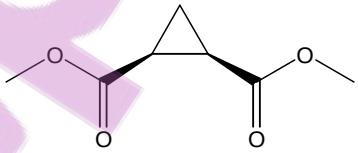

Sodium methoxide (25.60 g, 0.66 mol) was added to a stirring mixture of methylacrylate (100 ml, 1.54 mol) and methylchloroacetate (41.50 ml, 0.66 mol) in an ice bath at 20-32 °C over 1 hour. The reaction is strongly exothermic. The reaction mixture was stirred at 18-25 °C for 1 hour. Water (150 ml) was added, stirred for 10 minutes and the organic phase washed with brine (2 x 50 ml) and the combined aqueous phases were re-extracted with dichloromethane (2 x 50 ml). The combined organic phases were dried and the solvent evaporated to give a pale yellow oil. This oil was distilled at 1 mm Hg, and collected in four fractions. The fractions

were analysed by GLC. The programme: initial temperature was 80 °C for 1 minute, increase rate of 20 °C/minute up to 240 °C, and then for 1 minute at 240 °C. The oven temperature was 80 °C. Peaks observed were: at 0.94 minutes the *trans*-ester, at 1.15 minutes the *cis*-ester, at 1.55, 2.20, 1.93, 2.51, 3.09, 4.04 and 5.06 minutes high boiling point impurities. The rough composition of the different fractions was as follow:

Fraction	Yield	Boiling point	*trans*-ester	*cis*-ester	impurities
1	71 g	< 40 °C	0	0	0.2
2	40 g	40-70 °C	1.6	2.5	0.2
3	8.73 g	70-80 °C	0.1	4.2	0.7
4	1.2 g	80-95 °C	0.02	2.3	1.5

The fractions containing the *cis*-stereoisomer were separated by column chromatography on silica gel eluted with petroleum ether/diethyl ether (9:1) to give a colourless oil, *cis-cyclopropane-1,2-dicaboxylic acid-dimethylester* **(27b)** (32.74 g, 31%) (68).

Physical properties:

ν_{max}/cm^{-1}: 3626, 3003, 2955, 1720

δ_H (500 MHz, $CDCl_3$): 3.70 (6H, s), 2.08 (2H, dd, *J* 6.9, 8.5 Hz), 1.70 (1H, ddd, *J* 5, 6.6, 13.2 Hz), 1.26 (1H, dt, *J* 5.05, 8.55 Hz)

δ_C (500 MHz, $CDCl_3$): 170.21, 51.98(+), 21.23(+), 11.64(-), [- = CH_2, + = CH, CH_3]

$[\alpha]_D^{26}$: +0.18 ° (c = 1.51, $CHCl_3$)

*3.3.2.27 Preparation of (*cis*-2-hydroxymethylcyclopropyl)-methanol (28)*

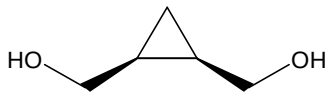

$LiAlH_4$ (0.2 g) was added to stirring THF (300 ml) at -20 °C under nitrogen to check the dryness of the THF. Then $LiAlH_4$ (9.00 g, 237.09 mmol, 2 mol eq.) was added. A solution of *cis*-cyclopropane-1,2-dicaboxylic acid dimethyl ester **(27b)** (18.73 g, 118.55 mmol) in THF (100 ml) was added drop-wise at -20 °C and the mixture refluxed for 1 hour. A freshly prepared saturated solution of sodium sulfate decahydrate (30 ml) was added at -20 °C and

stirred for 30 minutes at RT. The mixture was filtered through a pad of silica gel, dried and the solvent evaporated to give a colourless oil of *(cis-2-hydroxymethylcyclopropyl)-methanol* **(28)** (11.42 g, 95%) (68).

Physical properties:

ν_{max}/cm^{-1}: 3320, 3003, 2885

δ_H (500 MHz, $CDCl_3$): 4.09 (2H, m), 3.24 (2H, m), 1.28 (2H, m), 0.80 (1H, m), 0.20 (1H, m)

δ_C (500 MHz, $CDCl_3$): 62.95(+), 17.48(-), 8.49(+), [+ = CH_2, - = CH, CH_3]

$[\alpha]_D^{26}$: -0.2 ° (c = 1.15, $CHCl_3$)

3.3.2.28 Preparation of butyric acid cis-*2-butyryloxymethylcyclopropylmethyl ester (29)*

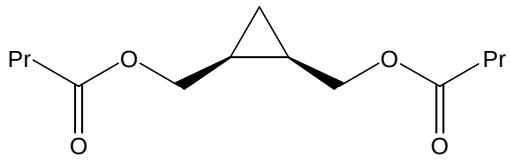

Butyric anhydride (37.53 g, 237.25 mmol, 2.2 mol eq.) was added to (*cis*-2-hydroxymethylcyclopropyl)-methanol **(28)** (11.00 g, 107.84 mmol). The mixture was refluxed at 140 °C for 1 hour and then cooled to RT. Dichloromethane (200 ml) and sodium hydroxide solution (14 g in 200 ml water) were added and then extracted. The aqueous layer was re-extracted with dichloromethane (2 x 50 ml) and the combined organic layers were washed with sodium bicarbonate solution (100 ml). The organic phase was dried, the solvent evaporated and the excess butyric anhydride distilled at high vacuum. The crude product was purified by column chromatography eluted with petroleum ether/diethyl ether (5:1) to give a colourless oil of *butyric acid cis-2-butyryloxymethylcyclopropylmethyl ester* **(29)** (23.69 g, 91%) (68).

Physical properties:

ν_{max}/cm^{-1}: 2966, 2877, 1725

δ_H (500 MHz, $CDCl_3$): 4.25 (2H, dd, *J* 6.9, 11.95 Hz), 3.97 (2H, dd, *J* 7.85, 11.95), 2.30 (4H, t, *J* 7.55 Hz), 1.67 (4H, sextet, *J* 7.25 Hz), 1.33 (2H, m), 0.96 (6H, t, *J* 7.25 Hz), 0.90 (1H, dt, *J* 5.05, 8.2 Hz), 0.35 (1H, q, *J* 5.65 Hz)

δ_C (500 MHz, $CDCl_3$): 173.52, 64.12(+), 36.15(+), 18.40(+), 14.65(-), 13.59(-), 8.58(+), [+ = CH_2, - = CH, CH_3]

$[\alpha]_D^{26}$: +0.2 ° (c = 1.65, $CHCl_3$)

3.3.2.29 Preparation of butyric acid cis-*2-hydroxymethylcyclopropylmethyl ester (30)*

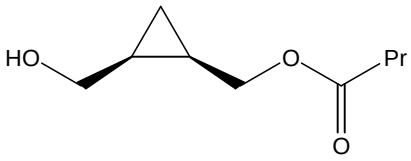

Lipase (1 g, PPL (Pig pancreas lipase), type II) was added to a flask fitted with a glass pH electrode which had been accurately calibrated, containing a gently stirring solution of distilled water (161 ml) and ethylene glycol (41 ml) at 3 °C under a steady stream of nitrogen. Butyric acid *cis*-2-butyryloxymethylcyclopropylmethyl ester **(29)** (10.50 g, 43.38 mmol) was then added. When hydrolysis began, pH decreased due to the formation of butyric acid. The pH was brought back to 6.5 by the careful addition of sodium hydroxide (1M) whilst maintaining the temperature at 3 °C. More lipase (0.75 g) was added to the reaction mixture after 1 hour and sodium hydroxide solution was added drop-wise during the reaction to keep the pH at 6.5. The total added sodium hydroxide solution was 45 ml and it took 4 ¼ hours. The mixture was filtered through a pad of celite; the pad of celite was then washed with water (25 ml) and then ether (50 ml). A saturated solution of sodium bicarbonate (60 ml) was added, pH 8.44, and then neutralised by ammonium chloride solution to pH 7.4. The mixture was extracted with ether (2 x 300 ml) and the combined organic layers were dried. The solvent was evaporated and the crude product was purified by column chromatography on silica gel eluted with petroleum ether/diethyl ether (1:1) to give a colourless oil of *butyric acid cis-2-hydroxymethylcyclopropylmethyl ester* **(30)** (5.39 g, 72%) (68).

Physical properties:

ν_{max}/cm^{-1}: 3417, 2966, 1732, 1186, 1046

δ_H (500 MHz, $CDCl_3$): 4.46 (1H, dd, *J* 5.7, 12 Hz), 3.83 (2H, m), 3.39 (1H, dd, *J* 9.15, 11.65 Hz), 2.30 (2H, t, *J* 7.55 Hz), 2.21 (1H, broad s), 1.65 (2H, sextet, *J* 7.25 Hz), 1.30 (2H, m), 0.94 (3H, t, *J* 7.55 Hz), 0.84 (1H, dt, *J* 5.05, 8.5 Hz), 0.22 (1H, q, *J* 5.65 Hz)

δ_C (500 MHz, $CDCl_3$): 173.62, 64.37(+), 62.46(+), 36.20(+), 18.58(-), 18.37(+), 14.36(-), 13.56(-), 7.68(+), [+ = CH_2, - = CH, CH_3]

$[\alpha]_D^{26}$: +19.35 ° (c = 1.33, $CHCl_3$), *reported as* $[\alpha]_D^{22}$*: +18.2 ° (c = 1.58,* $CHCl_3$*) by Grandjean et al. (68)*

3.3.2.30 Preparation of butyric acid cis*-2-bromomethylcyclopropylmethyl ester (31)*

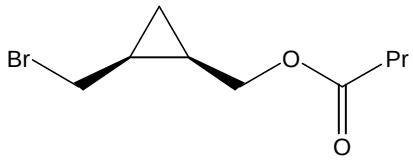

Triphenylphosphine (8.78 g, 33.43 mmol, 1.15 mol eq.) and butyric acid *cis*-2-hydroxymethylcyclopropylmethyl ester **(30)** (5 g, 29.07 mmol) were dissolved in dichloromethane (150 ml) at RT and then cooled to 0 °C. *N*-bromosuccinimide (6.57 g, 36.92 mmol, 1.27 mol eq.) was added portion wise over 20 minutes at 0-4 °C. The mixture was allowed to reach RT and then stirred for 1 hour. When TLC showed that no starting material was left, a saturated solution of sodium bisulfate (140 ml) was added and the mixture was extracted. The aqueous layer was re-extracted with dichloromethane (2 x 50 ml) and the combined organic layers were washed with water (100 ml). The solution was dried and the solvent evaporated. Petroleum ether/diethyl ether (1:1, 250 ml) was added and the mixture stirred for 30 minutes at RT. The triphenylphosphonium oxide was filtered off and washed thoroughly with a mixture of petroleum ether/diethyl ether (1:1). The solvent was evaporated and the crude product purified by column chromatography on silica gel eluted with petroleum ether/diethyl ether (4:1) to give a colourless oil of *butyric acid cis-2-bromomethylcyclopropylmethyl ester* **(31)** (6 g, 88%).

Physical properties:

ν_{max}/cm^{-1}: 2966, 2876, 1734, 1181, 986

δ_H (500 MHz, $CDCl_3$): 4.22 (1H, dd, *J* 6.95, 12 Hz), 4.03 (1H, dd, *J* 8.5, 12.3 Hz), 3.51 (1H, dd, *J* 7.55, 10.4 Hz), 3.38 (1H, dd, *J* 8.2, 10.4 Hz), 2.29 (2H, t, *J* 7.6 Hz), 1.65 (2H, sextet, *J* 7.25 Hz), 1.48 (2H, m), 1.01 (1H, dt, *J* 5.35, 8.2 Hz), 0.94 (3H, t, *J* 7.6 Hz), 0.36 (1H, q, *J* 5.65 Hz)

δ_C (500 MHz, $CDCl_3$): 173.52, 63.31(+), 36.13(+), 33.96(+), 19.29(-), 18.36(+), 17.96(-), 13.59(-), 12.49(+), [+ = CH_2, - = CH, CH_3]

$[\alpha]_D^{24}$: -9.69 ° (c = 1.37, $CHCl_3$); *reported as* $[\alpha]_D^{23}$*: -10.6 ° (c = 0.81,* $CHCl_3$*)*

*3.3.2.31 Preparation of butyric acid (1*R*,2*S*)-2-(1-phenyl-1*H*-tetrazol-5-ylsulfanylmethyl)-cyclopropyl methyl ester (32)*

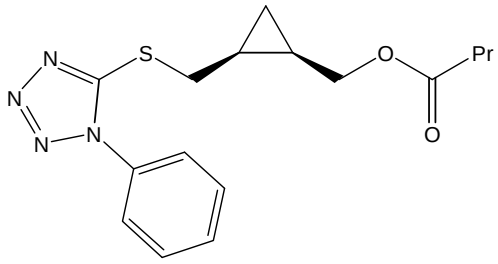

Butyric acid *cis*-2-bromomethylcyclopropylmethyl ester **(31)** (8.00 g, 34.04 mmol) was added to a stirring solution of 1-phenyl-1H-tetrazol-5-thiol (6.67 g, 37.44 mmol) and potassium carbonate (9.89 g, 71.48 mmol) in acetone (250 ml) at RT and the reaction mixture was stirred for 19 hours at RT. When TLC showed that no starting material was left, the mixture was added to water (1.5 L) and extracted with dichloromethane (250 ml). The aqueous layer was re-extracted with dichloromethane (2 x 80 ml) and the combined organic layers were washed with brine (2 x 200 ml), dried and evaporated. The crude product was purified by column chromatography on silica gel eluted with petroleum ether/diethyl ether (2:1) to give a pale yellow oil of *butyric acid (1*R*,2*S*)-2-(1-phenyl-1H-tetrazol-5-ylsulfanylmethyl)-cyclopropylmethyl ester* **(32)** (10.95 g, 88%).

Physical properties:

Found M + Na^+: 355.1185, $C_{16}H_{20}N_4NaO_2S$ requires: 355.1199

ν_{max}/cm^{-1}: 2965, 2875, 1732, 1500, 1174, 983, 763

δ_H (500 MHz, $CDCl_3$): 7.57 (5H, m), 4.34 (1H, dd, *J* 6.6, 12.25 Hz), 3.96 (1H, dd, *J* 9.15, 11.95 Hz), 3.59 (1H, dd, *J* 7.85, 13.25 Hz), 3.43 (1H, dd, *J* 7.9, 13.55 Hz), 2.27 (2H, t, *J* 7.55 Hz), 1.64 (2H, sextet, *J* 7.55 Hz), 1.51 (1H, m), 1.41 (1H, m), 0.97 (1H, dt, *J* 5.4, 8.2 Hz), 0.93 (3H, t, *J* 7.25 Hz), 0.40 (1H, q, *J* 5.7 Hz)

δ_C (500 MHz, $CDCl_3$): 173.45, 154.25, 133.81, 130.05(+), 129.73(+), 123.84(+), 63.72(-), 36.20(-), 34.18(-), 18.38(-), 16.39(+), 15.53(+), 13.61(+), 10.96(-), [- = CH_2, + = CH, CH_3]

$[\alpha]_D^{24}$: -1.28 ° (c = 1.14, $CHCl_3$); *reported as* $[\alpha]_D^{22}$*: -1.2 ° (c = 1.06, $CHCl_3$)*

*3.3.2.32 Preparation of butyric acid (1*R*,2*S*)-2-(1-phenyl-1*H*-tetrazole-5-sulfonylmethyl)-cyclopropyl methyl ester (33)*

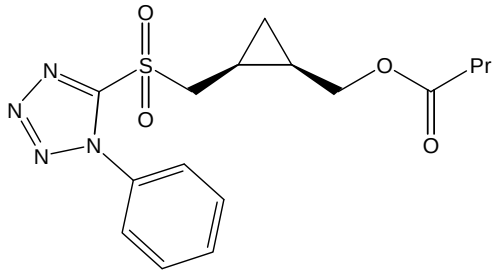

A solution of ammonium heptamolybdate(VI)tetrahydrate (18.59 g, 15.06 mmol) in ice cold H_2O_2 35% (w/w, 50 ml) was added to a stirring solution of butyric acid (1*R*,2*S*)-2-(1-phenyl-1*H*-tetrazol-5-ylsulfanylmethyl)-cyclopropylmethyl ester **(32)** (10.00 g, 30.12 mmol) in THF (125 ml) and IMS (250 ml) at 10 °C and stirred at RT for 2 hours. A further solution of ammonium heptamolybdate(VI)tetrahydrate (5.03 g, 4.07 mmol) in ice cold H_2O_2 35% (w/w, 15 ml) was added and the mixture stirred for 19 hours at RT. The reaction mixture was poured into water (1.5 L) and extracted with dichloromethane (1 x 300 ml, 2 x 80 ml). The combined organic layers were washed with water (700 ml), dried and evaporated to give a residue which was purified by column chromatography on silica gel eluted with petroleum ether/diethyl ether (2:1) to give a thick pale yellow oil of *butyric acid (1*R*,2*S*)-2-(1-phenyl-1H-tetrazole-5-sulfonylmethyl)-cyclopropylmethyl ester* **(33)** (10.18 g, 93%).

Physical properties:

Found M + Na^+: 387.1079, $C_{16}H_{20}N_4NaO_4S$ requires: 387.1097

ν_{max}/cm^{-1}:	2967, 1731, 1343, 1153, 765
δ_H (500 MHz, $CDCl_3$):	7.70 (2H, m), 7.63 (3H, m), 4.37 (1H, dd, *J* 5.7, 12.3 Hz), 4.03 (1H, dd, *J* 5.4, 14.85 Hz), 3.92 (1H, dd, *J* 8.2, 12 Hz), 3.67 (1H, dd, *J* 8.85, 15.15 Hz), 2.31 (2H, t, *J* 7.55 Hz), 1.67 (2H, sextet, *J* 7.55 Hz), 1.49 (2H, m), 1.03 (1H, dt, *J* 5.7, 8.5 Hz), 0.97 (3H, t, *J* 7.55 Hz), 0.60 (1H, q, *J* 5.7 Hz)
δ_C (500 MHz, $CDCl_3$):	173.33, 153.70, 133.14, 131.45(+), 129.68(+), 125.17(+), 63.37(-), 56.76(-), 36.13(-), 18.41(-), 14.73(+), 13.61(+), 9.70(-), 8.68(+), [- = CH_2, + = CH, CH_3]
$[\alpha]_D^{24}$:	+44.22 ° (c = 1.10, $CHCl_3$); *reported as* $[\alpha]_D^{23}$*: +52.7 ° (c = 1.45, $CHCl_3$)*

3.3.2.33 Preparation of 6-bromo-hexanal (34)

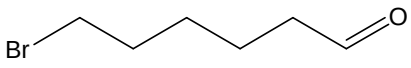

6-Bromo-hexan-1-ol (10.00 g, 55.25 mmol, see Preparation of 6-Bromo-hexan-1-ol, section 3.3.2.11) in dichloromethane (30 ml) was added to a stirring suspension of pyridinium chlorochromate (29.95 g, 138.94 mmol) in dichloromethane (300 ml) at RT. The mixture was stirred for 3 hours at RT. When TLC showed no starting material was left, the mixture was poured into diethyl ether (500 ml) and filtered through a pad of silica gel, then washed well with diethyl ether. The filtrate was evaporated to give a residue which was purified by column chromatography on silica gel eluted with petroleum ether/diethyl ether (5:1, then 1:1) to give *6-bromo-hexanal* **(34)** as a colourless oil (6.31 g, 64%).

Physical properties:

δ_H (500 MHz, $CDCl_3$): 9.77 (1H, t, *J* 1.25 Hz), 3.40 (2H, t, *J* 6.9 Hz), 2.46 (2H, dt, *J* 7.25, 1.25 Hz), 1.88 (2H, pent, *J* 6.6 Hz), 1.66 (2H, pent, *J* 7.25 Hz), 1.48 (2H, m)

δ_C (500 MHz, $CDCl_3$): 201.96(+), 43.59 (-), 33.23 (-), 32.42 (-), 27.64(-), 21.16(-), [- = CH_2, + = CH, CH_3]

*3.3.2.34 Preparation of butyric acid (1**R**,2**S**)-2-(7-bromo-heptyl)-cyclopropyl methyl ester (35)*

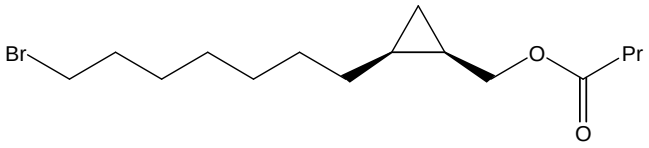

Lithium bis(trimethylsilyl)amide (46.66 ml, 49.56 mmol, 1.06 M, 2 mol eq.) was added drop-wise to a stirring solution of butyric acid (1*R*,2*S*)-2-(1-phenyl-1*H*-tetrazole-5-sulfonylmethyl)-cyclopropylmethyl ester **(33)** (9.00 g, 24.73 mmol) and 6-bromo-hexanal **(34)** (5.31 g, 29.67 mmol, 1.2 mol eq.) in dry THF (130 ml) under nitrogen at - 20 °C. The reaction mixture was allowed to reach RT and was then stirred for 16 hours. The reaction was quenched with water (100 ml) and petroleum ether/diethyl ether (1:1, 100 ml). The organic layer was separated and the aqueous layer re-extracted with petroleum ether/diethyl ether (1:1, 2 x 50 ml). The combined organic layers were washed with brine (2 x 100 ml), dried and evaporated to give a

thick dark yellow oil which was purified by column chromatography on silica gel eluted with petroleum ether/diethyl ether (9:1) to give *butyric acid 2-((E/Z)-7-bromo-hept-1-enyl)-cyclopropylmethyl ester* (5.80 g, 74%).

Butyric acid 2-((*E*/*Z*)-7-bromo-hept-1-enyl)-cyclopropylmethyl ester (5.75 g, 18.14 mmol) was dissolved in THF (150 ml). 2,4,6-Triisopropylbenzene sulfonohydrazide (14.88 g, 49.88 mmol, 2.75 mol eq.) was added and the reaction mixture was stirred at 50 °C for 20 hours. A further 2,4,6-triisopropylbenzene sulfonohydrazide (3.7 g, 12.40 mmol, 0.68 mol eq.) was added and the reaction was stirred at 50 °C for 22 hours. The mixture was diluted with petroleum ether/diethyl ether (1:1, 200 ml) and a solution of NaOH in water (100 ml, 2%) and extracted. The aqueous layer was re-extracted with petroleum ether/diethyl ether (1:1, 2 x 50 ml) and the combined organic layers were washed with water (100 ml), dried and evaporated. ^{1}H NMR showed that there was still some starting material left. The hydrogenation was repeated: Butyric acid 2-((*E*/*Z*)-7-bromo-hept-1-enyl)-cyclopropylmethyl ester (5.75 g, 18.14 mmol) was dissolved in THF (70 ml). 2,4,6-Triisopropylbenzene sulfonohydrazide (5.4 g, 18.14 mmol, 1 mol eq.) was added and the reaction mixture was stirred at 50 °C for 3 hours. A further 2,4,6-triisopropylbenzene sulfonohydrazide (5.4 g, 18.14 mmol, 1 mol eq.) was added and the reaction was stirred at 50 °C for 24 hours. The mixture was diluted with petroleum ether/diethyl ether (1:1, 100 ml) and a solution of NaOH in water (200 ml, 2%) and extracted. The organic layer was separated and the aqueous layer re-extracted with petroleum ether/diethyl ether (1:1, 2 x 100 ml). The combined organic layers were washed with water (150 ml), dried and evaporated. ^{1}H NMR showed that there was no more starting material left. The crude product was purified by column chromatography on silica gel eluting with petroleum ether/diethyl ether (10:1) to give *butyric acid (1*R,*2*S*)-2-(7-bromo-heptyl)-cyclopropylmethyl ester* **(35)** as a colourless oil (4.61 g, 80%).

Physical properties:

Found M + Na^{+}: 341.1021, $C_{15}H_{27}BrNaO_2$ requires: 341.1087

ν_{max}/cm^{-1}: 3066, 2962, 2855, 1734

δ_H (500 MHz, $CDCl_3$): 4.19 (1H, dd, *J* 6.9, 11.65 Hz), 3.93 (1H, dd, *J* 8.8, 11.65), 3.41 (2H, t, *J* 6.95 Hz), 2.30 (2H, t, *J* 7.25 Hz), 1.86 (2H, pent, *J* 6.9 Hz), 1.67 (2H, sextet, *J* 7.25 Hz), 1.4 (5H, m), 1.32 (4H, m), 1.23 (1H, m), 1.13 (1H, m), 0.96 (3H, t, *J* 7.25 Hz), 0.87 (1H, m), 0.74 (1H, dt, *J* 4.75, 8.55 Hz), 0.02 (1H, q, *J* 5.4 Hz)

δ_C (500 MHz, $CDCl_3$): 173.81, 65.07(+), 36.32(+), 33.93(+), 32.79(+), 29.81(+), 29.28(+), 28.74(+), 28.53(+), 28.12(+), 18.50(+), 16.17(-), 14.17(-), 13.66(-), 9.77(+) [+ = CH_2, - = CH, CH_3]

$[\alpha]_D^{24}$: +10.03 ° (c = 1.50, $CHCl_3$); *reported as* $[\alpha]_D^{23}$*: -14.31 ° (c = 1.2, $CHCl_3$)*

*3.3.2.35 Preparation of (1*R*,2*S*)-2-(7-bromo-heptyl)-cyclopropyl methanol (36)*

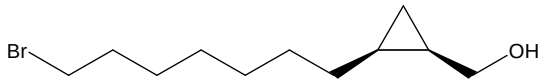

Anhydrous potassium carbonate (5.17 g, 37.39 mmol, 2.65 mol eq.) was added to a stirring solution of butyric acid (1*R*,2*S*)-2-(7-bromo-heptyl)-cyclopropylmethyl ester **(35)** (4.5 g, 14.11 mmol) in methanol (30 ml) and THF (20 ml) at room temperature. The reaction was stirred for 4 hours at 45 °C. When TLC showed that no starting material was left, the mixture was diluted with water (200 ml) and diethyl ether (100 ml). The organic layer was separated and the aqueous layer re-extracted with diethyl ether (2 x 50 ml). The combined organic layers were washed with brine, dried and evaporated to give an oily residue which was purified by column chromatography on silica gel eluting with petroleum ether/diethyl ether (5:1) to give (1*R*,2*S*)-*2-(7-bromo-heptyl)-cyclopropyl-methanol* **(36)** (2.97 g, 85%).

Physical properties:

Found M + Na^+: 271.0623, $C_{11}H_{21}BrNaO$ requires: 271.0668

ν_{max}/cm^{-1}: 3345, 2934, 2859

δ_H (500 MHz, $CDCl_3$): 3.65 (1H, dd, *J* 7.25, 11.35 Hz), 3.57 (1H, dd, *J* 8.2, 11.35 Hz), 3.41 (2H, t, *J* 6.95 Hz), 1.86 (2H, pent, *J* 6.95 Hz), 1.43 (6H, m), 1.33 (4H, m), 1.22 (1H, m), 1.10 (1H, m), 0.86 (1H, m), 0.71 (1H, dt, *J* 4.7, 8.5 Hz), -0.03 (1H, q, *J* 5.05 Hz)

δ_C (500 MHz, $CDCl_3$): 63.27(+), 33.97(+), 32.78(+), 29.98(+), 29.28(+), 28.70(+), 28.47(+), 28.10(+), 18.13(-), 16.09(-), 9.45(+), [+ = CH_2, - = CH, CH_3]

$[\alpha]_D^{24}$: +12.87 ° (c = 1.65, $CHCl_3$); *reported as* $[\alpha]_D^{23}$*: -18.9 ° (c = 1.04, $CHCl_3$)*

3.3.2.36 Preparation of (1S,2R)-2-(7-bromo-heptyl)-cyclopropane carbaldehyde (37)

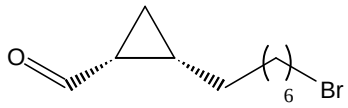

(1*R*,2*S*)-2-(7-Bromo-heptyl)-cyclopropyl-methanol **(36)** (1.0 g, 4.02 mmol) in dichloromethane (10 ml) was added to a stirring suspension of pyridinium chlorochromate (2.17 g, 10.05 mmol, 2.5 mol eq.) in dichloromethane (35 ml) at RT. The mixture was stirred for 3 hours at RT and when TLC showed that no starting material was left, the mixture was poured into diethyl ether (200 ml) and filtered through a pad of silica gel, then washed thoroughly with diethyl ether and the filtrate evaporated to give a residue which was purified by column chromatography on silica gel eluted with petroleum ether/diethyl ether (5:2) to give *(1S,2R)-2-(7-bromo-heptyl)-cyclopropane carbaldehyde* **(37)** as a colourless oil (0.75 g, 76%).

Physical properties:

Found M + Na^+: 269.04, $C_{11}H_{19}BrNaO$ requires: 269.0511

ν_{max}/cm^{-1}: 3436, 2928, 2855, 1704

δ_H (500 MHz, $CDCl_3$): 9.37 (1H, d, *J* 5.4 Hz), 3.41 (2H, t, *J* 6.6 Hz), 1.87 (3H, m), 1.60 (1H, m), 1.49 (2H, m), 1.41 (3H, m), 1.32 (5H, m), 1.24 (1H, dt, *J* 4.75, 7.9 Hz), 1.19 (1H, dt, *J* 5.05, 6.6 Hz)

δ_C (500 MHz, $CDCl_3$): 201.64(-), 33.90(+), 32.71(+), 29.79(+), 28.98(+), 28.59(+), 28.05(+), 28.02(+), 27.71(-), 24.75(-), 14.71(+), [+ = CH_2, - = CH, CH_3]

$[\alpha]_D^{24}$: +8.19 ° (c = 1.28, $CHCl_3$); *reported as* $[\alpha]_D^{23}$*: -10.1 ° (c = 1.62, $CHCl_3$)*

3.3.2.37 Preparation of (1S,2R)-1-(7-bromo-heptyl)-2-((17R,18R)-17-methoxy-18-methyl-hexatriacontyl)-cyclopropane (38)

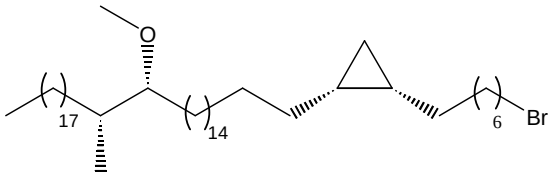

Lithium bis(trimethylsilyl)amide (46.70 ml, 49.56 mmol, 1.06 M, 2 mol eq.) was added drop wise to a stirring solution of (1*S*,2*R*)-2-(7-bromo-heptyl)-cyclopropane carbaldehyde **(37)** (5.31 g, 29.67 mmol) and 5-((16*R*,17*R*)-16-methoxy-17-methyl-pentatriacontane-1-sulfanyl)-1-phenyl-1*H*-tetrazole **(26)** (9 g, 24.73 mmol, 1.2 mol eq.) in dry THF (50 ml) under nitrogen at -2 °C. The reaction mixture was allowed to reach RT and stirred for 1 hour. When TLC showed that no starting material was left, the reaction mixture was quenched with a saturated solution of ammonium chloride (100 ml) and petroleum ether/diethyl ether (1:1, 100 ml). The organic layer was separated and the aqueous layer re-extracted with petroleum ether/diethyl ether (1:1, 2 x 50 ml). The combined organic layers were washed with brine (100 ml), dried and evaporated to give a pale yellow oil which was purified by column chromatography on silica gel eluted with petroleum ether/diethyl ether (9:1) to give (1*S*,2*R*)-*1-(7-bromo-heptyl)-2-((E/Z)-17-methoxy-18-methyl-hexatriacontyl)-cyclopropane* as a colourless oil (5.80 g, 74%).

Physical properties:

δ_H (500 MHz, $CDCl_3$): 5.52 (1H, m), 5.17 (1H, dd, J 8.55, 15.45 Hz), 3.41 (2H, t, *J* 6.95 Hz), 3.35 (3H, s), 2.96 (1H, m), 2.01 (2H, q, *J* 6.95 Hz), 1.87 (2H, pent, *J* 6.9 Hz), 1.64 (1H, m), 1.46-1.20 (70H, m including s), 1.11 (2H, m), 0.89 (3H, t, *J* 6.95 Hz), 0.85 (3H, d, *J* 6.95 Hz), 0.80 (1H, dt, *J* 4.4, 8.5 Hz), 0.12 (1H, q, *J* 5.35 Hz)

δ_C (500 MHz, $CDCl_3$): 127.84(-), 125.56(-), 85.45(-), 57.71(-), 35.36(-), 33.95(+), 32.85(+), 32.74(+), 32.39(+), 31.93(+), 30.51(+), 29.98(+), 29.94(+), 29.79(+), 29.70(+), 29.62(+), 29.56(+), 29.36(+), 29.30(+), 29.17(+), 29.07(+),28.87(+), 28.77(+), 28.17(+), 27.58(+), 26.17(+), 22.69(+), 18.43(-), 18.20(-), 14.88(-), 14.10(-), 12.30(+), [+ = CH_2, - = CH, CH_3]

2,4,6-Triisopropylbenzene sulfonohydrazide (14.88 g, 49.88 mmol, 2.75 mol eq.) was added to a stirring solution of (1*S*,2*R*)-1-(7-bromo-heptyl)-2-((E/Z)-17-methoxy-18-methyl-hexatriacontyl)-cyclopropane (5.75 g, 18.14 mmol) in THF (150 ml) at RT. The reaction mixture was stirred at 52 °C for 3 hours, followed by the addition of another mole equivalent of 2,4,6-triisopropylbenzene sulfonohydrazide (5.41 g, 18.14 mmol) and stirred under the same conditions for another 24 hours. The mixture was diluted with petroleum ether/diethyl ether (1:1, 100 ml) and a solution of NaOH in water (100 ml, 2%) and extracted. The organic layer was separated and the aqueous layer was re-extracted with petroleum ether/diethyl ether (1:1, 2 x 50 ml) and the combined organic layers were washed with brine (100 ml), dried, filtered through a pad of silica gel and washed with petroleum ether. The filtrate was evaporated to give a colourless residue. ^{1}H NMR showed that there was still some starting material left and the same procedure was repeated. The crude product was purified by column chromatography on silica gel eluting with petroleum ether/diethyl ether (10:1) to give (1*S*,2*R*)-*1-(7-bromo-heptyl)-2-(17-methoxy-18-methyl-hexatriacontyl)-cyclopropane* **(38)** as a colourless oil (4.61 g, 80%).

Physical properties:

ν_{max}/cm^{-1}:	2922, 1464, 1098, 720
δ_H (500 MHz, $CDCl_3$):	3.42 (2H, t, *J* 6.95 Hz), 3.35 (3H, s), 2.96 (1H, m), 1.87 (2H, pent, *J* 6.9 Hz), 1.64 (1H, m), 1.48-1.2 (73H, m including s), 1.18-1.06 (4H, m), 0.89 (3H, t, *J* 6.95 Hz), 0.86 (3H, d, *J* 6.95 Hz), 0.66 (2H, m), 0.57 (1H, dt, *J* 4.1, 7.9 Hz), -0.32 (1H, q, *J* 5.35 Hz)
δ_C (500 MHz, $CDCl_3$):	85.45(-), 57.71(-), 35.35(-), 34.01(-), 32.86(+), 32.39(+), 31.92(+), 30.50(+), 30.22(+), 30.07(+), 29.98(+), 29.94(+), 29.70(+), 29.41(+), 29.36(+), 28.82(+), 28.72(+), 28.65(+), 28.19(+), 27.58(+), 26.16(+), 24.10(-), 22.69(+), 15.78(-), 15.72(-), 14.88(-), 14.10(-), 10.93(+), [+ = CH_2, - = CH, CH_3]
$[\alpha]_D^{24}$:	+5.17 ° (c = 1.44, $CHCl_3$); *reported as* $[\alpha]_D^{22}$*: +5.5 ° (c = 1.29, $CHCl_3$)*

3.3.2.38 Preparation of 5-(7-[1S,2R]-2-((17R,18R)-17-methoxy-18-methyl-hexatriacontyl)-cyclopropyl)-heptyl sulfanyl)-1-phenyl-1H-tetrazole (39)

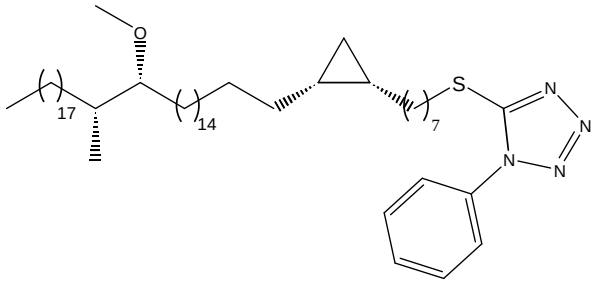

1-(7-Bromo-heptyl)-2-((17*R*,18*R*)-17-methoxy-18-methyl-hexatriacontyl)-cyclopropane **(38)** (0.5 g, 0.65 mmol) in THF (10 ml) was added to a stirring solution of 1-phenyl-1*H*-tetrazol-5-thiol (0.13 g, 0.72 mmol, 1.1 mol eq.) and potassium carbonate (0.35 g, 2.50 mmol, 3.8 mol eq.) in acetone (30 ml) at RT. The reaction mixture was stirred for 5 hours at 40 °C and then at RT for 16 hours. When TLC showed that no starting material was left, the mixture was diluted with water (50 ml) and dichloromethane (100 ml). The organic layer was separated and the aqueous layer was re-extracted with dichloromethane (2 x 50 ml). The combined organic layers were washed with brine (2 x 200 ml), dried and evaporated to give an oil which solidified later. The crude product was purified by column chromatography on silica gel eluted with petroleum ether/diethyl ether (2:1) to give a oil of *5-(7-[1S,2R]-2-((17R,18R)-17-methoxy-18-methyl-hexatriacontyl)-cyclopropyl)-heptyl sulfanyl)-1-phenyl-1H-tetrazole* **(39)** (10.95 g, 88%).

Physical properties:

Found M + Na^+: 887.7434, $C_{55}H_{100}N_4NaOS$ requires: 887.7510

ν_{max}/cm^{-1}: 2926, 2851, 1509, 1464, 1097

δ_H (500 MHz, $CDCl_3$): 7.57 (5H, m), 3.41 (2H, t, *J* 7.55 Hz), 3.35 (3H, s), 2.96 (1H, m), 1.83 (2H, pent, *J* 7.25 Hz), 1.63 (1H, m), 1.45-1.25 (72H, m including s), 1.13 (4H, m), 0.89 (3H, t, *J* 6.6 Hz), 0.85 (3H, d, *J* 7.05 Hz), 0.65 (2H, m), 0.57 (1H, dt, *J* 4.1, 8.2 Hz), -0.33 (1H, q, *J* 5.05 Hz)

δ_C (500 MHz, $CDCl_3$): 130.03(-), 129.75(-), 123.87(-), 85.45(-), 57.71(-), 35.35(-), 33.40(+), 32.38(+), 31.92(+), 30.50(+), 30.22(+), 30.08(+), 29.98(+), 29.94(+), 29.75(+), 29.70(+), 29.41(+), 29.36(+), 29.09(+), 28.72(+), 28.64(+), 27.57(+), 26.16(+), 22.69(+),

15.76(-), 15.70(-), 14.88(-), 14.10(-), 10.93(+), [+ = CH_2, - = CH, CH_3]

$[\alpha]_D^{25}$: +4.44 ° (c = 1.07, $CHCl_3$); *reported as* $[\alpha]_D^{22}$*: +3.9 ° (c = 1.21, $CHCl_3$)*

3.3.2.39 Preparation of 5-(7-[1S,2R]-2-((17R,18R)-17-methoxy-18-methyl-hexatriacontyl)-cyclopropyl)-heptyl sulfonyl)-1-phenyl-1H-tetrazole (40)

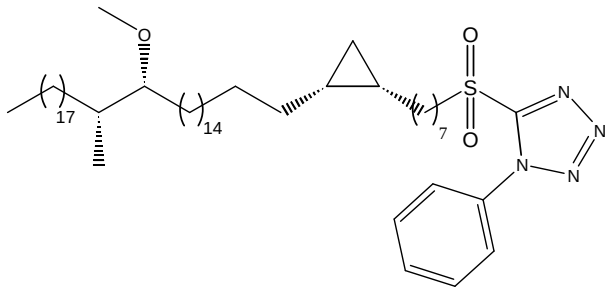

A solution of ammonium heptamolybdate(VI)tetrahydrate (0.36 g, 0.29 mmol, 0.5 mol eq.) in ice cold H_2O_2 35% (w/w, 5 ml) was added drop-wise to a stirring solution of 5-(7-[1*R*,2*S*]-2-((17*R*,18*R*)-17-methoxy-18-methyl-hexatriacontyl)-cyclopropyl)-heptyl sulfanyl)-1-phenyl-1*H*-tetrazole **(39)** (0.50 g, 0.58 mmol) in THF (20 ml) and IMS (20 ml) at 5 °C and stirred at RT for 1 hour, then 3 more identical solutions of ammonium heptamolybdate(VI)tetrahydrate in ice cold H_2O_2 35% (w/w) were added over the next hour. The reaction mixture was stirred for 16 hours at RT and then diluted with water (100 ml) and dichloromethane (50 ml). The organic layer was separated and the aqueous layer was re-extracted with dichloromethane (2 x 50 ml). The combined organic layers were washed with brine (100 ml), dried and evaporated to give a residue which was purified by column chromatography on silica gel eluting with petroleum ether/diethyl ether (5:1) to give an oil of *5-(7-[1S,2R]-2-((17R,18R)-17-methoxy-18-methyl-hexatriacontyl)-cyclopropyl)-heptyl sulfonyl)-1-phenyl-1H-tetrazole* **(40)** (10.18 g, 93%).

Physical properties:

Found M + Na^+: 919.7339, $C_{55}H_{100}N_4NaO_3S$ requires: 919.6469

ν_{max}/cm^{-1}: 2908, 1596, 1499, 1464, 1343, 1153, 1099, 760

δ_H (500 MHz, $CDCl_3$): 7.71 (2H, m), 7.63 (3H, m), 3.74 (2H, distorted t, *J* 7.9 Hz), 3.35 (3H, s), 2.96 (1H, m), 1.97 (2H, pent, *J* 7.55 Hz), 1.63 (1H, m), 1.52 (2H, m), 1.48-1.2 (70H, m including s), 1.13 (4H, m), 0.89

(3H, t, *J* 6.65 Hz), 0.86 (3H, d, *J* 6.65 Hz), 0.66 (2H, m), 0.58 (1H, dt, *J* 3.75, 7.85 Hz), -0.32 (1H, q, *J* 5.05 Hz)

δ_C (500 MHz, $CDCl_3$): 131.44(-), 129.70(-), 125.08(-), 85.45(-), 57.71(-), 56.05(+), 35.35(-), 31.92(+), 30.49(+), 30.22(+), 29.99(+), 29.94(+), 29.76(+), 29.69(+), 29.36(+), 29.16(+), 28.96(+), 28.73(+), 28.59(+), 28.16(+), 27.57(+), 26.16(+), 25.07(+), 22.68(+), 21.95(+), 15.76(-), 15.66(-), 14.88(-), 14.10(-), 10.93(+), [+ = CH_2, - = CH, CH_3]

$[\alpha]_D^{25}$: +4.40 ° (c = 1.0, $CHCl_3$); *reported as* $[\alpha]_D^{23}$*: +4.13 ° (c = 1.45, $CHCl_3$)*

3.3.2.40 Preparation of 2-(8-iodo-octyloxy)-tetrahydro-pyran (41)

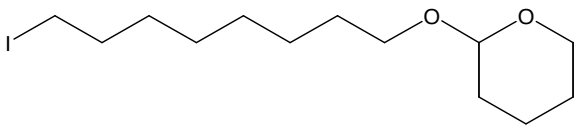

3,4-Dihydro-2*H*-pyran (29.67 g, 0.35 mol, 1.5 mol eq.) and pyridinium-*p*-toluene sulfonate (3.02 g, 0.012 mol, 0.05 mol eq.) were added to a stirring solution of 8-bromo-octan-1-ol (49.14 g, 0.235 mol, section 3.3.2.17) in dry dichloromethane (300 ml) under nitrogen at 5-10 °C. The reaction was stirred for 2 hours at RT, when TLC showed no starting material was left, the reaction mixture was washed with saturated solution of $NaHCO_3$ (200 ml), and then extracted with dichloromethane (3 x 200 ml). The organic layer was dried and evaporated to give *2-(8-bromo-octyloxy)-tetrahydro-pyran* (68.91 g, >99%).

NaI (109 g, mol, 3 mol eq.) was dissolved in acetone (400 ml) and stirred at RT. 2-(8-bromo-octyloxy)-tetrahydro-pyran (68.91 g, 0.235mol) was added and then $NaHCO_3$ (19.77 g, 1 mol eq.) was added. The reaction mixture was refluxed for 3 hours and then stirred overnight at RT. The reaction mixture was cooled down and the solvent was evaporated. The residue was diluted with water (400 ml) and dichloromethane (300 ml), the organic layer was separated and the aqueous layer re-extracted with dichloromethane (2 x 200 ml). The organic layer was dried and evaporated to give a yellow residue which was purified by column chromatography on silica gel eluted with petroleum ether/diethyl ether (10:1) to givean oil of *2-(8-iodo-octyloxy)-*

tetrahydro-pyran **(41)** (71.47 g, 89%). A few drops of triethylamine were added to the silica gel when the column was packed.

Physical properties:

ν_{max}/cm^{-1}: 2936, 2854

δ_H (500 MHz, $CDCl_3$): 4.57 (1H, t, *J* 2.5 Hz), 3.86 (1H, m), 3.72 (1H, ddd, *J* 6.95, 9.45, 16.4 Hz), 3.49 (1H, m), 3.38 (1H, ddd, *J* 6.6, 9.45, 16.05 Hz), 3.18 (2H, t, *J* 7.25 Hz), 1.82 (3H, m), 1.71 (1H, m), 1.63-1.48 (6H, m), 1.42-1.28 (8H, m)

δ_C (500 MHz, $CDCl_3$): 98.82(-), 67.56(+), 62.32(+), 33.49(+), 30.75(+), 30.40(+), 29.66(+), 29.20(+), 28.43(+), 26.12(+), 25.48(+), 19.67(+), 7.17(+), [+ = CH_2, - = CH, CH_3]

3.3.2.41 Preparation of 11-(tetrahydro-pyran-2-yloxy)-undecan-1-ol (42)

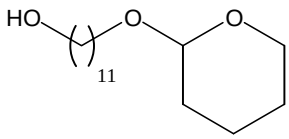

Ammonia gas was condensated to liquid ammonia into a 1 L flask (500 ml) and mechanically stirred while lithium wire (4.93 g, 0.68 mol, 2.5 mol eq. of alcohol) was cut up in tiny pieces and added one by one. The reaction mixture was stirred for 20 minutes where after propagyl alcohol (15.5 g, 0.27 mol, 1.3 mol eq.) in dry ether (30 ml) was added drop-wise and then stirred for another 40 minutes. 2-(8-Iodo-octyloxy)-tetrahydro-pyran **(41)** (71.00 g, 0.21 mol) in dry ether (30 ml) was added, the reaction mixture was stirred for 5 hours while being kept cool with liquid nitrogen. Then the stirring was stopped and the mixture was left overnight at RT for the ammonia to evaporate. Ether (700 ml) and sulfuric acid (100 ml, 10%) was added to the residue and stirred until the residue was dissolved. The ether layer was decanted off, more ether and sulfuric acid was added and the reaction mixture stirred. The ether layer was then decanted again, water was added and the mixture extracted with ether (2 x 250 ml). The combined organic layers were washed with water (500 ml), brine (500 ml) and $NaHCO_3$ (250 ml). The product was then dried and evaporated to give a dark oil of crude *11-(tetrahydro-pyran-2-yloxy)-undec-2-yn-1-ol* (52.36 g, 94%).

Physical properties:

δ_H (500 MHz, $CDCl_3$): 4.57 (1H, t, *J* 2.55 Hz), 4.24 (2H, s), 3.87 (1H, m), 3.73 (1H, m) 3.48 (1H, m), 3.38 (1H, m), 2.20 (2H, m), 1.91 (1H, broad s), 1.82 (1H, m), 1.70 (1H, m), 1.62-1.48 (8H, m), 1.40-1.28 (8H, m)

δ_C (500 MHz, $CDCl_3$): 98.83(-), 86.39, 78.39, 67.64(+), 62.32(+), 51.28(+), 30.73(+), 29.65(+), 29.24(+), 28.95(+), 28.69(+), 28.50(+), 26.12(+), 25.46(+), 19.65(+), 18.67(+), [+ = CH_2, - = CH, CH_3]

Nickel acetate tetrahydrate (10.20 g, 0.04 mol, 0.2 mol eq.) was stirred in ethanol (400 ml) while the flask was being filled with hydrogen. Sodium borohydride (1.81 g, 0.04 mol, 0.2 mol eq.) in ethanol (60 ml) was added and the mixture was stirred for 30 minutes at RT. 11-(Tetrahydro-pyran-2-yloxy)-undec-2-yn-1-ol (52.36 g, 0.21 mol) in ethanol (50 ml) was added and the reaction mixture stirred while being hydrogenated under hydrogen atmosphere. When no more hydrogen was absorbed, the mixture was filtrated through a pad of celite on silica gel and washed with ether (triethyl amine was added to the silica gel). Water and dichloromethane was added and the organic layer was separated. The aqueous layer was re-extracted with dichloromethane (2 x 300 ml). The combined organic layers were dried and evaporated to give a dark residue which was purified by column chromatography on silica gel eluted with petroleum ether/diethyl ether (5:2, then 1:1) to give a yellow oil of *11-(tetrahydro-pyran-2-yloxy)-undecan-1-ol* **(42)** (43.85 g, 83%).

Physical properties:

ν_{max}/cm^{-1}: 3416, 2940

δ_H (500 MHz, $CDCl_3$): 4.58 (1H, t, *J* 2.85 Hz), 3.88 (1H, m), 3.73 (1H, ddd, *J* 6.9, 9.45, 16.4 Hz), 3.64 (2H, ddd, *J* 5.65, 6.6, 13.25 Hz), 3.50 (1H, m), 3.38 (1H, ddd, *J* 6.6, 9.45, 16.05 Hz), 1.83 (1H, m), 1.71 (1H, m), 1.66 (1H, s), 1.62-1.50 (8H, m), 1.38-1.26 (14H, m)

δ_C (500 MHz, $CDCl_3$): 98.82(-), 67.67(+), 63.02(+), 62.31(+), 32.79(+), 30.77(+), 29.72(+), 29.55(+), 29.52(+), 29.48(+), 29.44(+), 29.38(+), 26.20(+), 25.71(+), 25.49(+), 19.67(+) [+ = CH_2, - = CH, CH_3]

3.3.2.42 Preparation of crude 2,2-dimethyl-propionic acid-11-(tetrahydro-pyran-2-yloxy)-undecyl ester (43)

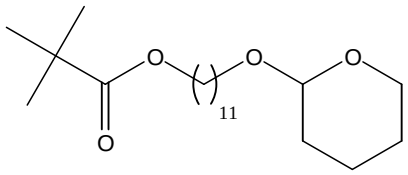

11-(Tetrahydro-pyran-2-yloxy)-undecan-1-ol **(42)** (43.66 g, 0.16 mol) and triethyl amine (24.49 g, 0.24 mol, 1.5 mol eq.) was stirred in dichloromethane (400 ml). 4-Dimethylaminopyridine (1.00 g, 0.01 mol) was added and the mixture was cooled to 5 °C. Trimethyl acetyl chloride (25.3 g, 0.21 mol, 1.3 mol eq.) was added slowly and the reaction mixture was stirred at RT for 3 hours. When TLC showed that no starting material was left, the reaction was quenched with water (500 ml) and dichloromethane. The organic layer was separated and the aqueous layer re-extracted with dichloromethane (2 x 150 ml). The combined organic layers were washed with water, dried and evaporated to give a yellow oil of crude *2,2-dimethyl-propionic acid-11-(tetrahydro-pyran-2-yloxy)-undecyl ester* **(43)** (57.32 g, >99%).

Physical properties:

ν_{max}/cm^{-1}: 2932, 2854, 1811, 1728

δ_H (500 MHz, $CDCl_3$): 4.57 (1H, t, *J* 2.55 Hz), 4.04 (2H, t, *J* 6.6 Hz), 3.87 (1H, m), 3.72 (1H, ddd, *J* 6.95, 9.45, 16.4 Hz), 3.50 (1H, m), 3.38 (1H, ddd, *J* 6.6, 9.45, 16.05 Hz), 1.83 (1H, m), 1.71 (1H, m), 1.63-1.50 (8H, m), 1.37-1.25 (14H, m), 1.19 (9H, s)

δ_C (500 MHz, $CDCl_3$): 178.60, 98.80(+), 67.64(-), 64.42(-), 62.29(-), 40.15(+), 39.09(-), 38.68(-), 30.75(-), 29.72(-), 29.51(-), 29.45(-), 29.44(-), 29.18(-), 28.58(-), 27.17(+), 26.47(+), 26.20(-), 25.87(-), 25.48(-), 19.66(-), [- = CH_2, + = CH, CH_3]

3.3.2.43 Preparation of 2,2-dimethyl-propionic acid-11-hydroxy-undecyl ester (44)

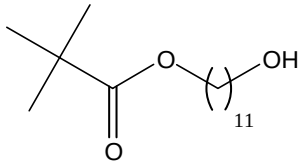

p-Toluenesulfonic acid monohydrate (3.00 g, 0.016 mol, 0.1 mol eq.) was added to a stirring solution of 2,2-dimethyl-propionic acid 11-(tetrahydro-pyran-2-yloxy)-undecyl ester **(43)** (57.32 g, 0.16 mol) in THF (100 ml), methanol (150 ml) and water (2 ml) at RT. The reaction mixture was stirred at RT for 5 hours. When TLC showed that no starting material was left, the mixture was diluted with a saturated solution of sodium bicarbonate (300 ml) and dichloromethane (300 ml). The organic layer was separated and the aqueous layer was re-extracted with dichloromethane (2 x 250ml). The combined organic layers were dried and evaporated to give a residue which was purified by column chromatography on silica gel eluted with petroleum ether/diethyl ether (5:2) to give *2,2-dimethyl-propionic acid-11-hydroxy-undecyl ester* **(44)** as a yellow oil (35.10 g, 80%).

Physical properties:

Found M + Na^+: 295.2238, $C_{16}H_{32}NaO_3$ requires: 295.2244

ν_{max}/cm^{-1}: 3384, 2929, 2855, 1731

δ_H (500 MHz, $CDCl_3$): 4.05 (2H, t, *J* 6.65 Hz), 3.64 (2H, t, *J* 6.6 Hz), 1.69 (1H, broad s), 1.65-1.54 (2H, m), 1.38-1.25 (14H, m), 1.19 (9H, s), 0.86 (2H, m)

δ_C (500 MHz, $CDCl_3$): 178.67, 64.44(-), 63.05(-), 38.71(-), 32.77(-), 29.53(-), 29.45(-), 29.44(-), 29.38(-), 29.18(-), 28.59(-), 27.18(+), 25.87(-), 25.71(-), 22.59(-), [- = CH_2, + = CH, CH_3]

3.3.2.44 Preparation of 2,2-dimethyl-propionic acid-11-oxo-undecyl ester (45)

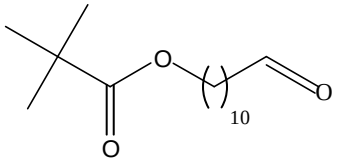

2,2-Dimethyl-propionic acid 11-hydroxy-undecyl ester **(44)** (17.50 g, 64.30 mmol) in dichloromethane (50 ml) was added to a stirring suspension of pyridinium chlorochromate (28.27 g, 128.60 mmol, 2 mol eq.) in dichloromethane (500 ml) at RT. The mixture was stirred for 3 hours at RT. When TLC showed that no starting material was left, the mixture was poured into diethyl ether (1 L), filtered through a pad of celite on silica gel, then washed thoroughly with diethyl ether. The filtrate was evaporated to give a residue which was purified by column chromatography on silica gel eluted with petroleum ether/diethyl ether (5:2) to give *2,2-dimethyl-propionic acid-11-oxo-undecyl ester* **(45)** as a yellow oil (15 g, 86%).

Physical properties:

ν_{max}/cm^{-1}: 2928, 1729, 1458, 1286

δ_H (500 MHz, $CDCl_3$): 9.76 (1H, t, *J* 1.55 Hz), 4.04 (2H, t, *J* 6.65 Hz), 2.41 (2H, dt, *J* 7.55, 1.9 Hz), 1.61 (4H, m), 1.37-1.25 (12H, m), 1.19 (9H, s)

δ_C (500 MHz, $CDCl_3$): 202.83(+), 178.62(-), 64.39(-), 43.86(-), 38.70(-), 29.38(-), 29.27(-), 29.14(-), 29.12(-), 28.57(-), 27.17(+), 25.85(-), 22.04(-), [- = CH_2, + = CH, CH_3]

3.3.2.45 Preparation of 13-(2,2-dimethyl-propionyloxy)-tridec-2-enoic acid methyl ester (46)

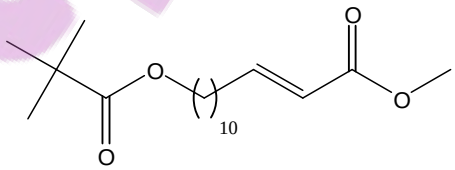

(Methoxycarbonylmethylene) triphenylphosphorane (43.31 g, 0.13 mol) was added to a stirring solution of 2,2-dimethyl-propionic acid 11-oxo-undecyl ester **(45)** (30.00 g, 0.11 mol) in toluene (500 ml). The reaction mixture was stirred overnight. The toluene was subsequently evaporated to give a residue which was diluted with petroleum ether/diethyl ether (5:2, 500 ml) and refluxed for 30 minutes. The mixture was filtrated and the precipitate washed with

petroleum ether/diethyl ether (5:2). The filtrate was evaporated to give a residue which was again diluted with petroleum ether/diethyl ether (5:2, 500 ml) and refluxed for 30 minutes. The mixture was then filtrated, the precipitate washed with petroleum ether/ diethyl ether (5:2) and the filtrate evaporated. The crude product was purified on silica gel gel eluted with petroleum ether/diethyl ether (5:2) to give a colourless oil of *13-(2,2-dimethyl-propionyloxy)-tridec-2-enoic acid methyl ester* **(46)** (31 g, 85%).

Physical properties:

Found M + Na^+: 349.2339, $C_{19}H_{34}NaO_4$ requires: 349.2349

ν_{max}/cm^{-1}: 2928, 2855, 1729, 1158

δ_H (500 MHz, $CDCl_3$): 6.97 (1H, dt, *J* 6.95, 15.45 Hz), 5.81 (1H, dt, *J* 1.6, 15.45 Hz), 4.04 (2H, t, *J* 6.6 Hz), 3.72 (3H, s), 2.19 (2H, m), 1.61 (2H, pent, *J* 6.6 Hz), 1.45 (2H, m), 1.37-1.25 (14H, m), 1.19 (9H, s)

δ_C (500 MHz, $CDCl_3$): 178.61, 167.16, 149.74(+), 120.80(+), 64.41(-), 51.32(+), 38.70(-), 32.17(-), 29.42(-), 29.37(-), 29.30(-), 29.16(-), 29.07(-), 28.58(-), 27.98(-), 27.18(+), 25.87(-), [- = CH_2, + = CH, CH_3]

*3.3.2.46 Preparation of (2**S**,3**R**)-13-(2,2-dimethyl-propionyloxy)-2,3-dihydroxy-tridecanoic acid methyl ester (47)*

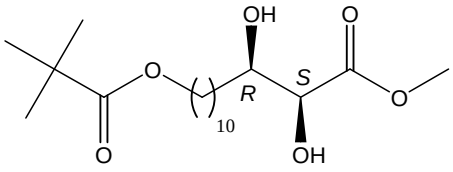

$(DHQD)_2PHAL$ ligand (0.55 g, 0.70 mmol, 0.01 mol eq.), K_3Fe_6 (69.27 g, 0.21 mol, 3 mol eq.), K_2CO_3 (29.08 g, 0.21 mol, 3 mol eq.) and OsO_4 (2.8 ml, 2.81 mmol, 0.04 mol eq.; 2.5 wt % solution in 2-methyl-2-propanol) were dissolved in a mixture of water and 2-methyl-2-propanol (800 ml, 1:1) at RT. $MeSO_2NH_2$ (6.67 g, 0.07 mol, 1 mol eq.) was added and the mixture was cooled to 2 °C while being stirred vigorously. 13-(2,2-Dimethyl-propionyloxy)-tridec-2-enoic acid methyl ester **(46)** (23 g, 0.07 mol) was added at 2 °C. The reaction was stirred at 2-4 °C for 8 hours. When TLC showed that no starting material was left, sodium metabisulfite (20 g, mol) was carefully added. The mixture was allowed to reach RT and stirred for 45 min, then extracted with dichloromethane (3 x 500 ml), dried and evaporated. The crude product was purified on column chromatography on silica gel eluted with petroleum

ether/ethyl acetate (5:1, then 1:1) to give *(2S,3R)-13-(2,2-dimethyl-propionyloxy)-2,3-dihydroxy-tridecanoic acid methyl ester* **(47)** as a colourless oil (25.60 g, >99%).

Physical properties:

Found M + Na^+: 383.2395, $C_{19}H_{36}NaO_6$ requires: 383.2404

ν_{max}/cm^{-1}: 3449, 2930, 2855, 1729

δ_H (500 MHz, $CDCl_3$): 4.11 (1H, m), 4.04 (2H, t, *J* 6.6 Hz), 3.89 (1H, m), 3.83 (3H, s), 3.08 (1H, broad s), 2.04 (1H, s), 1.61 (4H, m), 1.46 (1H, m), 1.38-1.23 (12 H, m), 1.19 (9H, s)

δ_C (500 MHz, $CDCl_3$): 178.66, 174.08, 73.07(+), 72.46(+), 64.44(-), 52.77(+), 38.71(-), 33.71(-), 29.45(-), 29.43(-), 29.41(-), 29.17(-), 28.58(-), 27.18(+), 25.87(-), 25.67(-), [- = CH_2, + = CH, CH_3]

$[\alpha]_D^{26}$: +9.70, (c = 1.34, $CHCl_3$)

3.3.2.47 Preparation of (2S,3R)-5-[10-(2,2-dimethyl-propionyloxy)-decyl]-2,2-dioxo-2λ⁶-[1,3,2]-dioxathiolane-4-carboxylic acid methyl ester (48)

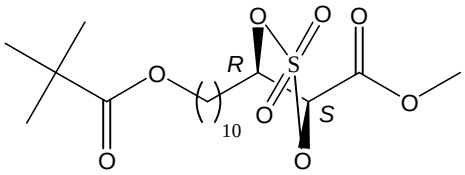

(2*S*,3*R*)-13-(2,2-Dimethyl-propionyloxy)-2,3-dihydroxy-tridecanoic acid methyl ester **(47)** (25.50 g, 70.44 mmol) was dissolved in CCl_4 (120 ml). Thionyl chloride (11.26 ml, 154.90 mmol, 2.2 mol eq.) was added and the mixture was vigorously refluxed for 2 hours. After cooling, the solution was carefully diluted with CH_3CN (120 ml), followed by the addition of ruthenium trichloride hydrate (0.73 g, 3.52 mmol, 0.05 mol eq.) and $NaIO_4$ (22.6 g, 105.66 mmol, 1.5 mol eq.). Water (180 ml) was then added drop-wise. The mixture was stirred overnight and then poured into diethyl ether (600 ml). The organic layer was separated and the aqueous layer re-extracted with diethyl ether (2 x 200 ml). The combined organic layers were washed with water (100 ml), saturated solution of sodium bicarbonate (100 ml) and brine (100 ml), then dried and evaporated to give a dark residue. Sodium thiosulfate pentahydrate was added to neutralise the iodine and the mixture was extracted with dichloromethane (2 x 200 ml). The organic layer was dried and evaporated. TLC showed that there was still starting material left and the reaction was repeated by addition of CCl_4 (60 ml), acetonitrile (60 ml),

ruthenium trichloride (0.5 g), $NaIO_4$ (15 g) and water (90 ml). The reaction mixture was stirred at RT and montored by TLC. After 30 min TLC showed that no starting material was left and the mixture was diluted with diethyl ether (400 ml). The organic layer was separated and the aqueous layer re-extracted with diethyl ether (2 x 100 ml). The combined organic layers were washed as described, dried and evaporated to give a very dark residue which was purified by column chromatography on silica gel eluted with petroleum ether/diethyl ether (1:1) to give a colourless oil of *(2S,3R)-5-[10-(2,2-dimethyl-propionyloxy)-decyl]-2,2-dioxo-2λ^6-[1,3,2]-dioxathiolane-4-carboxylic acid methyl ester* **(48)** (16.73 g, 56%).

Physical properties:

Found M + Na^+: 445.1857, $C_{19}H_{34}NaO_8S$ requires: 445.1867

ν_{max}/cm^{-1}: 2930, 2856, 1774, 1724

δ_H (500 MHz, $CDCl_3$): 4.95 (1H, dt, *J* 5.05, 7.25 Hz), 4.89 (1H, d, *J* 7.25 Hz), 4.05 (2H, t, *J* 6.6 Hz), 3.90 (3H, s), 1.98 (2H, m), 1.64-1.45 (4H, m), 1.58-1.45 (2H, m), 1.39-1.26 (12H, m), 1.20 (9H, s)

δ_C (500 MHz, $CDCl_3$): 178.63, 165.38, 84.06(+), 79.81(+), 64.39(-), 53.67(+), 38.71(-), 32.96(-), 29.36(-), 29.26(-), 29.15(-), 29.12(-), 28.81(-), 28.57(-), 27.18(+), 25.84(-), 24.76(-), [- = CH_2, + = CH, CH_3]

$[\alpha]_D^{26}$: +31.17 º (c = 1.03, $CHCl_3$)

3.3.2.48 Preparation of (R)-13-(2,2-dimethyl-propionyloxy)-3-hydroxy-tridecanoic acid methyl ester (49)

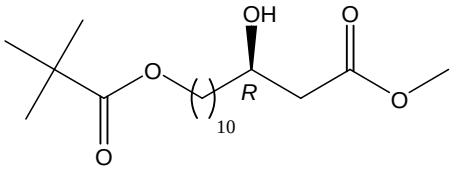

(2*S*,3*R*)-5-[10-(2,2-Dimethyl-propionyloxy)-decyl]-2,2-dioxo-2λ^6-[1,3,2]-dioxathiolane-4-carboxylic acid methyl ester **(48)** (22 g, 51.88 mmol) was dissolved in DMAC (300 ml) and NaBH4 (2.26 g, 59.67 mmol, 1.15 mol eq.) was slowly added at 0 °C. The reaction mixture was stirred at RT for 1 hour. When TLC showed that no starting material was left, the solvent was distilled under high vacuum. The residue was diluted with THF (250 ml) and water (0.5 ml) and concentrated sulfuric acid (1.35 ml) added. The mixture was stirred for 1 hour where after sodium metabisulfate (25 g) was added and stirred for another 30 minutes. This was then

filtered through a pad of silica gel and washed with THF. The filtrate was evaporated to give a residue which was purified by column chromatography on silica gel eluting with petroleum ether/ethyl acetate (10:3) to give *(R)-13-(2,2-dimethyl-propionyloxy)-3-hydroxy-tridecanoic acid methyl ester* (9.20 g, 52%).

Physical properties:

Found M + Na^+: 367.2427, $C_{19}H_{36}NaO_5$ requires: 367.2455

ν_{max}/cm^{-1}: 3517, 2922, 2854, 1732

δ_H (500 MHz, $CDCl_3$): 4.04 (2H, t, *J* 6.6 Hz), 3.99 (1H, m), 3.71 (3H, s), 2.51 (1H, dd, *J* 3.15, 16.4 Hz), 2.41 (1H, dd, *J* 9.15, 16.4 Hz), 1.61 (2H, pent, *J* 6.6 Hz), 1.53 (1H, m), 1.43 (2H, m), 1.37-1.25 (5H, m), 1.19 (9H, s)

δ_C (500 MHz, $CDCl_3$): 178.61, 173.42, 67.99(+), 64.41(-), 51.66(+), 41.12(-), 38.68(-), 36.50(-), 29.46(-), 29.44(-), 29.42(-), 29.41(-), 29.15(-), 28.57(-), 27.16(+), 25.85(-), 25.42(-), [- = CH_2, + = CH, CH_3]

$[\alpha]_D^{26}$: -10.0 º (c = 1.23, $CHCl_3$)

*3.3.2.49 Preparation of (2**R**,3**R**)-2-allyl-[11-(2,2-dimethyl-propionyloxy)-1-hydroxy-undecyl]-pent-4-enoic acid methyl ester (50)*

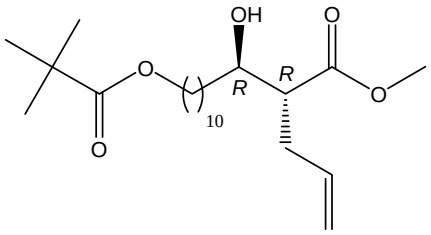

Butyl lithium (3.05 ml, 6.40 mmol, 2.2 mol eq.) was added to a stirred solution of diisopropylamine (0.65 g, 6.40 mmol, 2.2 mol eq.) in dry THF (40 ml) under nitrogen at -78 °C. The reaction mixture was allowed to reach RT and was re-cooled to -78 °C before (*R*)-13-(2,2-dimethyl-propionyloxy)-3-hydroxy-tridecanoic acid methyl ester **(49)** (1 g, 2.91 mmol) in dry THF (20 ml) was added drop-wise. The reaction mixture was allowed to slowly warm to 0 °C in the cold bath over 2 hours and then re-cooled to -65 °C before allylic iodide (0.32 ml, 3.49 mmol, 1.2 mol eq.) and HMPA (1.01 ml, 5.81 mmol, 2 mol eq.) in dry THF (2 ml) was added drop-wise. The reaction mixture was allowed to slowly warm to -5 °C in the cold bath over 2 hours and the reaction monitored by TLC. When TLC showed that little starting

material was left, ammonium chloride (10 ml) was added and the product extracted with diethyl ether/ethyl acetate (1:1, 3 x 50 ml). The combined organic layers were washed with brine (50 ml), dried and evaporated to give a residue which was purified by column chromatography on silica gel eluted with petroleum ether/ethyl acetate (4:1) to give *(2R,3R)-2-allyl-[11-(2,2-dimethyl-propionyloxy)-1-hydroxy-undecyl]-pent-4-enoic acid methyl ester* **(50)** as a pale yellow oil (614 mg, 55%).

Physical properties:

Found M + Na^+: 407.2751, $C_{22}H_{40}NaO_5$ requires: 407.2768

ν_{max}/cm^{-1}: 3524, 2930, 2854, 1736, 1642

δ_H (500 MHz, $CDCl_3$): 5.75 (1H, m), 5.11 (1H, dd, J 0.95, 17 Hz), 5.05 (1H, br d, *J* 10.05 Hz), 4.05 (2H, t, *J* 6.65 Hz), 3.71 (3H, s), 2.55 (1H, m), 2.50-2.38 (2H, m), 1.62 (3H, pent, *J* 6.3 Hz), 1.50-1.42 (4H, m), 1.37-1.25 (16H, m), 1.20 (9H, s)

δ_C (500 MHz, $CDCl_3$): 178.65, 175.33, 134.89(+), 117.18(+), 71.78(+), 64.44(-), 51.56(+), 50.54(+), 38.72(-), 35.57(-), 33.81(-), 29.50(-), 29.49(-), 29.47(-), 29.45(-), 29.20(-), 28.61(-), 27.21(+), 25.89(-), 25.71(-), [- = CH_2, + = CH, CH_3]

$[\alpha]_D^{25}$: +1.08, (c = 1.15, $CHCl_3$); *reported as* $[\alpha]_D^{19}$*: +1.94 (c = 1.19, $CHCl_3$)*

3.3.2.50 Preparation of (1R, 2R)-1-acetoxy-11-oxoundecyl hexacosanoic acid methyl ester (52)

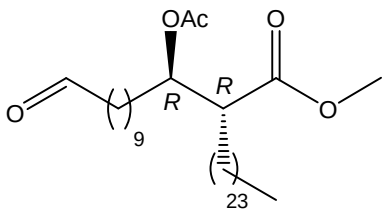

Methyl (2*R*,3*R*)-3-acetoxy-2-tetracosanyl-13-hydroxytridecanoate **(51)** (0.18 g, 0.286 mmol, kindly provided by Dr J. Al Dulayymi, University of Wales, Bangor, UK) in dichloromethane (5 ml) was added to a stirring suspension of pyridinium chlorochromate (2.50 g, 1.13 mmol, 4 mol eq.) in dichloromethane (15 ml) at RT. The mixture was stirred for 1 hour at RT. When TLC showed that no starting material was left, the mixture was poured into diethyl ether (200

ml) and filtered through a pad of celite on silica gel, then washed thoroughly with diethyl ether. The filtrate was evaporated to give a residue which was purified by column chromatography on silica gel eluted with petroleum ether/diethyl ether (5:2) to give *(1R, 2R)-1-acetoxy-11-oxoundecyl hexacosanoic acid methyl ester* **(52)** as an oil (0.17 g, 96%).

Physical properties:

ν_{max}/cm^{-1}:	2917, 2849, 1741
δ_H (250 MHz, $CDCl_3$):	9.73 (1H, t, *J* 1.8 Hz), 5.03 (1H, ddd, *J* 4.2, 7, 11.3 Hz), 3.64 (3H, s), 2.57 (1H, ddd, *J* 4.2, 6.7, 10.7 Hz), 2.38 (2H, dt, *J* 1.8, 7.2 Hz), 2.03 (3H, s), 1.95-1.08 (62H, br s), 0.88 (3H, t, *J* 7 Hz)
δ_C (250 MHz, $CDCl_3$):	202.9, 173.6, 170.3, 74.1, 51.5, 49.6, 43.9, 31.9, 31.7, 29.7, 29.3, 29.1, 28.1, 27.5, 25.0, 22.6, 22.0, 21.0, 14.1, [- = CH_2, + = CH, CH_3]
$[\alpha]_D^{22}$:	*reported as +9.8 ° (c = 1.06, $CHCl_3$)*

3.3.2.51 Preparation of (R)-2-{(R)-1-acetoxy-18-[(1S,2R)-2-((17R,18R)-17-methoxy-18-methyl hexatriacontyl)-cyclopropyl]-octadecyl}-hexacosanoic acid methyl ester (53)

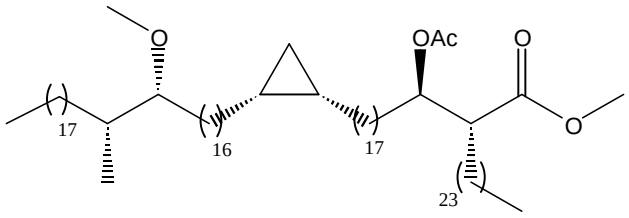

Lithium bis(trimethylsilyl)amide (0.45 ml, 0.427 mmol, 1.06 M, 1.3 mol eq. to sulfone) was added drop wise to a stirring solution of (1*R*,2*R*)-1-acetoxy-11-oxoundecyl hexacosanoic acid methyl ester **(52)** (0.174 g, 0.274 mmol) and 5-(7-[1*S*,2*R*]-2-((17*R*,18*R*)-17-Methoxy-18-methyl-hexatriacontyl)-cyclopropyl)-heptyl sulfonyl)-1-phenyl-1*H*-tetrazole **(40)** (0.30 g, 0.33 mmol, 1.2 mol eq.) in dry THF (10 ml) under nitrogen at - 10 °C. The reaction mixture was allowed to reach RT and was then stirred for 1 hour. When TLC showed that no starting material was left, the reaction mixture was quenched with a saturated solution of ammonium chloride (5 ml) and diethyl ether (10 ml). The organic layer was separated and aqueous layer was re-extracted with diethyl ether (3 x 10 ml). The combined organic layers were washed with brine (20 ml), dried and evaporated to give a white solid which was purified by column chromatography on silica gel eluting with petroleum ether/diethyl ether (10:1) to give *(R)-2-*

{(E/Z)-(R)-1-acetoxy-18-(1S,2R)-2-((17R,18R)-17-methoxy-18-methyl hexatriacontyl)-cyclopropyl}-octadec-11-enyl}-hexacosanoic acid methyl ester (0.22 g, 60%).

(*R*)-2-{(*E/Z*)-(*R*)-1-Acetoxy-18-(1*S*,2*R*)-2-((17*R*,18*R*)-17-methoxy-18-methyl hexatriacontyl)-cyclopropyl}-octadec-11-enyl}-hexacosanoic acid methyl ester (0.215 g, 0.165 mmol) was stirred in THF (10 ml) and methanol (5 ml), cooled to 5 °C and excess of dipotassium azodicarboxylate was added. Acetic acid (3 ml) in methanol (2 ml) was added drop-wise to the reaction mixture over 3 hours at RT. After 6 hours another portion of dipotassium azodicarboxylate was added, followed by the addition of acetic acid (1ml) in methanol (1 ml) and this was repeated 12 hours later. The reaction was stirred for a further 20 hours and then poured into ammonium chloride (20 ml). A mixture of petroleum ether/diethyl ether (1:1, 50 ml) was added, the organic layer was separated and the aqueous layer was re-extracted with petroleum ether/diethyl ether (1:1, 2 x 30 ml). The combined organic layers were dried and evaporated. The procedure was repeated again for another 24 hours to give a white solid which was purified by column chromatography on silica gel eluting with petroleum ether/ diethyl ether (5:1) to give *(R)-2-{(R)-1-acetoxy-18-(1S,2R)-2-((17R,18R)-17-methoxy-18-methyl hexatriacontyl)-cyclopropyl}-octadecyl-hexacosanoic acid methyl ester* **(53)** (194 mg, 90%).

Physical properties:

ν_{max}/cm^{-1}: 2920, 1743, 1469, 1375, 1237, 1162, 719

δ_H (500 MHz, $CDCl_3$): 5.09 (1H, dt, *J* 3.8, 7.9 Hz), 3.69 (3H, s), 3.35 (3H, s), 2.96 (1H, m), 2.62 (1H, ddd, *J* 4.4, 6.95, 14.8 Hz), 2.04 (3H, s), 1.68-1.58 (4H, m), 1.56-1.48 (1H, m), 1.46-1.20 (138 H, m including s), 1.18-1.05 (4H, m), 0.89, (6H, t, J 6.6 Hz), 0.85 (3H, d, J 6.9 Hz), 0.65 (2H, m), 0.57 (1H, dt, *J* 4.1, 7.9 Hz), -0.32 (1H, q, *J* 5.05 Hz)

δ_C (500 MHz, $CDCl_3$): 173.65, 170.33, 85.45(-), 74.11(-), 57.70(-), 51.52(-), 49.59(-), 35.35(-), 32.39(+), 31.92(+), 31.72(+), 30.500(-), 30.32(+), 30.22(+), 29.98(+), 29.94(+), 29.70(+), 29.65(+), 29.56(+), 29.47(+), 29.44(+), 29.40(+), 29.36(+), 28.72(+), 28.12(+), 27.58(+), 27.47(+), 26.16(+), 24.99(+), 22.68(+), 22.61(+), 21.01(-), 15.78(-), 14.88(-), 14.10(-), 10.91(+), [+ = CH_2, - = CH, CH_3]

$[\alpha]_D^{25}$: +7.69 ° (c = 1.04, $CHCl_3$); *reported as* $[\alpha]_D^{22}$*: +7.17 ° (c = 1.32, $CHCl_3$)*

*3.3.2.52 Preparation of (**R**)-2-{(**R**)-1-hydroxy-18-[(1**S**,2**R**)-2-((17**R**,18**R**)-17-methoxy-18 methyl hexatriacontyl)-cyclopropyl]-octadecyl}-hexacosanoic acid (1)*

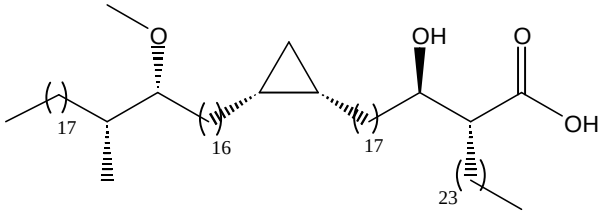

Lithium hydroxide monohydrate (22 mg, 0.535 mmol) was added to a stirring solution of (*R*)-2-{(*R*)-1-acetoxy-18-[(1*S*,2*R*)-2-((17*R*,18*R*)-17-methoxy-18-methylhexatriacontyl)-cyclopropyl]-octadecyl}-hexacosnoic acid methyl ester **(53)** (50 mg, 0.038 mmol) in tetrahydrofuran (8 ml), methanol (1 ml) and water (0.5 ml) at RT. The reaction mixture was stirred at 43 ^oC for 24 hrs. When TLC showed that no starting material was left, the reaction was cooled to room temperature and diluted with petroleum ether/diethyl ether (1:1, 30 ml) and ammonium chloride (5 ml) and acidified with 5% HCl. The organic layer was separated and the aqueous layer extracted with petroleum ether/diethyl ether (1:1, 2 x 20ml). The combined organic layers were dried and evaporated to give a white solid which was purified by column chromatography on silica gel eluted with petroleum ether/ethyl acetate (5:2) to give *(R)-2-{(R)-1-hydroxy-18-[(1S,2R)-2-((17R,18R)-17-methoxy-18-methylhexatri-acontyl)-cyclopropyl]-octadecyl}-hexacosnoic acid* **(1)** (32 mg, 67%).

Physical properties:

Found M – H^+: 1252.2804, $C_{85}H_{167}O_4$ requires: 1252.2859

ν_{max}/cm^{-1}: 3516, 2917, 2850, 1718, 1462

m.p. 59-61 ºC

δ_H (500 MHz, $CDCl_3$): 3.73-3.70 (1H, m), 3.35 (3H, s), 2.99-2.95 (1H, m), 2.48-2.44 (1H, m), 1.79-1.71 (1H, m), 1.67-1.61 (2H, m), 1.55-1.08 (145H, m), 0.90-0.83 (9H, including a t, *J* 7 Hz and a d, *J* 7 Hz), 0.68-0.63 (2H, m), 0.56 (1H, br, dt, *J* 4.05, 8.15 Hz), -0.32 (1H, br, q, *J* 5.05 Hz)

δ_C(500 MHz, $CDCl_3$): 178.84, 85.56(-), 72.11(-), 57.67(-), 50.71(-), 35.55(+), 35.33(-), 32.35(+), 31.92(+), 30.47(+), 30.31(+), 30.22(+), 29.97(+), 29.93(+), 29.70(+), 29.66(+), 29.61(+), 29.58(+), 29.50(+), 29.42(+), 29.36(+), 28.71(+), 27.56(+), 27.33(+), 26.14(+), 25.72(+), 22.68(+), 15.77(-), 14.89(-), 14.11(-), 10.90(+), [+ = CH_2, - = CH, CH_3].

$[\alpha]_D^{25}$: +6.95 ^{o} (c = 1.05, $CHCl_3$)

3.4 Biological activity/antigenicity of different synthetic mycolic acids

3.4.1 Results and discussion

The ability to synthesize complex molecules like MAs is in itself quite a challenge, especially if the size, hydrophobicity, restricted solubility properties, huge variety and stereochemical features of these molecules are taken into acount. To be able to select the correct structure amongst the natural MAs and then synthesize it in such a way that it displays the same biological activity as the natural product, eg. so perfectly that these molecules are also recognised by TB antibodies the way the natural MAs are, is the ultimate achievement sought to clearly understand how the molecules are put together in nature and for what reason. Prof Baird and his group (University of Wales, Bangor, UK) are doing pioneering work on the stereochemically synthesis of MAs and have synthesized a few different MAs, including a α-MA, a keto-MA and a couple of different diastereomers of methoxy-MA (6-8), the latter in which I had the opportunity to participate.

As shown in Chapter 2 (section *2.4.1*), antibodies in TB^+ and TB^- patient serum recognised the natural MA as well as the methoxy-MA subtype. This led to other questions: How important is the stereochemistry of the functional groups in the methoxy-MA for recognition by antibodies? The only way to determine this is to synthetize a particular enantiomer of one particular MA subtype that is recognised by human antibodies and then to synthesize structural variants of this basic structure that probes particular structural aspects in a systematic way to interrogate every structural aspect of MA that may play a role in biological activity. The first challenge was to synthesise a synthetic MA that was identical in structure to the natural MA of *M. tuberculosis* and to test it for antigenicity against human TB patient serum. For the antigenicity/biological activity assay, different synthetic methoxy-MAs were kindly provided by Dr J. Al Dulayymi (University of Wales, Bangor, UK) in addition to the synthesized

methoxy-MA described in this chapter. Apart from the methoxy-MA, different synthetic keto- and hydroxy-MAs were kindly provided by Gani Koza (University of Wales, Bangor, UK). For antigenicity determination, the same ELISA assay was followed that was used in Chapter 2 for the determination of activity of the natural MA and their sub-types.

The exact stereochemistry of the cyclopropane group in the mero chain of natural MA is not known. The two possibilities of *cis*-stereochemistry around the cyclopropane group (*S,R* and *R,S*) were included in two of the methoxy-MAs to determine if one would be favoured above the other by antibodies in TB^+ serum. The stereochemistry of the methyl methoxy-group in the distal position in natural MA is thought to be *S,S*. NMR analyses showed that the stereochemistry is definitely either *S,S* or *R,R*, but not *S,R* or *R,S*. The different stereochemistries around the two loci of methoxy-MA, represented in the three synthetic variants that were tested are shown in Figure 3.20.

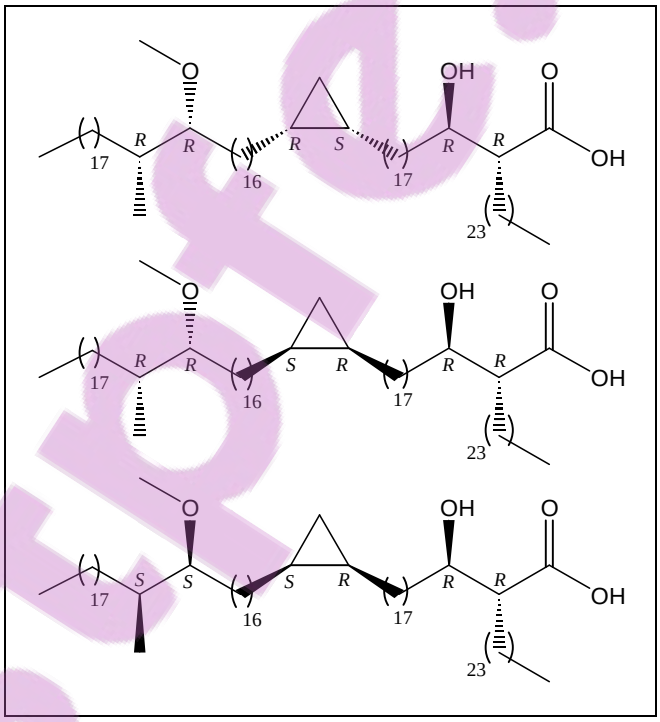

Figure 3.20: *The different diastereomers of synthetic methoxy-MAs tested for antigenicity against TB patient serum.*

Figure 3.21 shows the structures of the synthetic keto- and hydroxy-MAs that were also included in the antigenicity assay. It is known that there is a small amount of *trans*-cyclopropane MAs present in the natural MA. Should the synthetic keto- and hydroxy-MA be recognized by patient antibodies, it would be interesting to learn how either the *cis*- or the

trans-cyclopropane influences this. Although, hydroxy-MA is not present in *M. tuberculosis*, it was included in this assay to see if the oxygenated group at that locus in the mero chain was sufficient to be recognized by antibodies in TB^{+} serum.

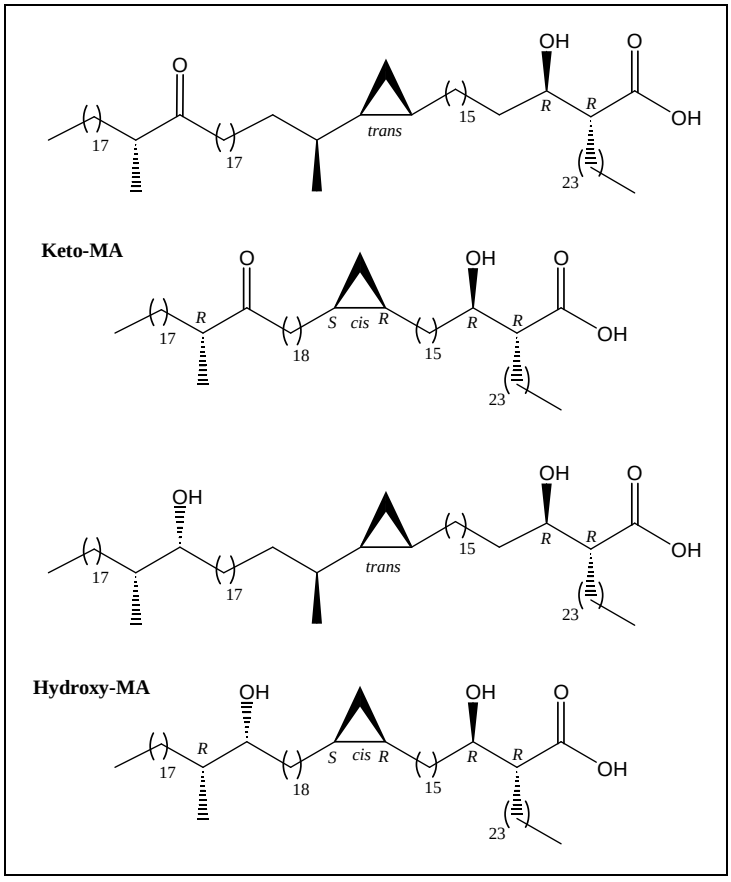

Figure 3.21: *Synthetic keto- and hydroxy-MAs*

To prove that the interaction between sera and MAs are specific, a synthetic alpha-MA (7), was O-acetylated at the β-OH and methylated at the carboxylic acid (Figure 3.22) and was included in the assay as a negative control.

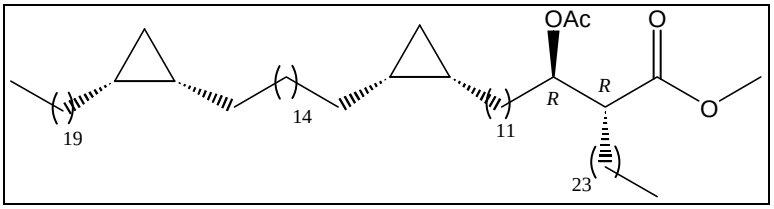

Figure 3.22: *Synthetic acetylated alpha-MA methyl ester (MB)*

This compound was chosen because it does not have a hydrogen donor group, which decreases the possibility of hydrogen bonds with antibodies. Moreover, the protection of the polar groups

in the mycolic motif will also discourage the "W" structural arrangement which is already less feasible for the alpha-MAs subclass. Therefore, this change in the three dimensional structure should disrupt its hydrophobic interactions with antibodies against MAs (145, 146).

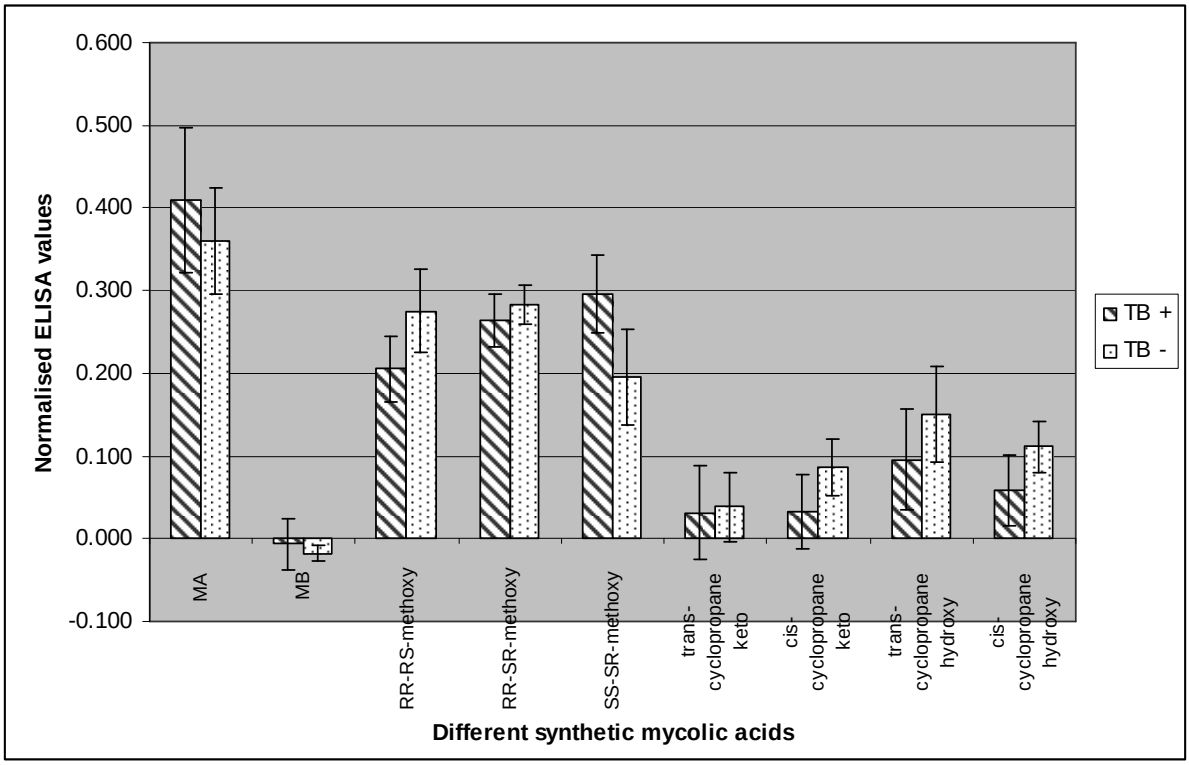

Figure 3.23: *ELISA results of human antibody binding to natural MA (MA) and various synthetic MA structures. Antigens are natural MA isolate (MA, n=92 for positive serum, n=30 for negative serum); a synthetic protected α-MA (MB, n=19 for positive serum, n=5 for negative serum); a few different diastereomers of a synthetic methoxy-MA, of which RR/SS describes the stereochemistry around the distal methoxy-methyl group, and RS/SR describes the stereochemistry around the proximal cis-cyclopropane group respectively, i.e. RR-RS-methoxy (n=20 for positive serum, n=8 for negative serum), RR-SR-methoxy (n=15 for positive serum, n=5 for negative serum), SS-SR-methoxy (n=20 for positive serum, n=5 for negative serum); trans-cyclopropane-keto-MA (n=20 for positive serum, n=8 for negative serum) and cis-cyclopropane-keto-MA (n=20 for positive serum, n=7 for negative serum); and trans-cyclopropane-hydroxy-MA (n=20 for positive serum, n=8 for negative serum) and cis-cyclopropane-hydroxy-MA (n=20 for positive serum, n=8 for negative serum). The source of the antibodies was sera collected from either TB positive or TB negative South African hospitalised patients of various adult age groups. (Values are given as a mean ± standard deviation).*

Figure 3.23 summarises the ELISA results of the different synthetic MAs. It must be noted that although the stereochemistry of these at the hydroxyl acid part is the same as that in the natural material, the stereochemistry at the other functional parts may or may not be as in the natural MA.

Antibodies in TB^+ patient serum recognised the natural MA, and a number of the deprotected synthetic MAs. All of these were also recognised by serum from TB^- patients, as was seen before with the different subclasses of natural MA (Fig 2.21, Chapter 2). There were, however, no significant differences in the way that the various MAs were recognised by sera from TB^+ and TB^- patients. However, as seen in Fig 3.23 this is reversed and is statistically significant ($P < 0.01$) only for the synthetic *SS*-*SR*-methoxy-MA, which is recognised preferentially by TB positive serum. This synthetic diastereomer is also the one that closest approximates the signal strength of antibody binding to natural MA by TB positive patient sera. One can therefore conclude that, *SS*-*SR*-methoxy-MA is the best antigen for use in a serodiagnostic assay for tuberculosis that is based on free MAs as antigen. In addition, *SS*-*SR*-methoxy-MA may well represent one of the antigenically active components that occurs in natural MA and that elicit specific antibody production in patients with TB. *RR*-*RS*-methoxy-MA was also recognised significantly better by TB^- serum compared to the TB^+ serum ($P < 0.01$). It might be that this diastereomer could be used to distinguish better between TB^+ and TB^- sera than with the natural MAs, but more sera will have to be analyzed to substantiate this.

Similar to the negative control antigen, MB, the *trans*-, *cis*-cyclopropane-keto-MA, and *cis*-cyclopropane-hydroxy-MA were also not recognised by TB^+ patient antibodies, but *trans*-cyclopropane-hydroxy-MA was recognised weakly. This demonstrates that the antigenicity of MA is not only dependent on the mycolic motif, but that the mero chain is critical in the manifestation of biological activity. In terms of the oxygenated groups in the mero chain, the methoxy is by far the most active, while some activity can be retained with a hydroxy group substituting for methoxy. Irrespective of whether the keto- and hydroxy-MA represent the natural material, the data clearly demonstrates the that structure of the mero chain is importance for antigenicity. By comparing the resolution in signals of TB^- and TB^+ sera between *SS*-*SR*-methoxy-MA to *RR*-*RS*- and *RR*-*SR*-MA it is clear that the stereochemistry of the mero chain plays a decisive role in their antigenicity. The nature of the stereochemistry of the keto- and the hydroxyl groups are not known and therefore more structures need to be analyzed.

I show, for the first time, that synthetic, stereochemically and diastereomerically pure MAs showed biological activity and were recognised by TB^+ patient serum. Surprisingly, these were also recognised by TB^- patient serum. One reason could be that cross-reactivity with cholesterol antibodies might play a role. It is also possible that there are antibodies to other

mycobacteria involving MAs, eg the saprophytic types. There may also be other unrecognised explanations.

The hydrophobicity of both MA and cholesterol and their apparent molecular relation (discussed in 1.1.7.4 and 3.1.3) suggests that the two entities could snugly fit together, stabilized by hydrophobic forces. The specificity of MA for attracting cholesterol is determined more by the type of oxygenated group (methoxy preferred) and its stereochemistry (*RR* preferred), than by the stereochemistry of the cyclopropane group in the mero chain. These two structural properties appear to be critical for defining the structural similarity of part of the MA structure to cholesterol.

The similarity in structure of MA to cholesterol may have a profound effect on the virulence of *M. tuberculosis,* in particular to their mechanism of entry into the host macrophage and their sustenance, as referred to in Chapter 1 (section 1.1.2). This applies especially to the ability of MA to attract cholesterol. To determine whether MA, in comparison to methylated MA (mMA) and synthetic protected alpha-MA (MB) attracts cholesterol, a biosensor cuvette was coated with MA-, mMA-, or MB-containing liposomes. Sensorgrams were generated by exposing the coated surface to cholesterol-containing liposomes. This was done with a resonant mirror biosensor as described by Siko (134). The resonant mirror biosensor works on the principle that the angle at which light is internally reflected from a sensing surface supported on a dielectric resonant layer, changes as mass accumulates onto it (41). This allows real time analyses of dynamic molecular binding of soluble ligates to ligands that are immobilised on the sensing surface (31). Figure 3.24 shows the coating of MA to the cuvette surface of more than 2 000 arc seconds, and then binding of cholesterol. MB could be coated to a similar degree of efficiency, while mMA coated even better at 3 000 arc seconds.

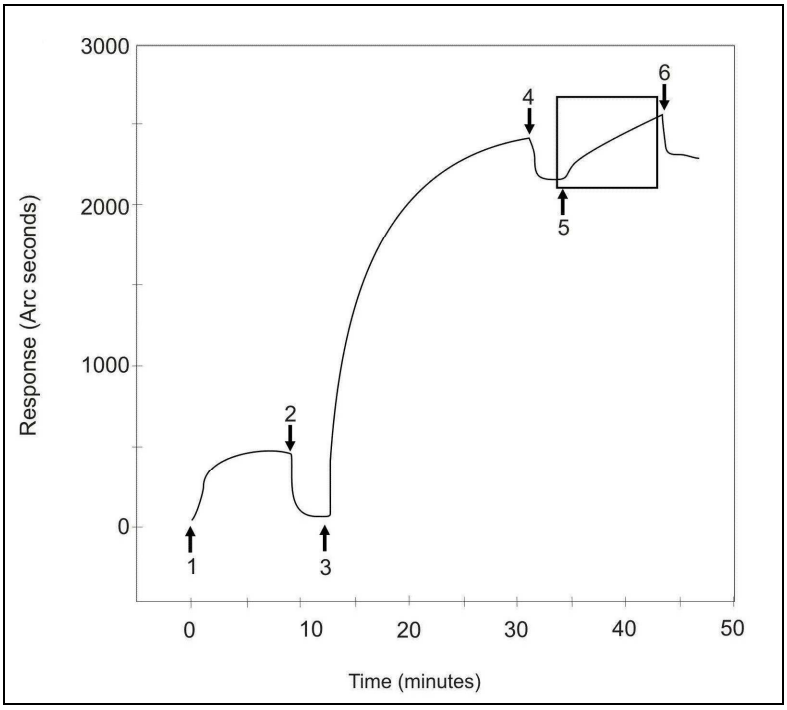

Figure 3.24: *A typical IAsys sensorgram to monitor binding of cholesterol to MA. 1: Activation of surface with CPC, 2: PBS/AE wash step, 3: addition of MA liposomes, 4: PBS/AE wash step, 5: addition of cholesterol liposomes, 6: PBS/AE wash step.*

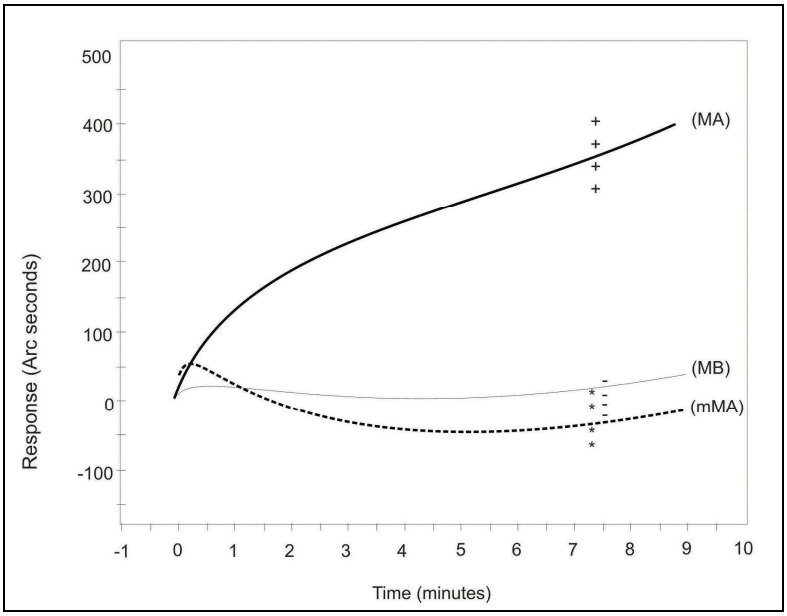

Figure 3.25: *Biosensor binding curves (the framed part of Figure 3.24) of cholesterol attraction to immobilized natural MAs (MA, thick line / +), MA methyl esters (mMA, dashed line / *) or acetylated synthetic alpha-MA methyl ester (MB, thin line / -). Each line represents the typical curve of five repeats with the exact end points of each indicated after 7.5 minutes exposure.*

Figure 3.25 shows that the MA-liposomes coated cuvette surface accumulated cholesterol from the solution, but that the MA methyl esters and the acetylated synthetic MA methyl ester (MB) were unable to do so (Student's t-test showed no significant difference between mMA and MB ($P > 0.1$), while the difference in binding of cholesterol to MA and MB was significant ($P < 0.001$).

It is clear that the attraction of cholesterol to MA is determined by the fine structure of the ligand-receptor pair. The loss of antigenicity and cholesterol binding capability of the methyl esters of MAs might be due to the requirement of free carboxylic acid to stabilize a conformational folding of the long meromycolate chain to which cholesterol can bind. Retzinger *et al*. (118) and Villeneuve *et al*. (145, 146) proposed that the long MA mero chain is kinked and folded in the lipid bilayer as three tightly packed bends of hydrocarbon. Similar folded conformations of oxygenated MA are proposed that can explain experimental observations obtained in different studies (70). The alignment of the acyl chains by folding may allow hydrophobic interactions by intra-molecular stacking that is enabled by the hairpin bend induced by the proximal *cis*-cyclopropane group. Methoxy-MA may bind better to cholesterol than keto-MA by retaining a tetrahedral structure around the oxygenated carbon, homologous to the structural architecture around the 3-hydroxy group of cholesterol. The carboxylic acid part of the molecule plays an important role in its antigenicity for both TB^+ and TB^- patient antibodies.

3.4.2 Materials and methods

3.4.2.1 Mycolic acids used as antigens in ELISA

For the antigenicity/cholesterol binding activity assay, different synthetic MAs were kindly provided by Dr J. Al Dulayymi and Gani Koza (University of Wales, Bangor, UK) in addition to the synthesized methoxy-MA described in Chapter 3 (6, 7, 90).

3.4.2.1.1 Natural mycolic acids

Mycobacterial MAs were isolated from a culture of *M. tuberculosis* H37Rv as described by Goodrum *et al.* (67), as a mixture of α-, keto- and methoxy-MAs (Figure 1.7).

3.4.2.1.2 Synthetic acetylated alpha mycolic acid methyl ester (MB)

An α-MA was synthesized by Al Dulayymi *et al.* (7) and was O-acetylated at the β-OH and methylated at the α-carboxylic acid.

3.4.2.1.3 Synthetic methoxy-MA (RR-RS-methoxy)

Deprotected as described in section 3.3.2.52.

3.4.2.1.4 Synthetic methoxy-MA (RR-SR-methoxy)

Demethylated and kindly provided by Dr J. Al Dulayymi (University of Wales, Bangor, UK).

3.4.2.1.5 Synthetic methoxy-MA (SS-SR-methoxy)

Deprotected and kindly provided by Dr J. Al Dulayymi (University of Wales, Bangor, UK).

3.4.2.1.6 Synthetic trans-*cyclopropane-keto-MA*

Synthesized and kindly provided by Gani Koza (University of Wales, Bangor, UK).

3.4.2.1.7 Synthetic cis-*cyclopropane-keto-MA*

Synthesized and kindly provided by Gani Koza (University of Wales, Bangor, UK).

3.4.2.1.8 Synthetic trans-*cyclopropane-hydroxy-MA*

Synthesized and kindly provided by Gani Koza (University of Wales, Bangor, UK).

3.4.2.1.9 Synthetic cis-*cyclopropane-hydroxy-MA*

Synthesized and kindly provided by Gani Koza (University of Wales, Bangor, UK).

3.4.2.2 Reagents and apparatus used in ELISA

As describe above in section 2.4.2.2 to 2.4.2.7.

3.4.2.3 Reagents and apparatus used in Biosensor assay

Natural mycolic acid (MA): Mycobacterial MAs were isolated from a culture of *M. tuberculosis* H37Rv as described by Goodrum *et al.* (67), as a mixture of α-, keto- and methoxy-MAs (Figure 1.7).

Synthetic α-mycolic acid (MB): Synthesized and kindly provided by Dr J. Al Dulayymi (University of Wales, Bangor, UK) (7).

Phosphatidyl choline-99 (PC): stock solution of 100 mg/ml in chloroform (99%, Sigma, USA).
Cholesterol (5-cholesten-3β-ol, Standard for chromatography, Sigma, St. Louis, MD, USA): stock solution of 100 mg/ml in chloroform.

Phosphate buffered saline (PBS): 20 x PBS stock was prepared by dissolving sodium chloride (160 g; 99%, Merck, SA), potassium chloride (4 g; 99%, Merck, SA), di-hydrogen potassium phosphate (4 g; 99%, Merck, SA) and di-sodium hydrogen phosphate (23 g; 99%, Merck, SA) in double distilled de-ionized water to a final volume of 1000 ml.

1 x PBS: 50 ml 20 x PBS in 950 ml dddH_2O. The pH of the solution was adjusted to 7.4 with 1 M NaOH.

PBS/Azide-EDTA (PBS/AE): EDTA (1 mM, Sigma, USA) and sodium azide (0.025% m/v, Sigma, USA) in 1 x PBS.

Saline: 0.9% NaCl (Merck, SA).
Potassium hydroxide (KOH): 12.5 M (Merck, SA).
Ethanol (EtOH): 95% (Saarchem, SA).
Cetyl-pyridinium chloride (CPC): 0.02 mg/ml in PBS/AE (Sigma, St. Louis, MD, USA).
IAsys resonant mirror biosensor: IAsys Affinity Sensors, Bar Hill, Cambridge, UK.
Sonicator: Branson Sonifier B-30, USA.

3.4.2.4 Preparation of liposomes containing mycolic acids, synthetic acetylated α-mycolic acid methyl ester (MB) or cholesterol

For the preparation of MA containing liposomes, PC (90 µl) was added to an amber glass vial containing MA (1 mg), mixed well to dissolve the MA, dried at 80 ˚C under a stream of N_2, and then sonicated in saline (2 ml) for 2 minutes at RT. The MB containing liposomes and the 'empty' PC liposomes were made in the same way, MB liposomes with 1 mg of MB, and PC liposomes with omission of the MAs. For the cholesterol-containing liposomes, PC (60 µl) and cholesterol (30 µl) were added to an amber glass vial without MA, mixed well, dried,

suspended in saline (2 ml) and sonicated as above. The liposomes were divided into 200 µl aliquots, freeze-dried and stored at -20 ˚C until used. Before use, the liposomes were reconstituted with PBS/AE (2 ml), heated at 80 ˚C for 15 minutes and then sonified as above. The final liposome concentration came to 500 µg/ml.

3.4.2.5 Measurements of interaction between MA, MB and cholesterol

IAsys software was used to set the IAsys affinity biosensor at a data-sampling interval of 0.4 s, temperature of 25 ^{0}C and stirring rate of 75%. Prior to use, the wells were regenerated by washing 5 times with EtOH (50 µl), for 30 seconds, followed by washing 7 times with PBS/AE (70 µl). The surface was then treated 5 times with KOH (50 µl) for 1 minute and finally washing 7 times with PBS/AE (70 µl). PBS/AE (60 µl) was pipetted into each well of the cuvette to obtain a stable baseline for 1 minute. The PBS/AE was subsequently aspirated and the surface activated with CPC (50 µl) for 10 minutes. This was followed by washing five times with PBS/AE (60 µl) and then substituting with PBS/AE (25 µl) for a new baseline before immobilization of MA-containing or MB-containing liposomes (25 µl) to the surface for 20 minutes. The immobilized liposomes were then washed 5 times with PBS/AE (60 µl) and again substituted with PBS/AE (25 µl) before the cholesterol-containing liposomes (25 µl) were added. Direct interaction between the immobilized MAs and cholesterol was monitored for 10 minutes, after which the cuvette was washed 3 times with 60 µl PBS/AE and regenerated as before.

Chapter 4

Discussion

This study set out to resolve the structure-activity relationship of MAs from *M. tuberculosis* in terms of both their antigenicity, i.e. their capacity to be recognised by TB patient serum antibodies, and the ability of MAs to attract cholesterol, because it may play a critical role in the entry of the bacillus into the host macrophage and its mechanism to survive in that normally hostile environment.

The first indication that MAs are antigenic was obtained indirectly by the production of antibodies against cord factor in mice and rabbits by a Japanese research group. They injected rabbits with methylated bovine serum albumin complex of cord factor to obtain antiserum. The anti-cord factor IgM antibodies were detected by a precipitin reaction. It was suggested that the antigenic epitope may be the trehalose moiety (82). In 2005, Fujita *et al.* (64) published evidence that suggested that the MA rather than the sugar component of trehalose di- and monomycolates, was the antigenic determinant that was recognized by anti-cord factor antibodies from tuberculosis patients. This same notion was more directly demonstrated by Pan *et al.* (112) who coated ELISA plate wells with the pure, separated MA methyl esters from hexane solutions and showed that the methoxy-mycolates were the predominant antigens, while little TB patient antibody binding could be demonstrated with the α- or keto-mycolates. Fujiwara *et al.* (65) showed that anti-cord factor IgG in rabbits recognized MA subclasses of *M. tuberculosis* and *M. avium.* All this work on the antigenicity of cord factor stemmed from Japanese laboratories that focused on bringing a commercial kit for serodiagnosis of TB on the market. This kit is currently on clinical trial.

Yano *et al.* (157) found that antibodies in TB patients recognized not only MA esterified to a mono- or disaccharide (cord factor), but also free MAs with a carbon number of 14 or more as antigens. The MAs were extracted from *Mycobacterium, Nocardia, Rhodococcus* and *Corynebacterium* species and were esterified to trehalose. The trehalose MA esters comprised of trehalose bound to 1 to 4 MAs. These antigens were then brought into contact with an antibody-containing sample and analyzed by ELISA. They also showed that *M. tuberculosis*

derived antibodies that react with cord factor were present in the serum of TB^+ patients, but not in healthy controls.

The preferred antigenicity of cord factor in TB patients was confirmed in this study by showing that MA bound to trehalose was recognised by TB^+ patient serum, but not by the TB^- patient serum when analysed by ELISA. In chapter 2 the issue around the antibodies responsible for recognition of cord factor and MA was discussed. It is in fact not that simple to determine. Although cord factor was not recognised by TB^- patient serum, free MA was recognised. It seems that there are different types of antibodies, one type that is only found in TB^+ patients and that can recognise MA bound to trehalose as cord factor, and another type that can only recognise free MA, but not the MA bound to trehalose. TB^+ patients have both types of antibodies in their serum. The epitope on cord factor that is important for recognition by TB^+ patient serum is not the trehalose, but a combination of trehalose with MA. Our results therefore confirms that of Fujiwara *et al.* (65). They found that the different types of MA from different *Mycobacterium* species have unique antibody specificity in TB patients. Therefore, trehalose is not a public cross-reactive epitope, but forms a unique complex epitope that depends on the MA it associates with. The results show a possible epitope that exists on MA and which disappears when bound to trehalose. The MA epitope is a natural epitope that is recognised by antibodies from both TB^+ patients and healthy people.

To determine the fine specifity of interaction of MA with antibodies, the three subclasses of MA from *M. tb* were separated and the antigenicity of two of the subclasses determined. The antigenicity of the MAs initially appeared not to reside in only one of the subclasses, but this finding was not entirely convincing, because of possible contamination of the α-MA with methoxy-MA and the lack of sufficient amounts of keto-MA to be tested. This finding therefore does not yet support my hypothesis i.e. that the recognition of MAs by TB patient serum antibodies resides in only one of the subclasses. However, the statement could still hold true if contamination of one preparation of subclass with other subclasses can be totally ruled out. This may be easier to achieve by chemical synthesis of each of the various subclasses, rather than their isolation from a natural extract.

Both the mycolic acid motif and the mero chain components of natural MA are important epitopes for antigenicity (Chapter 2 and 3). It may be possible that this epitope on MA is

hidden when MA is bound to arabinogalactan in the cell wall, or that this epitope can only be recognised as free MA that might be found in lipoproteins in TB patients. It might well be that this is the immunogen that induces the formation of anti-MA antibodies in TB patients.

In recent years free MAs were used as antigens for the serodiagnosis of tuberculosis. They had good potential because HIV-TB co-infected patients maintained high antibody levels to MAs (127). It has been shown with ELISA that free MAs were not adequate for serodiagnosis of tuberculosis; it was only 57% accurate. An association between MAs and cholesterol was hypothesized (134) that might explain the low accuracy.

AmB accumulates to a cholesterol coated surface and also to a natural MA coated surface in a waveguide resonant mirror biosensor, but not to a synthetic protected α-MAs coated surface (24). Similarly, I demonstrated that cholesterol accumulated on a natural MA surface, but not on the synthetic protected α-MAs surface or a surface of methylated natural MA. The association of both AmB and cholesterol to MA depended on the formation of hydrogen bonds that also affect the structural rigidity of the molecules. The attraction between MA and cholesterol was specific and depended on a particular conformation that the free MAs assume in the phospholipid bilayer of liposomes. This will probably also apply to biological membranes.

Cholesterol may be attracted to MAs through hydrophobic Van der Waals interactions or by a more specific interaction between certain similar features present in both molecules. Free MAs assume a ‘W’ conformation with all the four alkyl chains folded to each other (145, 146). The condensed conformation of MAs was proposed by several groups and is based on Langmuir studies. The ‘W’ conformation could resemble the shape of cholesterol. In its extended form, the structure of MA can hardly relate to that of cholesterol or be able to attract cholesterol to any degree of specific association. According to Alving *et al.* (9, 10) naturally occuring autoantibodies against cholesterol reacting with the 3β-hydroxy group of cholesterol are present in the serum of almost every healthy individual. This was confirmed by Horváth *et al.* (79) and Bíró *et al.* (26). If MAs are able to attract cholesterol, it might be possible that cholesterol antibodies from TB^- patients recognise these MAs.

Retzinger *et al*. (118) and Villeneuve *et al.* (145, 146) proposed that the long MA mero chain is kinked and folded in the lipid bilayer to form three tightly packed bends of hydrocarbon. Similar folded conformations of oxygenated MA was proposed to explain experimental observations obtained in different studies (70, 75, 76). The alignment of the acyl chains due to folding may allow hydrophobic interactions by intra-molecular stacking that is enabled by the hairpin bend induced by the proximal *cis*-cyclopropane group. Methoxy-MA may relate better to cholesterol than keto-MA by retaining a tetrahedral structure around the oxygenated carbon, homologous to the structural architecture around the 3-hydroxy group of cholesterol. This all supports the folded conformation proposed by Siko (134).

The stereochemically controlled synthesis of MAs was first achieved by Al Dulayymi and co-workers (3-8, 38, 90), but to clarify the absolute stereochemistry of the functional groups in the mero chain as it occurs in nature, these compounds must be tested for biological activity and antigenicity.

Antibodies that are present in TB^+ patient serum recognise a number of synthetic MAs. All of these were also recognised by serum from TB^- patients. The α-MA, the negative control antigen, and the different keto- and hydroxy-MAs were not recognised by TB^+ patient antibodies. This demonstrates that the antigenicity of MA is not only dependent on the mycolic motif, but that the mero chain is critical in the manifestation of biological activity. In terms of the oxygenated groups in the mero chain, the methoxy seems to be more active.

One diastereomer of synthetic methoxy-MA was more avidly recognised by TB^+ serum than the other, and weaker by TB- serum compared to the rest of the MAs. It also is the one that most closely approximates the signal strength of antibody binding to natural MA by TB^+ patient sera. It can therefore be concluded that, of these synthetic compounds, *SS*-*SR*-methoxy-MA would be the most appropriate antigen to use in a serodiagnostic assay for tuberculosis. It may well represent one of the antigenically active components that occurs in natural MA and that elicits specific antibody production in patients with TB.

There are other questions. Can the mycolic acid motif retain its activity if it is esterified with some other groups, for instance arabinogalactan or 5-BMF. In these cases, a hydroxyl group would still be in the vicinity of the carboxyl group to form hydrogen bonds with the methoxy-

group in the folded mero chain? What is the role of the C_{24} chain? Is the C_{24} chain important for biological activity? It would be worthwhile to investigate in order to manipulate MAs for its exploitation as biologically active compound, eg. to find a minimum antigenic structure.

Proving that these synthetic MAs are recognized by antibodies in TB^+ patient serum when analyzed by ELISA, is only the beginning. It would be worthwhile to investigate other biological properties of the different subtypes of these synthetic MAs. MAs elicit an immune response, stimulate double negative T-cells (67) and stimulates mainly the macrophages following intraperitoneal administration of MAs into mice. This is achieved by converting the MAs into cholesterol-rich foam cells (89).

This thesis reports a stereocontrolled chemical synthesis of a biologically active MA. The chemical synthesis of MA and its derivatives can be used to control TB and other lung diseases in a variety of ways. In diagnostics it now can allow the determination of the minimum antigenic structure for recognition by antibodies in TB^+ patient serum as well as for other mycobacterial diseases like leprosy, Crohn's disease, Buruli ulcer and *M. avium* complex diseases. In biosensor technology the synthetic MA can be directly coupled to the gold disc surface of the cuvettes, eliminating additional washing and coating steps. In therapy, a synthetic medicine based on MA structure can be designed against asthma and arthritis, as well as in TB, eg. as an inhibitor of MA biosynthesis or the inhibition of the TACO-proteins. Synthetic MA can be included into nanoparticles for immunomodulation to exploit its anti-inflammatory effect.

References

1. **Aaron, L., D. Saadoun, I. Calatroni, O. Launay, N. Memain, V. Vincent, G. Marchal, B. Dupont, O. Bouchaud, D. Valeyre, and O. Lortholary.** 2004. Tuberculosis in HIV-infected patients: A comprehensive review. Clin. Microbiol. Infect. **10:**388-398.

2. **Ainsa, J. A., C. Martin, and B. Gicquel.** 2001. Molecular approaches to tuberculosis. Mol. Microbiol. **42:**561-570.

3. **Al Dulayymi, J. R., M. S. Baird, H. H. Hussain, B. J. Alhourani, A. Y. Alhabashna, S. J. Coles, and M. B. Hursthouse.** 2000. The cycloaddition of cyclopropenes to enones. Tetrahedron Lett. **41:**4205-4208.

4. **Al Dulayymi, J. R., M. S. Baird, and K. Jones.** 2004. The absolute stereochemistry of grenadamide. Tetrahedron **60:**341-345.

5. **Al Dulayymi, J. R., M. S. Baird, H. Mohammed, E. Roberts, and W. Clegg.** 2006. The synthesis of one isomer of the α-methyl-*trans*-cyclopropane unit of mycolic acids. Tetrahedron **62:**4851-4862.

6. **Al Dulayymi, J. R., M. S. Baird, and E. Roberts.** 2003. The synthesis of a single enantiomer of a major α-mycolic acid of *Mycobacterium tuberculosis*. Chem. Commun.**:**228-229.

7. **Al Dulayymi, J. R., M. S. Baird, and E. Roberts.** 2005. The synthesis of a single enantiomer of a major α-mycolic acid of *Mycobacterium tuberculosis*. Tetrahedron **61:**11939-11951.

8. **Al Dulayymi, J. R., M. S. Baird, and E. Roberts.** 2000. The synthesis of single enantiomers of a meromycolic acid. Tetrahedron Lett. **41:**7107-7110.

9. **Alving, C. R., and G. M. J. Swartz.** 1991. Antibodies to cholesterol, cholesterol conjugates and liposomes: Implications for atherosclerosis and autoimmunity. Crit. Rev. Immunol. **10:**441-453.

10. **Alving, C. R., G. M. J. Swartz, and M. Wassef.** 1989. Naturally occuring autoantibodies to cholesterol in humans. Biochem. Soc. Trans. **629:**637-639.

11. **Anderson, R. J.** 1941. Structural peculiarities of acid-fast bacterial lipids. Chem. Rev. **29:**225-243.

12. **Antonucci, G., E. Girardi, M. Raviglione, and G. Ippolito.** 1995. Risk factors for tuberculosis in HIV-infected persons. A prospective study. JAMA **274:**143-148.

13. **Armstrong, J. A., and P. D. A. Hart.** 1971. Response of cultured macrophages to *Mycobacterium tuberculosis,* with observations on fusion of lysosomes with phagosomes. J. Exp. Med. **134:**713-740.

14. **Asselineau, J.** 1950. Sur la structure chimique des acides mycoliques isolés de *Mycobacterium tuberculosis* var. *hominis*; determination de la position de l'hydroxyle. C. R. Hebd. Seances. Acad. Sci. **230:**1620-1622.

15. **Asselineau, J., and G. Lanéelle.** 1998. Mycobacterial lipids: A historical perspective. Frontiers in Bioscience **3:**e164-174.

16. **Asselineau, J., and E. Lederer.** 1950. Structure of the mycolic acids of mycobacteria. Nature **166:**782-783.

17. **Av-Gay, Y., and R. Sobouti.** 2000. Cholesterol is accumulated by mycobacteria but its degradation is limited to non-pathogenic fast-growing mycobacteria. Can. J. Microbiol. **46:**826-831.

18. **Baba, T., Y. Natsuhara, K. Kaneda, and I. Yano.** 1997. Granuloma formation activity and mycolic acid composition of mycobacterial cord factor. Cell. Mol. Life Sciences **53:**227-232.

19. **Barry, C. E., R. E. Lee, K. Mdluli, A. E. Sampson, B. G. Schroeder, R. A. Slayden, and Y. Yuan.** 1998. Mycolic acids: Structure, biosynthesis and physiological functions. Prog. Lipid Res. **37:**143-179.

20. **Bean, A. G., D. R. Roach, and H. Briscoe.** 1999. Structural deficiencies in granuloma formation in TNF gene targeted mice underlie the heightened susceptibility to aerosol

Mycobacterium tuberculosis infection, which is not compensated for by lymphotoxin. J. Immunol. **162:**3504-3511.

21. **Beckman, E. M., S. A. Porcelli, C. T. Morita, S. M. Behar, S. T. Furlong, and M. B. Brenner.** 1994. Recognition of a lipid antigen by CD1-restricted ab+ T cells. Nature **372:**691-694.

22. **Bekierkunst, A., I. S. Levij, and E. Yarkoni.** 1968. Acute granulomatous response produced in mice by trehalose-6,6'-dimycolate. J. Bacteriol. **96:**958-961.

23. **Bekierkunst, A., I. S. Levij, and E. Yarkoni.** 1971. Suppression of urethan-induced lung adenomas in mice treated with trehalose-6,6'-dimycolate (cord factor) and living BCG. Science **174:**1240-1242.

24. **Benadie, Y.** 2007. Amphotericin B as a mycolic acid specific targeting agent in tuberculosis. MSc. Department of Biochemistry, University of Pretoria, Pretoria.

25. **Besra, G. S., K. H. Khoo, M. R. McNeil, A. Dell, H. R. Morris, and P. J. Brennan.** 1995. A new interpretation of the structure of the mycolyl-arabinogalactan complex of *Mycobacterium tuberculosis* as revealed through characterization of oligoglycosyladitol fragments by fast-atom bombardment mass spectrometry and ^{1}H nuclear magnetic resonance spectroscopy. Biochemistry **34:**4257-4266.

26. **Biro, A.** 2003. Serum anti-cholesterol antibodies in chronic hepatitis-C patients during IFN-α-2b treatment. Immunobiol. **207:**161-168.

27. **Bloch, H.** 1950. Studies on the virulence of tubercle bacilli. Isolation and biological properties of a constituent of virulent organism. J. Exp. Med. **91:**197-217.

28. **Brennan, P. J.** 1989. Structure of mycobacteria: recent developments in defining cell wall carbohydrates and proteins. Rev. Infect. Dis. **11:**S420-S430.

29. **Brennan, P. J.** 2003. Structure, function and biogenesis of the cell wall of *Mycobacterium tuberculosis*. Tuberculosis **83:**91-97.

30. **Brennan, P. J., and H. Nikaido.** 1995. The envelope of mycobacteria. Annu. Rev. Biochem. **64:**29-63.

31. **Buckle, P. E., R. J. Davies, T. Kinning, D. Yeung, P. R. Edwards, and D. Pollard-Knight.** 1993. The resonant mirror: A novel optical biosensor for direct sensing of biomolecular interactions. I: Principle of operation and associated instrumentation. Biosens. Bioelectron. **8:**347-355.

32. **Butler, W. R., and L. S. Guthertz.** 2001. Mycolic acids analysis by high-performance liquid chromatography for identification of *Mycobacterium* species. Clin. Microbiol. Rev. **14:**704-726.

33. **Chatterjee, D.** 1997. The mycobacterial cell wall: Structure, biosynthesis and sites of drug action. Curr. Opin. Chem. Biol **1:**579-588.

34. **Chatterjee, D., and K. H. Khoo.** 1998. Mycobacterial lipoarabinomannan: An extraordinary lipoheteroglycan with profound physiological effects. Glycobiol. **8:**113-120.

35. **Chatterjee, D., K. Lowell, B. Riviore, M. R. McNeil, and P. J. Brennan.** 1992. Lipoarabinomannan of *M. tuberculosis*. J. Biol. Chem. **267:**6234-6239.

36. **Collum, B. D., J. H. McDonald, and W. C. Still.** 1980. Synthesis of the polyether antibiotic monensin. 2. Preparation of intermediates. J. Am. Chem. Soc. **102:**2118-2120.

37. **Coxon, G. D., J. R. Al-Dulayymi, M. S. Baird, S. Knobl, E. Roberts, and D. E. Minnikin.** 2003. The synthesis of (11*R*,12*S*)-lactobacillic acid and its enantiomer. Tetrahedron: *Assymmetry* **14:**1221-1222.

38. **Coxon, G. D., J. R. Al Dulayymi, C. Morehouse, P. J. Brennan, G. S. Besra, M. S. Baird, and D. E. Minnikin.** 2004. Synthesis and properties of methyl 5-(1'*R*,2'*S*)-(2-octadecylcycloprop-1-yl)pentanoate and other ω-19 chiral cyclopropane fatty acids and esters related to mycobacterial mycolic acids. Chemistry and Physics of Lipids **127:**35-46.

39. **Coxon, G. D., S. Knobl, E. Roberts, M. S. Baird, J. R. Al Dulayymi, G. S. Besra, P. J. Brennan, and D. E. Minnikin.** 1999. The synthesis of both enantiomers of lactobacillic acid and mycolic acid analogues. Tetrahedron Lett. **40:**6689-6692.

40. **Crowe, L. M., B. J. Spargo, T. Ioneda, B. L. Beaman, and J. H. Crowe.** 1994. Interaction of cord factor (trehalose-6,6'-dimycolate) with phospholipids. Biochim. Biophys. Acta. **1194:**53-60.

41. **Cush, R., J. M. Cronin, and W. J. Stewart.** 1993. The resonant mirror: A novel optical biosensor for direct sensing of biomolecular interactions Part I: Principle of operation and associated instrumentation. Biosens. Bioelectron. **8:**347-354.

42. **Daffé, M., and P. Draper.** 1998. The envelope layers of mycobacteria with reference to their pathogenicity. Adv. Microb. Physiol. **39:**131-203.

43. **Daffé, M., and D. Lanéelle.** 1988. Distribution of phthiocerol diester, phenolic mycosides and related compounds in mycobacteria. J. Gen. Microbiol. **134:**2049-2055.

44. **Daffé, M., and M. A. Lanéelle.** 1991. Structure and stereochemistry of mycolic acids of *Mycobacterium tuberculosis* and *Mycobacterium ulcerans*. Res. Microbiol. **142:**397-403.

45. **Daffé, M., M. A. Lanéelle, G. Puzo, and C. Asselineau.** 1981. Acide mycolique epoxidique: un nouveau type d'acide. Tetrahedron Lett. **22:**4515-4516.

46. **De Chastellier, C., T. Lang, and L. Thilo.** 1995. Phagocytic processing of the macrophage endoparasite, *Mycobacterium avium*, in comparison to phagosomes which contain *Bacillus subtile* or latex beads. Eur. J. Cell. Biol. **68:**167-182.

47. **De Chastellier, C., and L. Thilo.** 1997. Phagosome maturation and fusion with lysosomes in relation to surface property and size of the phagocytic particle. Eur. J. Cell. Biol. **74:**49-62.

48. **Dobson, G., D. E. Minnikin, S. M. Minnikin, J. H. Parlett, and M. Goodfellow.** 1985. Systematic analysis of complex mycobacterial lipids, p. 237-265. *In* M. Goodfellow and D. E. Minnikin (ed.), Chemical methods in bacterial systematics. The society for applied bacteriology.

49. **Draper, P.** 1998. The outer parts of the mycobacterial envelope as permeability barriers. Frontiers in Bioscience **3:**1253-1261.

50. **Dubnau, E., J. Chan, C. Raynaud, V. P. Mohan, M. A. Lanéelle, K. Yu, A. Quémard, I. Smith, and M. Daffé.** 2000. Oxygenated mycolic acids are necessary for virulence of *Mycobacterium tuberculosis* in mice. Mol. Microbiol. **36:**630-637.

51. **Dubnau, E., M. A. Lanéelle, S. Soares, A. Benichou, T. Vaz, D. Promé, J. C. Promé, M. Daffé, and A. Quémard.** 1997. *Mycobacterium bovis* BCG genes involved in the biosynthesis of cyclopropyl keto- and hydroxy-mycolic acids. Mol. Microbiol. **23:**313-322.

52. **Durand, E., M. Gillois, J. F. Tocanne, and G. Lanéelle.** 1979. Property and activity of mycoloyl esters of methyl glucoside and trehalose. Effect on mitochondrial oxidative phosphorylation related to organization of suspensions and to acyl-chain structures. Eur. J. Biochem. **94:**109-118.

53. **Durand, E., M. Welby, G. Lanéelle, and J. F. Tocanne.** 1979. Phase behaviour of cord factor and related bacterial glycolipid toxins. A monolayer study. Eur. J. Biochem. **93:**103-112.

54. **Ehlers, S., M. E. A. Milke, and H. Hahn.** 1994. Progress in TB research: Robert Koch's dilemma revisited. Immunol. Today **15:**1-4.

55. **Ellner, J. J.** 1997. Review: The immune response in human tuberculosis: implications for tuberculosis control. J. Infect. Dis. **176:**1351-1359.

56. **Fenton, M. J., and M. W. Vermeulen.** 1996. Immunopathology of tuberculosis: Roles of macrophages and monocytes. Infect. Immun. **64:**683-690.

57. **Ferrari, G., H. Langen, N. M., and J. Pieters.** 1999. A coat protein on phagosomes involved in the intracellular survival of mycobacteria. Cell **97:**435-437.

58. **Filling, C., K. D. Berndt, J. Benach, S. Knapp, T. Prozorovski, E. Nordling, R. Ladenstein, H. Jornvall, and U. Oppermann.** 2002. Critical residues for structure and catalysis in short-chain dehydrogenases/reductases. J. Biol. Chem. **277:**25677-25684.

59. **Flynn, J. L., and J. Chan.** 2001. Tuberculosis: Latency and reactivation. Infect. Immun. **69:**4195-4201.

60. **Flynn, J. L., and J. D. Ernst.** 2000. Immune responses in tuberculosis. Curr. Opin. Immunol. **12:**432-436.

61. **Flynn, J. L., M. M. Goldstein, and J. Chan.** 1995. Tumour necrosis factor-alpha is required in the protective immune response against *Mycobacterium tuberculosis* in mice. Immunity **2:**561-572.

62. **Frieden, T. R., T. R. Sterling, S. S. Munsiff, C. J. Watt, and C. Dye.** 2003. Tuberculosis. Lancet **362:**887-899.

63. **Fujita, Y., T. Doi, R. Maekura, M. Ito, and I. Yano.** 2006. Differences in serological responses to specific glycopeptidolipid-core and common lipid antigens in patients with pulmonary disease due to *Mycobacterium tuberculosis* and *Mycobacterium avium* complex. J. Med. Microbiol. **55:**189-199.

64. **Fujita, Y., T. Doi, K. Sato, and I. Yano.** 2005. Diverse humoral immune responses and changes in IgG antibody levels against mycobacterial lipid antigens in active tuberculosis. Microbiol. **151:**2065-2074.

65. **Fujiwara, N., J. Pan, K. Enomoto, Y. Terano, T. Honda, and I. Yano.** 1999. Production and partial characterization of anti-cord factor (trehalose-6,6'-dimycolate) IgG antibody in rabbits recognizing mycolic acid subclasses of *Mycobacterium tuberculosis* or *Mycobacterium avium*. FEMS Immunol. Med. Microbiol. **24:**141-149.

66. **Gatfield, J., and J. Pieters.** 2000. Essential role for cholesterol in entry of mycobacteria into macrophages. Science **288:**1647-1650.

67. **Goodrum, M. A., D. G. R. Siko, T. Niehues, D. Eichelbauer, and J. A. Verschoor.** 2001. Mycolic acids from *Mycobacterium tuberculosis*: Purification by countercurrent distribution and T-cell stimulation. Microbios **106:**55-67.

68. **Grandjean, D., P. Pale, and J. Chuche.** 1991. Enzymatic hydrolysis of cyclopropanes. Total synthesis of optically pure dictyopterens a and c. Tetrahedron **47:**1215-1230.

69. **Grange, J. M.** 1988. Mycobacteria and human disease. Edward Arnold Ltd, London.

70. **Grant, E. P., E. M. Beckman, S. M. Behar, M. Degano, D. Frederique, G. S. Besra, I. A. Wilson, S. A. Porcelli, S. T. Furlong, and M. B. Brenner.** 2002. Fine specificity

of TCR compementarity-determining region residues and lipid antigen hydrophilic moieties in the recognition of a CD1-lipid complex. J. Immunol. **168:**3933-3940.

71. **Gray, G. R., M. Y. H. Wong, and S. J. Danielson.** 1982. The major mycolic acids of *Mycobacterium smegmatis*. Prog. Lip. Res. **21:**91-107.

72. **Grzybowski, S., and E. A. Allen.** 1964. The challenge of tuberculosis in decline. A study based on the epidemiology of tuberculosis in Ontario, Canada. Am. Rev. Resp. Dis. **90:**707-720.

73. **Hart, P. D., J. A. Armstrong, C. A. Brown, and P. Draper.** 1972. Ultrastructural study of the behavior of macrophages toward parasitic mycobacteria. Infect. Immun. **5:**803-807.

74. **Hasan, Z.** 1997. Isolation and characterization of the mycobacterial phagosome: segregation from the endosomal/lysosomal pathway. Mol. Microbiol. **24:**545-553.

75. **Hasegawa, T., S. Amino, S. Kitamura, L. Matsumoto, S. I. Katada, and J. Nishijo.** 2003. Study of the molecular conformation of α- and keto-mycolic acid monolayers by Langmuir-Blodgett technique and fourier transform infrared reflection-absorption spectroscopy. Langmuir **19:**105-109.

76. **Hasegawa, T., and R. M. Leblanc.** 2003. Aggregation properties of mycolic acids molecules in monolayers films: A comparative study of compounds from various acid-fast bacterial species. Biochim. Biophys. Acta. **1617:**89-95.

77. **Hashimoto, N., T. Aoyama, and S. Takayuki.** 1981. New methods and reagents in organic synthesis. 14. A simple efficient preparation of methyl esters with trimethylsilyl diazomethane (TMSCHN2) and its applications to gas chromatography analysis of fatty acids. Chem. Pharm. Bull. **29:**1475-1478.

78. **He, H., S. Oka, Y. Han, M. Yamamura, E. Kusunose, M. Kusunose, and I. Yano.** 1991. Rapid serodiagnosis of human mycobacteriosis by ELISA using cord factor (trehalose-6,6'-dimycolate) purified from *Mycobacterium tuberculosis* as antigen. FEMS Microbiol. Immunol. **76:**201-204.

79. **Horvath, A.** 2001. High level of anticholesterol antibodies (ACHA) in HIV patients. Normalization of serum ACHA concentration agter introduction of HAART. Immunobiol. **203:**756-768.

80. **Huang, H. C., J. K. Rehmann, and G. R. Gray.** 1982. Total synthesis of naturally occuring mycolic acids. (*E*)- and (*Z*)-threo-2-docosyl-3-hydroxytetracont-21-enoate. J. Org. Chem. **47:**4018-4023.

81. **Kaneda, K., S. Imiaiszumi, T. Baba, M. Tsukamura, and I. Yano.** 1988. Structure and molecular species composition of three homologous series of α-mycolic acids from *Mycobacterium* spp. J. Gen. Microbiol. **134:**2213-2229.

82. **Kato, M.** 1972. Antibody formation to trehalose 6,6'-dimycolate (cord factor) of *Mycobacterium tuberculosis*. Infect. Immun. **5:**203-212.

83. **Kaufmann, S. H.** 2001. How can immunology contribute to the control of tuberculosis? Nat. Rev. Immunol. **1:**20-30.

84. **Kaul, D.** 2001. Molecular link between cholesterol, cytokines and atherosclerosis. Mol. Cell. Biochem. **219:**65-71.

85. **Kaul, D., P. K. Anand, and I. Verma.** 2004. Cholesterol-sensor initiates *M. tuberculosis* entry into human macrophages. Mol. Cell. Biochem. **258:**219-222.

86. **Kaul, D., and M. Kaur.** 1998. Receptor-C_k controls the expression of Bcl-2 and cyclin d genes. Leuk. Res. **22:**671-675.

87. **Kawamura, M., N. Sueshige, K. Imayoshi, I. Yano, R. Maekura, and H. Kohno.** 1997. Ensyme immunoassay to detect antituberculous glycolipid antigen (anti-TBGL antigen) antibodies in serum for diagnosis of tuberculosis. J. Clin. Lab. Anal.**:**140-145.

88. **Keet, D. F., N. P. Kriek, M. L. Penrith, A. Michel, and H. Huchzermeyer.** 1996. Tuberculosis in buffaloes (*Syncerus caffer*) in the Kruger National Park: spread of the disease to other species. Onderstepoort J. Vet. Res. **63:**239-244.

89. **Korf, J. E., A. C. Stoltz, J. A. Verschoor, P. de Baetselier, and J. Grooten.** 2005. The *Mycobacterium tuberculosis* cell wall component mycolic acid elicits pathogen-associated host innate immune responses. Eur. J. Immunol. **35:**890-900.

90. **Koza, G., and M. S. Baird.** 2007. The first synthesis of a single enantiomer of a ketomycolic acid. Tetrahedron Letters **48:**2165-2169.

91. **Lacave, C., M. A. Lanéelle, M. Daffé, H. Montrozier, M. P. Rols, and C. Asselineau.** 1987. Structural and metabolic study of the mycolic acids of *Mycobacterium fortuitum*. Eur. J. Biochem. **163:**369-378.

92. **Lanéelle, M. A., and G. Lanéelle.** 1970. Structure d'acides mycoliques et d'un intermediaire dans la biosynthese d'acides dicarboxyliques. Eur. J. Biochem. **12:**296-300.

93. **Laval, F., M. A. Lanéelle, C. Deon, B. Monsarrat, and M. Daffé.** 2001. Accurate molecular mass determination of mycolic acids by MALDI-TOF mass spectrometry. Anal. Chem. **73:**4537-4544.

94. **Long, R., and M. Gardam.** 2003. Tumour necrosis factor-α inhibitors and the reactivation of latent tuberculosis infection. CMAJ **168:**1153-1156.

95. **Lopez-Marin, L. M., E. Segura, C. Hermida-Escobedo, A. Lemassu, and M. C. Salinas-Carmona.** 2003. 6,6'-Dimycoloyl trehalose from rapidly growing *Mycobacterium*: An alternative antigen for tuberculosis serodiagnosis. Immunol. Med. Microbiol. **36:**47-54.

96. **Luquin, M., J. Roussel, F. Lopez-Calahorra, G. Lanéelle, V. Ausina, and M. A. Lanéelle.** 1990. A novel mycolic acid in a *Mycobacterium* sp. from the environment. Eur. J. Biochem. **192:**753-759.

97. **Maekura, R., M. Nakagawa, Y. Nakamura, T. Hiraga, Y. Yamamura, M. Ito, E. Ueda, S. Yano, H. He, S. Oka, K. Kashima, and I. Yano.** 1993. Clinical evaluation of rapid serodiagnosis of pulmonary tuberculosis by ELISA with cord factor (trehalose 6,6'-dimycolate) as antigen purified from *Mycobacterium tuberculosis*. Am. Rev. Respir. Dis. **148:**997-1001.

98. **McNeil, M.** 1996. Targeted preclinical drug development for *Mycobacterium avium* complex: a biochemical approach, p. 263-283. *In* J. A. Korvick and C. A. Benson (ed.), *Mycobacterium avium* complex imfection. Marcel Dekker Inc, New York.

99. **Michel, A., R. G. Bengis, D. F. Keet, M. Hofmeyr, L. M. Klerk, P. C. Cross, A. E. Jolles, D. Cooper, I. J. Whyte, P. Buss, and J. Godfroid.** 2006. Wildlife tuberculosis in South African conservation areas: implications and challenges. Veterinary Microbiology **12:**91-100.

100. **Minnikin, D. E.** 1982. Lipids: Complex lipids, their chemistry, biosynthesis and roles., p. 95-184. *In* C. Ratledge and J. Stanford (ed.), The biology of the mycobacterium: Physiology, identification and classification. Academic Press, Inc, San Diego.

101. **Minnikin, D. E., and M. Goodfellow.** 1980. Lipid composition in the classification and identification of acid-fast bacteria. Soc. Appl. Bacteriol. Symp. Ser. **8:**189-256.

102. **Minnikin, D. E., L. Kremer, L. G. Dover, and G. S. Besra.** 2002. The methyl-branched fortifications of *Mycobacterium tuberculosis*. Chem. Biol. **9:**545-553.

103. **Minnikin, D. E., S. M. Minnikin, and M. Goodfellow.** 1982. The oxygenated mycolic acids of *Mycobacterium tuberculosis, M. farcinogenes and M. senegalese*. Biochim. Biophys. Acta. **712:**616-620.

104. **Minnikin, D. E., S. M. Minnikin, J. H. Parlett, M. Goodfellow, and M. Magnusson.** 1984. Mycolic acid patterns of some species of *Mycobacterium*. Arch. Microbiol. **139:**225-231.

105. **Minnikin, D. E., and N. Polgar.** 1967. The methoxymycolic and ketomycolic acids from human tubercle bacilli. Chem. Comm.**:**1172-1174.

106. **Minnikin, D. E., and N. Polgar.** 1967. The mycolic acids from human and avian tubercle bacilli. Chem. Comm.**:**916-918.

107. **Mohan, V. P., C. A. Scanga, K. Yu, H. M. Scott, K. E. Tanaka, E. Tsang, M. C. Tsai, J. L. Flynn, and J. Chan.** 2001. Effects of tumour necrosis factor-alpha on host ummune response in chronic persistent tuberculosis: Possible role for limiting pathology. Infect. Immun. **69:**1847-1855.

108. **Morimoto, Y., S. Kitao, Y. Okita, and T. Shoji.** 2003. Total synthesis and assignment of the double-bond position and absolute configuration of (-)-pyrinodemin A. Org. Lett. **5:**2611-2614.

109. **Nilsson, K., and C. Ullenius.** 1994. Stereoselectivity in the 1,4-addition reaction of organocopper reagents to ethyl 3-[(*S*)-2,2-dimethyl-1,3-dioxolan-4-yl]propenoate. Tetrahedron **50:**13173-13180.

110. **Noll, H., and H. Bloch.** 1955. Studies on the chemistry of the cord factor of *Mycobacterium tuberculosis*. J Biol Chem **214:**251-265.

111. **Nunn, P., B. Williams, K. Floyd, C. Dye, G. Elzinga, and M. Raviglione.** 2005. Tuberculosis control in the era of HIV. Nat. Rev. Immunol. **5:**819-826.

112. **Pan, J., N. Fujiwara, S. Oka, R. Maikura, T. Ogura, and I. Yano.** 1999. Anti-cord factor (trehalose-6,6'-dimycolate) IgG antibody in tuberculosis patients recognizes mycolic acid subclasses. Microbiol. Immunol. **43:**863-869.

113. **Peloquin, C. A., and S. E. Berning.** 1994. Infection caused by *Mycobacterium tuberculosis*. Annals of Pharmacotherapy **28:**72-84.

114. **Porcelli, S., C. T. Morita, and M. B. Brenner.** 1992. CD1b restricts the response of human $CD4^{-}8^{-}$ T lymphocytes to a microbial antigen.

115. **Pretorius, A.** 1999. Humoral and cellular immunogenicity of mycobacterail mycolic acids in tuberculosis. MSc. Department of Biochemistry, University of Pretoria, Pretoria.

116. **Qureshi, N., K. Takayama, H. C. Jordi, and H. K. Schones.** 1978. Characterization of the purified components of a new homologous series of α-mycolic acids from *Mycobacterium tuberculosis* H37Ra. J. Biol. Chem. **253:**5411-5417.

117. **Raja, A.** 2004. Immunology of tuberculosis. Indian J. Med. Res. **120:**213-232.

118. **Retzinger, G. S., S. C. Meredith, K. Takayama, R. L. Hunter, and F. J. Kezdy.** 1981. The role of surface in the biological activities of trehalose 6,6'-dimycolate. Surface properties and development of a model system. J. Biol. Chem. **256:**8208-8216.

119. **Ribi, E., D. L. Granger, K. C. Milner, K. Yamamoto, S. M. Strain, and R. Parker.** 1982. Induction of resistance to tuberculosis in mice with defined components of mycobacteria and with some unrelated materials. Immunol. **46:**297-305.

120. **Rodwell, T. C., N. P. Kriek, R. G. Bengis, I. J. Whyte, P. C. Viljoen, V. de Vos, and W. M. Boyce.** 2001. Prevalence of bovine tuberculosis in African buffalo at Kruger National Park. J. Wildlife Dis. **37:**258-264.

121. **Rozwarski, D. A., C. Vilcheze, M. Sugantino, R. Bittman, and J. C. Sacchettini.** 1999. Crystal structure of the *Mycobacterium tuberculosis* enoyl-ACP reductase, InhA, in complex with NAD^+ and a C16 fatty acyl substrate. J. Biol. Chem. **274:**15582-15589.

122. **Russell, D. G.** 2001. *Mycobacterium tuberculosis*: here today, and here tomorrow. Nat. Rev. Mol. Cell Biol. **2:**569-577.

123. **Ryll, R., Y. Kumazawa, and I. Yano.** 2001. Immunological properties of trehalose dimycolate (cord factor) and other mycolic acid-containing glycolipids. Microbiol. Immunol. **45:**801-811.

124. **Ryosuke, M., T. Ueki, H. Katakai, K. Takao, and K. Tadano.** 2001. Synthetic study of macquarimicins: Highly stereoselective construction of the AB-ring system. Org. Lett. **3:**3029-3032.

125. **Saita, N., A. Fujimura, I. Yano, and K. K. Soejima.** 2000. Trehalose-6,6'-dimycolate (cord factor) of *Mycobacterium tuberculosis* induces corneal angiogenesis in rats. Infect. Immun. **68:**5991-5997.

126. **Sakaguchi, I., N. Ikeda, M. Nakayama, Y. Kato, I. Yano, and K. Kaneda.** 2000. Trehalose-6,6'-dimycolate (cord factor) enhances neovascularization through vascular endothelial growth factor production by neutrophilis and macrophages. Infect. Immun. **68:**2043-2052.

127. **Schleicher, G. K., C. Feldman, Y. Vermaak, and J. A. Verschoor.** 2002. Prevalence of anti-mycolic acid antibodies in patients with pulmonary tuberculosis co-infected with HIV. Clin. Chem. Lab. Med. **40:**882-887.

128. **Schluger, N. W., and W. N. Rom.** 1997. The host immune response to tuberculosis. Am. J. Resp. Crit. Care Med. **157:**679-691.

129. **Sechi, L. A., M. Mura, F. Tanda, A. Lissia, A. Solinas, G. Fadda, and S. Zanetti.** 2001. Identification of *Mycobacterium avium* subsp. *paratuberculosis* im biopsy

specimens from patients with Crohn's disease identified by *in situ* hybridization. **39:**4514-4517.

130. **Sekanka, G., M. S. Baird, D. E. Minnikin, and J. Grooten.** 2007. Mycolic acids for the control of tuberculosis. Expert Opin. Ther. Patents **17:**315-331.

131. **Selwyn, P. A., D. Hartel, V. A. Lewis, E. E. Schoenbaum, S. H. Vermund, R. S. Klein, A. T. Walker, and G. H. Freidland.** 1989. A prospective study of the risk of tuberculosis among intravenous drug users with human immunodeficiency virus infection. N. Engl. J. Med. **320:**545-550.

132. **Seyferth, D., H. Menzel, A. W. Dow, and T. C. Flood.** 1972. Trimethylsilyl-substituted diazoalkanes. I Trimethylsilyl diazomethane. J. Organomet. Chem. **44:**279-290.

133. **Sieling, P. A., D. Chatterjee, S. A. Porcelli, T. L. Prigozy, R. J. Massaccaro, T. Soriano, B. R. Bloom, M. B. Brenner, M. Kronenberg, P. J. Brennan, and R. L. Modlin.** 1995. CH1-restricted T cell recognition of microbial lipoglycan antigens. Science **269:**227-230.

134. **Siko, D. G. R.** 2002. Mycobacterial mycolic acids as immunoregulatory lipid antigens in the resistance to tuberculosis. PhD. Department of Biochemistry, University of Pretoria, Pretoria.

135. **Sodhi, A., J. Gong, C. Silva, D. Qian, and P. F. Barnes.** 1997. Clinical correlates of interferon-gamma production in patients with tuberculosis. Clin. Infect. Dis. **25:**617-620.

136. **Spargo, B. J., L. M. Crowe, T. Ioneda, B. L. Beaman, and J. H. Crowe.** 1991. Cord factor (trehalose-6,6'-dimycolate) inhibits fusion between phospholipid vesicles. PNAS **88:**737-740.

137. **Spencer, H.** 1985. Pathology of the lung, 4th ed, vol. 1. Pergamon Press, Oxford.

138. **Stead, W. W., and J. P. Lofgren.** 1983. Does the risk of tuberculosis increase in old age? J. Infect. Dis. **147:**951-955.

139. **Steck, P. A., B. A. Schwartz, M. S. Rosendahl, and G. R. Gray.** 1978. Mycolic acids: A reinvestigation. J. Biol. Chem. **253:**5625-5629.

140. **Stodola, F. H., A. Lesuk, and R. J. Anderson.** 1938. The chemistry of the lipids of tubercle bacilli. LIV The isolation and properties of mycolic acid. J. Biol. Chem. **126:**505-513.

141. **Styblo, K.** 1980. Recent advances in epidemiological research in tuberculosis. Adv. Tuberc. Res. **20:**1-63.

142. **Thanyani, T. S.** 2003. A novel application of affinity biosensor technology to detect antibodies to mycolic acid in tuberculosis patients. MSc. Department of Biochemistry, University of Pretoria, Pretoria.

143. **Van Deventer, S. J. H.** 2001. Transmembrane TNF-α, induction of apoptosis and the efficacy of TNF-targeting therapies in Crohn's disease. Gastroenterology **121:**1242-1246.

144. **van Regenmortel, M.** 1999. The antigenicity of tobacco mosaic virus. Philosophical Transactions: Biological Sciences **354:**559-568.

145. **Villeneuve, M., M. Kawai, H. Kanashima, M. Watanabe, D. E. Minnikin, and H. Nakahara.** 2005. Temperature dependence of the Langmuir monolayer packing of mycolic acids form *Mycobacterium tuberculosis*. Biochim. Biophys. Acta **1715:**71-80.

146. **Villeneuve, M., M. Kawai, M. Watanabe, Y. Aoyagi, Y. Hitotsuyanagi, K. Takeya, H. Gouda, S. Hirono, D. E. Minnikin, and H. Nakahara.** 2007. Conformational behavior of oxygenated mycobacterial mycolic acids from *Mycobacterium bovis* BCG. Biochim. Biophys. Acta **1768:**1717-1726.

147. **Vrey, P. J.** 2004. Lipid ligand-protein receptor interactions characterised by a resonant mirror biosensor. MSc. Department of Biochemistry, University of Pretoria, Pretoria.

148. **Wang, L., R. A. Slayden, C. E. Barry, and J. Liu.** 2000. Cell wall structure of a mutant of *Mycobacterium smegmatis* defective in the biosynthesis of mycolic acids. J. Biol. Chem. **275:**7224-7229.

149. **Watanabe, M., Y. Aoyagi, H. Mitome, T. Fujita, H. Naoki, M. Ridell, and D. E. Minnikin.** 2002. Location of functional groups in mycobacterial meromycolate chains; the recognition of new structural principles in mycolic acids. Microbiol. **148:**1881-1902.

150. **Watanabe, M., Y. Aoyagi, M. Ridell, and D. E. Minnikin.** 2001. Separation and characterization of individual mycolic acids in representative mycobacteria. Microbiol. **147:**1825-1837.

151. **Watanabe, M., A. Ohata, S. Sasaki, and D. E. Minnikin.** 1999. Structure of a new glycolipid from *Mycobacterium avium-Mycobacterium intracellulare* complex. J. Bacteriol. **181:**2293-2297.

152. **WHO.** 2005. Fact sheet No 104: Tuberculosis.

153. **WHO.** 2001. Fact sheet No 199: Buruli ulcer.

154. **WHO.** 2006. Global Tuberculosis control. Surveillance, planning, financing. World Health Organization.

155. **WHO.** 2004. Status rapport: Leprosy elimination project.

156. **Williams, B. G., and C. Dye.** 2003. Anti-retroviral drugs for tuberculosis control in the era of HIV/AIDS. Science **301:**1535-1537.

157. **Yano, I., S. Oka, Y. Ueno, Y. Natsuhara, J. Yoshinaga, and Y. Kato.** 1990. Reagent for detecting antibody corresponding to acid-fast bacterium antigen and application thereof. Japan patent PCT/JP89/01341.

158. **Yuan, Y., D. Mead, B. G. Schroeder, Y. Zhu, and C. E. Barry.** 1998. The biosynthesis of mycolic acids in *Mycobacterium tuberculosis*. J. Biol. Chem. **273:**21282-21290.

159. **Zimmerli, S., S. Edwards, and J. D. Ernst.** 1996. Selective receptor blockade during phagocytosis does not alter the survival and growth of *Mycobacterium tuberculosis* in human macrophages. Am. J. Respir. Cell Mol. Biol. **15:**760-770.